UNIVERSITY OF EDINBURGH

PROBLEMS IN THE PHYSICAL CHEMISTRY OF POLYSACCHARIDES: THE STRUCTURE AND SOLUTION BEHAVIOUR OF POTATO AMYLOSE

by

ALAN R. PROCTER, B.Sc.

THESIS

submitted for the degree of

DOCTOR OF PHILOSOPHY

April, 1965.

TO MY PARENTS

AND ISOBEL

CONTENTS

PREFACE

Throughout this research, Dr. C. T. Greenwood has been a constant source of advice and encouragement, for which I am most grateful. Some of the work in Section 4A has been published in conjunction with Dr. Greenwood and colleagues, and a reprint is inserted at the end of this thesis.

I wish to thank Professors Sir Edmund Hirst and T.L. Cottrell for the provision of laboratory facilities, the Department of Scientific and Industrial Research for a Maintenance Grant during the period 1962-63, and the Potato Marketing Board for a Post-graduate Studentship Award for the period 1963-65.

The University Chemistry Department,
The King's Buildings,
Edinburgh 9.

INTRODUCTION

INTRODUCTION

It is now generally recognised that starch consists of two chemically-distinct components - amylose and amylopectin, which were first obtained in a pure state by Schoch (1942). Starch, which occurs as granules under the microscope, may be fractionated into its components by aqueous leaching (Meyer et al., 1940), but this is inferior to Schoch's method of completely dispersing the granules in hot water, and precipitating the amylose with a polar organic substance. The amylopectin is recovered from the supernatant and the amylose may be purified by repeated recrystalization. The ease of fractionation and percentage of amylose and amylopectin varies widely with the starch source. Pretreatment of the granule is often necessary to render it more amenable to dispersion, and methods using boiling organic liquids (Montgomery and Senti, 1958; Banks et al., 1959), alkali at $0^{o}C$ (Potter et al., 1953), and liquid ammonia (Hodge et al., 1948) have been tried. Starch fractionation procedures have recently been reviewed by Muetgeert (1961). Both components are α-1,4 glucans and their principal chemical and physical distinctions are shown in Table 1.

Starch chemistry, and in particular the physical chemistry of the starch components, is the subject of extensive reviews by Greenwood (1956) and Whelan (1958). Only a brief résumé of the more recent trends is therefore presented here.

Amylose:- Amylose is incompletely degraded by the enzyme

TABLE 1

A comparison of the properties of amylose and amylopectin

Property	Amylose	Amylopectin
Molecular configuration	Essentially linear	Highly branched
Molecular weight	ca 10^6	ca 10^8
Stability in aqueous solution	Unstable - tends to retrograde	Stable
Complex formation	Readily with iodine and polar substances	Very limited with iodine and polar substances
Colour with iodine	Deep blue	Purple-red
β-Amylolysis limit	ca 70-90% conversion into maltose	ca 55% conversion into maltose
Action of α-amylase + Z-enzyme	Complete hydrolysis	High molecular weight dextrans
X-ray diffraction	Crystalline	Amorphous or weakly crystalline patterns

β-amylase, and is therefore not a completely linear chain of unmodified α-1,4 linked anhydroglucose units. The presence of 'anomalous' amylose has long been known, but its structure and relation to the two major starch components is still a mystery. This problem is investigated fully in this thesis. The heterogeneous nature of amylose is established in Section 4A, and its structure and distribution with respect to starch intermediate fractions is discussed in Section 6.

Much interest has been recently given to the solution behaviour of amylose. The fractionation method for amylose of Everett and Foster (1959) has enabled conformation of the polysaccharide molecule to be studied in detail. Unfortunately, no absolute agreement in experiment has yet been reached. The conformation of amylose in aqueous solutions is studied in Sections 3 and 4B, where other results are critically examined, but it is generally considered to be of a flexible coil form.

The stability of amylose in aqueous solution has been the subject of many investigations. Acid and neutral solutions favour retrogradation, (Lansky et al., 1949), whereas alkali solvents promote degradation unless the strict conditions of nitrogen atmosphere and low temperatures are adhered to (see Section 3B). In fact, Baum and Gilbert (1954) have suggested that amylose contains oxygen sensitive bonds which hydrolyse in the presence of oxygen. This is an important factor to be considered in starch fractionation and amylose recrystalization. Failure to exclude oxygen may not only yield a low molecular weight product, but also a modified

product with possible oxidation at the glucose hydroxyl groups. In spite of the above difficulties, amylose solutions may easily be prepared by dissolving the butan-1-ol complex directly in the required solvent at room temperatures. Use of the complex has the additional advantage that possible degradation in the drying procedure of amylose is avoided.

In view of the many difficulties in handling amylose solutions, the measurement of molecular weight would be difficult. However, amylose derivatives, which are more stable in solution, may be prepared, and with particular attention to the elimination of degradation, their molecular weights determined. Recent results on amylose acetate indicate a molecular weight of ca 10^6 (D.P. ca 6000) by sedimentation diffusion in 0.2M alkali (Cowie, 1958; Bryce, 1958), and lightscattering (Everett and Foster, 1959) for the native polysaccharide. Husemann et al., (1961) used the tri-carbanilate derivative and also found a molecular weight of ca 10^6. Muetgeert (1961) has suggested that the maximum limiting viscosity number, $[\eta]$, for potato amylose in alkali is 280, whereas values of 400-500 are consistently found in these laboratories (see for example Greenwood and McKenzie, 1963). Moreover, these higher viscosity values are confirmed by high molecular weight values of ca 4×10^6 from lightscattering (Geddes, 1964).

The molecular weight distribution of amylose has been found by Everett and Foster (1959) and by Banks (1960), to be broad and continuous. Indeed, both workers found an exponential distribution toward higher molecular weight species. Such distributions

would be highly polydisperse and this is confirmed by an $\overline{M}_w/\overline{M}_n$ value of ca 5 by Geddes (1964).

Recently some biosynthesis studies on potatoes by McKenzie (1964) have shown that the starch and its components change on maturity of the potato tuber. He found that the size of the starch granules and the percentage of amylose, as well as the molecular size of the starch components, increased with age.

McGregor (1964) has also recently established the action pattern of some amylolytic enzymes. He showed that soya bean Z-enzyme attacked α-1,4 glycosidic linkages randomly, which is a similar action to the α-amylase isolated from other sources. The action pattern of β-amylase was also shown to be multichain, i.e. the enzyme attacks each substrate molecule (amylose) simultaneously.

The solution behaviour of amylose derivatives, notably the acetate, has been recently studied by Cowie (1961a) and Cowie and Toporowski (1964). The results indicate that the molecule is a flexible coil with negligible draining in chloroform and nitromethane. The coil seems to be less flexible than native amylose, with the additional possibility of some helical character. Valuable information on the fine structure of amylose can be gained from its sedimentation behaviour. Very few such measurements have been made to date. A detailed investigation into the sedimentation velocity behaviour of amylose is therefore presented in Section 5.

Amylopectin:- Methylation studies and latterly periodate

oxidations have indicated the structure of amylopectin to be mainly α-1,4 linked glucose units with some α-1,6 linkages, to form a complex branched structure, with an average chain length, $\overline{C.L.}$ of ca 25 anhydroglucose units (Thomson and Wolfrom, 1951). There is some evidence for 1,3 and 1,2 branch points, but this has not been confirmed (Manners and Mercer, 1963).

Three possible structures due to Haworth et al. (1937), Staudinger and Husemann (1937) and Meyer (1940a) were proposed for amylopectin and are shown in Fig. 1. By successive use of β-amylase and R-enzyme, Peat et al. (1952) were able to assign Meyer's structure as the most probable for amylopectin.

The β-amylolysis limit of amylopectin is generally about 55% and is a measure of the external chain length (Greenwood and Thomson, 1962), but this can vary with source (Whelan, 1958) and maturity (McKenzie, 1964). The 'tree-like' structure of amylopectin also has an internal chain length, which may be calculated as ca 9 anhydroglucose units.

The presence of esterified phosphate at C_6 of the glucose unit was first noted by Posternak (1935) in root starches. This phosphate is chiefly associated with amylopectin (Schoch, 1942) and confers some unusual solution properties on the polysaccharide. Ionic repulsion by the charges associated with the phosphate groups, confer an 'expanded' conformation on the amylopectin molecule in aqueous solution. The presence of neutral salt neutralises this charge effect, subsequently contracting the molecule. This 'pseudo-polyelectrolyte' behaviour is exemplified in the sedimentation and

FIG 1

Haworth

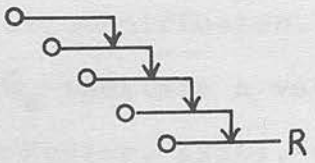

Staudinger

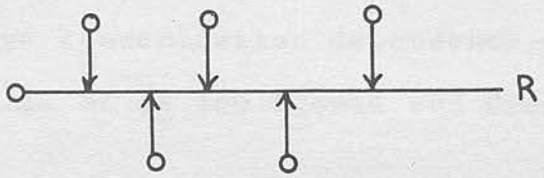

Meyer

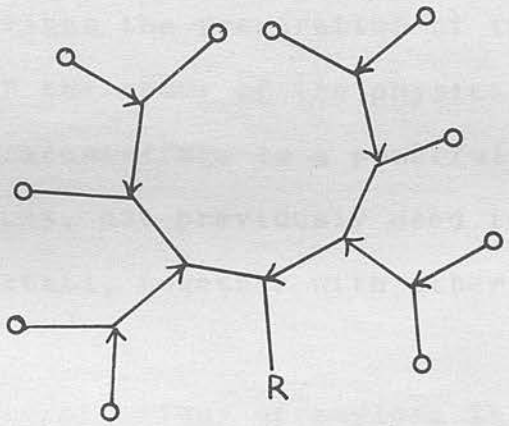

R reducing end group

o non-reducing end group

↓ α-1,6 link

viscosity measurements of Jones (1959).

Molecular weight determination of various acylated derivatives by osmotic pressure have indicated 10^5-10^6 (Greenwood, 1956). However, many higher values - up to 10^8 - have been obtained by light-scattering and sedimentation-diffusion. The wide variety of results between $\overline{M}_n$ and $\overline{M}_w$ indicate a very large molecular weight distribution (Stacy and Foster, 1956), which is exemplified by sedimentation analysis. Spurious molecular weights may be obtained, due to aggregation of the complex branched structure - suggested by the large concentration dependence during sedimentation, and a $[\eta]$ -value of ca 150 (Cowie and Greenwood, 1957).

Outline of Thesis:- In this thesis, some of the outstanding problems in the fine structure of amylose are studied in detail, and Section 1 describes the preparation of the samples used in the investigation. In the study of the physical properties of macromolecules, the ultracentrifuge is a powerful tool. Several ultracentrifuge techniques, not previously used in these laboratories, are described in detail, together with other experimental methods, in Section 2.

The viscometric behaviour of amylose in aqueous solution is considered in Section 3, with particular reference to the changes in viscosity with solvent power. In Section 4, subfractions of amylose are considered - first with respect to the existence of an 'anomalous' amylose, and secondly with respect to the hydrodynamic behaviour of the molecule in aqueous solution.

Section 5 deals with the sedimentation velocity of amylose in

various solvents. In the course of this study, the sedimentation coefficient was found to be dependent on the applied force field - this phenomenon is also investigated in this section.

Finally, the existence of a third component, other than amylose or amylopectin, is considered in Section 6. Attempts are made to isolate this component and determine its structure. This work is further complimented with a detailed analysis of amylose subfractions containing the 'anomalous' amylose.

SECTION 1

THE PREPARATION OF SAMPLES

1A. THE ISOLATION AND FRACTIONATION OF POTATO STARCH

Potatoes (var. Pentland Crown), kindly supplied by the Scottish Plant Breeding Station, Roslin, Midlothian, were harvested in October 1962 and October, 1963. Starch was isolated and fractionated by the method of Banks and Greenwood (1959) and was stored at $2^{o}C$ in a distilled water suspension layered with toluene (see Table 1.1).

Amylose was stored as the butan-1-ol complex, in water saturated with butan-1-ol, at $2^{o}C$. Amyloses were characterized by their intrinsic viscosity number, $[\eta]$ in 0.15M KOH, and by their β-amylolysis limits. These values were found to be constant for each preparation, but varied slightly for the two crops. The reason for this may lie in the different maturity of the potato tubers (McKenzie, 1964).

Amylopectins were characterized by their iodine affinities (Anderson and Greenwood, 1955) and β-amylolysis limits.

TABLE 1.1

The fractionation scheme for starch

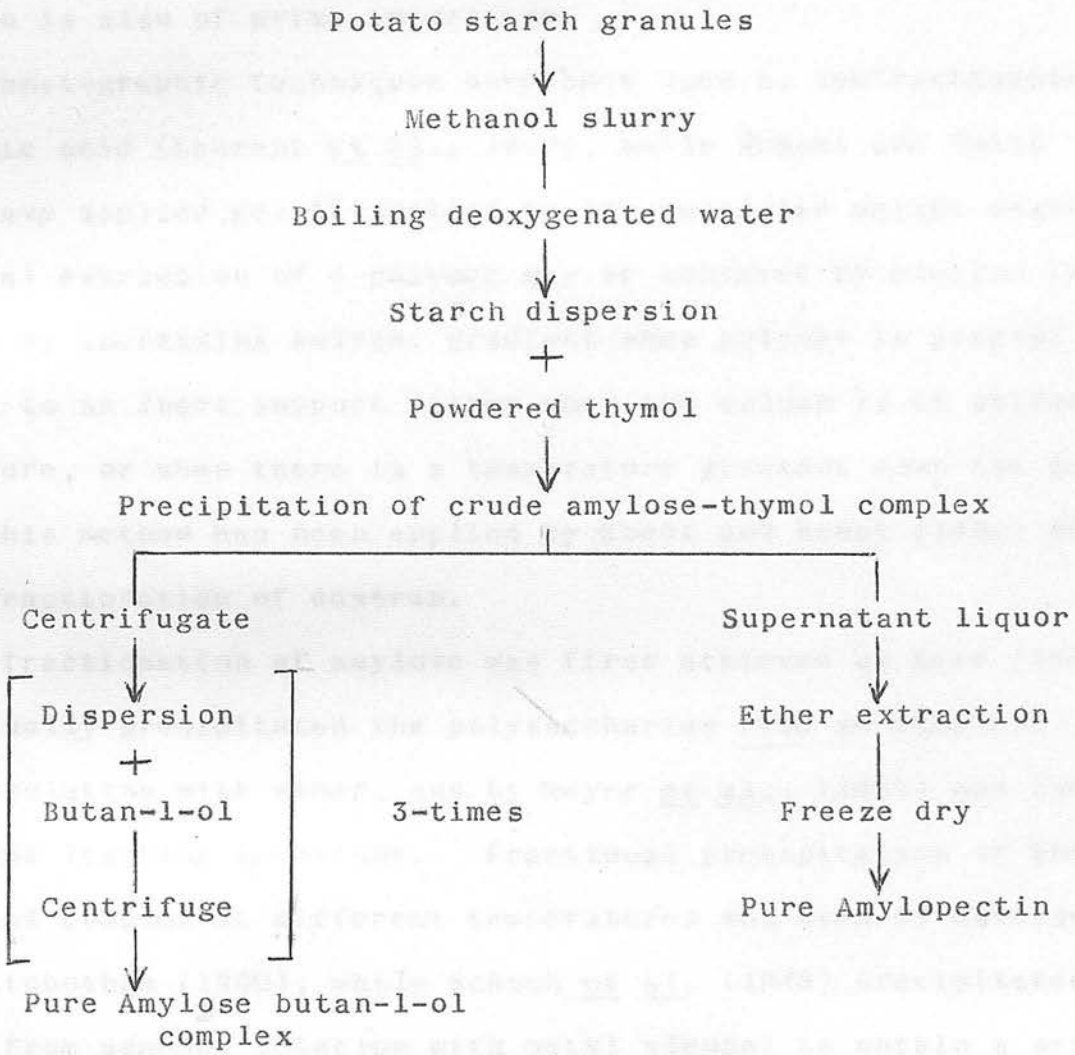

1B. THE SUBFRACTIONATION OF AMYLOSE

For the hydrodynamic study of a polymer, it is essential to have a series of narrow molecular weight fractions. This can be particularly difficult in the polysaccharide field, where broad and heterogeneous molecular weight distributions are often encountered. The elimination of possible degradation during subfractionation is also of prime importance.

Chromatographic techniques have been used to subfractionate hyaluronic acid (Laurent *et al.*, 1960), while Hummel and Smith (1962) have applied gel filtration to low molecular weight dextran. Fractional extraction of a polymer may be achieved by elution from a column by increasing solvent gradient when polymer is precipitated on to an inert support either when the column is at uniform temperature, or when there is a temperature gradient down the column. This method has been applied by Ebert and Ernst (1962) to the subfractionation of dextran.

Subfractionation of amylose was first achieved by Kerr (1945) who gradually precipitated the polysaccharide from an ethylenediamine solution with ether, and by Meyer *et al.*, (1949) who used an aqueous leaching technique. Fractional precipitation of the butan-1-ol complex at different temperatures was used by Goodison and Higginbotham (1950), while Schoch *et al.* (1949) precipitated amylose from aqueous solution with octyl alcohol to obtain a series of subfractions. However, these methods were either experimentally difficult or inefficient, and often produced degraded fractions. These and other methods have been critically examined by

Jones (1959). The most efficient subfractionation procedure to date involves precipitation from a dimethyl sulphoxide (DMSO) solution of dry amylose by the stepwise addition of ethanol at $4^{o}C$, and was first described by Everett and Foster (1959).

EXPERIMENTAL

The subfractionation of amylose was achieved by the method of Everett and Foster (1959). Fractions, which appeared as a clear gel, were collected on a Sharples super centrifuge, and hardened with ethanol. The ethanol precipitates were dispersed in hot de-oxygenated water with vigorous stirring in a nitrogen atmosphere, and reprecipitated as butan-1-ol complexes. A series of 14 fractions (P-series) were collected by this method, and their properties are examined in Sections 3C, 3D and 4A.

Several modifications were later made to Everett and Foster's method; (a) the amylose butan-1-ol complex was dissolved directly in DMSO, thus avoiding possible degradation to amylose during the drying procedure. (b) Subfractionation appeared as efficient at room temperature as at $4^{o}C$. (c) Fractions of a narrower molecular weight distribution were obtained if primary fractions were redissolved in more DMSO and refractionated. A variation in the precipitant was also tried, and fraction series with acetone (PA-series), ethanol (PE-series) and benzene (PB-series) were obtained (Table 1.2). The precipitation curves for these fraction series are shown in Fig. 1.1, and indicate that the efficiency of fractionation is in the order acetone > ethanol > benzene. With acetone, fractions of approximately equal weight were easily obtained by regular additions of the non-solvent, but the nature of the benzene precipitation curve is such that a major part of the amylose was precipitated on the first addition of non-solvent. The properties of these fractions are critically examined in Section 4A.

TABLE 1.2

Subfractionation of potato (var. Pentland Crown) amylose by precipitation from dimethylsulphoxide solution

Acetone[a]			Ethanol[a]			Benzene[a]		
Fraction	% non-solvent	%[c]	Fraction[b]	% non-solvent	%[c]	Fraction[b]	% non-solvent	%[c]
PA1	40.7	17.1	PE1a	44.6	10.6	PB1a	37.0	23.9
PA2	42.1	13.2	PE1b	45.0	9.7	PB1b	37.3	2.8
PA3	43.1	16.1	PE1c	45.3	6.4	PB1c	38.5	25.0
PA4	44.7	20.2	PE2a	44.8	15.5	PB1d	41.6	14.2
PA5	45.9	4.1	PE2b	45.5	3.6	PB2	38.4	8.5
PA6	47.8	16.1	PE2c	50.0	5.9	PB3	39.6	11.9
PA7	55.2	13.1	PE3	48.2	32.0	PB4	41.1	2.3
			PE4	60.5	16.1	PB5	46.8	11.4

a) Precipitant

b) a, b, c, d represent refractionated products

c) Expressed as the percentage of total amylose recovered.

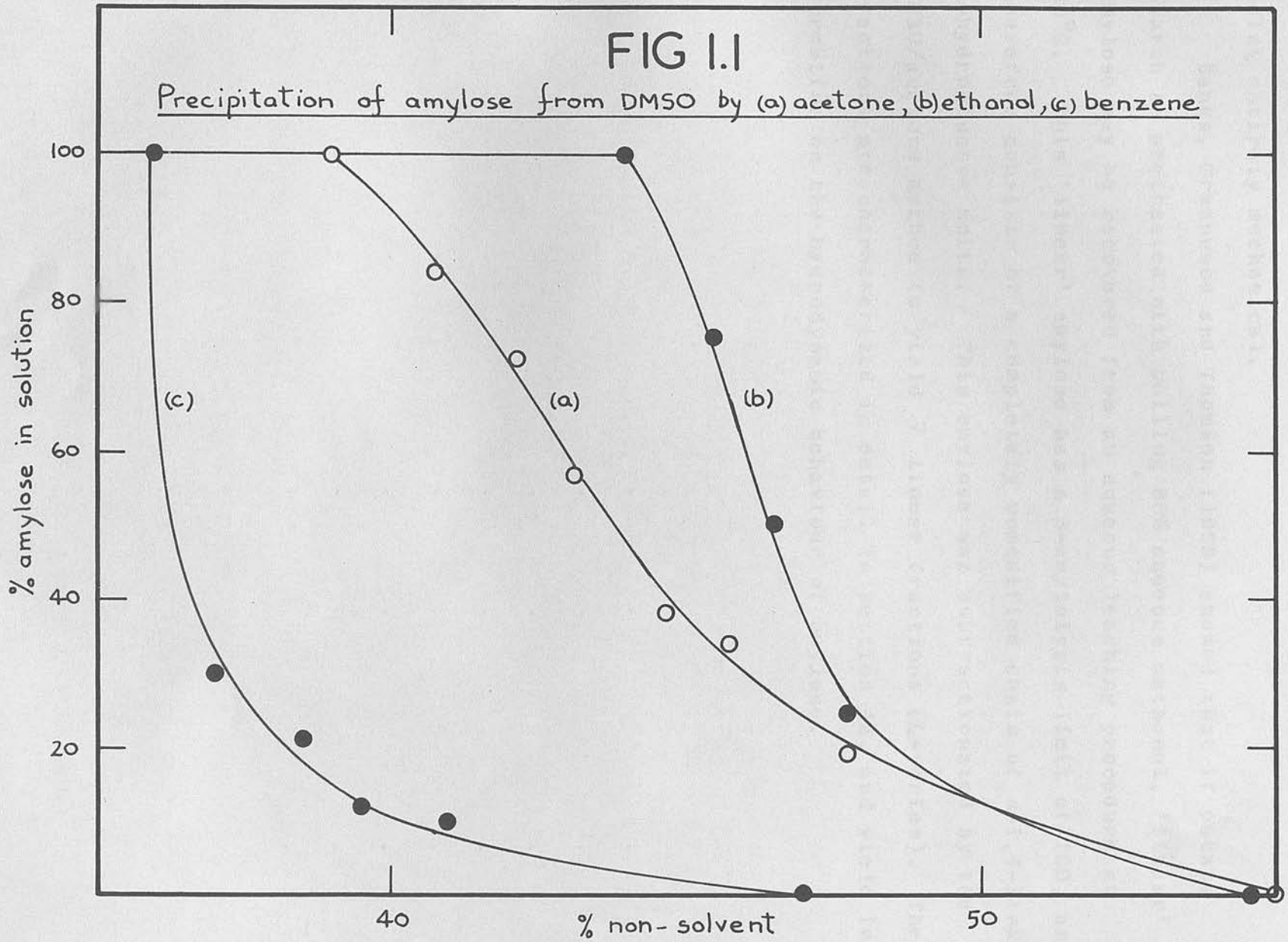
FIG 1.1
Precipitation of amylose from DMSO by (a) acetone, (b) ethanol, (c) benzene
% amylose in solution
100
80
60
40
20
(c)
(a)
(b)
40
% non-solvent
50

The percentage recovery with these procedures was ca 90%; losses being entirely mechanical.

Banks, Greenwood and Thomson (1959) showed that if potato starch is pretreated with boiling 80% aqueous methanol, 'linear' amylose may be recovered from an aqueous leaching procedure at 60°C. This 'linear' amylose has a β-amylolysis limit of 100, and therefore consists of a completely unmodified chain of α-1,4-linked anhydroglucose units. This amylose was subfractionated by the DMSO/acetone method to yield 7 linear fractions (L-series). These fractions are characterized in detail in section 4B, and yield information on the hydrodynamic behaviour of amylose.

SECTION 2

EXPERIMENTAL METHODS

2A. CAPILLARY VISCOMETRY

One of the most characteristic properties of a polymer is its ability to increase the viscosity of the medium in which it is dissolved. The extent of this viscosity increase reflects, in general, the molecular size and shape of the dissolved polymer, and provides a quick and simple method of comparing a series of samples. Precision viscometry has been reviewed in detail by Öhrn (1958).

Definitions:- The relative increase in viscosity

$$\eta_{sp} = \eta_{rel} - 1 = \frac{\eta - \eta_o}{\eta_o}$$

where η and η_o are the solution and solvent viscosities respectively. Since the viscosity of a solution depends on the concentration of the polymer, c, it is usual to extrapolate viscosity values to infinite dilution, and obtain the limiting viscosity number

$$[\eta] = \lim_{c \to o} (\eta_{sp}/c) \qquad 2.1$$

The limiting viscosity number, or Standinger index, has the dimensions of reciprocal concentration. Throughout this thesis, concentrations were expressed in units of gm ml^{-1} as recommended by I.U.P.A.C. (J.Polymer Sci., 8, 257, 1952).

Viscosity and Concentration:- Huggins (1942) suggested the relation

$$\eta_{sp}/c = [\eta] + k [\eta]^2 c \qquad 2.2$$

Here η_{sp}/c is a linear function of c, and $[\eta]$ is easily obtained by extrapolation. Relations by Martin (1942) and Schulz and Sing (1945) have also been suggested, but it is generally accepted that at low concentrations, Huggin's equation is most appropriate. The theoretical significance of the Huggin's constant k is uncertain, but recently Gillespie (1963) has shown it to be related to molecular entanglement.

Viscosity and Solvent:- For a given polymer, the limiting viscosity number depends on the nature of the solvent (Alfrey et al., 1942). In thermodynamically "good" solvents, where the polymer is contained in an energetically favourable environment, polymer-polymer interactions are small, allowing a linear polymer like amylose to take up an extended conformation, leading to a high $[\eta]$ -value. Conversely, in a thermodynamically "poor" solvent, polymer-polymer interactions promote a compact shape, and hence a low $[\eta]$ -value.

Viscosity and Shear:- The measurement of viscosity involves the measurement of a flow property of the solution. During this measurement, a shearing force is necessarily applied to the solution under study. In a capillary viscometer, where the viscosity of a fluid is measured from the time required for a fixed volume to flow through a capillary tube, the fluid is subjected to a tangental shearing force against the walls of the capillary (Fig. 2.1). Similar shearing forces exist with a rotating or Couette viscometer (Fig. 2.2). The viscosity of liquids like water or butan-1-ol is independent of such effects, and are termed Newtonian liquids.

FIG 2.1

Telescopic shear

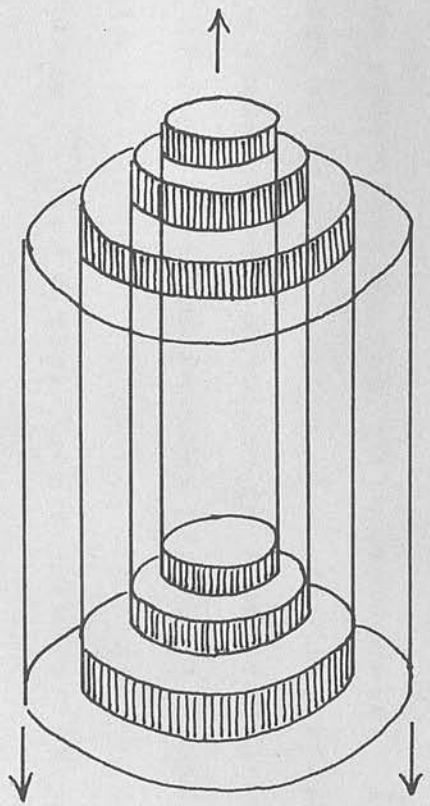

FIG 2.2

Rotational shear

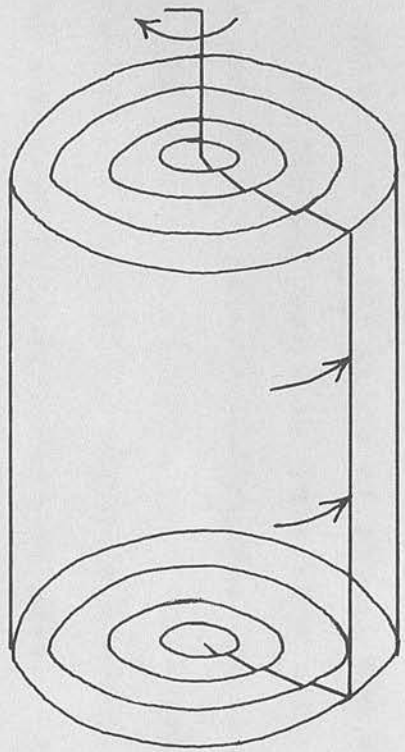

However, the apparent viscosity of most polymer solutions is dependent on shear stress (or rate of shear), and such solutions are said to be non-Newtonian. This behaviour is due to the increasing orientation of the molecules in the direction of flow opposing the effect of Brownian motion. At low rates of shear, the molecules are orientated nearly at random, and thus interfere with the motions of their neighbours and of the solvent molecules. As they line up more and more under the influence of flow, this interference becomes less and less, and hence the viscosity, which is a measure of the internal friction of the solution, also becomes less. For any given shear rate, the effect is greater, the higher the concentration, and the longer the polymer molecule. By definition, intrinsic viscosity is free from the influence of polymer-polymer interactions, but as polymer solvent interactions persist down to infinite dilution, the value of $[\eta]$ derived from measurements of the viscosities of solutions at finite concentration, may depend on the conditions of flow prevailing during the measurements. $[\eta]$ -values therefore, although quite satisfactory in a relative sense, must be corrected to zero shear, if any absolute or theoretical conclusions are to be drawn, (for details see reviews by Peterlin and Copic, 1956; Yang, 1961).

The shear stress τ for a capillary viscometer is given by:

$$\tau = hdg\, {}^{R}/_{2L} \text{ dynes cm}^{-2} \qquad 2.3$$

where d = liquid density
R = capillary radius
L = capillary length
h = driving head of liquid

$h = (m_1 - m_2)/\ln(m_1/m_2)$ for cylindrical bulbs, where m_1, m_2 are respectively, the initial and final distance between the top of the liquid level and the lower end of the capillary. The average shear rate $\bar{G}$ is given by

$$\bar{G} = \tau/\eta \ \text{sec}^{-1}$$

where η is the viscosity of the liquid.

Viscosity and Molecular weight:- The most generally used empirical relation is that put forward by Kuhn (1934) and Mark (1938) -

$$[\eta] = K_1 M^a \qquad 2.4$$

where $a = 1$.

Houwink (1940) later confirmed its validity for $0.5 < a < 0.8$. K_1 and a are constants for a given solvent-polymer pair, a determining the flexibility of the dissolved polymer -

a = 0 for rigid spheres

= 0.5-0.8 for flexible polymer chains

= 0.9-1.2 for stiff polymer chains

= 1.7-2 for rigid ellipsoids and rods.

- Yang (1961).

Perhaps the most widely accepted theoretical approach to the problem is that developed by Flory and Fox (1949, 1950, 1951). They proposed that at a temperature "Θ" in a thermodynamically poor

solvent, a linear polymer molecule assumes its "unperturbed" dimensions. Thus a Θ-solvent and a Θ-temperature, which usually coincides with the precipitation temperature, are defined. The unperturbed root-mean-square end-to-end distance $(\overline{r_o^2})^{\frac{1}{2}}$, is related to that in a "better" solvent (i.e. where the solvent power is greater) by an expansion factor α

$$(\overline{r^2})^{\frac{1}{2}} = \alpha(\overline{r_o^2})^{\frac{1}{2}} \qquad 2.5$$

It was further shown that

$$[\eta] = K' M^{\frac{1}{2}} \alpha^3 \qquad 2.6$$

where $K' = \phi(\overline{r_o^2}/M)^{3/2}$, M = molecular weight, and ϕ is a universal constant = 2.1×10^{23} c.g.s. units. In particular, at Θ conditions $[\eta]_\Theta = K' M^{\frac{1}{2}}$ 2.7

Details of other polymer theories can be found in the review by Banks and Greenwood (1963a). In a recent refinement of the Flory-Fox theory, Stockmayer and Fixman (1963) show

$$[\eta] = K' M^{\frac{1}{2}} + 0.51 \phi BM \qquad 2.8$$

where ϕ now has a revised value of ca 2.8×10^{23} c.g.s. units, and B is a polymer-solvent interaction parameter.

Polymer theory for branched macromolecules (e.g. amylopectin) is less well developed and somewhat empirical (Banks and Greenwood, 1963a).

Most polymers, particularly natural polymers, have a broad distribution of molecular weight (polymolecular systems). Such a

distribution may be symmetrical (monodisperse) or skew (polydisperse). In some instances, a natural polymer may consist of a mixture of two or more discrete types of molecules, whose molecular weight distributions overlap (paucidisperse), or whose distributions do not overlap (heterogeneous). In measuring the molecular weight of a polymer, therefore, an average value is obtained depending on the method employed. If n_i and M_i are the number and molecular weight of species i, then the number average molecular weight ($\bar{M}_n$) and the weight average molecular weight ($\bar{M}_w$), are defined as

$$\bar{M}_n = \frac{\sum n_i M_i}{\sum n_i} \qquad 2.9$$

$$\bar{M}_w = \frac{\sum n_i M_i^2}{\sum n_i M_i} \qquad 2.10$$

$\frac{\bar{M}_w}{\bar{M}_n}$ ($\geqslant 1$) is a measure of polydispersity and equals unity for a monodispersed polymer. Flory (1943) defined the molecular weight average derived from viscosity measurements as

$$\bar{M}_v = \left[\frac{\sum n_i M_i^{1+a}}{\sum n_i M_i}\right]^{1/a} \qquad 2.11$$

where a is the exponent in the Mark-Houwink equation (equation 2.4). $\bar{M}_v$ is closely approximated by $\bar{M}_w$, which is the molecular weight average normally employed in polymer theory.

EXPERIMENTAL

Viscosities were measured in modified Ubbelohde suspended-level viscometers (Fig. 2.3) which were rigidly supported in a bath thermostatted at 25.00 ($\pm$ 0.01°C). In such a viscometer, the viscosity is given by

$$\eta = A\rho t - \frac{B\rho}{t} \qquad 2.11$$

where A and B are constants, ρ is the density of the fluid, and t the flow time of a fixed volume of liquid. The dimensions of the viscometers were such that the kinetic energy correction, $B\rho/t$, was negligible and the average shear rate calculated from equation 2.3 was $\bar{G}$ = ca 1200 sec^{-1}.

Hence $\eta = A\rho t$ for the solution

and $\eta_o = A\rho_o t_o$ for the solvent.

The specific viscosity is therefore given by

$$\eta_{sp} = \frac{\rho t - \rho_o t_o}{\rho_o t_o}$$

Since only dilute polymer solutions are concerned, $\rho \simeq \rho_o$ and therefore

$$\eta_{sp} = \frac{t - t_o}{t_o}$$

Procedure:- This was essentially the method described by Greenwood (1964), for the amylose-butan-1-ol complex in alkali.

Viscosity of Amylose:- In practice, the use of the butan-1-ol complex rather than the dried form of amylose has several advantages. The complex is more easily soluble - even in neutral solution, and

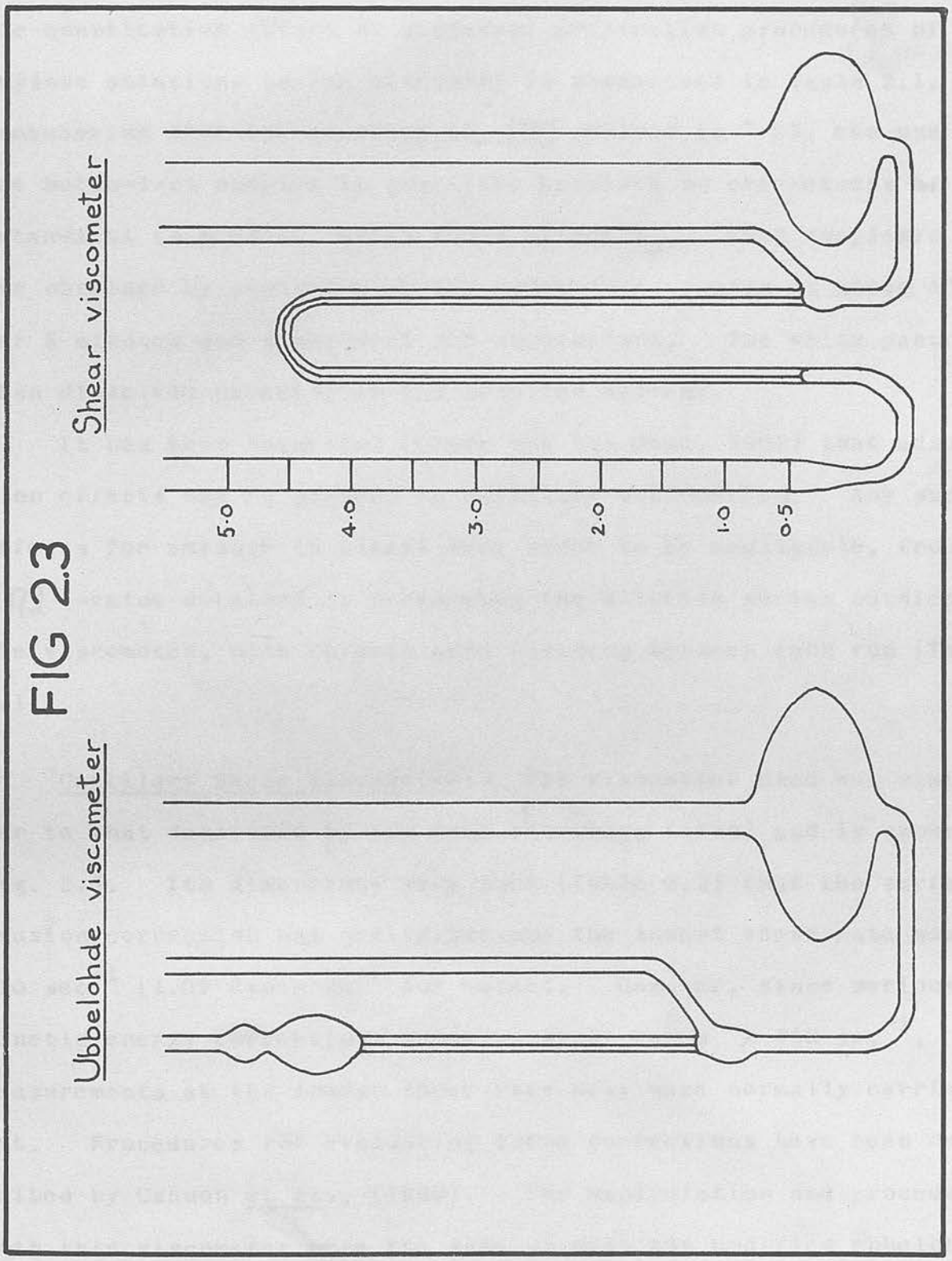

FIG 2.3

the possible degradation during the drying procedure is avoided. The quantitative effect of different preparation procedures of amylose solutions on the viscosity is summarised in Table 2.1. Remembering that the accuracy of $[\eta]$ -values is $\pm$ 2%, the use of the butan-1-ol complex is justified provided no over-excess of butan-1-ol is present, which would affect t_o. Such complexes are obtained by centrifuging the butan-1-ol complex at about 1000g for 5 minutes and discarding the supernatant. The white paste is then dissolved directly in the required solvent.

It has been suggested (Cragg and Van Oene, 1962) that adsorption effects may be present in capillary viscometers. Any such effects for amylose in alkali were shown to be negligible, from the $[\eta]$ -value obtained by performing the dilution series outside the viscometer, with chromic acid cleaning between each run (Table 2.1).

Capillary Shear Viscometer:- The viscometer used was similar to that described by Van Oene and Cragg (1962) and is shown in Fig. 2.3. Its dimensions were such (Table 2.2) that the surface tension correction was negligible and the lowest shear rate was 110 sec^{-1} (1.09 dynes cm^{-2} for water). However, since serious kinetic energy corrections arose at shear rates $>$ 110 sec^{-1}, measurements at the lowest shear rate only were normally carried out. Procedures for evaluating these corrections have been described by Cannon et al., (1960). The manipulation and procedure with this viscometer were the same as with the modified Ubbelohde type.

TABLE 2.1

The effect of butan-1-ol on $[\eta]$ of two amylose samples

Isolation procedure of amylose butan-1-ol complex	$[\eta]$ a)	k b)
Centrifuged 5 min. at 10^3g.	270	0.36
Centrifuged 30 min. at 10^3g.	260	0.38
Centrifuged 20 min. at 10^4g.	260	0.37
Dry sample	260	0.35
External dilution	255	0.35
Excess butan-1-ol present	970	0.42
No centrifugation	760	0.43
Centrifuged 5 min. at 10^3g.	730	0.40
Dry sample	730	0.40

a) Determined in 0.15M KOH

b) Huggin's constant.

TABLE 2.2

Dimensions of capillary shear viscometer (see fig. 2.3)

Mark	H[a] cm.	τ[b]	$\bar{G}$[c]
5.0	19.35	-	-
4.0	15.33	13.1	1380
3.0	11.13	9.90	1040
2.0	6.93	6.70	700
1.0	2.73	3.40	360
0.5	0.63	1.09	110

a) Height above capillary outflow

b) Calculated shear stress in dynes cm^{-2}

c) Calculated average shear rate in sec^{-1}.

2B. ROTATIONAL VISCOMETRY

The first practical rotational viscometer was that designed by Couette (1890). Couette's concentric-cylinder viscometer consisted of a rotating cup and an inner cylinder which was supported by a torsion wire and rested in a point bearing at the bottom of the cup. As the outer cup revolved, a twisting moment was applied to the inner cylinder through the intervening fluid under study. The magnitude of this moment was balanced by the torsion in the wire, which was measured, and enabled Couette to calculate the apparent viscosities of non-Newtonian fluids. Since 1940, many designs have appeared, (Ogston and Stanier, 1953; Zimm and Crothers, 1962; Kay and Saunders, 1964), some of which are available commercially (Van Wazer et al., 1963).

Couette Viscometers have several advantages over capillary instruments; the rate of shear (G) applied to the fluid, can reach far lower limits ($G < 1$ sec^{-1}) and corrections due to surface tension and kinetic energy are absent in a Couette instrument.

Theory:- The theory of rotational viscometry has been detailed by Van Wazer et al. (1963). In outline, if R_b and R_c are the radii of the bob and the cup respectively, then the rotating couple on the bob is given by

$$c\Theta = \frac{4\pi l \eta w}{(1/R_b^2 - 1/R_c^2)} \qquad 2.13$$

c = couple per unit angular displacement

θ = angular displacement of bob (radians)

ℓ = length of torsion wire

η = absolute viscosity of the fluid

w = cup speed in radians sec^{-1}

whence $\theta = (K''\ell)w\eta$ 2.14

and $K''\ell$ is a calibration constant for the instrument.

The velocity gradient in the liquid, contained in the annular gap between the bob and cup, at a distance r from the axis of rotation is given by

$$\frac{dv}{dr} = 2w \frac{1/r^2}{(1/R_b^2 - 1/R_c^2)} \qquad 2.15$$

The mean velocity gradient which equals the average shear rate, $\bar{G}$, is given by

$$\left(\frac{dv}{dr}\right)^{mean} = 2w \frac{R_c R_b}{R_c^2 - R_b^2} \qquad 2.16$$

$\bar{G}$ has the dimensions of sec^{-1} and is related to shear stress τ by

$$\tau = \eta \bar{G} \text{ dynes cm}^{-2} \qquad 2.17$$

Newtonian and non-Newtonian behaviour may be detected from a plot of η vs. $\bar{G}$. In the former case η is independent of $\bar{G}$, but in the latter case, which is typical of polymer solutions, η generally increases as $\bar{G}$ decreases.

Instrument and Calibration:- An instrument similar to that described by Ogston and Stanier (1953) was kindly constructed by Mr. G. Newall, Animal Genetics Department, Edinburgh University. A schematic diagram of the viscometer is shown in Fig. 2.4. The cup was thermostatted at 25°C by circulating water from a thermostat tank. Constant speeds of revolution were achieved by connecting the cup through a continuous thread to a synchronous motor via a multispeed gear box. The dimensions of the instrument were such that the speed of the cup (w) in revolutions per minute equals twice the average rate of shear ($\bar{G}$) in sec^{-1}. Speeds of 1-100 r.p.m. were possible, corresponding to $\bar{G}$ = 0.5-50 sec^{-1}. Above this speed turbulance in the solution under examination usually set in, leading to erratic deflections. Deflections (Δ), corresponding to the angular deflection (θ) of the bob, were measured by arranging the galvanometer mirror to project an image of a vertical hair line on to a hemi-circular scale at its focal length (100 cm.). The scale was made by bending a plastic strip, 100 cm. long, and marked in millimeters, into a hemi-circle of 100 cm. radius. After much experimentation, the following modifications to Ogston and Stanier's instrument were found essential to maintain steady and reproducable readings: (a) a non-magnetic bob of gold plated brass was found superior to stainless steel, readings being steady and unaffected by the slightly magnetised bearings in the cup. (b) a perspex box to exclude draughts was made to fit round the tortion wire and damping assembly. (c) Diala oil B (Shell) was found to be superior as an inert damping fluid. Readings were read to the nearest

FIG 2.4

COUETTE VISCOMETER

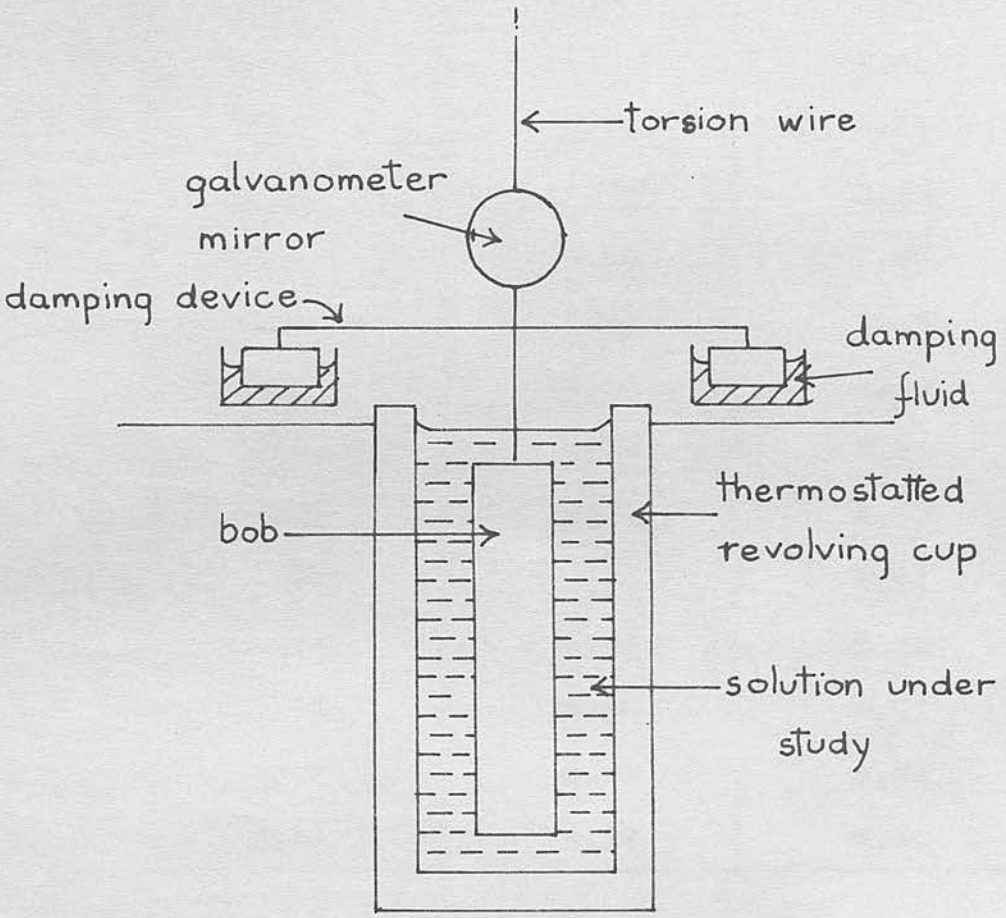

TABLE 2.3

Calibration of the Couette viscometer

$S^{a)}$ r.p.m.	$\Delta^{b)}$ cm.	$\eta^{c)}$ calc.
49.0	12.3	8.94
41.8	10.4	8.86
34.0	8.52	8.93
29.7	7.39	8.86
24.1	6.08	8.99
19.5	4.85	8.88
13.7	3.48	9.05
11.0	2.66	8.61
9.50	2.38	8.92
3.24	0.81	8.91
2.21	0.55	8.87
1.39	0.34	8.71
1.07	0.30	9.98
0.74	0.18	8.66

a) $\omega = S \times 2\pi/60$ rads.sec^{-1}

b) $\theta = \Delta \cdot 10^{-2}$ rads.

c) Calculated from equation 2.18.

0.01 cm., and were steady to 0.02 cm.

The instrument was calibrated with de-ionised distilled water. Redistilled butan-1-ol was also used as a secondary standard (Table 2.3). By plotting Θ vs. w, and knowing the absolute viscosity of water, the calibration constant $K''\ell$ in equation 2.14 was determined. The following calibration equation was thence derived for this instrument at 25°C:-

$$\eta = \Delta/_s \times 35.6 \text{ millipoises} \qquad 2.18$$

where Δ = deflection in cm.

s = cup speed in r.p.m.

From the standard deviation, viscosity values were found to be accurate to $\pm$ 1%.

EXPERIMENTAL

The cup was carefully levelled with the aid of a sensitive inclinometer. 10 ml. of amylose solution were pipetted into the cup and left for ca 30 minutes to attain the temperature of the circulating thermostat. As greater precision is obtained with a viscous fluid, concentrated amylose solutions were always prepared. The bob was carefully lowered and centred by eye, and the draught excluder fitted. The zero reading was noted. Readings at several speeds, which were found by timing revolutions of the cup with a stop-watch, were taken for each concentration. Concentrations at C, $^4/_5$C, $^2/_5$C, $^1/_5$ C were achieved by withdrawing volumes of solution from the cup and replacing with an equal volume of solvent. Throughout, care was taken to see that no bubbles were introduced in the annular gap between the bob and the cup. Between each dilution, the solution in the cup was stirred with a glass rod, and the solvent kept in the thermostat bath so that temperature equilibrium was achieved quickly. The solvent alone was also run in the viscometer.

The absolute viscosity, η , of the solutions was plotted against the rate of shear G, and extrapolated to zero G to yield η^o, the viscosity at zero rate of shear. η^o_{sp} values were calculated and from a plot of η^o_{sp}/C vs. C (Huggins, 1942), $[\eta]^o$ values were obtained. $[\eta]^o$, the intrinsic viscosity number at zero shear, is accurate to $\pm$ 2% for high viscosity amylose samples. This accuracy however, decreases markedly with smaller viscosity amylose samples, and $[\eta]^o$ values below ca 200 are uncertain. Concentra-

tions of amylose solutions were determined by the alkali ferricyanide method (Lampitt et al., 1955) in triplicate. Since the amylose solutions were usually concentrated, 0.5 ml. samples were taken for analysis instead of the normal 1 ml. samples.

2C. ULTRACENTRIFUGE - SEDIMENTATION VELOCITY

The idea of a high speed centrifuge to create force fields, sufficiently high to sediment colloidal particles in solution, was first exploited by Svedberg and Nichols (1923). The development of this technique, and its application to polymers, has been discussed by Svedberg and Pederson (1940), and the recent advances reviewed in monographs by Schachman (1959) and Williams (1963).

Theory:- The sedimentation coefficient, S, is the rate of movement of the macromolecules per unit force field, i.e.

$$S = \frac{1}{w^2 x} \cdot \frac{dx}{dt} = \frac{1}{w^2} \cdot \frac{d(\ell n\, x)}{dt} \qquad 2.19$$

where w is the angular velocity. The sedimentation coefficient usually depends on the concentration of macromolecules in solution, c, and hence S-values have to be extrapolated to infinite dilution. The limiting value, S_o, is achieved by an empirical plot of S^{-1} vs. c, where $S = \frac{S_o}{1 + k'c}$, (Gralén, 1944).

Sedimentation and Molecular Weight:- S_o is related to the molecular weight (M) of the macromolecules by Svedberg's equation,

$$M = \frac{RT\, S_o}{(1 - \bar{V}\rho) D_o} \qquad 2.20$$

where R = gas constant

T = absolute temperature

D_o = diffusion coefficient at infinite dilution

$\bar{V}$ = partial specific volume of the solute

ρ = density of the solution.

$\bar{V}$ may be easily measured by pyknometry, but D_o is usually quite difficult to obtain. Because of this, and the fact that the molecular weight obtained corresponds to none of the usual molecular weight averages, the equation is seldom used in this form.

To overcome these difficulties, Scheraga and Mandelkern (1953) proposed the equation

$$M = \left[\frac{N.\eta_o.S_o}{\beta(1 - \bar{V}\rho)}\right]^{3/2} . [\eta]^{1/2} \qquad 2.21$$

where N is Avagandro's number and β is a constant related to the axial ratio of the molecule (Ogston, 1953). This equation is more strictly valid for proteins. For flexible polymer chains, Mandelkern and Flory (1952) proposed

$$M^{2/3} = \frac{S_o\, N\, [\eta]^{1/3}.\eta_o}{\phi^{1/3}\, P^{-1}(1 - \bar{V}\rho)} \qquad 2.22$$

where $\phi^{1/3}P^{-1} = 2.5 \times 10^6$ c.g.s. units; η_o = solvent viscosity in c.g.s. units, and $[\eta]$ is in ml. gm^{-1}.

A similar relation to the Mark-Houwink equation (equation 2.4) exists for the sedimentation coefficient, i.e.

$$S_o = K_2 M^b \qquad 2.23$$

where K_2 and b are constant for a given polymer-solvent system (Flory, 1953). Wales and Rehfeld (1962) showed that by combining equations 2.4, 2.21 and 2.23, it can be shown that:-

$$b = \frac{2 - a}{3} \qquad 2.24$$

$$\text{and} \quad K_2 = \frac{1}{K_1^{1/3}\,\delta} \qquad 2.25$$

$$\text{where} \quad \delta = \frac{\eta_o . N}{\beta(1 - \bar{V}\rho)}$$

However, the validity of these relations for 'non-Θ' conditions is questionable.

EXPERIMENTAL.

A Spinco Model 'E' Ultracentrifuge, capable of speeds up to 60,000 r.p.m., and fitted with Schlieren optics was used for this work. During experiments, the temperature was kept constant by means of a Rotor Temperature Indicator and Control (RTIC) unit. Calibration showed that the temperature, T, was related to 'balance dial readings', R, by T = 33.12 - R(0.02085), (Table 2.4).

The Determination of Sedimentation Coefficients:- Photographs of sedimentation boundaries were taken at equal time intervals, and were measured by means of a micro-comparator. The absolute distance of the boundaries from the axis of rotation (x) were determined to the nearest 0.01 mm. S-values were calculated from the gradient of the line of least squares of the log x vs. time plot. The maximum ordinate of the Schlieren diagram was taken as the boundary position, but this is only true for symmetrical boundaries (Goldberg, 1953). However, the error involved is usually small (Williams et al., 1958).

S-values at several concentrations were measured through a dilution series to yield S_o-values which are accurate to ca. $\pm$ 2%.

Determination of the Square Root of the Second Moment Boundary Position:- For Schlieren patterns, which arise from skew molecular weight distribution, the true boundary position is defined by the square root of the second moment. At this point, the sedimenting macromolecules suffer displacement at unit time equal to that of those ahead. The calculation of this position,

TABLE 2.4

Calibration of the ultracentrifuge 'RTIC' unit

Temperature ^{o}C	Rheostat range	Balance dial readings
6.0	6	466
6.5	6	441
7.1	6	413
8.3	6	353
9.1	6	314
10.6	6	240
11.2	6	209
12.0	6	171
12.4	6	148
12.5	5	990
15.35	5	854
15.4	6	008
17.0	5	777
20.95	5	580
24.35	5	421

TABLE 2.5

Radius cubed scale (Z-scale)

Z $(10x/x_r)^3$	$Z^{1/3}/10$ x/x_r	$100Z^{-2/3}$ $(x_r/x)^2$	$x_r = 161.86$ mm x (mm)
500	0.793701	1.5874	128.55
520	804145	1.5464	130.16
540	814325	1.5080	131.81
560	824257	1.4719	133.41
580	833955	1.4376	134.98
600	843433	1.4059	136.52
620	852702	1.3753	138.02
640	861774	1.3464	139.49
660	870659	1.3191	140.93
680	879366	1.2932	142.33
700	887904	1.2684	143.72
720	896280	1.2447	145.07
740	904504	1.2223	146.40
760	912580	1.2008	147.71
780	920516	1.1802	149.00
800	928317	1.1604	150.26
1000	1.000000	1.0000	161.86

which is not only profitable, but frequently essential (Trautman et al., 1954), was by Trautman's method (1956).

A radius-cubed scale table was constructed as suggested by Trautman (1956), an abbreviated version of which is shown in Table 2.5. Here Z values from 500-800 are tabulated with their corresponding magnified values of x, which are measured in cm. from the axis of rotation on the photographic plate. x_r = 16.186 cm. was taken as the magnified distance of the outer reference line from the axis of rotation (7.300 cm. x 2.22). The x value 16.186 cm. was indexed on the comparator x scale, and the photographic plate then positioned such that the reference line coincided with the 'hair line'. x values in cm., corresponding to specific Z values, were then indexed on the comparator, and the corresponding Δy values were recorded in cm. to the nearest 0.001 cm. In this manner, the whole Schlieren boundary was traversed at Z increments of 4. Δy values were more easily determined if the sedimentation velocity experiment was carried out in a double sector cell, whence a correct 'base line' was present beneath the Schlieren peak. Each Δy value was multiplied by the corresponding $(x_r/x)^2$ value from the table, and the expression

$$\frac{\sum_{i}^{peak} (x_r/x_i)^2 \, \Delta y_i}{\sum_{i}^{peak} \Delta y_i} = (x_r/\bar{x})^2 \qquad 2.26$$

evaluated for $\bar{x}$, where $\bar{x}$ is the magnified distance of the square root of the second moment in cm. from the axis of rotation. This $\bar{x}$ value was then converted to an actual distance from the axis of

rotation, and the sedimentation coefficient evaluated in the usual manner. The position of this boundary and the corresponding S-value are weight average properties of the sedimenting polymer; whereas when the position of maximum ordinate is used to evaluate S, the sedimentation coefficient of the most abundant species only, is measured.

Determination of Heterogeneity:- The ultracentrifuge is most valuable in detecting heterogeneity in a polymer. This is apparent when two or more peaks are present in the Schlieren diagram, (although skew peaks also indicate incipient heterogeneity). The areas beneath the peaks have been related to the actual concentrations of components by Johnston and Ogston (1946). They showed that the apparent concentration of the slower component in a two-component system is enhanced at the expense of the faster. This effect is most prominent at high concentrations of the fast component, and when its concentration dependence of S (expressed by k') is large. Harrington and Schachman (1953) also showed this Johnston-Ogston effect to be more prominent when the S-values of the two components are similar. Trautman et al. (1954) have outlined a procedure for analysing a heterogeneous two-component system. They derived the equation

$$\frac{(\bar{x}_s^{obs}/x_m)^2 \, C_s^{obs}}{C_s^o} = \frac{(\bar{x}_f^{obs}/x_m)^{2(1-\Psi)} - 1}{(\bar{x}_f^{obs}/\bar{x}_s^{obs})^2 - 1} \qquad 2.27$$

where $\bar{x}$ = radial distance of the boundary

x_m = radial distance of the meniscus

C_s^o = actual concentration of the slower component

C_s^{obs} = observed concentration of the slower component

subscripts s and f refer to the slow and fast components respectively, and $\Psi = {}^{S}s/S_f$ at infinite dilution. In practice, the polymer system is examined at several concentrations, whence a value of Ψ may be obtained. By substitution in equation 2.27, C_s^o is determined and hence C_f^o. Other treatments of heterogeneous systems are detailed in Schachman (1959).

2D. ULTRACENTRIFUGE - SEDIMENTATION EQUILIBRIUM

If the ultracentrifuge operating speeds are sufficiently low (ca. 10,000 r.p.m.), sedimentation of the macromolecules may be balanced by their diffusion. The time taken to reach this equilibrium state may be impractically long. This disadvantage however, is offset in that sedimentation equilibrium theory, derived by thermodynamics (Young et al. 1954), is sound, and possesses none of the assumptions made in other ultracentrifugal analyses.

Theory:- At equilibrium the material migrating across a given surface in a centrifugal direction is exactly balanced by the transport centripetally due to diffusion, and the expression,

$$c\, Sw^2x = D\,(^{dc}/_{dx}) \qquad 2.28$$

where c is the concentration of the polymer, applies to all levels in the cell. Application of Svedberg's equation yields

$$M = \frac{2RT}{(1 - \bar{V}\rho)w^2} \cdot \frac{d(\ell n\, c)}{dx^2} \qquad 2.29$$

For a two-component system of homogeneous solute and a solvent this becomes

$$M = \frac{RT}{(1 - \bar{V}\rho)w^2} \cdot \frac{1}{xc}\,\frac{dc}{dx}\left(1 + \frac{cd(\ell n\, y)}{dc}\right) \qquad 2.30$$

where y is the activity coefficient of the solute on the c scale. If ideal behaviour is assumed, as is the case with many protein solutions, then

$$M = \frac{RT}{(1 - \bar{V}\rho)w^2} \cdot \frac{1}{xc} \cdot {}^{dc}/_{dx} \qquad 2.31.$$

Molecular weights may be calculated from the slope of the $\ell n\, c$ vs. x^2 plot, which may also yield information on the homogeneity of the sample. Plots which are concave upward indicate polydispersity, and those which are concave downward are an index of the non-ideality of the solution. Other methods of plotting the data have been suggested by Lamm (1929) - $\ell n({}^{1}/_{x})({}^{dc}/_{dx})$ vs. x^2; and Archibald (1947) - $({}^{1}/_{xc})({}^{dc}/_{dx})$ vs. x. However, all these methods are laborious when employing only one optical system.

However, if the position in the cell, where the concentration was equal to the original concentration c_o were known, the concentration gradient $({}^{dc}/dx)_o$ at this point could be determined and equation 2.30 evaluated for M. Van Holde and Baldwin (1958) showed that if very short solution columns were used (1 mm.), then this point corresponds closely to the midpoint of the column. Here the concentration is within 1% of the initial concentration if $H < 0.25$, where

$$H = w^2M(1 - \bar{V}\rho)(b^2 - a^2)/4RT \qquad 2.32$$

Even shorter columns were proposed by Yphantis (1960), where from equation 2.31, the molecular weight of ribonuclease in a 0.7 mm. column at 24,000 r.p.m. was determined. Short columns have the additional advantage that equilibrium times, which are proportional to the square of the column height, are drastically reduced; this, however, is at the expense of the precision and resolving power of longer columns. The molecular weight obtained by this method is a weight

average, and Yphantis (1960) also showed that a Z-average molecular weight $\overline{M}_z$ may be determined from the slope of a $^{dn}/_{dx}$ vs. x plot (n = refractive index) in a short column, but results were rather imprecise.

Recently Hermans (1964), Lütje (1964) and Yphantis (1964) have shown that various molecular weight averages may be assessed in a paucidisperse system, if the speed is chosen such that the concentration at the meniscus c_m is much less than that at the base, c_b. At equilibrium, the following relations apply,

$$\overline{M}_{w,x} = \frac{RT}{(1 - \overline{V}\rho)w^2} \cdot \frac{(^{dc}/_{dx})_x}{x.c_x} \qquad 2.33$$

$$\overline{M}_w = \frac{RT}{(1 - \overline{V}\rho)w^2} \cdot \frac{c_b}{x_b \int_m^b c_x.dx} \qquad 2.34$$

$$\overline{M}_n = \frac{RT}{(1 - \overline{V}\rho)w^2} \cdot \frac{{}_m\int^b c_x dx}{x_b \, {}_m\int^b \, {}_m\int^b c_x.dr.dr} \qquad 2.35$$

where the subscript x refers to the level in the cell at x cm. from the axis of rotation. Extrapolation of equation 2.33 to x = b gives $\overline{M}_z$.

Since, from equations 2.30 and 2.31, the apparent molecular weight, M_{app}, is

$$M_{app} = \frac{M}{(1 + c \frac{d(\ell n\, y)}{dc})} \qquad 2.35$$

true molecular weights for a non-ideal system may be obtained by plotting $1/M_{app}$ vs. c and extrapolating to infinite dilution. Thus

$$1/M_{app} = 1/\overline{M}_w + B.c \qquad 2.37$$

where B is a coefficient that equals the light-scattering virial coefficient (Kegeles et al., 1957).

EXPERIMENTAL

Equilibrium runs were made using the short column method of Yphantis (1960). The necessary low speeds were attained by means of a 6.4:1 stepdown gear box fitted to the ultracentrifuge drive unit. 12 mm. epoxy resin double sector cells were used. Into one sector was introduced ca 0.025 ml. of silicone oil to give a sharp base line to the column, and exactly 0.025 ml. of solution from an 'Agla' micrometer syringe. Ca. 0.1 ml. of pure solvent was put into the other sector. This procedure gave a liquid column of approximately 0.7 mm. An appropriate speed for the equilibrium run was chosen using equation 2.32. To determine the initial concentration, c_o, a synthetic boundary was used - an interference synthetic boundary centre piece, which used 0.15 ml. solution, was found the most satisfactory. To ensure that equilibrium had been reached in the short column run, photographs were taken at half-hour intervals; equilibrium was established when successive photographs were identical (by measurement). Using the solvent pattern as a base line, the magnified $(^{dc}/_{dx})$ value at the mid-point of the solution column, and its absolute distance from the axis of rotation, $\bar{x}$, were determined. The area beneath the synthetic boundary peak was measured and corrected for radial magnification, and is equal to c_o in area units if the bar-angle is kept constant throughout the experiment. The most suitable bar angle was found to be 80^o. For dilute solutions, $(^{dc}/_{dx})$ was magnified using a 30 mm. double sector cell and subsequently divided by $2\frac{1}{2}$ for the calculation. Values were substituted in

$$\overline{M}_w = \frac{RT}{(1 - \overline{V}\rho)w^2} \cdot \frac{1}{\overline{x}\, c_o} \cdot \left(\frac{dc}{dx}\right)_{x=\overline{x}} \qquad 2.38$$

which is equivalent to equation 2.31. With a lower speed limit of 2000 r.p.m., the upper molecular weight limit is ca 1.5 x 10^6, for 0.7 mm columns, by this technique.

The Molecular Weight of Sucrose:- To test the short column method in practice, the molecular weight of sucrose (M = 342), in a 2% aqueous solution, was measured. The results, using $\overline{V}$ = 0.618, are shown in Table 2.6,

Table 2.6

The molecular weight of sucrose by the short column equilibrium method

Speed r.p.m.	Equilibrium time min.	Column height mm.	$\overline{M}_w$ calc.
50,740	120	2.1	338
50,740	30	0.7	341

and are within the experimental accuracy of 3% quoted by Yphantis (1960).

The Molecular Weight of Amylolytic Enzymes:- Salivary α-amylase (kindly supplied by Professor W. J. Whelan) and crystalline sweet potato β-amylase (Worthington Biochem. Corp.) were used and the results are shown in Table 2.7. The pure solvent required for the synthetic boundary runs was taken as the dialysate, obtained

TABLE 2.7

The molecular-weight of some Amylolytic enzymes

Enzyme	Speed r.p.m.	Equilibrium time, hours	Column height, mm	$10^{-5} . \bar{M}_w$
α-amylase[a]	9,320	ca 3	0.7	0.35
"	12,560	ca 3	0.7	0.34
β-amylase[b]	6,570	ca 2½	0.7	2.03

a) Dissolved in 0.1M acetate buffer at pH = 5.5, plus 0.1% $CaCl_2$

b) Dissolved in water at pH = 5.

after dialysing the enzyme for 24 hours at 2°C against buffer or water.

The results for α-amylase are lower than the 45,000 reported by Danielsson (1947), whereas, for β-amylase, there is good agreement with the literature value of 215,000 (Thoma et al., 1963). Both samples were homogeneous on sedimentation velocity. The β-amylase was chromatographed down a Sephadex column, and the eluate concentrated for a molecular weight determination. The resultant value of 112,000 is half that of the native enzyme. A molecular weight of 50,000 has been suggested for the depolymerised enzyme (Thoma et al., 1963), thus the chromatographed enzyme would appear to be the dimer. It was noted that the recovery from the column was only ca 12%. It would therefore seem that gel filtration has withheld the 'double-dimer' rather than split the enzyme in two, although the pH-history during and after gel filtration might also affect its state of aggregation. Banks (1960) found a molecular weight of ca 150,000 for sweet potato β-amylase, although his sample contained low molecular weight contaminant.

2E. ULTRACENTRIFUGE - APPROACH TO SEDIMENTATION EQUILIBRIUM

Another method of overcoming the disadvantage of the long times to attain sedimentation equilibrium is to consider the transient state, or approach to sedimentation equilibrium. Archibald (1947) showed that molecular weights can be determined from a knowledge of the concentration distribution (at any time) in the regions of the solution column near the meniscus and bottom of the cell.

Theory:- Archibald pointed out that across the meniscus and cell bottom, the net transport of solute is zero, and therefore equation 2.28 is valid; i.e.

$$c_m S w^2 x_m = D(^{dc}/_{dx})_m \qquad 2.39$$

and

$$c_b S w^2 x_b = D(^{dc}/_{dx})_b \qquad 2.40$$

where

$$c_m = c_o - \frac{1}{x_m^2} \int_{x_m}^{x_p} x^2 \frac{dc}{dx} \cdot dx \qquad 2.41$$

and

$$c_b = c_o - \frac{1}{x_b^2} \int_{x_p}^{x_b} x^2 \frac{dc}{dx} \cdot dx \qquad 2.42$$

if a plateau region at x_p exists in the cell (Klainer and Kegeles, 1955).

At constant speed, values of $^S/_D$ may be calculated to yield values for the molecular weight at the meniscus and cell bottom

from Svedberg's equation 2.20. For a homogeneous solute, these values will be equal; but in practice, separate values are determined at different times and extrapolated to zero time. In this procedure, heterogeneity or aggregation may readily be detected, which is the main advantage of the Archibald technique.

Disadvantages lie in the uncertainty of $(^{dc}/_{dx})_{m,b}$ and the laborious computations involved in equations 2.41 and 2.42.

An improvement was, therefore, suggested by Trautman (1956), who recommended a plot of concentration gradient (at the meniscus and/or the bottom of the cell) vs. the integrals in equations 2.41 and 2.42. The evaluation of these is facilitated by the use of Trautman's radius cubed (Z) scale (Table 2.5). Homogeneous materials give a straight line Trautman plot, of gradient $^{S}/_{D}$, whence $\overline{M}_w$ and $\overline{M}_z$ values may be calculated. The advantage of this method is that runs at several speeds are incorporated on the same plot, which is, in effect, an average of several Archibald experiments. Errors in the determination of $(^{dc}/_{dx})$ are therefore averaged out. Erlander and Foster (1959) have also applied this technique to the analysis of paucidisperse systems.

Determination of molecular weights by Archibald-Trautman:-

Runs were made in 30 mm. double sector cells at four or five selected speeds ranging from 3,000-12,000 r.p.m., with the aid of the 6.4:1 reduction gear. Photographs at various time intervals between 10-50 minutes were taken at each speed. At the highest speed, the peak was allowed to break completely away from the meniscus, to yield a measure of the initial concentration c_o in area units

beneath the peak. Between each speed the rotor was stopped and the contents of the cell thoroughly mixed before the next run. A bar angle of 80^{o} provided the best conditions for an easy extrapolation of the Schlieren pattern to the meniscus.

Data at the meniscus only was used, and a radius cubed scale was constructed for Z-values between 500 and 800; (an abbreviated version is shown in Table 2.5). The Schlieren pattern was traversed at Z increments of 2, in a similar manner to that described on p 39 . In the region of the meniscus, Δy values were read at Z increments of 1. The data was further magnified by plotting on graph paper, whence the area A_z was determined by counting squares. As a radius cubed x scale was used, this area corresponds exactly to the required concentration integral in the theory (equation 2.41). $(^{dc}/_{dx})_m$, which is equivalent to Δy_m, was read from the graph after a straight line extrapolation of the Schlieren pattern to the meniscus. The initial concentration c_o was determined on the Z-scale, in similar manner, to give A_z^o.

Now, from Trautman (1956) and Erlander and Foster (1959), -

$$Y^* = -X^*(^{S}/_{D}) + X^{*o}(^{S}/_{D}) \qquad 2.43$$

where

$$Y^* = \frac{\Delta y_m \tan \theta}{w^2 x_m} \qquad 2.44$$

$$X^* = \frac{x_r^3 \tan \theta}{3000\, G_x^2} \cdot \frac{\Delta z \sum \Delta y_i}{x_m^2} \qquad 2.45$$

$$X^{*o} = \frac{G_y}{G_x} \cdot a'b' n_c^o \qquad 2.46$$

where

n_c^o = refractive index of the solution at the initial concentration,

x = magnified radius,

G_x = total radial magnification = 2.22,

G_y = magnification of the cylindrical lens,

a' = optical path length of the cell,

b' = optical lever arm,

θ = Schlieren bar angle,

Δy_i = distance between the height of the solution pattern and the baseline at radius i = Z

$\Delta Z \sum \Delta y_i = A_z$ = area determined on Z-scale.

Since the bar angle was kept constant, and x_m varied negligibly with w, equation 2.43 may be multiplied by $G_x/\tan\theta$, whence-

$$Y^* = \frac{\Delta y_m \; 2.22}{w^2 \; x_a} \qquad 2.47$$

$$X^* = \frac{(16.186)^3 \cdot A_z}{(3000)(2.22)x_a^2} = 0.635\left(\frac{A_z}{x_a^2}\right) \qquad 2.48$$

$$X^{*o} = (\Delta Z \sum \Delta y_i)^o = A_z^o \qquad 2.49$$

Y* and X* values, computed from equations 2.47, 2.48 and 2.49, were plotted as Y* vs. - X* (Fig. 2.5). The gradient (from equation 2.43) is given by

$$\left|\frac{Y^*}{X^{*o} - X^*}\right| = (S/D)_w^o = \frac{\bar{M}_w(1 - \bar{V}\rho)}{RT} \qquad 2.50$$

For a polydisperse system, which yields a curved Trautman plot,

FIG 2.5

Trautman plot for β-amylase

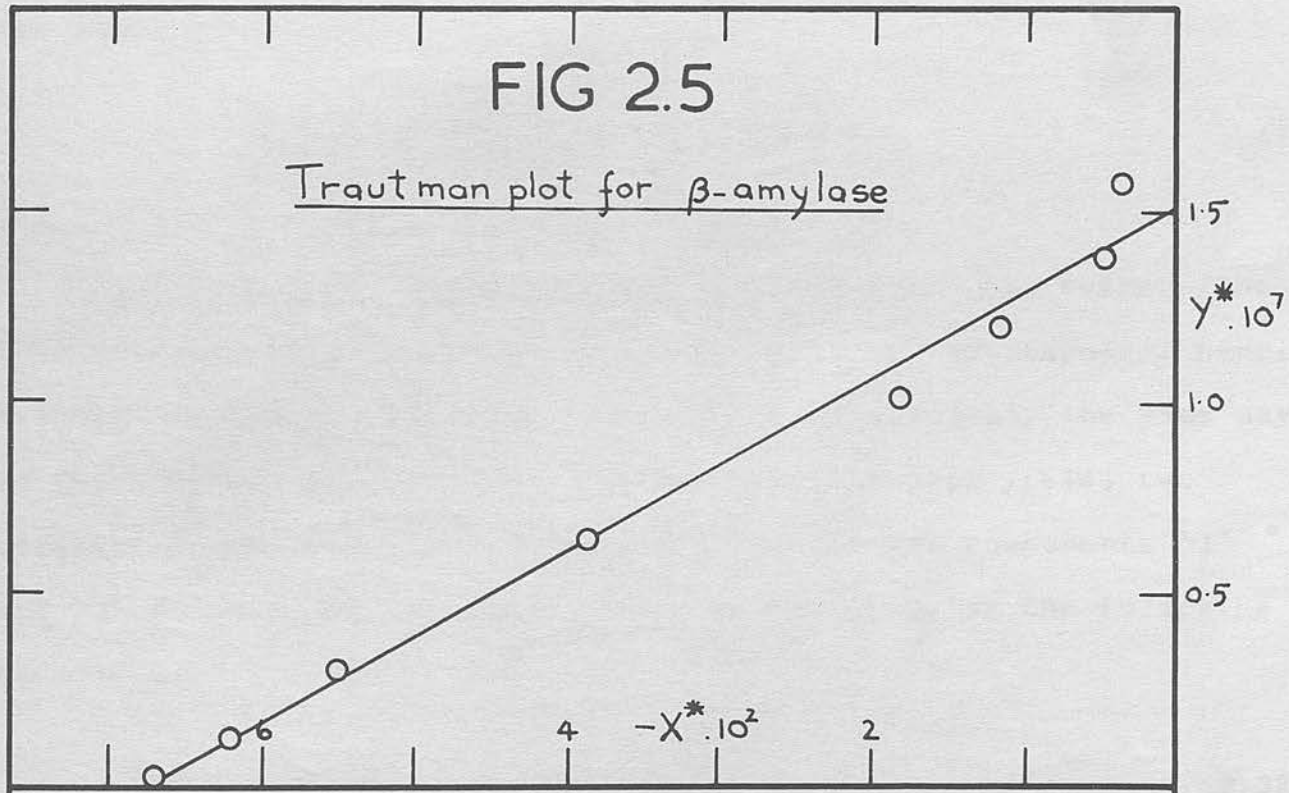

FIG 2.6

Trautman plot for a paucidisperse system

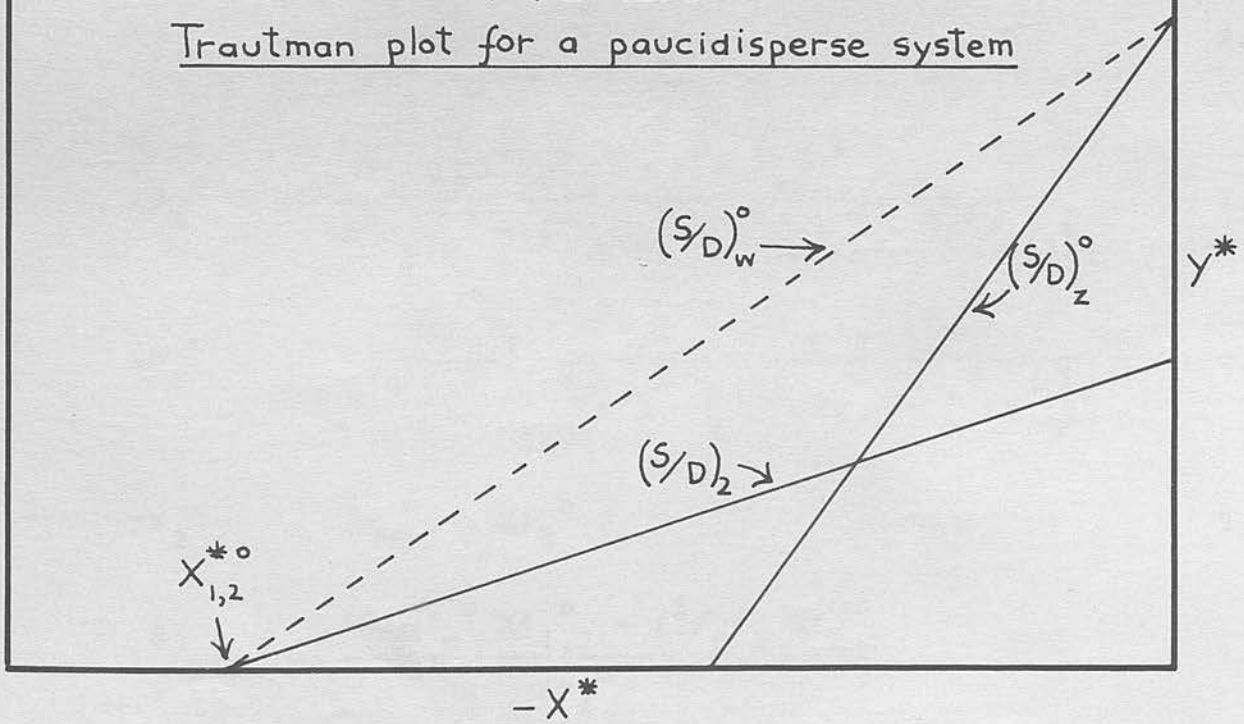

the Z average molecular weight is calculated from the gradient of the curve at X* = O.

$$\left|\frac{\Delta Y^*}{\Delta X^*}\right| = (S/D)^o_z = \frac{\bar{M}_z (1 - \bar{V}\rho)}{RT} \qquad 2.51$$

Analysis of paucidisperse systems:- Erlander and Foster (1959) have extended this procedure to the analysis of two-component paucidisperse systems. The data is collected in precisely the same way as for a monodisperse system, but the Trautman plot yields two straight lines (Fig. 2.6). The data for the two components '1' and '2' is analysed for $(S/D)_1$, X^{*o}_1 and X^{*o}_2, using the following equations:-

$$X^{*o}_{1,2} = \frac{G_y}{G_x} a' b' (n_c^o)_{1,2} = A_{z\,1,2} \qquad 2.52$$

$$M_i = \frac{RT}{(1 - \bar{V}_i\rho)} (S/D)_i \qquad 2.53$$

$$X^{*o}_1 = \frac{X^*_{1,2}\left[(S/D)_w^o - (S/D)_2\right]^2}{(S/D)_2^2 + (S/D)_w^o\left[(S/D)_z^o - 2(S/D)_2\right]} \qquad 2.54$$

$$X^{*o}_2 = \frac{X^*_{1,2}\left[(S/D)_w - (S/D)_1^o\right]^2}{(S/D)_1^2 + (S/D)_w^o\left[(S/D)_z^o - 2(S/D)_1\right]} \qquad 2.55$$

$$X^{*o}_2 = X^{*o}_{1,2} - X^{*o}_1 \qquad 2.56$$

$$(S/D)_1 = \frac{(S/D)_w^o X^{*o}_{1,2} - (S/D)_2 X^{*o}_1}{X^{*o}_1} \qquad 2.57$$

where the superscript "o" refers to the initial concentration, and the subscripts "1" and "2" refer to the fast and slow components respectively. In practice, the two lines are altered within experimental error, until the values of $X^*_2{}^o$ obtained from equations 2.55 and 2.56 agree. Values of $(S/D)_w^o$, $(S/D)_z^o$, $(S/D)_2$ and $X^*_{1,2}{}^o$ are determined directly from the Trautman plot (Fig. 2.6). From a knowledge of n_c^o and $\bar{V}$ for each component, their respective molecular weights and concentrations may be determined.

The choice of meniscus:- This is the most critical point in the whole method, and can affect the final result quite markedly, especially at low speeds where the meniscus image appears broader. The fine structure of the meniscus has been discussed by Trautman (1958) and later by Erlander and Babcock (1961), who reasoned the broad image to be due to the curvature on the meniscus surface (Fig. 2.7). They suggested that the 'meniscus' should be one-third the distance of the 'central shadow' from the 'apex line.'

There was a large scatter (outwith experimental error) of experimental points on Trautman plots employing the 'Erlander/Babcock' meniscus. This error was attributed to an incorrect meniscus. These authors used only 12 mm. and 3 mm. cells, with 30 mm. cells one might expect the largest portion of the meniscus to be located at the 'apex line.' Moreover, it was noted that their meniscus tends toward the 'apex line' at speeds $>$ 2000 r.p.m. Using an 'apex meniscus' as defined in Fig. 2.7, a better Trautman plot was obtained.

Although rigorous light-source alignment has been suggested

FIG 2.7

Meniscus fine structure

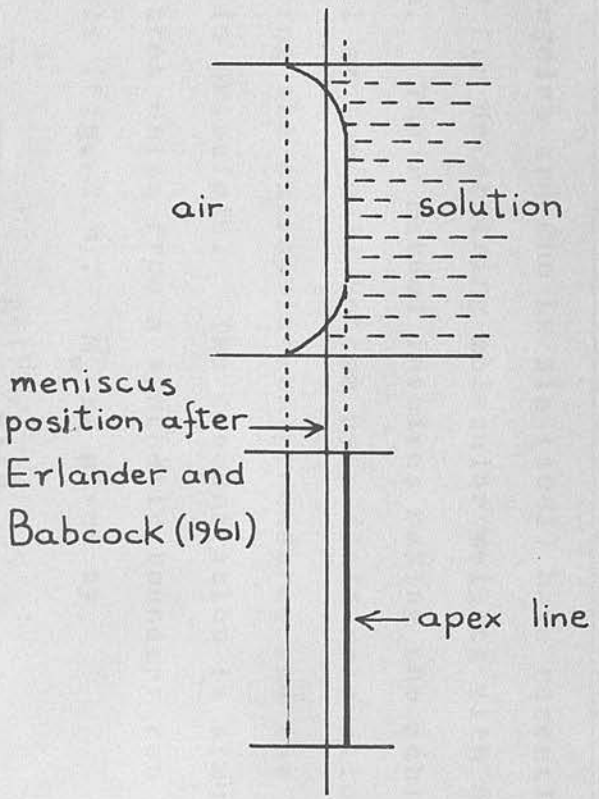

FIG 2.8

Field relaxation technique

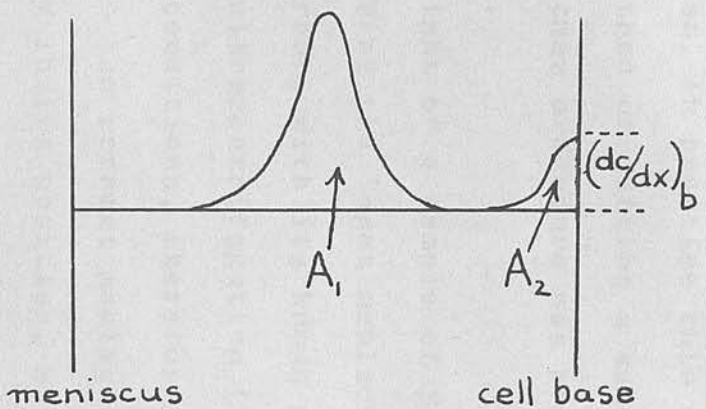

(Trautman, 1958) as an essential preliminary to determining the exact meniscus position, in practice this would be laborious. The semi-empirical method of putting a sample of known molecular weight through a Trautman procedure was preferred, as a check on the meniscus position.

The molecular weight of a sample of β-amylase was found to be 220,000 (Fig. 2.5), using the 'apex meniscus'. This agrees, to within experimental error, with its known molecular weight determined by equilibrium ultracentrifugation (Table 2.7). Under the present experimental conditions, therefore, the 'apex-line' appears to correspond to the correct meniscus, but, in view of the well-known uncertainty in its position, molecular weights determined by this method must be regarded as qualitative only (ca $\pm$ 5%).

Determination of molecular weights by the Field Relaxation Technique:- Kegeles and Cho Lu Sia (1963) have recently proposed a rapid method for determining molecular weights with one ultracentrifuge run. Their method involves making the Schlieren pattern horizontal at the cell bottom by a field relaxation technique, thus facilitating the extrapolation procedure, and the application of the Archibald principle. The concentration is simultaneously determined in area units from a synthetic boundary run in the main body of the cell (Fig. 2.8). $\overline{M}_w$ is given by

$$\overline{M}_w = \frac{RT(dc/dx)_b}{(1 - \overline{V}\rho)w^2 . x_b(A_1 + A_2)} \qquad 2.58$$

where A_1 and A_2 are the appropriate areas indicated in Fig. 2.8, corrected for radial magnification; $(dc/dx)_b$ is the magnified distance measured on the plate; and x_b is the absolute radial distance of the cell base.

A 12 mm. double sector epoxy resin cell was used with the interference synthetic boundary centre piece. Into one sector was introduced ca 0.025 ml. of silicone oil to give a clear base line, and 0.15 ml. of solution from an 'Agla' micrometer syringe. The other sector was filled with pure solvent. The 'high speed' chosen for the run is arbitrary, depending on the concentration and molecular weight of the solute, but ca 20,000 r.p.m. is used for material of $\bar{M}_w = 10^5$ in a 1% solution. After a sufficient build up of material at the base of the cell, the rotor is braked slowly to the 'low speed' - generally about one-third of the 'high speed'. A photograph was taken when the Schlieren pattern was horizontal at the cell base. The molecular weight of sucrose (M = 342) in a 2% aqueous solution was determined by this method and found to be 343.

The molecular weight obtained is heavily biased in favour of the heavier species of a polymer of broad molecular weight distribution. Thus in conjunction with sedimentation equilibrium, this technique can provide a rapid detection of heterogeneity or aggregation.

2F. ULTRACENTRIFUGE - DENSITY GRADIENT EQUILIBRIUM

At sedimentation equilibrium, a low molecular weight solute will be distributed unevenly throughout the cell to form a concentration gradient, and consequently a density gradient, the solute concentration and solution density increasing with radial distance. If now a small quantity of macromolecule is present in the system and the density of the solution is near the buoyant density of the macromolecule, the latter will move to a unique position in the liquid column, where the density of the solution is equal to the buoyant density of the macromolecule.

Meselson et al. (1957) and Meselson and Stahl (1958) first applied these techniques analytically, by studying deoxyribonucleic acid (DNA) in concentrated aqueous caesium chloride (CsCl) solutions. They showed that the concentration distribution of the macrospecies at equilibrium in the density gradient is Gaussian, and that the width of the distribution is inversely proportional to the molecular weight. Moreover, if macrospecies of different buoyant densities are present, they will be segregated with respect to their buoyant densities along the density gradient.

The buoyant density corresponds closely to the solvated density (the reciprocal of the partial specific volume, $\bar{V}$, of the solvated species at atmospheric pressure), and depends on the composition and solvation of the anhydrous species. Material homogeneous in buoyant density and molecular weight gives rise to a Gaussian concentration distribution. Examples of skewed concentration distributions and bimodal and polymodal bands arising

from molecular weight and/or density heterogeneity can be found in the review by Vinograd and Hearst (1962).

Solutions of sucrose and salts other than CsCl may also be used to establish a density gradient (Ifft et al., 1961), whereas Buchdahl et al. (1963, 1963a) have used mixtures of dense and light organic solvents to study polymers at density gradient equilibrium.

This relatively new method of polymer characterization has been recently reviewed by Hermans and Ende (1964).

Theoretical considerations:- At equilibrium in a density gradient, the macromolecules concentrate in a band where the sum of the forces acting on a given molecule is zero. From this consideration Meselson et al. (1957) formulated the equation

$$M_{1\ app} = \frac{RT\ \rho_o}{(d\rho/dr)_o\ w^2 r_o\ \sigma^2} \qquad 2.59$$

for the apparent molecular weight polymer species '1', where r_o is the radial distance at the centre of the Gaussian polymer band where the buoyant density is ρ_o. $(d\rho/dr)_o$ is the density gradient of the solution at r_o, and σ is the standard deviation of the Gaussian concentration distribution of the polymer. The molecular weight is thus inversely proportional to the square of the band width.

The distribution of a single polymeric species is defined by the Gaussian function,

$$c_1(r) = c_1(r_o) \exp \frac{-(r-r_o)^2}{2\sigma^2} \qquad 2.60$$

where c(r) is the concentration of polymer at radial distance r. σ may be determined from a plot of $\ln c$ vs. $(r - r_o)^2$ which has a gradient of $-\frac{1}{2}\sigma^{-2}$. Such a plot also provides a convenient test for heterogeneity. A concave downward curve indicates heterogeneity with respect to effective (buoyant) density; a concave upward curve indicates heterogeneity with respect to molecular weight, and the slope at any point is proportional to $\bar{M}_w$ at the appropriate position in the polymer band. Moreover, linearity of the $\ln c$ vs. $(r - r_o)^2$ plot, indicates the monodispersity of the banded macromolecules (Meselson and Stahl, 1958).

The determination of $(^{d\rho}/_{dr})_o$ has been discussed by Ifft et al. (1961) for aqueous solutions of sucrose and various salts. They proposed an isoconcentration point r_e in the liquid column, where the density ρ_e is equal to that of the initial solution before application of the centrifugal field. They also proposed the function $\beta(\rho)$, where

$$\beta(\rho) = \frac{d \ln a}{d\rho} \cdot \frac{RT}{(1 - \bar{V}\rho)M} \qquad 2.61$$

and

$$\beta(\rho)\,(^{d\rho}/_{dr})_e = w^2 r_e \qquad 2.62$$

(a is the activity coefficient of the solute). r_e may be calculated from

$$r_e' = \sqrt{\frac{r_b^2 + r_m^2}{2}} \qquad 2.63$$

where r_b = radial distance of cell bottom

r_m = radial distance of the meniscus and r_e' tends to r_e as $\beta(\rho)$ becomes constant (Vinograd and Hearst, 1962). From tabulated values of $\beta(\rho)$, $(d\rho/dr)_e$ may be calculated at r_e, which is equal to $(d\rho/dr)_o$ to a good approximation. Density values at the band centres, ρ_o, may be determined from

$$\rho_o = \rho_e + (d\rho/dr)_e \, (r - r_o) \qquad 2.64$$

to a good approximation.

The thermodynamic equilibrium theory of polydispersed systems in a mixture of two solvents has been described by Hermans (1963, 1963a) and Hermans and Ende (1963). They describe how such polymer bands may be analysed - especially with respect to molecular weight distribution.

The presence of other density gradients:- The density gradient due to the redistribution of low molecular weight solute, described on p. 60 is known as the composition density gradient. However, superimposed on this are other density gradients, which must be considered for a rigorous treatment of data. (a) The compression density gradient is due to the compressibility of the solution at high centrifugal field forces. Its magnitude can be up to 10.8% of the composition gradient for the $CsCl/H_2O$ system, and its calculation has been detailed by Hearst et al. (1961). (b) The physical density gradient equals the sum of the composition and compression density gradients. (c) The buoyancy density gradient is due to the distribution and compressibility

of the polymer. (d) The effective density gradient takes into account all the above density gradients, together with the activity of the polymer. This is the correct density gradient to use in the application of theory, but unfortunately it has only been evaluated for the DNA/CsCl/H_2O system to date (Vinograd and Hearst, 1962).

EXPERIMENTAL

A Spinco Model E analytical ultracentrifuge equipped with a Schlieren optical system was used. Aqueous solutions of CsCl were used to establish the density gradient, runs normally being made at 39,460 r.p.m. 30 mm. path length cells were found unsuitable due to the excessive refractive index of the dense solutions. This difficulty may be overcome by using a combination of negative wedge windows in the cells. However, 12 mm. path length cells were found more suitable and were used with plain and negative wedge windows routinely, (4mm and 2 mm path length cells were also found useful for small amounts of solution).

Procedure for a density gradient experiment with amylose:- For a 12 mm. cell operation, amylose butan-1-ol complex was dissolved in distilled water (ca 1 ml. complex to 10 ml. H_2O). Using an 'Agla' micrometer syringe, a known volume of this solution was added to a weighed amount of Analar CsCl to give approximately the required density. A graph showing the relation between percentage weight of solute and solution density, which was constructed from values in the International Critical Tables (1929), is shown in Fig. 2.9. The exact density of the resultant solution was determined to three decimal places by weighing a known volume (delivered from an 'Agla' micrometer syringe) to the nearest 0.00001 gm. With the aid of a negative wedge window, dual runs were possible, which were continued until equilibrium had been

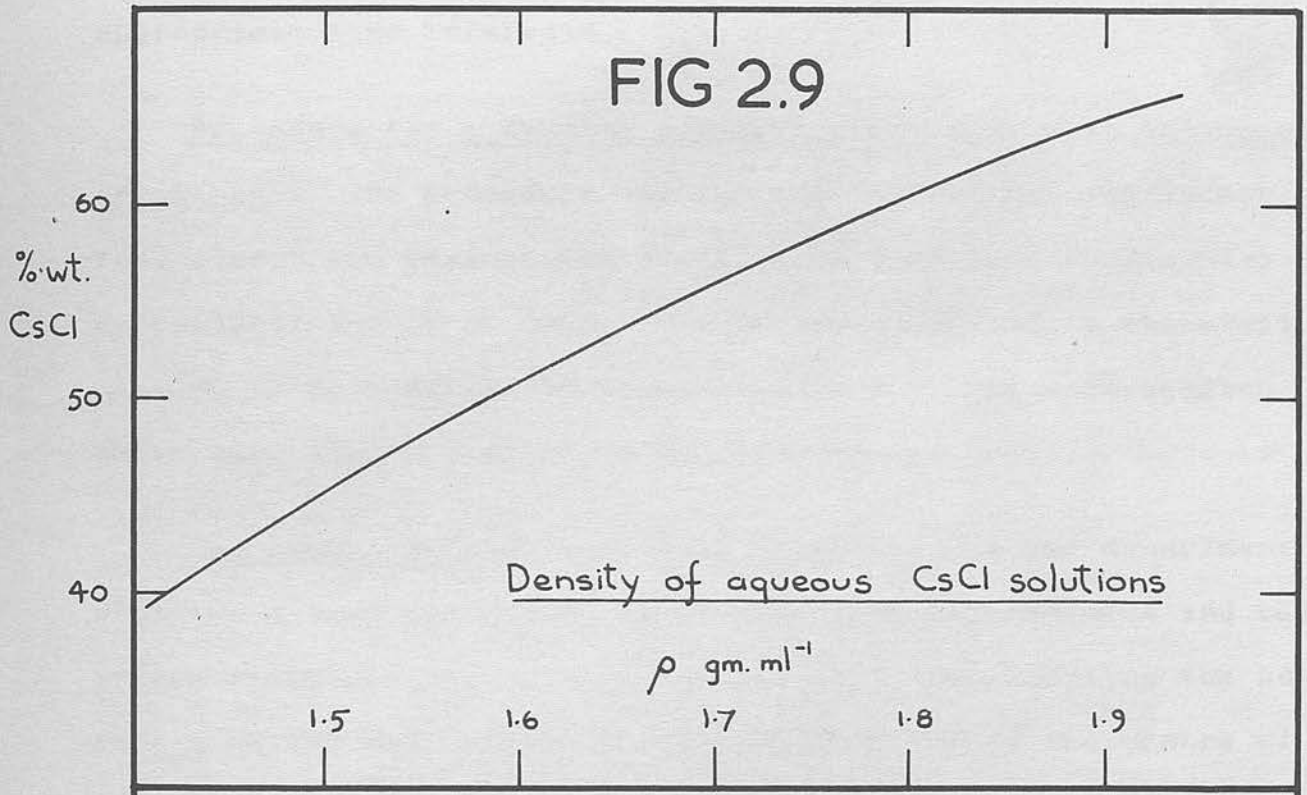

FIG 2.9

FIG 2.10

Distribution of a polymer at equilibrium in a density gradient

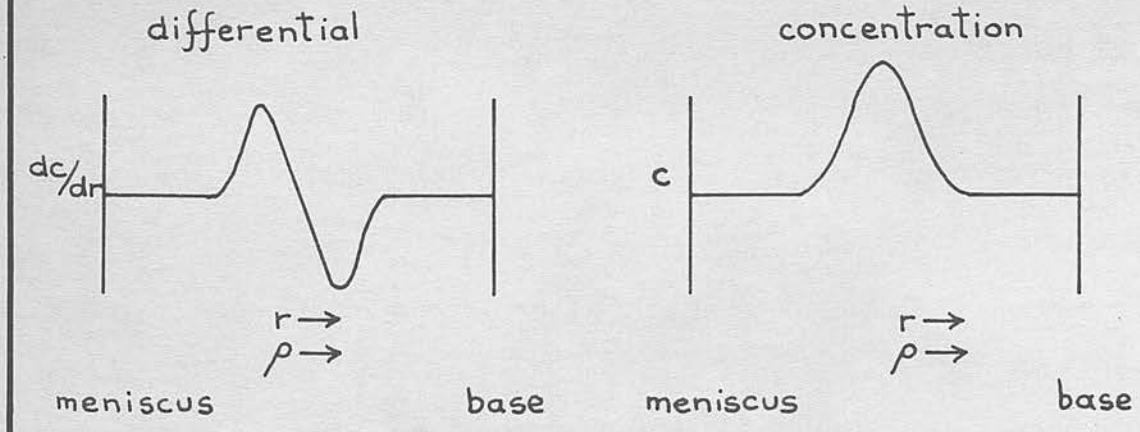

reached (usually about 48 hours), photographs being taken at appropriate time intervals.

Procedure for a density gradient experiment with amylopectin or starch:- The procedure was the same as for amylose except that starch and amylopectin dispersions were used to dissolve the appropriate amount of CsCl. These were prepared in the usual manner, by dispersing the polysaccharides in hot deoxygenated water with vigorous stirring and allowing to cool.

The determination of buoyant density:- As the experiment proceeds a peak and a well break away from the meniscus and cell bottom respectively. This peak and well, representing the boundaries of the macromolecule band, migrate toward the centre of the cell to form a biphasic differential curve at equilibrium at the appropriate density along the density gradient (Fig. 2.10). Equilibrium is established when no further change is observed in the Schlieren diagram.

The Schlieren pattern was traced on to graph paper using a micro-comparator and the slightly curved base line fitted by extrapolation. The radial distance, r_0, at which the Schlieren curve cut the base line was determined, and the buoyant density, ρ_0, of the polymer band calculated using equations 2.62, 2.63, and 2.64. For starch-type polysaccharides, ρ_0 was found to be between 1.65-1.70, so the $\beta(\rho)$ value used in the calculation of ρ_0 values was 1.190×10^9 c.g.s. units (Ifft et al., 1961). Since in this density range $\beta(\rho)$ is independent of ρ, equation 2.63 can be validly used to determine r_e. Strictly, the effective

density gradient should be used in the calculation of results, but values of the required parameters for the system under study were not available. Compression effects, which would increase $(^{d\rho}/_{dr})_e$ by about 8.7% (Hearst et al., 1961) were also ignored, as they had no effect on the conclusions drawn from these experiments. Only a composition density gradient was therefore assumed in the evaluation of data.

The determination of molecular weight:- The differential Schlieren curve was integrated with respect to radial distance r to yield the concentration distribution of the banded polymer (Fig. 2.10). This curve was analysed for σ by plotting $\ln$ of the concentration, c, against the square of the half band width $(r - r_o)^2$. In the absence of density heterogeneity, the weight average molecular weight was calculated from equation 2.59, at different points in the polymer band.

Where polymer distribution bands overlapped, a process of reflection and subtraction of the biphasic Schlieren curve yielded accurately the distribution of the two (or more) components at equilibrium (Adams and Schumaker, 1964).

The total amount of polymeric material in different bands was also determined from the areas beneath the concentration distribution curves (Buchdahl et al., 1963a).

2G. ENZYMIC CHARACTERIZATION

Enzymes, in particular β-amylase and Z-enzyme, are essential for the complete characterization of amyloses. β-Amylase degrades amylose from the non-reducing end by the stepwise removal of maltose (Kerr and Gehman, 1951). A linear and unmodified chain of α-1,4-linked anhydroglucose units is degraded completely to give a β-amylolysis limit = 100. Z-enzyme is non-specific, and in the presence of β-amylase degrades the α-1,4 amylose chain randomly. The limit of degradation by the concurrent action of β-amylase and Z-enzyme - the (β + Z) limit - is a measure of purity (Banks, Greenwood and Jones, 1960).

Experimental:- β-amylolysis limits, and (β + Z) limits were determined for amylose butan-1-ol complexes as described by Banks and Greenwood (1963b). The accuracy of such values is ±2%.

Crystalline sweet potato β-amylase (Worthington Biochemical Corp.) was used, and 'crude' β-amylase (Koch-Light Laboratories Limited) was used as a source of Z-enzyme. After incubation, the maltose concentration in the enzyme digest was determined from the reducing power of 3 ml. aliquots (Lampitt et al., 1955). The polysaccharide concentration was determined by estimating the glucose reducing power, after prior hydrolysis with 1.5N H_2SO_4. The β-amylolysis limit is expressed as the percentage conversion of polysaccharide into maltose and is given by

$$\frac{\text{Maltose concentration}}{\text{Polysaccharide concentration}} \cdot \frac{324}{342}$$

SECTION 3

THE VISCOMETRIC BEHAVIOUR OF AMYLOSE IN AQUEOUS ALKALINE SOLUTION

3A. VISCOSITY AS A FUNCTION OF ALKALI CONCENTRATION AND pH

It is well known that, in the solid state, amylose exists in two conformations; an extended form defined by an A or B type of X-ray diffraction pattern; and a helical form defined by a V-pattern (Rundle et al., 1944; Bear, 1944). This latter conformation exists in solid complexes formed with, for example, butanol and iodine, and in amylose precipitated from aqueous solution with ethanol. More recently, Germino et al. (1964) and Valletta et al. (1964) have shown the helical structure to exist in ketone and alcohol complexes from the results of X-ray powder patterns. However, the question of the conformation of amylose in solution remains uncertain.

Viscosity measurements provide a rapid, convenient method for measuring the hydrodynamic volume and hence characterizing the molecular size of a polymer in solution. Alkaline solutions have often been suggested as solvents for starch and amylose, although no agreement has been reached as to the best solvent for routine characterization. Koëts (1936), and Koëts and Kruyt (1937) first noted viscosity changes in aqueous starch solutions as a function of the alkali concentration, with a maximum at 0.1M NaOH. However, few complete studies of this effect have been made to date.

EXPERIMENTAL

A total (unfractionated) amylose was used for this work. Viscosities were determined on solutions of the butan-1-ol complex at 25°C. Concentrations of amylose in these solutions were determined by the alkaline-ferricyanide method (Lampitt et al., 1955), after prior hydrolysis with 1.5N H_2SO_4. In the alkaline solutions of high molarity, care was taken to make the normality 1.5N with respect to the acid during the hydrolysis procedure. 'Blank' determinations were run concurrently in all cases.

Preparation of solvents:- Aqueous solutions of KOH, NaOH, tetramethyl ammonium hydroxide (TMAH) and tetra-ethyl ammonium hydroxide (TEAH), were prepared, and their molarities determined by titration against standard HCl. For solutions at pH $<$ 11, various buffer systems were prepared and their exact pH values read from a 'Pye' pH-meter. The viscosity behaviour in five buffer systems was studied - (a) Boric acid/KOH; (b) Boric acid/KOH/KCl; (c) Borate/KOH/KCl at constant ionic strength (μ = 0.2M); (d) Ethanolamine-hydrochloride/KOH/KCl at constant ionic strength (μ = 0.2M); and (e) KH_2PO_4/NaOH at pH = 7.0. The detailed preparation of these systems is described by Clark (1923) and Bates (1954). Difficulty was experienced with the solution of amylose in some buffers, and therefore all solutions were prepared by firstly dissolving the amylose complex in water and then diluting twice with the requisite buffer. In the mixed KOH/KCl solvents, the KCl concentration was extended until either amylose or KCl itself was precipitated.

RESULTS AND DISCUSSION

The results are illustrated in Figs. 3.1, 3.2, 3.3 and 3.4. The variation of $[\eta]$ -values with solvent is interpreted as indicating changes in hydrodynamic volume of the dissolved amylose molecule. The cause of such changes is a difficult problem, which has recently been discussed by Rao and Foster (1963), and also noted by Hollo et al. (1961) and Husemann et al. (1961).

Like other polysaccharides, amylose behaves as a weak acid in alkali solution, due to the ionisation of hydroxyl groups. The pK_a of these have been measured by Saric and Schofield (1946) and found to be 13.3 and ca 15. With the stripping of protons from the polymer chain, negative charges are formed which may repel each other. This 'coulombic repulsion' will involve an increase in the hydrodynamic volume, and hence in the $[\eta]$ -value of the amylose molecule (Overbeek and Bungenberg de Jong, 1949).

It has been suggested by Reeves (1954), that in alkali, ionisation of hydroxyl groups is accompanied by a change in conformation of the glucose pyranose ring. The various ring conformations suggested by Reeves - 3B, C1 and B1 - are shown in Fig. 3.4. The ionisation of the C_2 and C_3 hydroxyl groups on the glucose ring involves an increase in their respective atomic volumes. Since these groups are sterically further apart in the 3B or C1 than in the B1 conformation, the former are favoured on ionisation. He proposed that in alkali $> 5M$, the ring conformation is entirely 3B (or C1), while in neutral solution alternate glucose units exist in the B1 form. At various intermediate

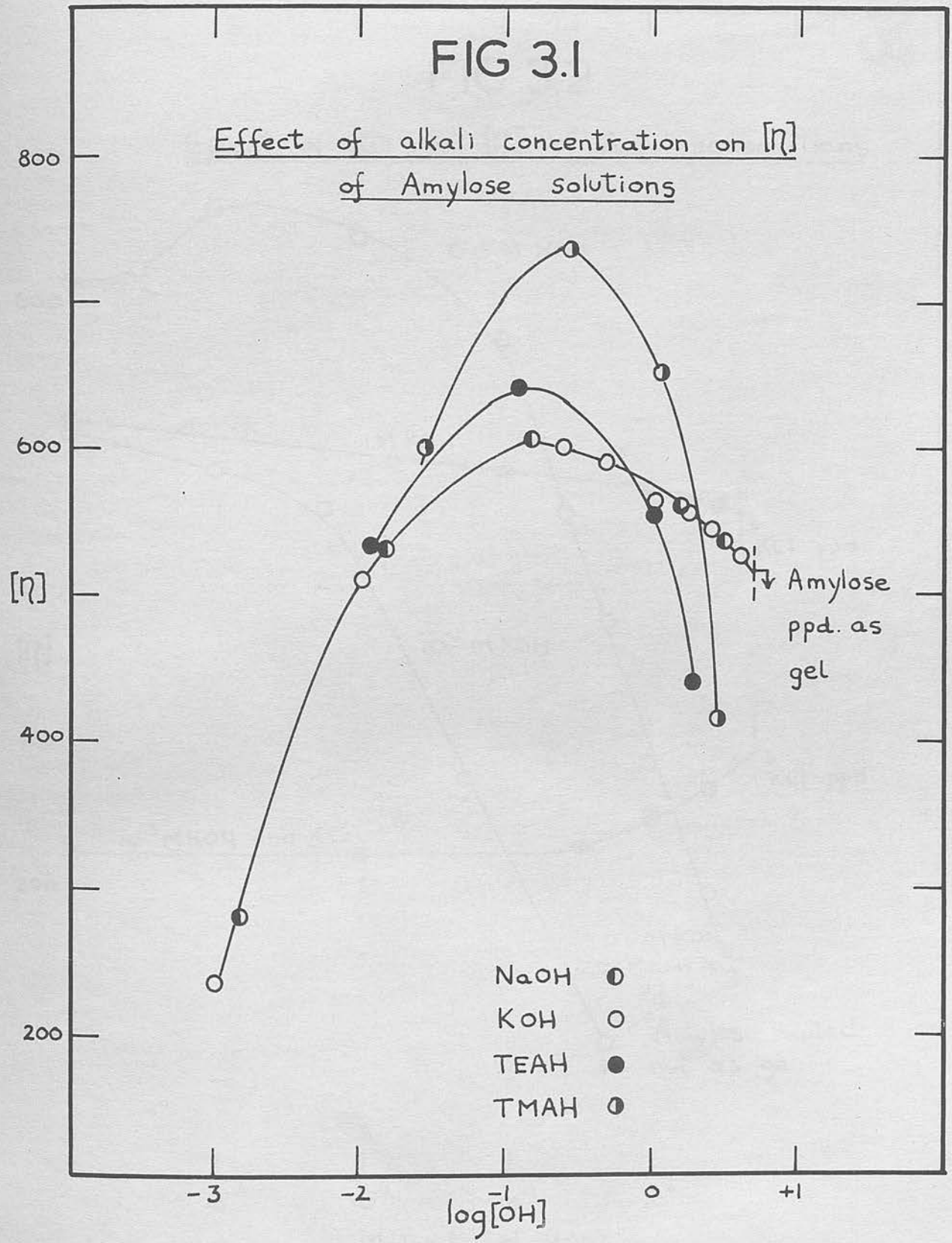
FIG 3.1
Effect of alkali concentration on [η] of Amylose solutions
800
600
400
200
[η]
Amylose ppd. as gel
NaOH
KOH
TEAH
TMAH
-3
-2
-1
0
+1
log[OH]

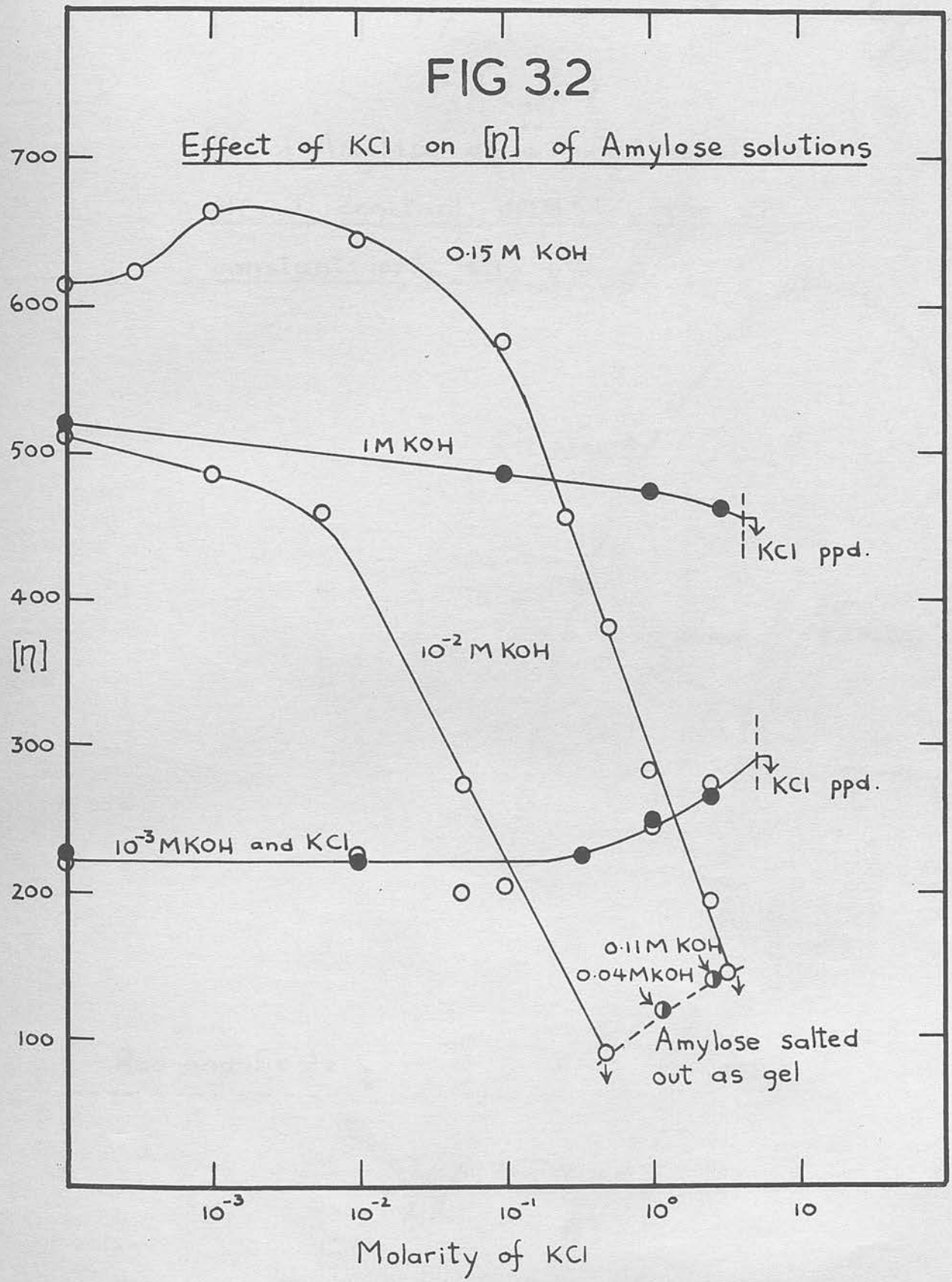
FIG 3.2
Effect of KCl on [η] of Amylose solutions
700
600
500
400
300
200
100
[η]
0·15 M KOH
1M KOH
KCl ppd.
10⁻² M KOH
KCl ppd.
10⁻³ MKOH and KCl
0·11M KOH
0·04MKOH
Amylose salted out as gel
10⁻³
10⁻²
10⁻¹
10⁰
10
Molarity of KCl

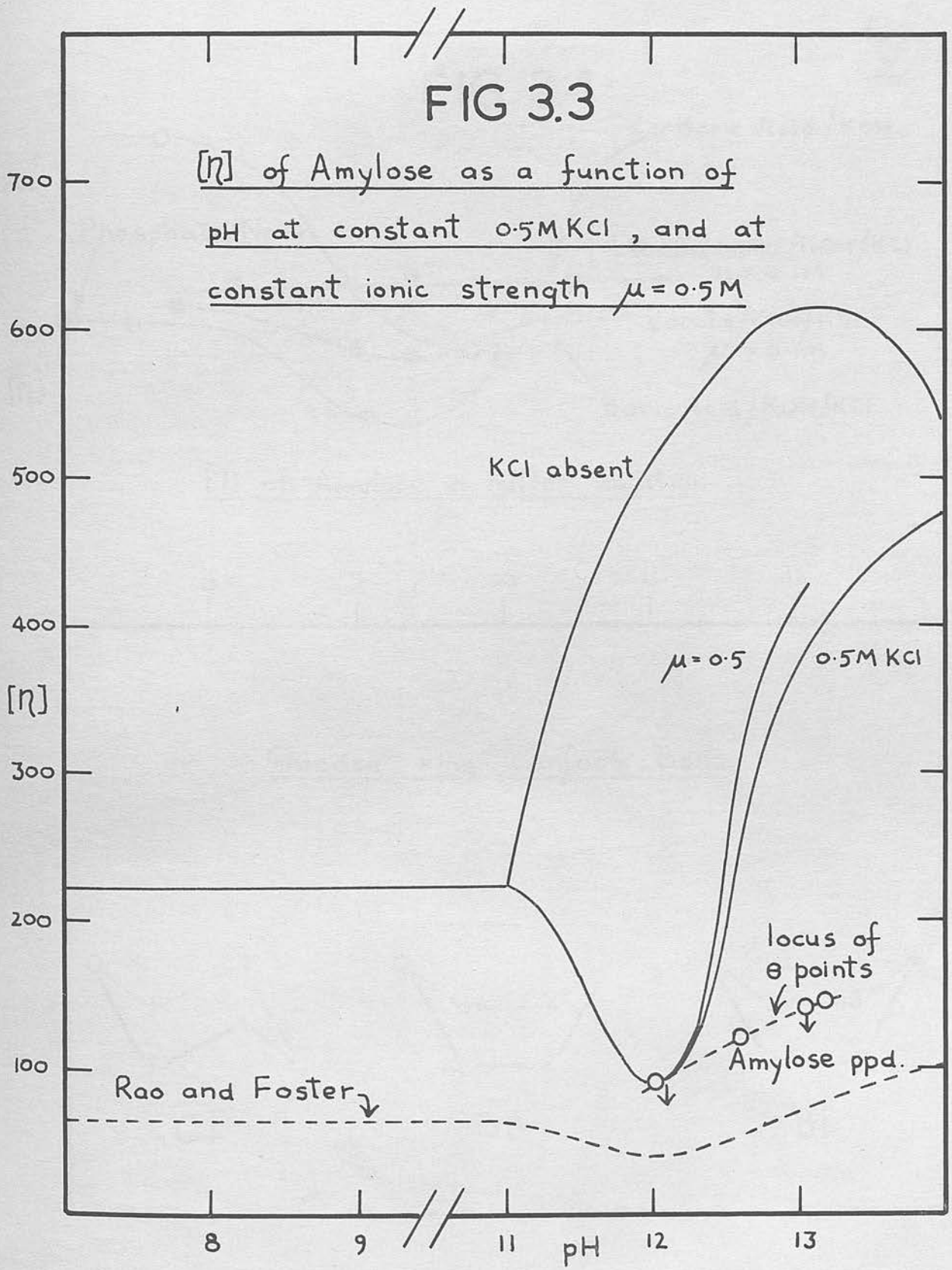
FIG 3.3
[η] of Amylose as a function of pH at constant 0.5M KCl, and at constant ionic strength μ = 0.5M
700
600
500
400
[η]
300
200
100
KCl absent
μ = 0.5
0.5M KCl
locus of θ points
Amylose ppd.
Rao and Foster
8
9
11
pH
12
13

molarities of alkali, there may be progressively more 3B (or C1) and less B1, giving stable, irregularly mixed ring conformations, which are readily soluble. Amylose in a regular, all-3B (or C1) conformation is insoluble. Greenwood and Rossotti (1958) also showed that amylose must exist in either B1, 3B or C1 ring conformations on consideration of models.

The results may be explained in terms of coulombic repulsion and glucose ring conformational changes.

Amylose in KOH and NaOH solutions (Fig. 3.1):- The $[\eta]$ - values are identical; the small K^+ and Na^+ gegen ions are therefore behaving similarly with respect to the amylose molecule. The $[\eta]$ -value rises to a maximum at about 0.15M KOH and then decreases to a value higher than that in neutral solutions, to be precipitated as a translucent gel at 4.7M KOH. At this point, amylose is thought to be entirely in its 3B (or C1) ring conformation and thence to have become insoluble. The maximum value at 0.15M KOH, is due to coulombic repulsion of neighbouring polymer segments. At higher molarities of alkali, ionisation is thought complete and there is therefore a build up of counter K^+ (or Na^+) ions, as well as further B1 $\rightarrow$ 3B (or C1) conformation changes. This gegen-ion activity, which effectively neutralises the charges and recontracts the polymer coil, is known as an electroviscous effect, (Overbeek and Bungenberg de Jong, 1949).

Amylose in 10^{-2}M KOH/KCl and 0.15M KOH/KCl solutions:- The addition of neutral salt (i.e. KCl) to the KOH solutions $> 10^{-3}$M and < 0.15M, decreases the $[\eta]$ -value, even to below that in

aqueous KCl solutions; the amylose being eventually salted out as a translucent gel (Fig. 3.2). These precipitation points are temperature dependent and therefore resemble ideal Θ-conditions (Fox and Flory, 1951). For brevity's sake, these precipitation conditions are hereafter referred to as 'aqueous Θ-points.' As amylose is gelled out at a low $[\eta]$ -value, it must be assumed that there is a regular structure of B1 conformations. Therefore, the build-up of neutral counter ions must effectively neutralise the hydroxyl groups on the molecule and change any 3B (or C1) to B1 conformations. The lower $[\eta]$ -value than in neutral solutions must indicate an even more ordered structure. Thus the ordered structure of alternate B1 ring forms, suggested by Reeves, in neutral solution, lies between the other two ordered extremes of all-B1 and all-3B (or C1) conformations.

The 3B (or C1) structure at 4.7M KOH is much larger than the B1 structure proposed at 'Θ-conditions', and it must therefore be concluded that in the former conformation, amylose occupies a larger hydrodynamic volume. The excess $[\eta]$ -values at 0.15M KOH above that at 4.7M KOH, is therefore solely due to the coulombic swelling by repulsion of neighbouring polymer segments.

The locus of 'Θ-points' from the 0.01M KOH to 0.15M KOH 'Θ-solvents' (Table 3.1) shows an increase in $[\eta]$ -values corresponding to the increase in $[\eta]$ from 0.01M KOH to 0.15M KOH alone (Fig. 3.3). It is suggested that this is, in effect, the corresponding coulombic swelling of amylose in its all-B1 conformation.

TABLE 3.1

Aqueous Θ-solvents for amylose at 25°C

Solvent	[η]
3.2M KCl + 0.16M KOH	145
2.5M KCl + 0.11M KOH	140
1.2M KCl + 0.04M KOH	120
0.50M KCl + 0.01M KOH	90

TABLE 3.2

[η] of amylose in mixed TMAH solvents

Solvent	[η]
0.27M TMAH	730
0.27M TMAH + 2M KCl	170
0.27M TMAH + 2M TMACl	100

Amylose in 1M KOH/KCl solution:- In this system no large fall in $[\eta]$ was detected up to 4.0M KCl when KCl itself was salted out (Fig. 3.2). It must be assumed that in 1M KOH the amylose conformation is so nearly all-3B (or C1) that not sufficient "neutralising" K^+ ions can be added to counter the B1 → 3B (or C1) effect. Thus the tendency of B1 → 3B (or C1) due to high alkalinity outweighs the 3B (or C1) → B1 due to counter ion activity.

Amylose in 10^{-3}M KOH/KCl and H_2O/KCl solutions:- The ring conformation of amylose glucose units in these near neutral systems, according to Reeves, is a regular structure of alternate B1 and 3B (or C1) ring forms. No ionisation can take place in these solvents on addition of KCl up to saturation at ca 4.9M KCl; therefore, some conformational change must take place at high K^+ concentrations to explain the slight increase in $[\eta]$. The presence of many K^+ ions in the neighbourhood of the C_2 and C_3 hydroxyl groups may force a limited B1 → 3B (or C1) conformation change.

Amylose in TMAH and TEAH solutions:- With aqueous solutions of these organic alkalis as solvents, higher maximum $[\eta]$-values are observed at ca 0.27M TMAH and 0.15M TEAH (Fig. 3.1.). This may be due to the larger gegen-ion within the ionised amylose molecule. Nightingale (1962) has shown the TMA^+ ion to be weakly peri-surface hydrated, whereas the TEA^+ ion is more hydrophobic and resists hydration. Moreover, Packter (1964) has recently suggested that TMA^+ and TEA^+ associate with polyelectrolytes, and that electrostatic effects predominate with these lower ammonium poly-salts. Although amylose is not strictly a polyelectrolyte in 0.27M TMAH

(or 0.15M KOH), this might explain why the TMAH maximum is so large; i.e. the more probable TMA^+-amylose associate occupies a larger hydrodynamic volume. The build-up of such large and probably immobile gegen ions at higher TMAH and TEAH concentrations must effectively neutralise the hydroxyl groups and rechange the conformations toward more B1, reducing the $[\eta]$-value. In this case, counter ion activity overrides the alkaline tendency of B1 → 3B (or C1).

Amylose in TMAH/KCl and TMAH/TMACl solutions:- The addition of KCl or tetra-methyl ammonium chloride (TMACl) to 0.27M TMAH reduces $[\eta]$ to a value similar to those in the KOH/KCl systems (Table 3.2). It must therefore be assumed that counter-ion activity is taking place, changing the amylose ring conformations toward a higher proportion of B1 forms. The TMACl reduces the $[\eta]$-value much lower than the KCl at the same molarity. It thus seems that the large hydrophobic TMA^+ is more effective than K^+ in promoting the 3B (or C1) → B1 transition. This substantiates the conclusion drawn above, where the moderate build-up of TMA^+ at 0.27M TMAH decreases the $[\eta]$-value below that in the corresponding KOH or NaOH case.

Huggin's constant and solvent power:- Huggin's constant k, may be interpreted in terms of degree of entanglement $\delta/d (= \frac{1}{2} - \frac{k}{3})$ as suggested by Gillespie (1963), where δ and d are parameters involved in the interaction of two polymer coils (Fig. 3.5; p82a). A summary of how k and δ/d values vary with solvent is shown in Table 3.3. k increases as the salt concentration is increased in

TABLE 3.3

Huggin's constant and degree of entanglement for amylose solutions

Solvent	$[\eta]$	k [a]	δ/d [b]
H_2O	220	0.81	0.23
2.5M KCl	265	0.58	0.31
10^{-3}M KOH	225	0.80	0.23
10^{-3}M KOH + 2.5M KCl	275	0.46	0.35
10^{-2}M KOH	510	0.40	0.37
10^{-2}M KOH + 0.50M KCl (θ)	90	4.6	-1.0
0.15M KOH	615	0.39	0.37
0.15M KOH + 3.2M KCl (θ)	145	3.9	-0.8
1M KOH	520	0.39	0.37
1M KOH + 3.0M KCl	460	0.14	0.45

a) Huggins constant

b) Degree of entanglement.

the 10^{-2}M and 0.15M KOH solutions; i.e. the degree of entanglement decreases as the molecules become more and more compressed in a 'poor' solvent. k is particularly high in Θ solvents, indicating very 'poor' ideal conditions with a minimum degree of entanglement. k is fairly constant in KOH between 0.01M-4M KOH, being less than that in H_2O or 10^{-3}M KOH which are 'poor' solvents. A small decrease in k is observed with increasing KCl concentration in H_2O, 10^{-3}M and 1M KOH, indicating an increase in the degree of entanglement. The significance of this, if any, is unknown.

Amylose solutions at pH = 12:- In the only other study of this kind, Rao and Foster (1963) indicate a $[\eta]$ minimum at pH = 12 (Fig. 3.3), which they attribute to a pH effect. These authors, however, prepared their solutions by partial neutralization of alkali dispersions of dry amylose, so that their solutions contained unknown and variable amounts of salt, whose effect on $[\eta]$ has not been appreciated. Although their experimental curve is not strictly valid, a similar curve may be obtained if the present results are considered at constant 0.5M KCl concentration, or at constant total ionic strength μ = 0.5M (Fig. 3.3).

Rao and Foster (1963) interpret their data as indicating a helix-coil transformation at pH = 12, which is tempting in view of the striking similarity of the curve with that of Doty *et al.* (1957) for polyglutamic acid. However, it seems unlikely that such a drastic transformation should depend only on the presence of sufficient salt. A salt concentration of $>$ 0.5M would involve amylose precipitation at pH = 12, and with $<$ 0.1M KCl no fall in

$[\eta]$ at pH = 12 would be detected at all (see Fig. 3.2). Rao and Foster's strongest argument is the change in skeletal backbone stiffness demonstrated by changes in K' in the Stockmayer-Fixman plot (see equation 2.8, p. 20). However, conflicting results are presented in Section 4 which show no change in K' for amylose in aqueous KCl, 'aqueous Θ-solvent' at pH 12, and 0.15M KOH. These results show amylose to be essentially a flexible coil in all aqueous solvents.

Reversible precipitation was observed for amylose solutions at the four experimental 'Θ-points' (Table 3.1), in common with Rao and Foster's 'pH 12 solvent' (which presumably contained 0.5M KCl). It is suggested that the systems are, in fact, true Θ-solvents at 25°C. This conclusion is substantiated by molecular weight and viscosity determinations (Section 4), and sedimentation studies (Section 5) on amylose under these conditions.

Burchard (1963) measured the $[\eta]$ -value for amylose under Θ-conditions, by employing a mixed organic Θ-solvent - 43.5% acetone/dimethyl sulphoxide (DMSO). In this solvent, amylose may be reversibly precipitated by raising or lowering the temperature about the Θ- temperature (25°C), in similar fashion to aqueous Θ-solvents. A similar solvent gave a $[\eta]$ -value of 125 for the present amylose sample. The present $[\eta]$ -values in different solvents compare very well with data from Burchard (1963) and Rao and Foster (1963) - (Table 3.4). This organic Θ-solvent compares with the 0.04M KOH/1.2M KCl aqueous Θ-solvent, from the $[\eta]$ -values. This is not surprising since DMSO is a strong ionising solvent giving $[\eta]$ -values for amylose comparable to those found in ca 0.04M

TABLE 3.4

$[\eta]$ of amylose in various solvents

Solvent	H_2O/KCl	Aqueous θ solv.	Organic θ solv.	1M KOH	0.5M KOH
a)	220	90	125	520	585
b)	222	-	125	-	-
b)	170	-	-	-	480
c)	63	40	-	105	*

a) Present data

b) Data from Burchard (1963)

c) Data from Rao and Foster (1963)

* Determined in presence of unknown KCl concentration.

KOH (Burchard, 1963).

It is interesting to note that the 'swamping effect' of the K^+ ions, reaching ultimately in Θ-solvent behaviour, is only an effect in alkali media where the amylose molecule is ionised. The presence of the ionised hydroxyl groups (on C_2 and C_3) is therefore essential to the ring conformational change in presence of K^+ ions, especially at Θ-and near Θ-conditions. Some form of close-range ionic attraction with K^+ ions is, therefore, possibly involved between the C_2 and C_3 ionised groups as well as gegen-ion activity neutralising long-range interactions. This close-range attraction leading to 3B (or C1) → B1 conformational changes where the C_2 and C_3 substituents are closer, would be especially evident at, and near, Θ conditions, where $[\eta]$ is lower than in neutral solutions, and a completely all B1 conformation is suspected. In its stable neutral solution conformation, amylose may be considered as being in a kind of potential-well from which it must rise out (by addition of alkali) before further changes can take place.

Cowie (1963) found amylose to be at its precipitation point in DMSO/aqueous 0.5M KCl (1:3) which was therefore acting as a Θ-solvent at 25°C. He explained the Θ-solvent activity in the following terms: DMSO is an ionising agent on the hydroxyl groups of amylose, and the presence of KCl would contract the molecule to its unperturbed dimensions, the amylose chain being drawn into a tighter form by the potassium ion - hydroxyl interactions. This is precisely the same mechanism as indicated in the aqueous Θ-solvents, and the systems appear analogous.

It should be stressed that the aqueous Θ-solvents detailed here are only valid at 25°C - at a higher temperature, a higher concentration of salt would be required to attain Θ conditions. It is also appreciated that these solvents have not been prepared by the method of Schultz and Flory (1953). They suggest that the percentage composition of solvent and non-solvent at the precipitation point, be determined over a wide concentration range for polymer fractions of different molecular weights, and the results extrapolated to zero concentration and infinite molecular weight. This procedure with solid KCl as the 'non-solvent' would present obvious difficulties.

Amylose in buffer solutions:- The results of viscosity measurements in buffers (Fig. 3.4) are similar to those in neutral solutions, but indicate a fall in the $[\eta]$ -values between pH 9-10, for the buffer systems that contain borate. This phenomenon is not an ionic strength effect, as it is present in buffers of constant ionic strength. The higher $[\eta]$ -values in the boric acid/KOH buffer system probably indicate a different ring conformation (more 3B or C1) than in the other buffers, which all contain KCl. The presence of the K^+ ions may have a 'swamping effect' in an analogous manner to solutions of higher pH. The characteristic well in $[\eta]$ -values is, however, still present.

The optimum pH for borate to complex with D-glucose is pH 9.2-9.7 (Smith and Montgomery, 1959), complexing favouring cis- rather than trans- hydroxyl groups. There is also a possibility of the formation of monobasic borospirans and cross-linking

between neighbouring polymer molecules. It is tentatively suggested that some kind of borate complexing is responsible for these lower $[\eta]$ -values. This could occur either between the C_2 and C_3 hydroxyl groups of the glucose ring, forcing it into a B1 form, or through hydroxyl groups of neighbouring glucose rings creating a kind of 'steric compression'.

A routine solvent for Amylose characterization:- The most suitable solvent for the routine viscosity characterization of amylose is 0.15M KOH, for the following reasons: (a) the $[\eta]$ -value is a maximum, facilitating the fine distinction between different samples; (b) the broad maximum between 0.1M and 0.2M KOH means that the solvent may be prepared easily without standardization; (c) any degrading enzyme inadvertantly introduced in the solution would be inactive in 0.15M KOH.

Cowie (1960), Everett and Foster (1959) and Burchard (1963) have used DMSO as a solvent, but its hygroscopic nature and lower solvent power render it inferior to 0.15M KOH. Schultz and Reitzer (1962), have also suggested a sodium iron-tartrate complex as a routine viscosity solvent. However, the solvent is difficult to prepare and store without undergoing modification. Foster and Hixon (1943) used ethylene diamine and Meyer et al. (1940) used hydrazine hydrate as solvents for amylose. However, both solvents appear to degrade amylose and are therefore also unsuitable.

3B. THE DEGRADATION OF AMYLOSE IN ALKALI

Degradation is a possible effect that might be complicating viscosity measurements in alkali. The alkaline degradation of amylose at high temperatures is well-known (Bottle *et al.*, 1953), whilst Wolff *et al.* (1950) and Lansky *et al.* (1949) have suggested that at low temperatures the effect is negligible. It was decided to verify this latter claim over a range of alkali concentrations.

Experimental:- The amylose sample was dissolved in alkali, and the degradation at three concentrations of polysaccharide was studied at 25°C in an air atmosphere. Results were plotted as change in $[\eta]$ -value with time.

Results and discussion:- The results (Fig. 3.5) show that degradation is more pronounced at the lower alkali concentrations. However, degradation is so small as not to effect normal viscosity determinations which are completed within an hour of solution.

Similar experiments at 2°C showed no change in $[\eta]$ after 72 hours, but a 20% fall in $[\eta]$ after 25 days, in 0.15M KOH.

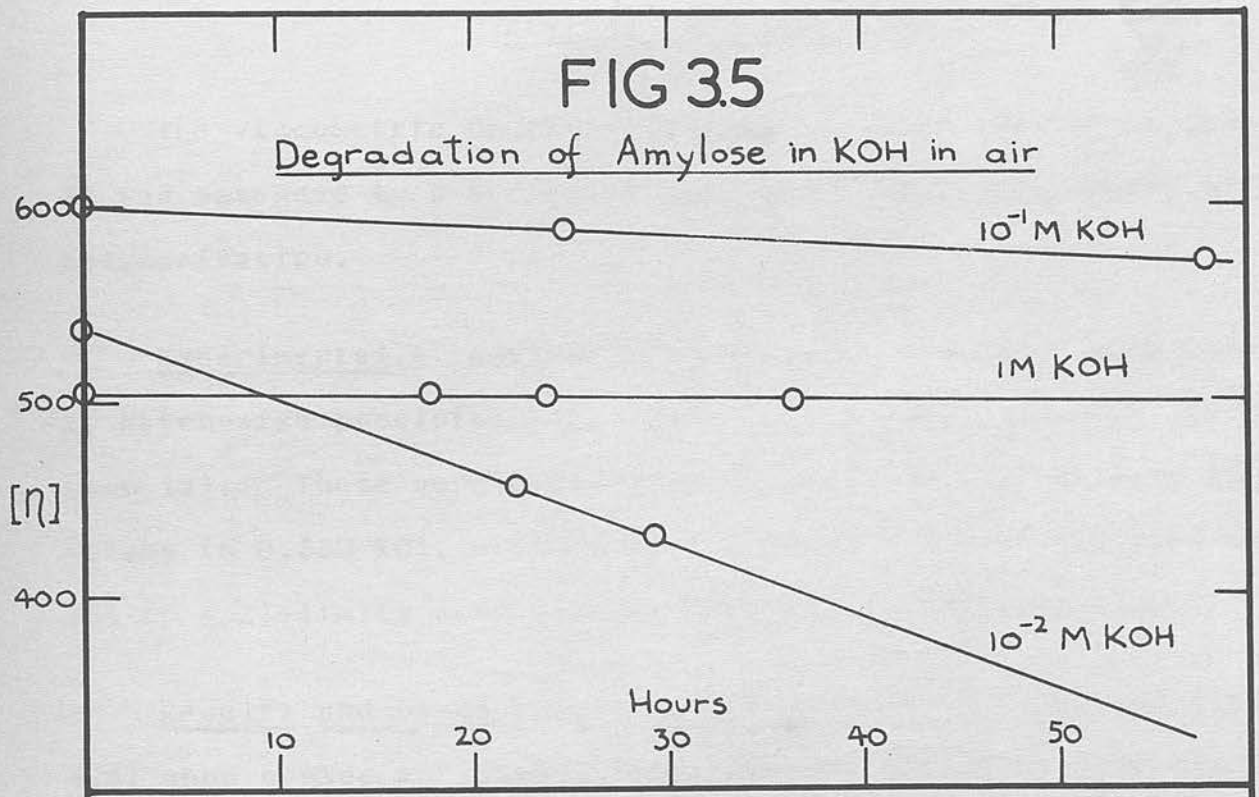

Doublet of two loosely coiled polymer molecules, (Gillespie, 1963)

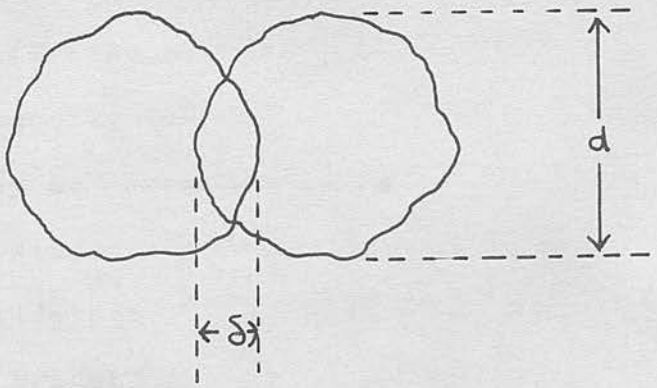

3C. THE VISCOMETRIC CHARACTERIZATION OF AMYLOSE SUBFRACTIONS.

The viscometric characterization of total amylose in Section 3A was extended to a series of samples of differing degree of polymerisation.

Experimental:- Amylose subfractions (P-series) were obtained by batch-wise precipitation, (Everett and Foster, 1959 - see Section 1B). These were characterized with respect to their $[\eta]$ - values in 0.33M KCl, 0.15M KOH, and 1M KOH. β-amylolysis limits and (β + Z)-limits were also determined for each fraction.

Results and Discussion:- $[\eta]$ -values of fractions (Table 3.5) show a wide variation, indicative of the broad molecular weight distribution of natural potato amylose. The 'coulombic' expansion and contraction discussed for total amylose, is evident in all the fractions.

The range in β-amylolysis limits (Table 3.6) illustrates the well-known presence in amylose of an anomaly or a barrier to β-amylase action (Greenwood, 1960). This anomaly is concentrated in the high viscosity fractions, and it has been suggested that this barrier may be 'branched amylose', although phosphate groups, non-α-1,4 glycosidic links and oxidised glucose units cannot be ruled out. Gillespie (1963) has shown that Huggin's constant k increases with branching. k is generally larger for the anomalous fractions, indicating perhaps some branching, but this tendency is masked somewhat by the opposite effect of k increasing

TABLE 3.5

The viscometric characterization of amylose subfractions

Fraction	0.33M KCl		0.15M KOH		1M KOH	
	$[\eta]$	$k^{a)}$	$[\eta]$	$k^{a)}$	$[\eta]$	$k^{a)}$
P1	350	0.76	1010	0.42	810	0.40
P2	295	0.84	855	0.44	695	0.46
P3	255	0.85	770	0.39	550	0.45
P4	220	0.80	600	0.38	510	0.40
P5	190	-	510	0.36	450	0.36
P6	160	-	415	0.38	380	0.32
P7	150	-	390	0.39	355	0.33
P8	135	-	315	0.38	320	0.36
P9	110	-	285	0.38	250	0.35
P10	105	-	250	0.35	205	-
P11	92	-	210	-	205	-
P12	66	-	135	-	110	-
P13	52	-	110	-	70	-
P14	38	-	75	-	65	-
Total	210	0.80	575	0.41	480	0.39

a) Huggin's constant.

TABLE 3.6

The degree of polymerization and enzymic characterization of amylose subfractions

Fraction	$\overline{D.P.}$ [a]	$[\beta]$ [b]	$[\beta + Z]$ [c]
P1	6000	84	100
P2	5100	84	101
P3	4100	86	99
P4	3800	86	99
P5	3300	88	100
P6	2800	89	99
P7	2600	91	100
P8	2400	93	100
P9	1850	95	100
P10	1500	94	101
P11	1500	98	100
P12	800	99	100
P13	500	100	99
P14	500	100	100
Total	3500	90	100

a) Calculated from $\overline{D.P.} = 7.4\,[\eta]_{1M\ KOH}$

b) β-amylolysis limit

c) $(\beta + Z)$ limit.

as the molecular size decreases (Table 3.5). Fractions P11-P14 have β-amylolysis limits of 100%, and therefore consist of linear-amylose. This branched material is unlikely to be contaminating amylopectin, as the (β + Z) limits indicate 'pure' amylose fractions. This anomaly is studied in detail in later sections.

Cowie and Greenwood (1957), have found the relation

$$\overline{D.P.} = 7.4 \times [\eta] \qquad 3.1$$

for amylose in 1M KOH, where $\overline{D.P.}$ = degree of polymerisation. Although the relation was obtained from acid degraded material and may be in error, calculated $\overline{D.P.}$ values are shown in Table 3.6 to give some indication of relative size.

Assuming the Mark-Houwink equation to apply to this fraction series, (which is not unlikely since there is a <u>regular</u> gradation of β-amylolysis limit and viscosity), we may write

$$[\eta]_{KCl} = AM^a \qquad 3.2$$

$$[\eta]_{KOH} = BM^b \qquad 3.3$$

for amylose in KCl and KOH respectively. On elimination of M,

$$\log[\eta]_{KOH} = {}^b/_a \log[\eta]_{KCl} + (\log B - {}^b/_a \log A) \qquad 3.4$$

$\log[\eta]_{KOH}$ is thus a linear function of $\log[\eta]_{KCl}$ with a gradient ${}^b/_a$. Such a plot for amylose in 0.33M KCl and 0.15M KOH is shown in Fig. 3.6, where ${}^b/_a = 1.23$, which is in excellent agreement with a similar plot obtained by Banks (1960) for a different

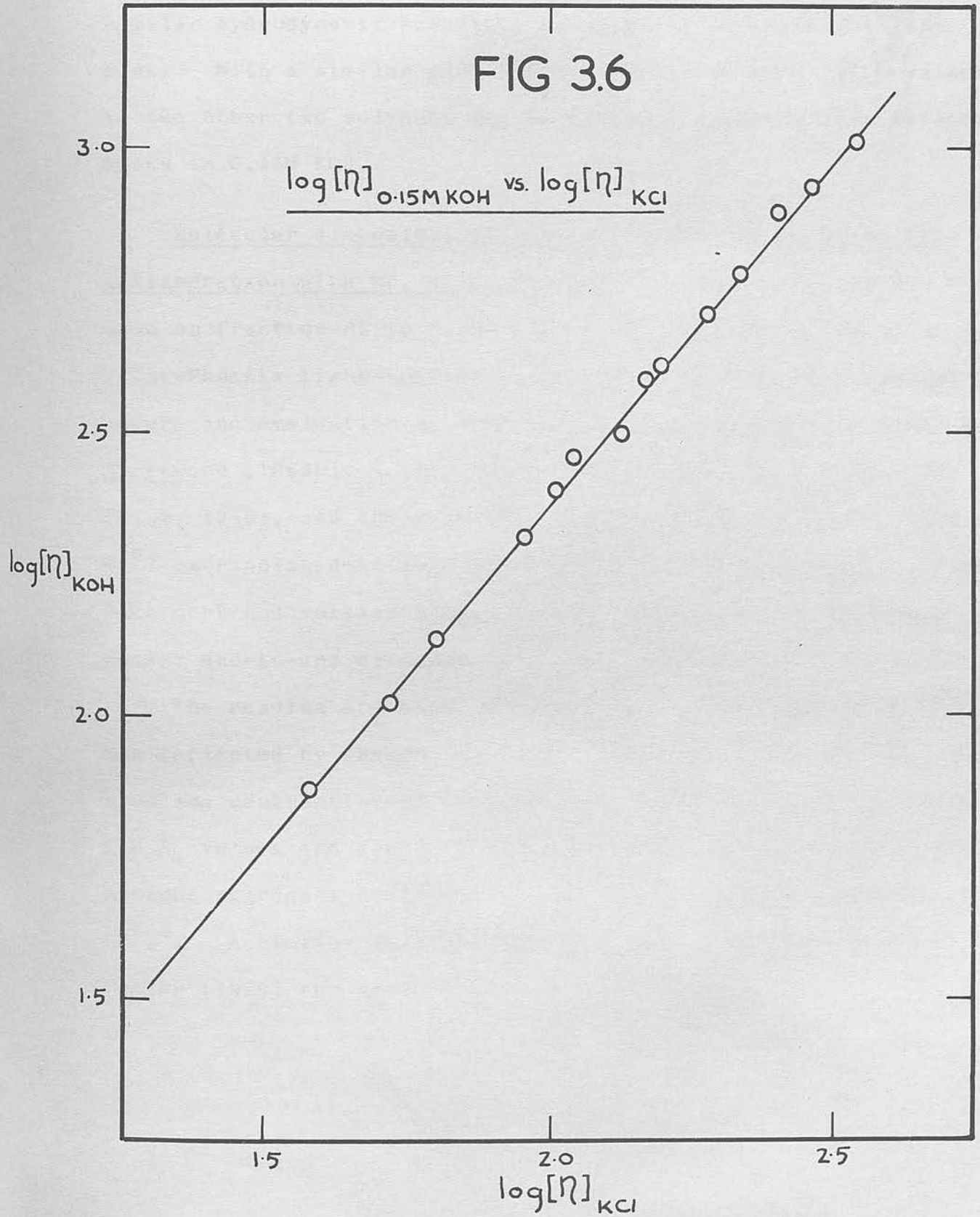
FIG 3.6
log [η]0·15M KOH vs. log [η]KCl
3·0
2·5
2·0
1·5
log[η]KOH
1·5
2·0
2·5
log[η]KCl

series of potato amylose fractions. That the fractions are of similar hydrodynamic behaviour is shown by the straight line plot. With a similar plot for amylose in 1M KOH, $[\eta]$ -values in the other two solvents may be calculated merely from measurements in 0.15M KOH.

Molecular dimensions of Amylose in aqueous solution (in collaboration with Mr. R. Geddes):- Turbidity measurements were made on fraction P5 in 0.33M KCl, 0.15M KOH and 1M KOH using a Brice-Phoenix light-scattering photometer. The experimental procedure and evaluation of results has been described by Banks and Greenwood (1963b). The results were plotted on a Zimm plot (Zimm, 1948), and the experimental points at high angles (above 45^{o}) extrapolated to zero angle and zero concentration. From the intercept and initial slope, values of $\bar{M}_w$ and the root-mean-square end-to-end distance $(\bar{r}^2)^{\frac{1}{2}}$ were calculated.

The results are shown in Table 3.7. The changes in $[\eta]$ are reflected by changes in $(\bar{r}^2)^{\frac{1}{2}}$, and clearly confirm the expansion and contraction of the amylose molecule in alkaline solution. The $\bar{M}_w$ values are constant in each solvent indicating that no serious aggregation effects are responsible for the changes in $(\bar{r}^2)^{\frac{1}{2}}$. A similar variation in $(\bar{r}^2)^{\frac{1}{2}}$ was found by Everett and Foster (1959) for amylose in 0.5M KCl and 1M KOH.

TABLE 3.7

Results of lightscattering measurements on fraction P5 in aqueous solution

Solvent	$10^{-6}.\bar{M}_w$	$[\eta]$	$(\bar{r}^2)^{\frac{1}{2}}_A$
0.33M KCl	5.6	190	1010
0.15M KOH	5.6	510	1300
1M KOH	5.6	450	1140

3D. THE SHEAR DEPENDENCE OF VISCOSITY

All viscosity measurements have been made in modified Ubbelohde capillary viscometers which have an average shear rate $\bar{G}$ = ca 1200 sec^{-1}. It is important to know if $[\eta]$ -values at zero shear are significantly different. Shear effects are important for rigid polymer chains (e.g. cellulose derivatives) of a sufficiently high molecular weight - generally $\bar{M}_w > 2 \times 10^5$ (Lohmander, 1964). Conversely for flexible polymer chains, like amylose, shear effects are relatively unimportant. Although a shear dependence for amylose has been reported by Cowie (1960) for $[\eta] > 300$, and a correction applied by Everett and Foster (1959), no satisfactory determinations at very low shear rates have been made to date.

Experimental:- The viscosities of amyloses of varying $\overline{D.P.}$ (P-fraction series - see Section 1B) in 0.33M KCl, 0.15M KOH and 1M KOH were measured at low shear rates. These values were compared to those obtained at $\bar{G}$ = 1200 sec^{-1} (Table 3.5). For measurements at shear rates below 50 sec^{-1} a Couette viscometer was used. Its manipulation and characterization have been described in Section 2B. As a check, $[\eta]$ -values at different shear rates were also determined in a capillary shear viscometer (see Section 2A).

Results and Discussion:- The results (Tables 3.8 and 3.9, and Fig. 3.7) show no shear dependence of $[\eta]$ between $\bar{G}$ = 0-1200 sec^{-1} even for the highest $\overline{D.P.}$ sample (fraction P1) available. A slight gradient dependence of Huggin's constant k is however

TABLE 3.8

$[\eta]$ of amylose fractions at zero shear from measurements in Couette viscometer

Fraction	$[\eta]$		
	0.33M KCl	0.15M KOH	1M KOH
P1	360	1040	790
P2	310	855	690
P3	250	760	520
P4	220	-	510
P5	190	510	450
P6	-	-	380
P8	-	310	-
P11	-	210	-

TABLE 3.9

$[\eta]$ and Huggin's constant of fraction P1 at various shear rates

(Fraction P1) $\bar{G}$ in sec^{-1}	0.33M KCl		0.15M KOH		1M KOH	
	$[\eta]$	k	$[\eta]$	k	$[\eta]$	k
0[a]	360	1.00	1040	0.62	810	0.61
100[b]	355	0.75	1010	0.46	810	0.45
1200[b]	350	0.76	1010	0.42	810	0.40

a) Measured in Couette viscometer

b) Measured in capillary viscometer.

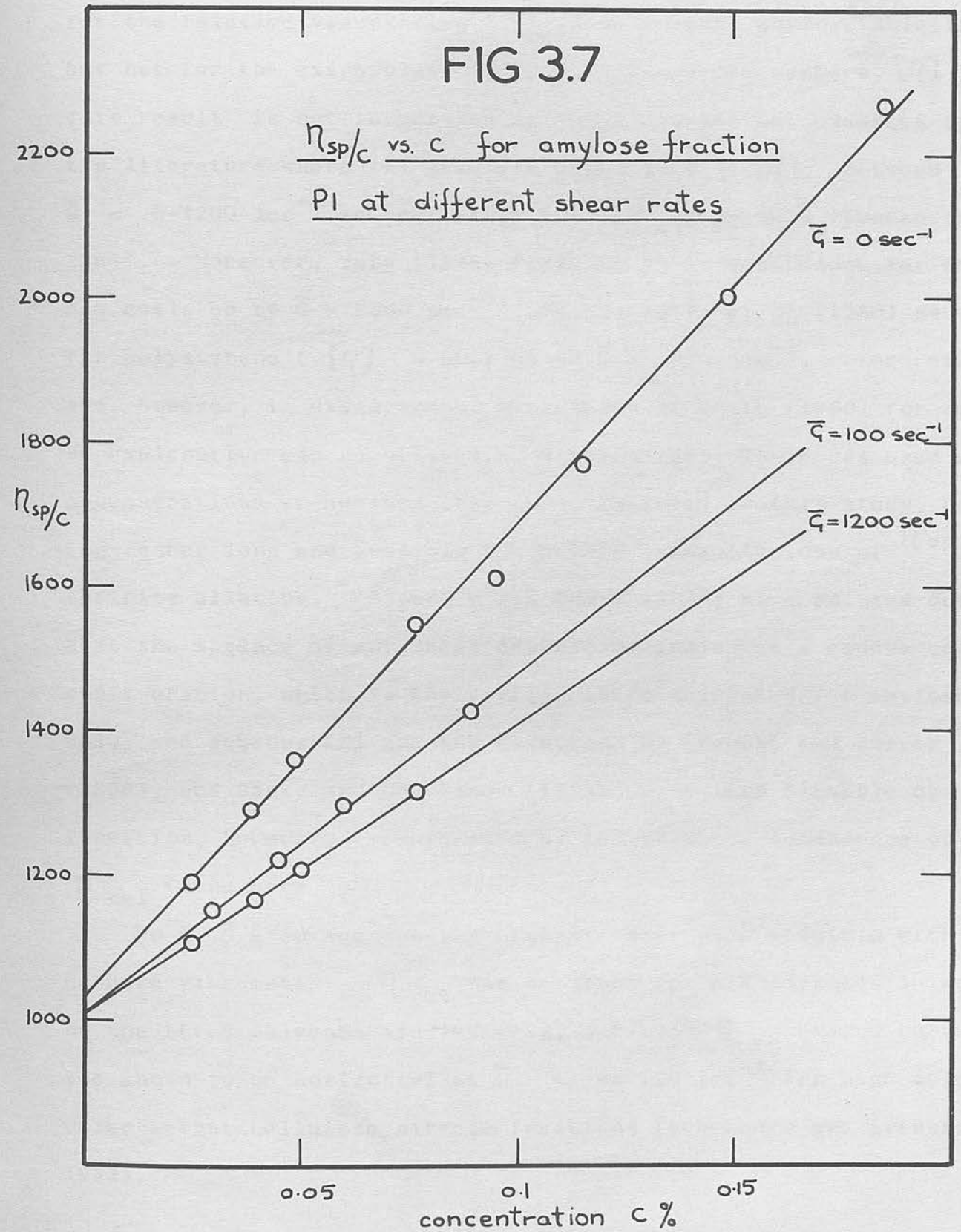
FIG 3.7
η_{sp}/c vs. c for amylose fraction
P1 at different shear rates
$\bar{G} = 0\ sec^{-1}$
$\bar{G} = 100\ sec^{-1}$
$\bar{G} = 1200\ sec^{-1}$
2200
2000
1800
1600
1400
1200
1000
η_{sp}/c
0.05
0.1
0.15
concentration c %

observed in this shear range, i.e. there is a shear dependence for the relative viscosities (η_{rel}) of aqueous amylose solutions, but not for the extrapolated intrinsic viscosity numbers, $[\eta]$. This result is not surprising as there are several examples in the literature where the gradient dependence of $[\eta]$ between $\bar{G}$ = 0-1200 sec^{-1} is negligible for $[\eta]$ < ca 3000 (Lohmander, 1964). Moreover, Yang (1958) finds no shear dependence for random coils up to $\bar{G}$ = 5000 sec^{-1}, and Passaglia et al (1960) none for polystyrene ($[\eta]$ = 500) up to $\bar{G}$ = 2000 sec^{-1}. The results are, however, in disagreement with those of Cowie (1960) for which no explanation can be offered. Nevertheless, Cowie has used higher concentrations of amylose than those employed in this study, rendering rather long and possibly inaccurate extrapolations of $\eta_{sp}/_c$ to infinite dilution. Peterlin and Copic (1956) have pointed out that the absence of any shear dependence indicates a random coil configuration, which is the configuration suggested for amylose in DMSO, and aqueous KCl and KOH solutions by Everett and Foster (1959), and Banks and Greenwood (1963b). A less flexible conformation, however, is suggested by the gradient dependence of η_{rel} found here.

Up to $\bar{G}$ = 50 sec^{-1} - the highest shear rate possible with the Couette viscometer - η_{rel} was constant for all amyloses in any of the three solvents studied (Fig. 3.8). η_{rel} vs. $\bar{G}$ curves are known to be horizontal at $\bar{G}$ < ca 200 sec^{-1} for high molecular weight cellulose nitrate fractions (Lohmander and Svensson, 1963).

FIG 3.8

η vs. $\bar{G}$ for amylose fractions

in various solvents

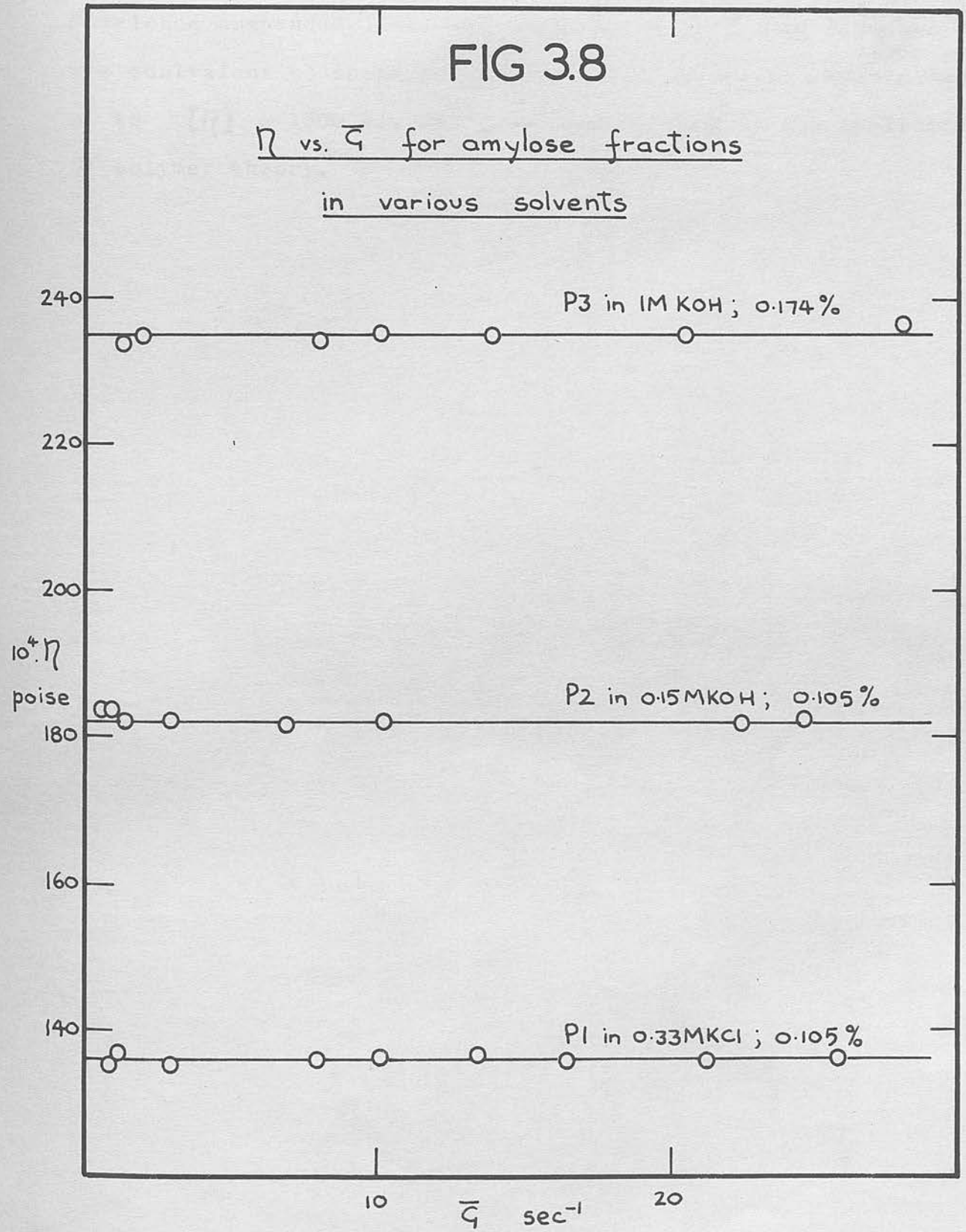

Conclusions:- $[\eta]$ -values measured in the more convenient Ubbelohde suspended level viscometers (where $\overline{G}$ = ca 1200 sec^{-1}), are equivalent to those measured at zero shear for amylose samples up to $[\eta]$ = 1000 ml. gm^{-1}, and may be used in the application of polymer theory.

SECTION 4

THE SUBFRACTIONATION OF AMYLOSE

4A. THE SUBFRACTIONATION OF TOTAL-AMYLOSE

4A. THE SUBFRACTIONATION OF TOTAL-AMYLOSE

Hess (1940) first proposed that amylose was not a completely linear α-1,4 linked glucan. This was confirmed by Peat et al. (1949) who showed that amylose was incompletely degraded by the enzyme β-amylase, but completely degraded by Z-enzyme. β-amylase is highly specific, and its degrading action is halted by the slightest anomaly in the amylose chain. Without care, such anomalies as oxidation at the C_2, C_3 or C_6 glucose hydroxyl groups may easily be introduced during the starch fractionation procedure (Banks et al., 1959a, Aspinall and Greenwood, 1962). Otherwise, the barrier to β-amylolysis may be a natural phenomenon, and be any of (a) a branch point, (b) a non α-1,4 glycosidic link, or (c) a phosphate ester group at the C_6 hydroxyl. The latter 'barrier' may be removed from the amylose chain artificially with phosphatase, and experiments by Banks and Greenwood (1961) showed no increase in the β-amylolysis limit after such treatment. A non-α-1,4 link seems most unlikely, which leaves the question of whether native amylose contains some branch points. This has been discussed by Greenwood (1960).

Subfractionation experiments have shown that this 'barrier' to β-amylolytic action is not confined to all amylose molecules (see for example, Section 3C). Amylose may be readily subfractionated, into samples with varying β-amylolysis limits, on successive aqueous leaching of starch granules (Greenwood and Thomson, 1962); with increasing temperature, amylose of increasing molecular size, shown by the limiting viscosity number, $[\eta]$, and decreasing β-amylolysis

limit is obtained. Banks (1960) also subfractionated total-amylose by the method of Everett and Foster (1959), and obtained fractions of varying β-amylolysis limit. These were characterized with respect to viscosity and molecular weight, and a Mark-Houwink plot was constructed from the results, which formed a straight line with the linear fractions. Points corresponding to the anomalous fractions - those with a β-amylolysis limit of less than 100 - fell below this line. This is strong evidence for branching in the anomalous fractions. Moreover, Banks showed that these fractions were heterogeneous on ultracentrifugation.

The subfractionation procedure for potato total-amylose was examined in more detail, with particular attention to the occurrence and distribution of anomalous fractions. Amyloses isolated from other botanical sources are also compared.

EXPERIMENTAL

Subfractionation of amyloses:- Amylose isolated from potato starch (var. Pentland Crown) was subfractionated by the method of Everett and Foster (1959). This has been described in Section 1B, where variations in the general procedure, by using acetone, ethanol and benzene as precipitants, yielded fraction series PA-, PE-, and PB- respectively.

Dried amylose was dispersed in KOH and subsequently neutralised with HCl on a pH-meter to give a solution in 0.14M KCl. Ethanol was added in a stepwise manner to the solution at 20°C. Precipitates (EK-fraction series) were removed on a centrifuge, dispersed in boiling deoxygenated water, and then reprecipitated as the butan-1-ol complex.

Amylose subfractions, which had been isolated by Dr. J. Thomson, the late Mr. I. Phillips, and Dr. A. W. McGregor from iris germanica starch, wheat starch, and potato starch (var. Redskin) respectively, were also examined in this investigation. Their properties, obtained by the above workers, are shown in Table 4.1.

Characterization of subfractions:- The limiting viscosity number in 0.15M KOH was determined on the butan-1-ol complex of the PA-, PE-, PB- and EK- fractions. These subfractions were also characterized by their β-amylolysis limits, $[\beta]$, and (β + Z)- limits, $[\beta + Z]$, as described in Section 2G. Sedimentation measurements on the complexes of all subfractions were made in 0.16M KCl at 39, 460 r.p.m. The calculation of S and S_o values has been described in Section 2C.

TABLE 4.1

Properties of subfractions obtained from various amyloses by dimethylsulphoxide/ethanol precipitation[x)]

Iris germanica amylose					Wheat amylose					Potato (var.Redskin) amylose			
Fraction[a)]	%[b)]	$[\eta]^{*}$[)]	β	β+Z	Fraction[a)]	%[b)]	$[\eta]^{*}$[)]	β	β+Z	Fraction[a,c)]	$[\eta]$	β	β+Z
I 1	1.9	540	62	101	W 1a[d)]	0.9	-	-	-	PR 1a	1200	58	101
I 2a	3.5	410	65	100	W 1b	3.7	560	66	100	PR 1b	700	66	101
I 2b	2.6	360	100	101	W 2a	11.6	535	71	101	PR 2	800	65	100
I 3a	2.1	380	70	101	W 2b	10.9	310	94	101	PR 3	525	72	99
I 3b	31.5	320	88	101	W 3a	12.1	410	80	101	PR 4	480	76	99
I 3c	9.4	260	100	100	W 3b	8.0	330	85	101	PR 5	410	82	101
I 4a	11.4	280	86	100	W 3c	5.6	265	99	100	PR 6	300	95	99
I 4b	10.4	150	92	100	W 4	13.4	210	94	100	PR 7	160	100	100
I 5	10.4	130	95	101	W 5	9.7	175	96	101	PR 8	90	100	100
I 6	11.4	110	95	101	W 6	10.9	130	99	100				
I 7	3.5	85	100	100	W 7	6.2	90	99	100				
I 8	1.9	80	100	100	W 8	7.0	60	100	101				
$\sum$-values[e)]	100	240	86	-	$\sum$-values[e)]	100	270	88	101	$\sum$-values[e)]	-	-	-
Orig. amylose	100	240	85	100	Orig. amylose	100	270	86	100	Orig. amylose	550	80	100

TABLE 4.1 contd.

a) a, b, c, represent refractionation products.

b) Expressed as percentage of total polysaccharide recovered.

c) Fraction weights were not determined as samples were obtained directly as butanol-complexes.

d) Insoluble fraction.

e) Calculated assuming percentage loss of each sample is identical.

*) Measured in 1M potassium hydroxide.

x) Results from Thomson (1961), Phyllips (1961), McGregor(1964).

RESULTS AND DISCUSSION

The efficiency of subfractionation:- Results of the subfractionation with a varying precipitant are shown in Table 4.2. As indicated in Section 1B, the efficiency of subfractionation is in the order acetone > ethanol > benzene, and this conclusion is substantiated on consideration of the physical properties of the separate fractions later. The most important feature, however, of these subfractionations is the agreement between the summated values of the physical properties of each fraction ($\sum$-values), and the corresponding values for the original sample. This is in agreement with the results of Thomson (1961), Phillips (1961) and McGregor (1964) shown in Table 4.1, and shows that the amyloses have undergone no degradation or modification during the subfractionation procedure. However, in the ethanol/KCl subfractionation (Table 4.3), no $[\eta]$ -value higher than that of the parent amylose was obtained, indicating some degradation. Moreover, the inferiority of this subfractionation procedure over Everett and Foster's (1959), is shown by the large size of fraction EK1.

Subfractionation and its relation to structural anomalies:- A study of Table 4.1 and 4.2 shows that not only are the amyloses subfractionated with respect to molecular size, but also β-amylolysis limit. Thus some of the subfractions are anomalous, or contain a barrier to β-amylolytic action. In common with the aqueous leached fractions of Greenwood and Thomson (1962), this structural anomaly is associated primarily with the high molecular weight fractions, the lower molecular-weight samples being essentially

TABLE 4.2

Properties of subfractions of potato (var. Pentland Crown) amylose obtained by precipitation from dimethylsulphoxide solution*

Acetone[a]				Ethanol[a]				Benzene[a]			
Fraction[b]	%[c]	$[\eta]$	$[\beta]$	Fraction[b]	%[c]	$[\eta]$	$[\beta]$	Fraction[b]	%[c]	$[\eta]$	$[\beta]$
PA 1	17.1	1040	85	PE 1a	10.8	1205	70	PB 1a	23.9	1040	81
PA 2	13.2	905	92	PE 1b	9.7	1135	73	PB 1b	2.8	-	84
PA 3	16.1	555	99	PE 1c	6.4	615	98	PB 1c	25.0	775	91
PA 4	20.2	460	100	PE 2a	15.5	690	82	PB 1d	14.2	490	98
PA 5	4.1	-	99	PE 2b	3.6	555	80	PB 2	8.5	530	94
PA 6	16.1	280	99	PE 2c	5.9	410	85	PB 3	11.9	340	96
PA 7	13.1	135	99	PE 3	32.0	340	97	PB 4	2.3	-	98
				PE 4	16.1	120	99	PB 5	11.4	155	101
$\sum$-values[d]	100	570	95	$\sum$-values[d]	100	560	89	$\sum$-values[d]	100	650	92
Original sample	100	575	92	Original sample	100	575	92	Original sample	100	575	92

*) The $(\beta + Z)$-limit was 100 for all subfractions

a) Precipitant

b) a, b, c represent refractionation products

c) Expressed as the percentage of total amylose recovered

d) Calculated assuming percentage loss of each sample is identical.

TABLE 4.3

Properties of subfractions of potato (var. Pentland Crown) amylose obtained by ethanol precipitation from KCl solution

Fraction	% ethanol	% a)	$[\eta]$	S_s b)	S_f b)
EK1	20.6	83.5	560	10.3	29
EK2	20.7	5.5	345	7.6	*
EK3	24.6	7.0	230	4.7	-
EK4	29.8	4.0	125	3.1	-
$\sum$-value c)			510		
Orig. amylose			575		

a) Expressed as the percentage of total amylose recovered

b) Determined in 0.16M KCl at a concentration of ca 0.2%

c) Calculated assuming percentage loss of each sample is identical

* Not measurable, minor peak present as small shoulder.

linear.

The distribution of this anomalous material in a fraction series, is also dependent on the precipitant used in the subfractionation procedure (Table 4.2). With acetone it is concentrated in the first two fractions, whereas with benzene it is distributed over almost all the fractions; the ethanol precipitated series is intermediate between the two. It would seem that the anomalous material is less soluble in the more polar acetone/DMSO solvent system.

It should be noted that contaminating branched material (amylopectin) could not be responsible for the incomplete degradation by β-amylase, as (β +Z)-limits for all fractions were 100 - indicating 'pure amylose' (Banks, Greenwood and Jones, 1960).

Ultracentrifugation of amylose and its subfractions:- The concentration dependence of sedimentation coefficient, S, was studied for two linear amylose fractions in 0.16M KOH, 0.16M KCl and 0.50M KCl at pH-12 at 25°C (aqueous Θ-solvent). The results (fig. 4.1), show a significant concentration dependence for the polysaccharide in alkali, which is reduced in aqueous salt solution, and absent in aqueous Θ solvent. It should be noted here that this concentration independence of S in this latter solvent is additional evidence that it is indeed an ideal Θ-solvent (see Section 3A).

However, the most important feature of these studies was that, although all fractions appeared homogeneous in alkali, anomalous fractions showed evidence of heterogeneity on sedimentation

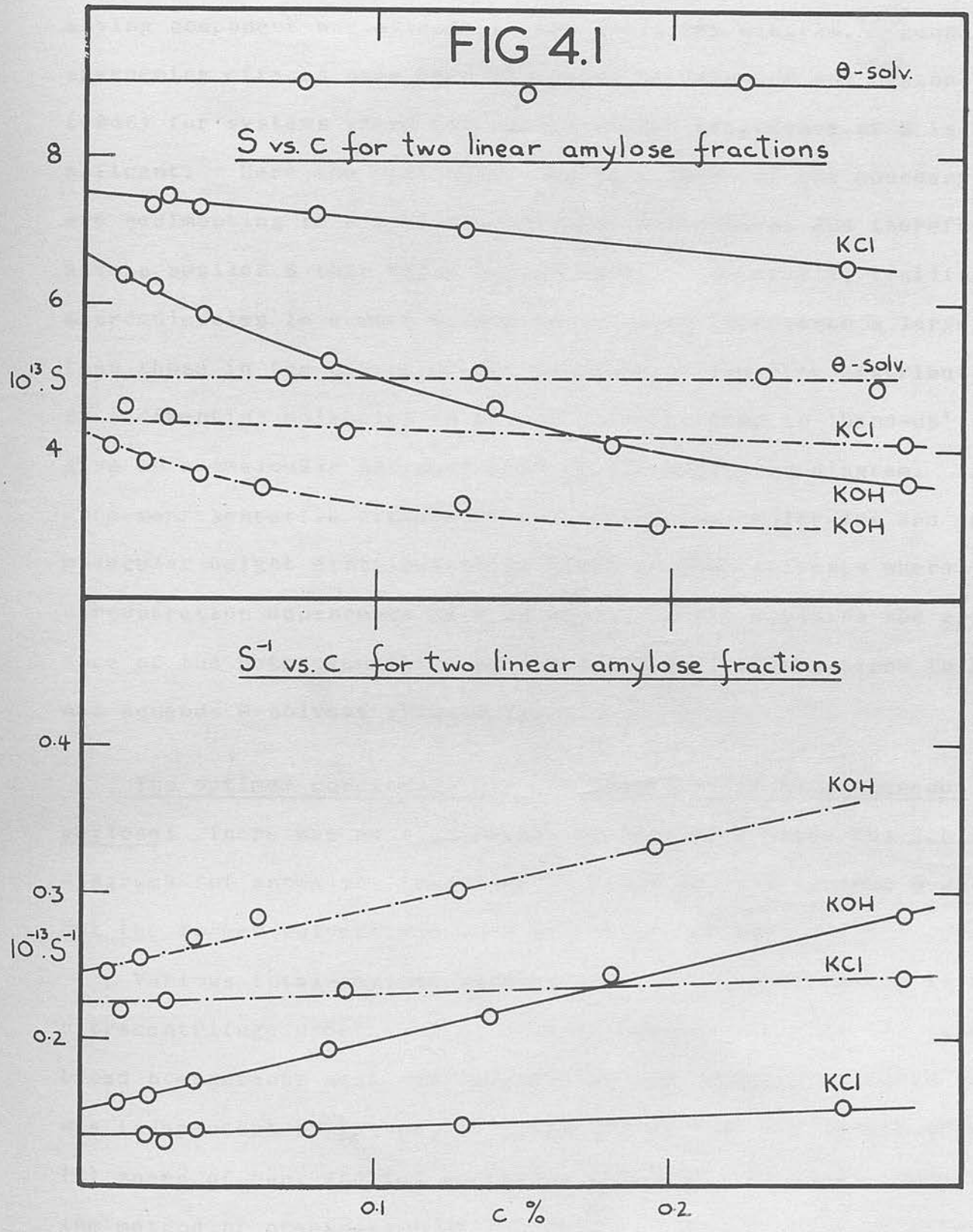
FIG 4.1
θ-solv.
S vs. C for two linear amylose fractions
8
6
$10^{13}.S$
4
KCl
θ-solv.
KCl
KOH
KOH
S^{-1} vs. C for two linear amylose fractions
0.4
0.3
$10^{-13}.S^{-1}$
0.2
KOH
KOH
KCl
KCl
0.1
C %
0.2

velocity in 0.16M KCl and aqueous Θ-solvent; i.e. a minor fast-moving component was evident in the Schlieren diagram. Boundary sharpening effects have been discussed by Johnston and Ogston (1946) for systems where the concentration dependence of S is significant. Here the macromolecules just ahead of the boundary are sedimenting in a more concentrated environment and therefore have a smaller S than those behind them. Conversely, trailing macromolecules in a more dilute environment experience a larger S than those in the centre of the boundary. Thus the distribution of sedimenting molecules in a good solvent, tend to 'band-up' and give an anomalously narrower peak in the Schlieren diagram. A more representative picture of the sedimenting molecules and their molecular weight distribution is given in poor solvents where the concentration dependence of S is small. This explains the appearance of the heterogeneities in anomalous amylose fractions in KCl and aqueous Θ-solvent (Fig. 4.2).

The optimum conditions for the detection of heterogeneous amylose: There was no significant difference between the Schlieren diagrams for anomalous fractions in 0.16M KCl and aqueous Θ-solvent, but the former solvent was more convenient to use.

Various total-amylose samples were spun qualitatively in the ultracentrifuge under various solvent conditions. In all cases a broad homogeneous peak was observed on the Schlieren diagram which was independent of (a) pH, (b) molarity of KCl, (c) length of run, (d) speed of run, and (e) whether a Θ-solvent was used. Moreover, the method of preparation of the solution had no apparent effect;

FIG 4.2

Sedimentation of fraction PA1 in KCl (lower) and KOH (upper)

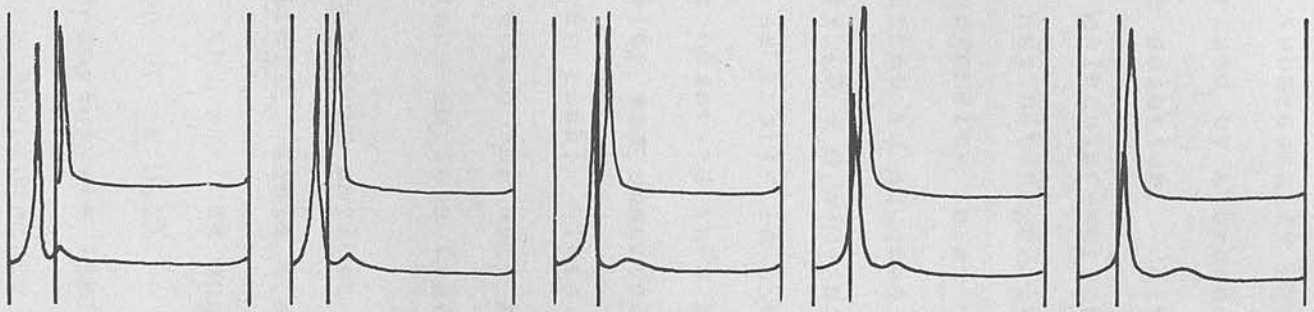

FIG 4.3

Typical schlieren patterns for the sedimentation of amylose subfractions in KCl

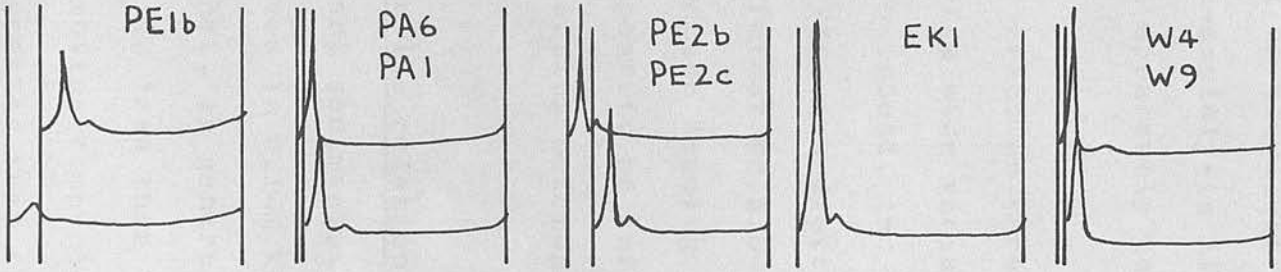

i.e. whether the butan-1-ol complex was dissolved directly in the required solvent, or the corresponding dry amylose was dispersed in alkali and subsequently neutralised. Total-amylose is therefore characterized by a broad homogeneous peak on ultracentrifugation in saline solution. Although it has a β-amylolysis limit of < 100, the molecular-weight distribution is apparently too broad to show any heterogeneity.

The heterogeneity in an anomalous amylose fraction (Fraction PA1), was apparent in aqueous salt solutions of a wide variation in KCl molarity (0 - 0.33M) and pH (5 - 9.5). Indeed, two peaks were observed as easily in water alone. However, two distinct peaks were not observed in a phosphate/KOH buffer at pH 5.5-7.4; the heterogeneity was observed as a shoulder on the leading edge of the Schlieren peak. This solvent would appear to be inferior to 0.16M KCl, which was used routinely, in detecting heterogeneities in anomalous amylose fractions.

Heterogeneity in amylose subfractions, and its relation to β-amylolysis limit: Table 4.4 shows the apparent sedimentation coefficients for the amylose subfractions dissolved in 0.16M KCl at a concentration of ca 0.2%. It can be seen that, in general, whenever the β-amylolysis limit for the sample is less than 95, the sample shows the presence of a minor fast-moving component with a sedimentation coefficient S_f some 2-4 times greater than that for the main, slower-moving, component, S_s. Some typical Schlieren patterns are shown in Fig. 4.3.

When the β-amylolysis limit is less than 95%, it would appear

TABLE 4.4

Apparent sedimentation coefficients for amylose subfractions dissolved in 0.16M potassium chloride at a concentration of ca. 0.2g/100 ml.

Fract.[a]	[β]	S_s	S_f	Fract.[a]	[β]	S_s	S_f	Fract.[a]	[β]	S_s	S_f
I 1[b]	62	14 →		W 1b	66	13	32	PR1a	58	12.9	27
I 3a	70	7.2	35	W 2b	94	6.7	16	PR2	65	11.0	24
I 4a	86	8.3	22	W 3a	80	11	24	PR6	95	8.6	21
I 5	95	5.0	-	W 4	94	7.6	23	PR7	100	6.7	-
I 7	100	3.6	-	W 8	100	4.5	-	PR8	100	4.0	-
PA 1	85	9.5	17.4	PE 1a[b]	70	11.2 →		PB 1a	81	12.8	-
PA 2	92	11.0	*	PE 1b	73	12.9	23	PB 1b	84	-	-
PA 3	99	12.4	-	PE 1c	98	14	-	PB 1c	91	9.3	-
PA 4	100	8.2	-	PE 2a	82	15	*)	PB 1d	98	6.9	-
PA 5	99	-	-	PE 2b	80	11	26	PB 2	94	8.0	-
PA 6	99	7.9	-	PE 2c	85	7.2	29	PB 3	96	6.2	-
PA 7	99	6.0	-	PE 3	97	6.5	-	PB 4	98	-	-
				PE 4	99	4.6	-	PB 5	101	4.9	-

a) Fractions labelled as in Tables 4.1 and 4.2

b) Pronounced asymmetrical peak

*) Not measurable, minor peak present as shoulder.

that a fraction of relatively narrow molecular-weight distribution is necessary before heterogeneity appears on ultracentrifugation. For example, none of the fractions of potato amylose obtained by precipitation with benzene from DMSO were heterogeneous (PB-series, Table 4.3). This was attributed to the fact that benzene is a 'poor' precipitant (see earlier), which yields fractions with a relatively wide range of molecular weights. Indirect evidence for this is shown by comparing the properties of the PB-fractions with those of the linear PA-fractions. For fractions with comparable values of S_s, the PB- fractions have much greater values of $[\eta]$, and it would appear that the minor fast-component is retarding the movement of the major one, although the heterogeneity is not apparent in the Schlieren pattern. That the sedimentation coefficient of a slower component, sedimenting in the presence of a faster species at a finite concentration, is less than that of the same material when migrating alone, is a consequence of the Johnston-Ogston effect (Schachman, 1959, p. 120). Further, some fractions (e.g. I1 and PE1a) gave an extremely broad asymmetric peak, which indicated incipient heterogeneity.

Some of the fractions obtained by ethanol/KCl fractionation also showed heterogeneity on ultracentrifugation in 0.16M KCl (Fig. 4.3, Table 4.3). This indicates that this phenomenon is not associated with the dimethylsulphoxide treatment of the amyloses.

The areas beneath the Schlieren peaks have been related to the actual concentration of the sedimenting species by Johnston and Ogston (1946), and this is considered in Section 6. However, it was apparent in this investigation that the peak area of the fast-

moving component was related to the β-amylolysis limit of the sample. For example, the apparent concentration ratio of slower- to faster-moving component for fraction PA1, where [β] = 85, was 11, whilst the corresponding ratio for fraction PE1b, where [β] = 73, was 4. If it is assumed that the heterogeneity in the anomalous fractions has a random distribution of branch points, its β-amylolysis limit would be 50%. On this basis, the percentage of non-linear material in the anomalous amylose fractions may be calculated from the relation,

$$\text{percentage} = 2(100 - \beta\text{-limit}).$$

Ultracentrifugal examination of a heterogeneous subfraction after β-amylolysis showed the absence of the major slow-moving component, but the appearance of peak with a sedimentation coefficient intermediate between S_f and S_s. Moreover, this 'β- limit dextrin' showed a distinctly asymmetric Schlieren peak; the implications of this, with regard to the structure of the dextrin, are considered in Section 6. Nevertheless, it seems most probable that the structural anomaly responsible for the incomplete β-amylolysis of amylose, is associated with the fast-moving component, which must correspond to higher molecular weight material.

The distribution of the heterogeneity in total-amylose: The distribution of material containing a barrier to β-amylolysis could not be easily deduced from such experiments, as simple molecular-weight fractionation will only occur for essentially linear series of polymer homologues. If there is any degree of branching in

amylose, the factors governing precipitation will be complex. However, from the sedimentation results presented here, and those of Banks (1960), it can be seen that heterogeneous (branched) amylose has a larger molecular-weight than linear-amylose. This has been estimated by Banks (1960) as ca 5-12 x 10^6.

The presence of aggregates in aqueous amylose solutions: It is well-known that in neutral aqueous solutions, amylose tends to retrograde (Lansky et al., 1949), and Paschall and Foster (1952) and Husemann et al. (1963) have suggested that natural amylose tends to aggregate in aqueous solution. The question therefore arises, as to whether the fast-moving peak observed on ultracentrifugation represents aggregated species. Assuming that β-amylolysis limit determinations are valid, and aggregation to be a general phenomenon, one would expect two peaks on ultracentrifugation for all fractions - and, indeed, for total-amylose if the aggregate was large enough. As this is not the case, (all PB-fractions and other fractions of β-amylolysis limit = 100, show one peak), it seems that the faster-moving minor peak is not due to aggregated amylose. This question of aggregation is important, and is discussed fully in later sections.

Additional evidence on the presence of a natural barrier to β-amylolysis: McKenzie (1964) isolated amyloses from immature potato tubers, and found that the β-amylolysis limit decreased with maturity. He concluded that the anomalous (branched) amylose was being progressively introduced with maturity. This is strong evidence for a natural barrier to β-amylolysis, as any artefact

introduced during the fractionation procedure would be expected to be present to the same extent in each sample.

McGregor (1964) isolated amylose from potato starch by the method of Killion and Foster (1960) and obtained samples that were incompletely degraded by β-amylase - comparable to amyloses obtained by a conventional fractionation procedure (Banks, Greenwood and Thomson, 1959). In McGregor's experiments, the temperature was always at room temperature or below. The introduction of artefacts through oxidation is most unlikely under these conditions, which further indicates a natural modification in amylose.

Precluding any artificial barriers to β-amylolysis, which may be introduced during fractionation, the evidence so far, indicates that native amylose - defined as the fraction of starch that forms a butan-1-ol complex - contains ca 20-40% of material with a structural modification. Kjølberg and Manners (1963) have shown the presence of ca 0.1% of α-1,6 glycosidic linkages in native amylose, by enzymic experiments. In its simplest form, therefore, this modification appears to be limited branching through α-1,6 linkages. Quantitative aspects of fractionation and possible structures for the 'branched amylose' are considered in Section 6.

4B. THE SUBFRACTIONATION OF LINEAR AMYLOSE

To evaluate the detailed hydrodynamic behaviour of a polymer, it is essential to have a homogeneous series of fractions. The measurement of molecular weight, viscosity and sedimentation coefficient on these fractions allows the application of the numerous polymer solution theories, which enables the conformation of the macromolecule to be determined in various solvents. Although several attempts to apply this procedure to amylose have been made, no satisfactory agreement in the molecular parameters has yet been reached. Ideally, the fractions should be monodispersed, homogeneous and cover a reasonably large molecular weight range; the viscosity values should also be determined at zero-shear.

Viscosity-molecular weight relations for amylose:- With the advent of a satisfactory subfractionation procedure, Everett and Foster (1959) found the following Mark-Houwink relations for natural amylose in 0.5M KOH, DMSO, and 0.33M KCl respectively

$$[\eta] = 8.50 \times 10^{-3} \bar{M}_w^{0.76} \qquad 4.1$$

$$[\eta] = 3.06 \times 10^{-2} \bar{M}_w^{0.64} \qquad 4.2$$

$$[\eta] = 1.13 \times 10^{-1} \bar{M}_w^{0.50} \qquad 4.3$$

From the Mark-Houwink exponents, the authors, concluded that amylose behaved as a random coil in 0.33M KCl which acted as a Θ-solvent at 25°C. Everett and Foster used lightscattering of amylose in DMSO to determine their molecular weights, but made no β-amylolysis limit determinations. Banks (1960) has shown that

non-linear amyloses, with β-amylolysis limits of less than 100, have anomalously high molecular weights. The question arises, therefore, whether Everett and Foster's amylose fractions were all linear and homogeneous.

Cowie (1960) applied a viscosity 'shear correction' and measured molecular weights in DMSO by lightscattering to obtain relations for 1M KOH, DMSO and ethylene diamine (EDA) of,

$$[\eta] = 1.8 \times 10^{-3} \bar{M}_w^{0.89} \qquad 4.4$$

$$[\eta] = 1.25 \times 10^{-3} \bar{M}_w^{0.87} \qquad 4.5$$

$$[\eta] = 1.55 \times 10^{-2} \bar{M}_w^{0.70} \qquad 4.6$$

respectively.

Cowie concluded that amylose had a randomly coiled conformation in EDA, but is much more extended in the other two solvents, and there was some evidence for a basic helical form in solution. Apart from the fact that a shear dependence of viscosity for amylose has not been confirmed (see Section 3D), Cowie again, quotes no β-amylolysis limit determinations. These considerations also cast doubt on the conclusion of Cowie (1963), that amylose may exist in at least two configurations from his study of the viscosity behaviour in mixed solvents.

Banks (1960) and Banks and Greenwood (1963b), using enzymically characterized linear-amylose fractions, determined the relations in 0.2M KOH and 0.33M KCl as

$$[\eta] = 6.92 \times 10^{-3} \bar{M}_w^{0.78} \qquad 4.7$$

and

$$[\eta] = 1.12 \times 10^{-1} \bar{M}_w^{0.50} \qquad 4.8$$

respectively. This latter relation is almost identical to that of Everett and Foster (equation 4.3).

All the above measurements have been made on natural amylose fractions. Synthetic amylose fractions, prepared by the enzyme phosphorylase, have been used in the studies of Burchard (1963). He found the following relations,

$$[\eta] = 0.276\ P_w^{0.85} \equiv 3.64 \times 10^{-3}\ \bar{M}_w^{0.85} \qquad 4.9$$

$$[\eta] = 0.257\ P_w^{0.82} \equiv 3.95 \times 10^{-3}\ \bar{M}_w^{0.82} \qquad 4.10$$

$$[\eta] = 1.112\ P_w^{0.51} \equiv 8.3 \times 10^{-2}\ \bar{M}_w^{0.51} \qquad 4.11$$

$$[\eta] = 0.684\ P_w^{0.67} \equiv 2.26 \times 10^{-2}\ \bar{M}_w^{0.67} \qquad 4.12$$

$$[\eta] = 0.420\ P_w^{0.68} \equiv 1.32 \times 10^{-2}\ \bar{M}_w^{0.68} \qquad 4.13$$

for synthetic amylose in 0.5M NaOH, DMSO, DMSO/43.5% acetone (an organic Θ-solvent), Formamide, and water respectively, where P_w is the weight average degree of polymerization, measured from light-scattering.

The discrepancy between the Mark-Houwink exponents of different authors is large. For example, with amylose in DMSO, exponents of 0.64, 0.87 and 0.82 (equations 4.2, 4.5 and 4.10), and for aqueous neutral solutions, 0.50 and 0.68 (equations 4.3, 4.8 and 4.13) have been found. Other discrepances for the alkaline solutions are also apparent. In view of the negligible shear dependence of $[\eta]$ for amylose, found in Section 3D, it is unlikely that these discrepancies arise from the viscosity determinations (apart

from, perhaps, the work of Cowie,(1960). This leaves the question of the molecular weight distribution of the fractions and their weight average molecular weights.

As no β-amylolysis limit determinations were made by Everett and Foster (1959) or by Cowie (1960), the homogeneity of their natural amylose fractions is in doubt. Moreover, it has been suggested by Paschall and Foster (1952) and Husemann et al. (1963) that aqueous solutions of natural amylose are unstable and tend to aggregate. This phenomenon could markedly affect the $\overline{M}_w$-values of Banks (1960) and Banks and Greenwood (1963b) determined by lightscattering in neutral salt solutions (see Husemann et al., 1963; Burchard, 1963a). Moreover, there is the question of the absolute molecular-weight distributions of the amylose fractions obtained by a DMSO/ethanol fractional precipitation. The value of K_1 in the Mark-Houwink equation (equation 2.4, p 19) depends on the homogeneity of each fraction - the larger the ratio $\overline{M}_w/\overline{M}_n$, the larger is K_1. However, if $\overline{M}_w/\overline{M}_n$ varies from fraction to fraction, then the exponent a will be in error. Since extreme precautions are necessary with regard to fraction homogeneity in a fractional precipitation scheme, such as that used here for amylose, there is potentially a large source of error for a in the above relations.

Burchard's (1963) results are of particular interest, as his enzymically prepared fractions were of very narrow distribution ($\overline{M}_w/\overline{M}_n < 1.04$) and, of course, true linear homologues. Moreover, these synthetic amyloses did not seem to possess the aggregative disadvantages to the same extent as natural amyloses, therefore

verifying Burchard's lightscattering data. It was concluded from these results that synthetic amylose existed as a coil which was drained to different extents in various solvents. Nevertheless, there may be unknown differences between natural and synthetic amyloses which could render Burchard's results incomparable with other work.

It was therefore decided to subfractionate a total linear amylose sample with regard to the molecular weight distribution and attempt to measure their molecular weight by ultracentrifugation.

EXPERIMENTAL

Linear amylose, isolated from potato total-amylose, was subfractionated by acetone precipitation from a DMSO solution, to yield the L-fraction series, as described in Section 1B. The procedure was carried out at 25 ± 0.1°C and since it is known that an acetone precipitant yields narrower molecular-weight subfractions (see Section 4A), the subfractions were considered fairly monodisperse.

Viscosity measurements:- Limiting viscosity numbers in 0.15M KOH, 0.15M KCl and 0.50M KCl/10^{-2}M KOH (aqueous Θ-solvent) were determined at 25.0°C on the butan-1-ol complexes of the amylose subfractions as described in Section 2A.

Molecular weight determinations by the short column method:- (see Section 2D). Molecular weight determinations were made on the dry amylose in neutral KCl solution. At the low speeds necessary for equilibrium runs of such large material ($\bar{M}_w > 10^5$), it was found better to omit the silicone oil at the cell bottom because of severe interface distortions on the schlieren diagram. The solution column was made exactly 0.50 mm long by introducing 0.044 ml from an Agla syringe into one sector of a 30 mm epoxy-resin double-sector cell. Synthetic boundary cell runs were made in a 12 mm cell. Since the limit of dry amylose solubility in alkali is ca 0.6%, and the lower limit of concentration for

FIG 4.4

The approach to equilibrium for fraction L3a

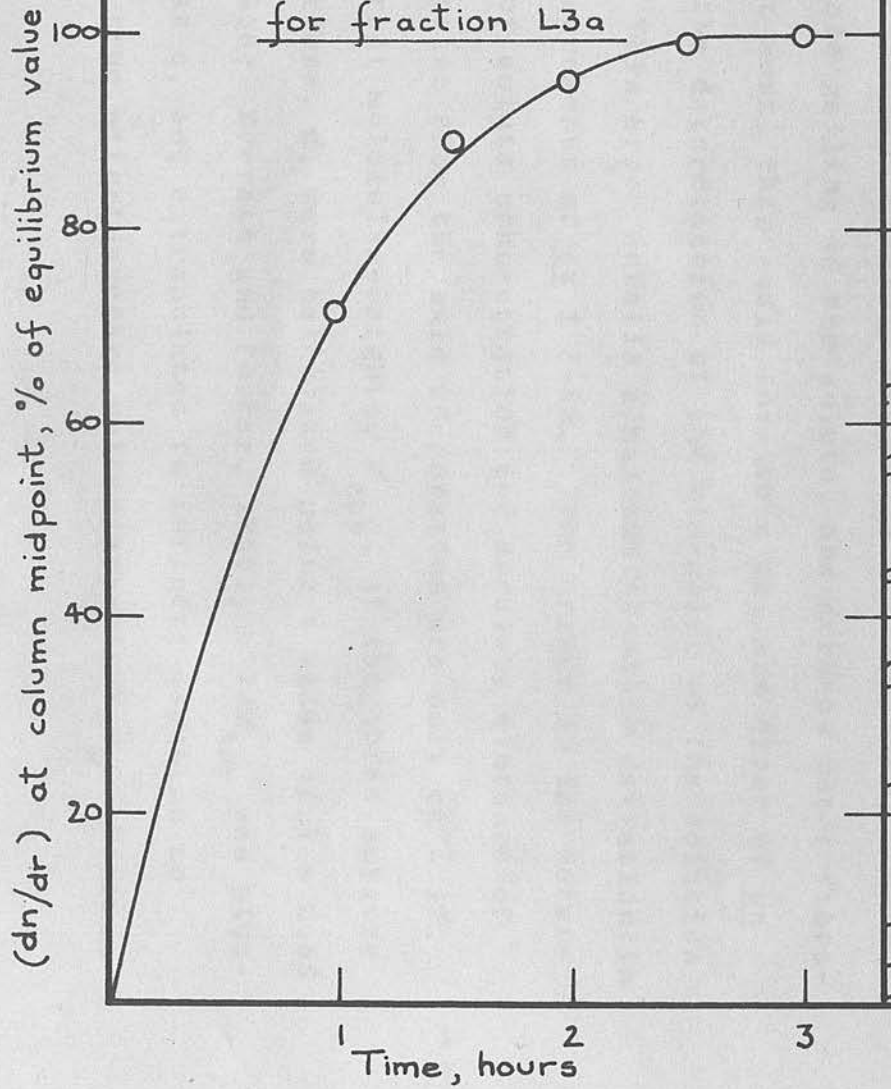

FIG 4.5

$1/M_{app}$ vs. C for some amylose fractions

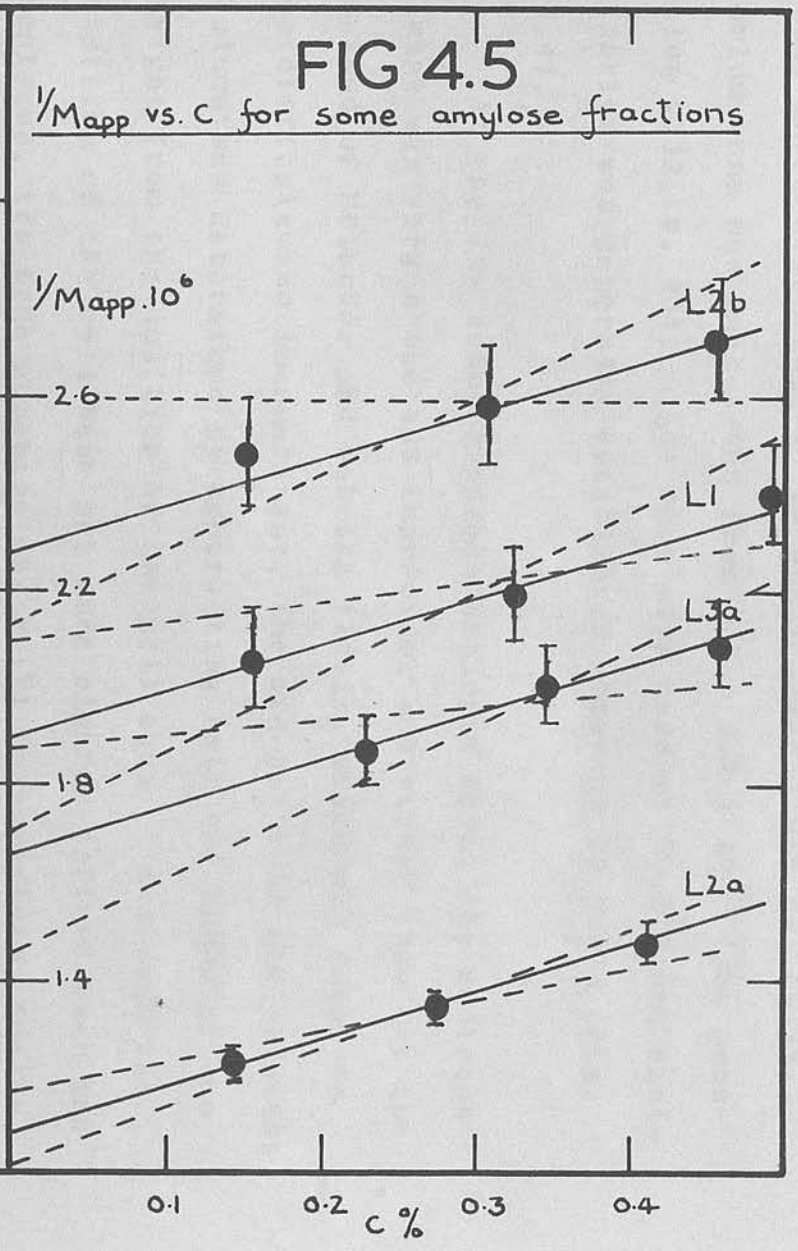

accurate molecular weight determinations by the equilibrium method is ca 0.2%, this narrow concentration range afforded only three dilutions. The upper speed limit for equilibrium runs was calculated from $w^2M = 9.8 \times 10^{10}$ (see equation 2.32, p. 43). All runs were made at 20.0°C and equilibrium was generally established after ca 2½ hours (Fig. 4.4).

At the low running speeds employed here, the meniscus image was very broad and imprecise, and rather than use the method of Erlander and Babcock (1961), which was found to be difficult and inconsistent, the mid-point of the solution column was determined by subtracting half the known column height from the position of the cell base. Although the position of the cell base was more clearly defined than the meniscus, its true position may still be uncertain, due to the possible gelling of the solute, and perhaps rotor vibrations. At most, this would involve a maximum error of ca ± 15% in the determination of the mid-point of the solution column. This error entails a maximum possible deviation in dn/dx measurements of ca ± 3-8%. The errors in the determination of solute concentration and absolute distance of this mid-point from the axis of rotation are only ca ± 1%.

Apparent molecular-weights, M_{app}, at the three amylose concentrations, c, were calculated using a value of $\bar{V} = 0.65$ (Cowie, 1958; Everett and Foster, 1959). $1/M_{app}$ was plotted against c, and extrapolated to infinite dilution to yield the true weight-average molecular weight $\bar{M}_w$. Maximum

possible errors in M_{app} were assessed for each concentration and amounted to ca ± 8% for the smaller fractions and ca ± 3% for the larger fractions. Maximum possible errors in the extrapolated $\overline{M}_w$ values were assessed from the $1/M_{app}$ vs. c plots (Fig. 4.5). These were ca ± 8% for the largest fractions and ca ± 15% for the smallest.

Molecular weight determinations by the Archibald-Trautman method:- This has been detailed in Section 2E. Runs were made on the amylose butan-1-ol complexes dissolved in aqueous Θ-solvent at 25.0°C. Under Θ-conditions, the second virial coefficient has been shown to be zero (Sotobayashi and Ueberreiter, 1964), and therefore, no extrapolation of $\overline{M}_w$ to infinite dilution was attempted. The procedure adopted was to dissolve the complex directly in aqueous Θ-solvent at 25°C at a concentration of ca 0.3%. This solution, together with solvent was introduced into preheated cells and rotor, and spun at 25°C. The error in the $\overline{M}_w$ values would be difficult to assess quantitatively, owing to the uncertainty in the meniscus position (see p. 55). However, as the Trautman procedure tends to average out such errors, the maximum variation in the slope of the Trautman plot (see Fig. 4.8) was taken as an estimate of the error in $\overline{M}_w$ as shown in column 3 of Table 4.5.

RESULTS AND DISCUSSION

The validity of equilibrium ultracentrifuge molecular weight determinations:- The $1/M_{app}$ vs. c plots for some of the amylose fractions are shown in Figure 4.5 in which an appreciation of the error in the extrapolated $\bar{M}_w$ values is indicated. The slopes of the lines are equal to the virial coefficient, but in view of the possible experimental error, these have not been explicitly evaluated.

To confirm the molecular weights in KCl by equilibrium centrifugation (see Table 4.5), repeat runs were made on fractions L3a and L4 dissolved in 0.15M KOH. The $1/M_{app}$ vs. c plots obtained, showed the pronounced upward curvatures characteristic of good solvents (Fig. 4.6). The extrapolation of such plots to infinite dilution is difficult, but this has been facilitated by the recent method of Inagaki and Kawai (1964), who suggested a plot of log $(1/M_{app})$ vs. c. Such plots for fractions L3a and L4 are shown in Figure 4.7, and yield intercepts corresponding to $\bar{M}_w$ values of $0.59 \pm 0.07 \times 10^6$ and $0.23 \pm 0.03 \times 10^6$ respectively. In spite of the proposed error, arising from an arbitrary uncertainty of $\pm$ 15% in the position of the mid-point of the solution column, the values are similar to those obtained in 0.15M KCl (Table 4.5).

Further confirmatory tests for the equilibrium $\bar{M}_w$-values were made by determining weight-average molecular weights by the Archibald-Trautman method. Good agreement

TABLE 4.5

A comparison of $\bar{M}_w$ determinations

for linear amylose fractions

Fraction*	$10^{-6}\ \bar{M}_w$		
	(a)	(b)	(c)
L1	0.85	0.54 ± 0.02	0.53 ± 0.06
L2a	1.50	0.78 ± 0.03	0.91 ± 0.08
L2b	0.59	0.45 ± 0.02	0.43 ± 0.05
L3a	0.91	-	0.60 ± 0.07
L3b	0.47	0.30 ± 0.02	0.31 ± 0.04
L4	0.28	-	0.21 ± 0.03
L5	0.15	-	0.12 ± 0.02

* a, b represent refractionated products

(a) Calculated from lightscattering data of Banks and Greenwood (1963); equation 4.8, p. 111.

(b) Determined by the Archibald-Trautman method.

(c) Determined by equilibrium ultracentrifugation.

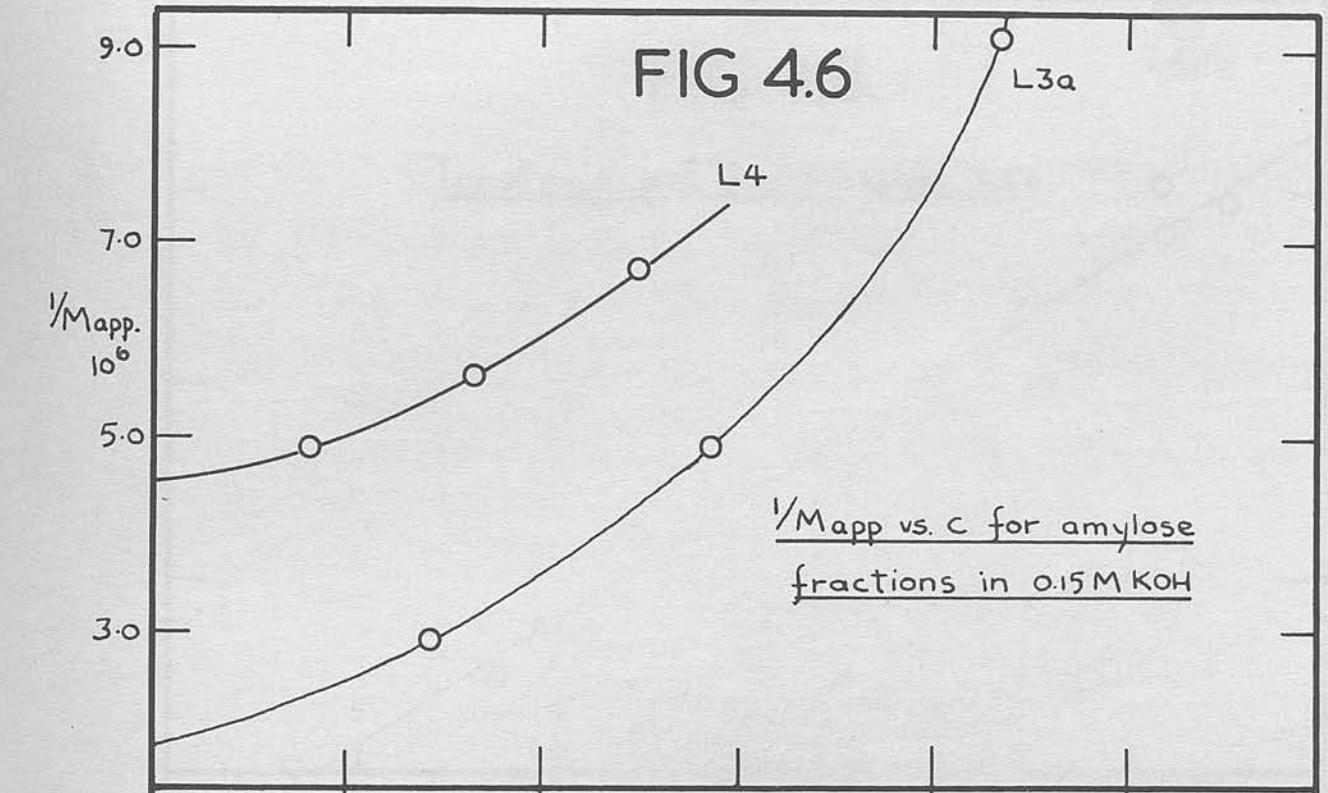

FIG 4.6

1/Mapp vs. C for amylose fractions in 0.15 M KOH

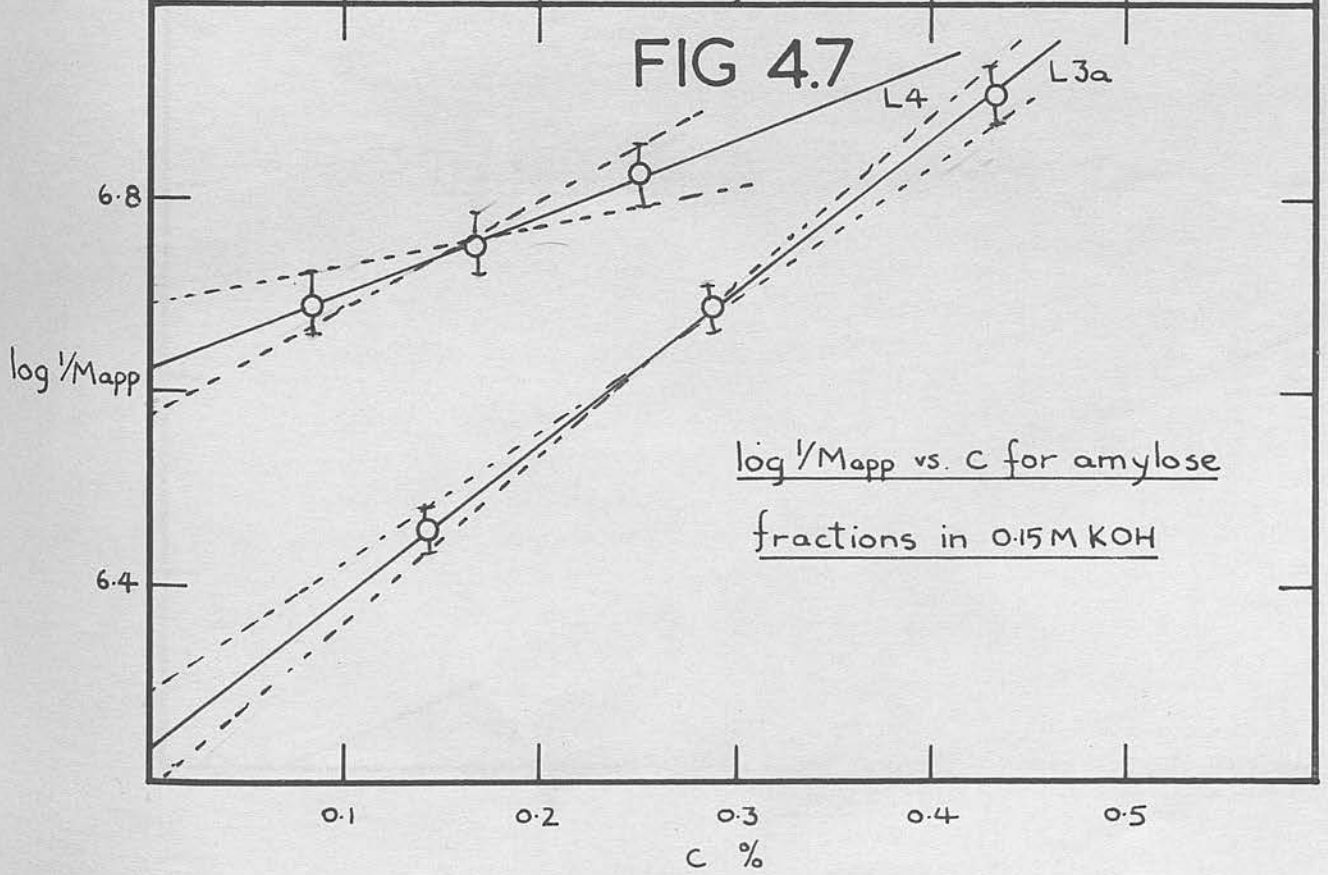

FIG 4.7

log 1/Mapp vs. C for amylose fractions in 0.15 M KOH

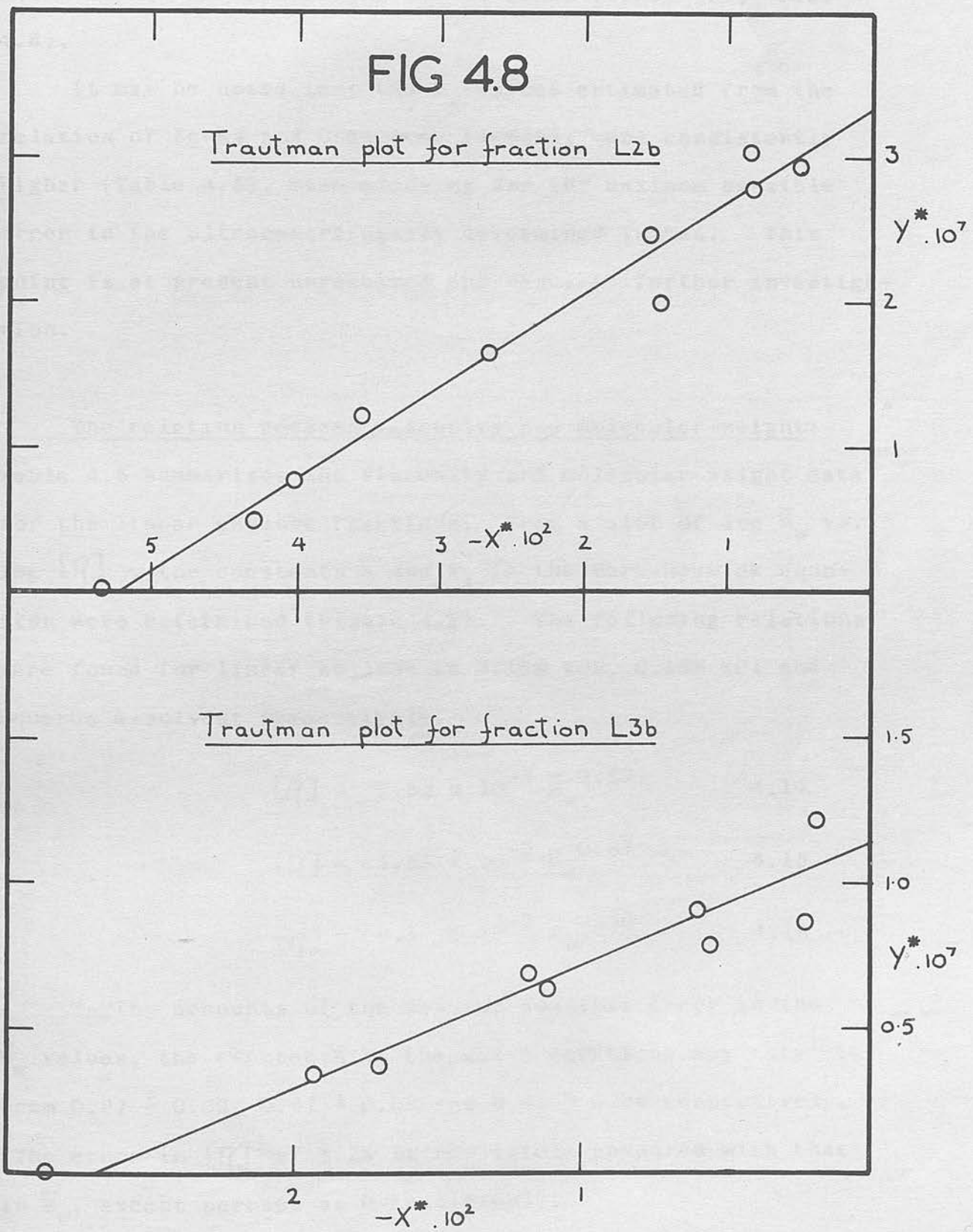
Trautman plot for fraction L2b
3
2
1
$y^* . 10^7$
5
4
3
$-X^* . 10^2$
2
1
Trautman plot for fraction L3b
1·5
1·0
0·5
$y^* . 10^7$
2
1
$-X^* . 10^2$

FIG 4.8

with the equilibrium values was obtained (Table 4.5; Fig. 4.8).

It may be noted that the $\overline{M}_w$-values estimated from the relation of Banks and Greenwood (1963b), were consistently higher (Table 4.5), even allowing for the maximum possible error in the ultracentrifugally determined values. This point is at present unresolved and requires further investigation.

The relation between viscosity and molecular-weight:- Table 4.6 summarises the viscosity and molecular weight data for the linear amylose fractions. From a plot of log $\overline{M}_w$ vs. log $[\eta]$, the constants a and K_1 in the Mark-Houwink equation were determined (Figure 4.9). The following relations were found for linear amylose in 0.15M KOH, 0.15M KCl and aqueous Θ-solvent respectively.

$$[\eta] = 2.82 \times 10^{-3} \overline{M}_w^{0.87} \qquad 4.14$$

$$[\eta] = 1.55 \times 10^{-2} \overline{M}_w^{0.67} \qquad 4.15$$

$$[\eta] = 8.1 \times 10^{-2} \overline{M}_w^{0.50} \qquad 4.16$$

Taking accounts of the maximum possible error in the $\overline{M}_w$ values, the exponents in the above equations may vary from 0.87 ± 0.09, 0.67 ± 0.09 and 0.45 ± 0.06 respectively. (The error in $[\eta]$ of ± 2% is negligible compared with that in $\overline{M}_w$, except perhaps at Θ-conditions).

TABLE 4.6

Viscosity and molecular-weight data for linear amylose fractions

Fraction	$10^{-6}.\bar{M}_w$ a)	[η]			$10^{-6}.M_w$ b)
		0.15M KOH	0.15M KCl	aqu. Θ-solv.	
L 1	0.53	285	107	62	0.59
L 2a	0.91	435	148	74	0.97
L 2b	0.43	210	85	49	0.41
L 3a	0.60	295	110	58	0.61
L 3b	0.31	167	71	47	0.30
L 4	0.21	120	55	41	0.19
L 5	0.12	75	38	30	0.11

a) Experimental data from equilibrium ultracentrifugation

b) Calculated from viscosity data using the relations of Burchard (1963), for water.

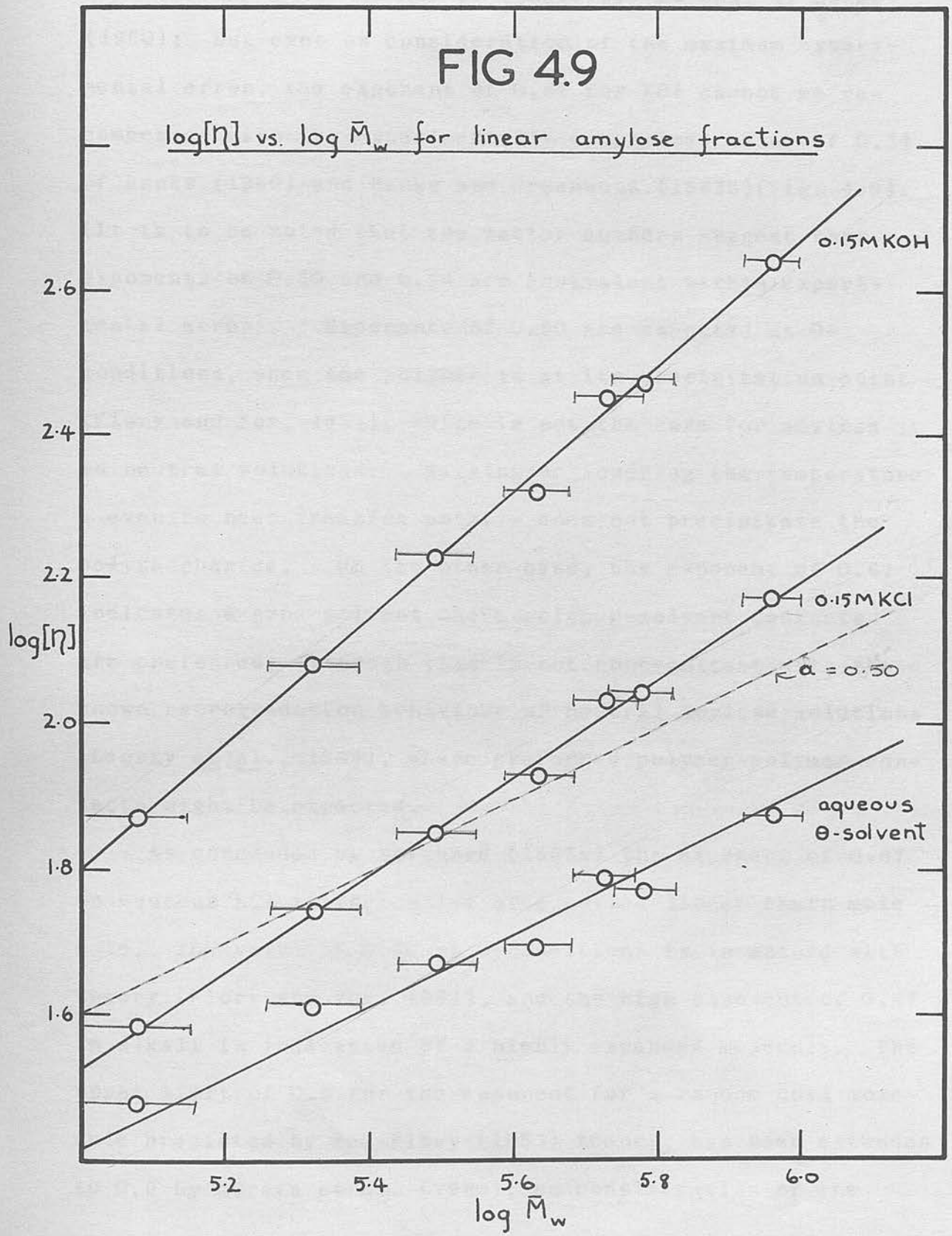
FIG 4.9
log[η] vs. log $\bar{M}_w$ for linear amylose fractions
0·15M KOH
0·15M KCl
a = 0·50
aqueous
θ-solvent
log[η]
2·6
2·4
2·2
2·0
1·8
1·6
5·2
5·4
5·6
5·8
6·0
log $\bar{M}_w$

The exponent for KOH is comparable to that of Banks (1960); but even on consideration of the maximum experimental error, the exponent of 0.67 for KCl cannot be recompensed with the experimentally determined value of 0.54 of Banks (1960) and Banks and Greenwood (1963b)(Fig. 4.9). (It is to be noted that the latter authors suggest that exponents of 0.50 and 0.54 are equivalent within experimental error). Exponents of 0.50 are expected at Θ-conditions, when the polymer is at its precipitation point (Flory and Fox, 1951), which is not the case for amylose in neutral solutions. Raising or lowering the temperature - even to near freezing point - does not precipitate the polysaccharide. On the other hand, the exponent of 0.67 indicates a good solvent where polymer-solvent contacts are preferred, although this is not concommitant with the known retrogradation behaviour of neutral amylose solutions (Lansky et al., 1949), where preferred polymer-polymer contacts might be expected.

As concluded by Burchard (1963a) the exponent of 0.67 in aqueous KCl is indicative of a coiled linear-chain molecule. The value of 0.50 at Θ-conditions is in accord with theory (Flory and Fox, 1951), and the high exponent of 0.87 in alkali is indicative of a highly expanded molecule. The upper limit of 0.8 for the exponent for a random coil molecule predicted by the Flory (1953) theory, has been extended to 0.9 by Kurata et al. (1960), on consideration of the

non-Gaussian character of the chains with excluded volume. The high degree of expansion is due to the coulombic swelling effects as a result of the ionisation of hydroxyl groups (see Section 3A).

It is perhaps interesting to compare the Mark-Houwink constants of other polymers at Θ-conditions (Table 4.7 from Kurata and Stockmayer, 1963). It seems more than fortuitous that many flexible linear polymers should have Flory constants, K', similar to that found here for amylose. Since K' determines the unperturbed dimensions of the polymer, it would seem that amylose has a similar hydrodyhamic behaviour to these other flexible linear polymers.

The unperturbed dimensions of amylose in aqueous solution:- The unperturbed dimensions of amylose were obtained by the recent method of Stockmayer and Fixman (1963). In this method a plot of $[\eta]M^{-\frac{1}{2}}$ vs. $M^{\frac{1}{2}}$ is constructed where the ordinate intercept equals the Flory constant, K', and the gradient is directly proportional to the polymer-solvent interaction parameter B(equation 2.8, p. 20). The unperturbed dimensions may be calculated from the relation,

$$K' = \phi\left[(\bar{r}_o^2)/M\right]^{3/2} \qquad 4.17$$

(Flory and Fox, 1951) where $\phi = 2.8 \times 10^{23}$ c.g.s. units.

Such a plot showed a common ordinate intercept of 8.1×10^{-2} (= K') for amylose in each of the three solvents studied

TABLE 4.7

Mark-Houwink constants of various polymers at Θ-conditions[a)]

Polymer	$10^2.K'$
Cellulose tributyrate	8.2
Poly (dimethylsiloxane)	8.1
Polystyrene	8.2
Poly (α-methyl styrene)	7.7
Poly (vinyl acetate)	8.2
Amylose[b)]	8.1

a) From list in Kurata and Stockmayer (1963)

b) This work.

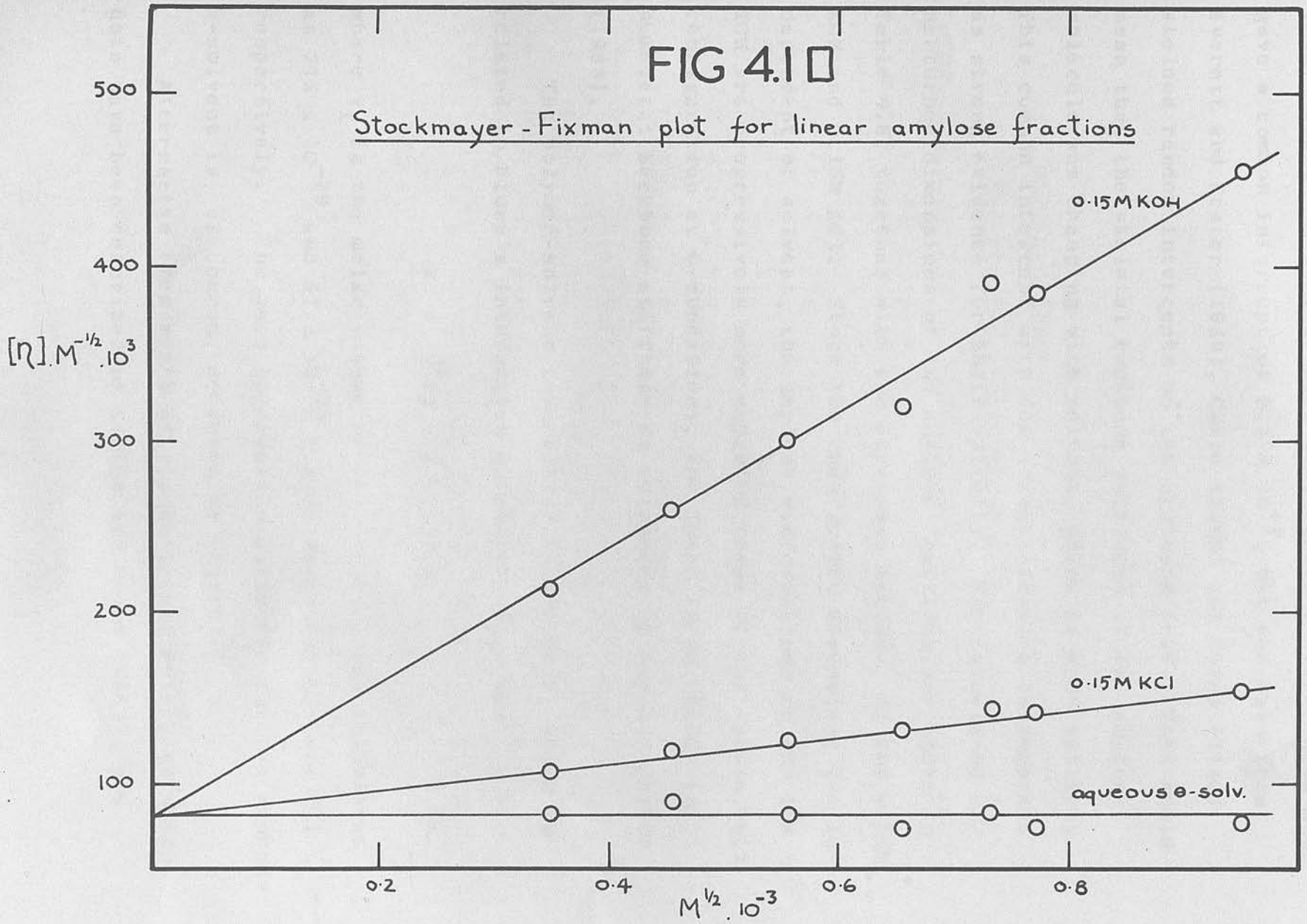
FIG 4.10
Stockmayer - Fixman plot for linear amylose fractions
0·15M KOH
0·15M KCl
aqueous θ-solv.
500
400
300
200
100
[η].M^-1/2.10^3
0·2
0·4
0·6
0·8
M^1/2.10^-3

(Fig. 4.10). A similar plot of Burchard's (1963) data also gave a common intercept of 8.1×10^{-2}, but the data from Everett and Foster (1959), Cowie (1960) and Banks (1960) yielded random intercepts on the ordinate axis. This would mean that the skeletal backbone stiffness of the amylose molecule was changing with solvent, which is most unlikely. This common intercept with the present results is regarded as strong evidence for their validity. The calculated unperturbed dimensions of the amylose fractions are shown in Table 4.8, together with the expansion factors, α, for 0.15M KOH and 0.15M KCl. Since the unperturbed dimensions are independent of solvent, the amylose conformations in KCl and KOH are progressively more expanded forms of the random coil configuration at Θ-conditions, and there is no change in skeletal backbone stiffness as suggested by Rao and Foster (1963).

The polymer-solvent interaction parameter B, which is related to Flory's interaction parameter χ_1, by,

$$B = \bar{V}^2(1 - 2\chi_1)/V_1N_A \qquad 4.18$$

where V_1 is the molar volume of the solvent, was calculated as 275×10^{-29} and 57×10^{-29} c.g.s. units for KOH and KCl respectively. The zero interaction parameter for the aqueous Θ-solvent is, of course, demanded by theory.

Alternative treatments of viscosity and molecular weight data have been described by Kamide and Moore (1964), and

TABLE 4.8

The unperturbed dimensions and expansion factors for linear amylose fractions

Fraction	$(\bar{r}_o^2)^{\frac{1}{2}}$ o A	$(\bar{s}_o^2)^{\frac{1}{2}}$ o A a)	α_{KOH} b)	α_{KCl} b)
L 1	482	197	1.66	1.20
L 2a	633	258	1.80	1.26
L 2b	436	178	1.63	1.20
L 3a	514	210	1.72	1.24
L 3b	368	150	1.52	1.15
L 4	303	124	1.43	1.10
L 5	230	94	1.36	1.08

a) Radius of gyration from $6\bar{s}_o^2 = \bar{r}_o^2$ (Debye, 1946)

b) Calculated from $[\eta]/[\eta]_\theta = \alpha^3$.

Kurata and Stockmayer (1963), from which equivalent values of K' may be obtained, though less precisely than from the Stockmayer-Fixman (1963) method.

The hydrodynamic behaviour of amylose:- To summarise, amylose behaves as a flexible coil in aqueous solutions. However, the possibility of at least an interrupted helical structure in the presence of excess complexing agent must be admitted (Hollo and SZejtle, 1958; Kuge and Sozaburo, 1961). Some form of inherent stiffness is implied in neutral aqueous solutions, which may arise from the uncharged regular structure of the polysaccharide in these solvents (see Section 3A).

Unfortunately, as no lightscattering measurements were made on these natural amylose fractions, a comparison between experimental and theoretical molecular dimensions could not be made. However, lightscattering measurements had been made on the synthetic amylose fractions of Burchard (1963) which have been shown to be comparable to the natural amylose samples examined here. In his study of fractions up to a degree of polymerisation, P_w, of 13,000 ($\bar{M}_w = 2.1 \times 10^6$), Burchard found a linear log-log relation between $[\eta]$ and P_w for $P_w > 100$ only. This he condluded was the limit of the statistical coil, and at $P_w < 100$ a strong solvent dependence of data was found. Burchard also indicated similarities in the amylose conformation at Θ-conditions, with polymethylmethacrylate and polystyrene, and that the Kirkwood-

Riseman (1948), Kuhn-Kuhn (1953) and Peterlin (1950) theories best fitted the experimental data. Burchard's conclusion that the amylose coil is drained to different extents in various solvents, seems feasible in view of the changing degrees of ionisation with solvent found earlier (Section 3A). These conclusions are in sharp discord with Rao and Foster (1963) who suggest that natural amylose approaches a stiff helical configuration in neutral aqueous solutions.

The existence of aggregates in aqueous solutions of natural amylose:- The presence of aggregated material was demonstrated by density gradient equilibrium experiments on amylose fractions dissolved in ca 6.5M CsCl (see Section 2F). Although such a high molarity of salt would probably favour any association reactions, the results are of some interest.

Fraction L2a was characterized by a symmetrical band, together with an aggregate band at equilibrium (see Fig. 6.9; p. 208a). The buoyant density, relative concentration, equilibrium time, T, and an estimation of relative molecular weight for the two bands are shown in Table 4.9. As both bands showed density heterogeneity from the downward curvature of the ln c vs. $(r - r_o)^2$ plot, absolute $\overline{M}_w$-values could not be calculated. However, their approximate relative molecular weights may be estimated from the inverse square of the band widths which are proportional to $\overline{M}_w$. It can be seen that under these experimental conditions (initial

amylose concentration ca 0.07%), some 6% of the total polysaccharide exists as an aggregate of about 20 times the molecular weight of the unaggregated amylose after 32 hours.

A closer study of this aggregation phenomenon was carried out, using different initial amylose concentrations. The results (Table 4.10) showed the buoyant density to decrease, as aggregation become more serious in the more concentrated amylose solutions, until a value of $\rho = 1.56$ ($\overline{V} = 0.64$) was attained for the completely salted out amylose. The density of solvated polysaccharide species would appear to be higher than the native (precipitated) polysaccharide. The buoyant density of unaggregated amylose molecules is higher than that of aggregated species (Table 4.9); this might be expected, due to the higher degree of solvation with a lower degree of intermolecular hydrogen bonding. The equilibrium times indicate that the rate of association is strongly concentration dependent, but the molecular weight (as estimated from the inverse square of the band width), was fiarly constant for each aggregate. However, it was found that the concentration (but not the molecular weight) of the aggregated species, increased with time.

Under the above experimental conditions, the observed trends in association are probably magnified versions of the phenomenon in low molarity KCl solutions. This association phenomenon, was shown to be unimportant in the sedi-

TABLE 4.9

Density gradient equilibrium data for linear amylose fraction L2a

Band	ρ a) $gm.ml^{-1}$	Rel. conc.	T b) hours	$(b.w)^{-2}$ c) cm^{-2}
Aggregate	1.628	6%	15	6.3
Amylose	1.663	94%	32	0.28

TABLE 4.10

Density gradient equilibrium data for linear amylose fraction L2b

Initial amylose concentration %	ρ a) $gm.ml^{-1}$	T b) hours
0.05	1.623	22
0.1	1.627	7
0.15	1.625	3
0.2	1.583	1
0.3	1.56	0

a) Buoyant density

b) Equilibrium time

c) Magnified inverse square of the band width $\propto \bar{M}_w$.

mentation equilibrium runs. A short column equilibrium run of fraction L5 in KCl solution was continued for 5 hours with a silicone oil base to the column. No thickening of the base line was observed, indicating the absence of serious aggregates (Yphantis, 1960). Moreover, no steep rise in the Schlieren pattern at the column base was observed for any of the equilibrium runs. It was therefore concluded that associated molecules must comprise a minor percentage of the total polysaccharide under these experimental conditions.

SECTION 5

THE SEDIMENTATION VELOCITY OF AMYLOSE

5A. THE CONCENTRATION AND FORCE FIELD DEPENDENCE OF SEDIMENTATION COEFFICIENT

Most polymers show a concentration dependence of sedimentation coefficient. The degree of dependence, however, varies according to the physical properties of the macromolecules (Schachman, 1959). A rigid, spherical molecule such as glycogen shows very little concentration dependence, whereas filamentous molecules such as amylose are usually markedly concentration dependent.

Little is known about the sedimentation velocity of amylose, and experiments to date have been confined to studies in 0.33M KCl and 0.2M KOH solution, (Banks, 1960). The concentration dependence in the former solvent was smaller than in the latter, but still significant. Moreover, sedimentation coefficients in KOH were lower than in KCl. In addition, sedimentation coefficients, S, measured by Rao and Foster (1963), are higher in aqueous Θ-solvents at pH 12 than in neutral solutions. As sedimentation velocity can elucidate solution behaviour of the dissolved polymer, the concentration dependence of S was studied for amylose in various solvents.

EXPERIMENTAL

During the study of sedimentation velocity, it was noted that the sedimentation coefficient, S, was apparently dependent on the force-field. For a total amylose of $[\eta]$ = 560 and $[\beta]$ = 90 the following results were obtained for S at ca 0.2% in 0.15M KCl and 0.15M KOH.

w r.p.m.	Force-field 10^{-3}.g	S_{KCl}	S_{KOH}
20,410	30	12.2	5.3
31,410	72	10.2	4.9
39,460	113	10.0	4.8
50,740	187	7.6	4.5

S is decreasing with force-field in the KCl, and KOH solutions. This phenomenon is not predicted by simple sedimentation velocity theory (Section 2C), and was therefore investigated more closely for various amyloses over a range in concentration.

Various linear and non-linear amyloses were studied in aqueous Θ-solvent, 0.15M KCl, 0.15M KOH and DMSO. Experiments were confined to amyloses that gave one peak on sedimentation in KCl, and sedimentation coefficients at constant temperature were measured using the maximum in the Schlieren peak as defining the boundary position of sedimenting macro-

molecules. In some experiments the boundary position was determined as the square root of the second moment of the Schlieren peak (see Section 2C).

During the study it was found that the S-values at different speeds were unaffected by the order in which the runs were made; and also unaffected by whether the ultracentrifuge was stopped between each speed and the cell contents replaced with fresh solution, or the speed changed during the run. Normally, therefore, runs were made at 20,410 r.p.m. and 50,740 r.p.m. with the speed being changed during the run. To compare results, the ratio of S at 20,410 r.p.m. to S at 50,740 r.p.m. was defined as γ.

The dependence of sedimentation coefficient on force-field:- The results of the speed dependence of a linear amylose fraction (L3a) in different solvents are shown in Table 5.1. It can be seen that the effect is not concentration dependent, and is in fact present at infinite dilution. As the phenomenon was common to all solvents, only behaviour in 0.15M KCl and aqueous Θ-solvent was studied in detail. The effect was present in both linear and non-linear amyloses and some typical results for KCl solutions are shown in Figure 5.1a - (fraction B1ab has the properties: $[\eta]$ = 395; $[\beta]$ = 84). Similar graphs, but with a concentration independence of S were obtained for amyloses in aqueous Θ-solvent at the two force

TABLE 5.1

Sedimentation coefficients at 20,410 r.p.m. and 50,740 r.p.m. for amylose fraction L3a in various solvents

Solvent	Conc. %	$10^{13}.S_1$ a)	$10^{13}.S_2$ b)	γ
DMSO	0.3	1.51	1.36	1.11
	0.15	1.85	1.70	1.09
0.15M KOH	0.2	5.05	4.9	1.03
	0.13	5.55	5.1	1.09
	0.1	6.05	5.5	1.10
0.15M KCl	0.478	7.5	5.9	1.10
	0.239	8.4	7.3	1.08
	0.179	9.2	7.5	1.09
	0.120	9.4	7.9	1.09
aqueous θ-solvent	0.466	9.5	7.2	1.32
	0.402	11.2	9.3	1.20
	0.15	11.8	10.2	1.15

a) Determined at w = 20,410 r.p.m.

b) Determined at w = 50,740 r.p.m.

FIG 5 IA

S vs. C for various amylose fractions in 0·15M KCl

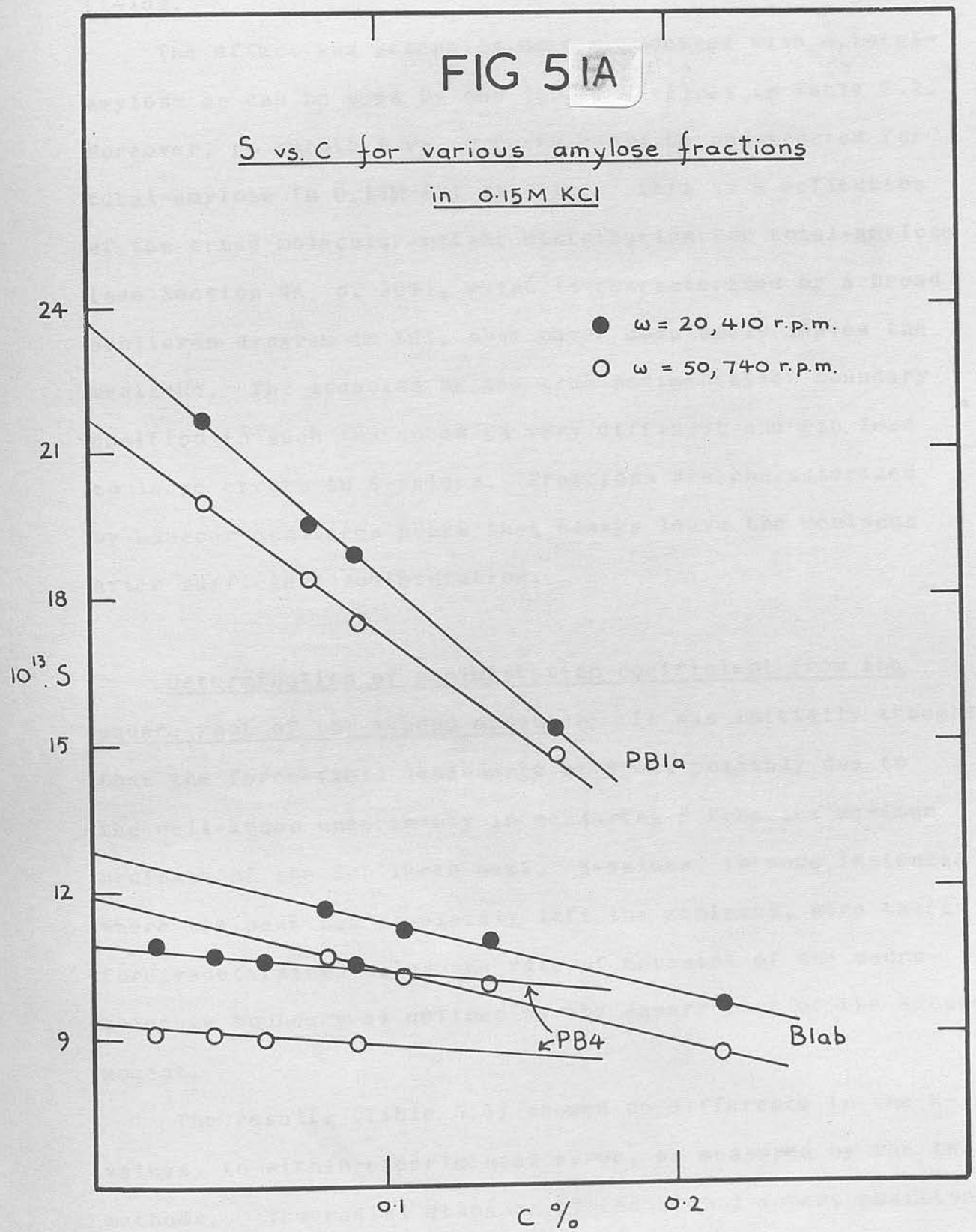

fields.

The effect was generally more pronounced with a total-amylose as can be seen by the larger γ-values in Table 5.2. Moreover, no smooth S vs. c curve could be constructed for total-amylose in 0.15M KCl solution. This is a reflection of the broad molecular-weight distribution for total-amylose (see Section 4A, p. 104), which is characterized by a broad Schlieren diagram in KCl, that never completely leaves the meniscus. The location of the true sedimentation boundary position in such instances is very difficult and can lead to large errors in S-values. Fractions are characterized by sharper Schlieren peaks that always leave the meniscus after sufficient sedimentation.

Determination of sedimentation coefficient from the square root of the second moment:- It was initially thought that the force-field dependence of S was possibly due to the well-known uncertainty in measuring S from the maximum ordinate of the Schlieren peak. S-values, in some instances where the peak had completely left the meniscus, were therefore redetermined using the rate of movement of the macromolecule boundary as defined by the square root of the second moment.

The results (Table 5.3) showed no difference in the S-values, to within experimental error, as measured by the two methods. The radial distance of the second moment position,

TABLE 5.2

Sedimentation coefficients of a total-amylose in 0.15M KCl at different concentrations

Conc. %	$10^{13}.S_1$ a)	$10^{13}.S_2$ b)	γ
0.232	12.0	10.2	1.20
0.166	12.8	10.1	1.26
0.145	13.7	9.8	1.40
0.116	12.0	9.7	1.24
0.110	10.2	9.4	1.09
0.083	10.9	8.9	1.22
0.058	13.8	8.2	1.69
0.055	11.9	9.8	1.21

a) Determined at w = 20,410 r.p.m.

b) Determined at w = 50,740 r.p.m.

TABLE 5.3

Comparison of sedimentation coefficients measured from the Schlieren peak maximum and the square root of the second moment

Fraction	Conc. %	Speed r.p.m.	$10^{13}.S_p$ a)	$10^{13}.S_m$ b)	$(\bar{x} - x_p)$ c) mm.
PB4 in KCl	0.091	20,410	10.5	10.5	0.04
		50,740	8.9	8.9	0.05
L2a in KCl	0.148	20,410	9.7	9.7	0.04
		50,740	9.1	9.1	0.04
Blab in KCl	0.134	20,410	11.0	11.0	0.01
		50,740	10.2	10.4	0.01
L2b in Θ	0.20	20,410	9.4	9.4	0.02
		50,740	8.4	8.4	0.23
L4 in Θ	0.20	20,410	6.3	6.3	0.02
		50,740	5.4	5.4	0.16
L3a in Θ	0.40	20,410	11.2	11.0	0.04
		50,740	9.3	9.6	0.44

a) Measured using peak maximum as boundary position

b) Measured using square root of the second moment as boundary position

c) Magnified radial difference between the peak maximum and the second moment boundary positions.

$\bar{x}$, and the derived S_m are weight average properties of the sedimenting macromolecules, and in all cases $\bar{x}$ was greater than the radial distance of the peak maximum, x_p. This means that the Schlieren peaks are skew - though this was undetectable visually - with some excess of higher molecular-weight material (Schachman, 1959).

Conclusions:- At present, this problem of the speed dependence of S is unresolved and requires further investigation. However, this phenomenon necessitates that in any study of the concentration dependence of S, the force-field should be kept constant.

Outline of investigation:- Sedimentation coefficients of linear amyloses (fractions P11, P13, L2a, L3a - see Section 1B) dissolved in seven different solvents, were measured over the concentration range 0.3 - 0.01%, as described in Section 2C. All runs were made at 25°C and 39,460 r.p.m. (except when stated otherwise), and the boundary position of the sedimenting macromolecules was taken as the maximum of the Schlieren peak. The amylose butan-1-ol complexes were dissolved directly in the following solvents: 0.50M KCl/ 10^{-2}M KOH (aqueous Θ-solvent), 0.15M KCl, 0.15M KOH, 1M KOH, tetra-methyl ammonium hydroxide (0.12M TMAH), tetra-ethyl ammonium hydroxide (0.12M TEAH), dimethyl sulphoxide (DMSO). Results were plotted as S vs. c and empirically as S^{-1} vs. c

(Gralen, 1944), and extrapolated to infinite dilution.

RESULTS AND DISCUSSION

The results for fraction P11 (Fig. 5.1 and 5.2) show a significant concentration dependence of sedimentation coefficient, S, for amylose in all solvents except aqueous Θ-solvent. This suggests that amylose is in an extended pliable conformation in these non-Θ-solvents, although molecular entanglement cannot be ruled out. Sedimentation is concentration independent in aqueous Θ-solvent up to ca 0.24%, and is compared with the sedimentation in KCl solution for amyloses of different molecular-weight in Fig. 5.3 (L2a data at 20,410 r.p.m.; P13 and L3a data at 50,740 r.p.m.). It should be noted that a concentration dependence of S has been found for some polymers at Θ-conditions (Billick, 1964).

Severe concentration dependences are evident in the ionising solvents, where amylose exists as a charged molecule, due to the ionisation of hydroxyl groups. Sitaramaiah et al. (1962) and Pedersen (1958) have explained the concentration dependence of S for a poly-electrolyte in terms of primary and secondary charge effects. The former, which is large, arises from the differential sedimentation of the macro-ion and its gegen ion. The macro-ion sediments more quickly than the small counter ions, builds up a charge at the base of the cell, and causes a decrease in the sedimentation rate by back electrophoresis of the sedimenting macro-ion. The secondary charge effects are due to the difference in the sedimentation rate of the positive and negative ions in the supporting electrolyte. Although amylose in

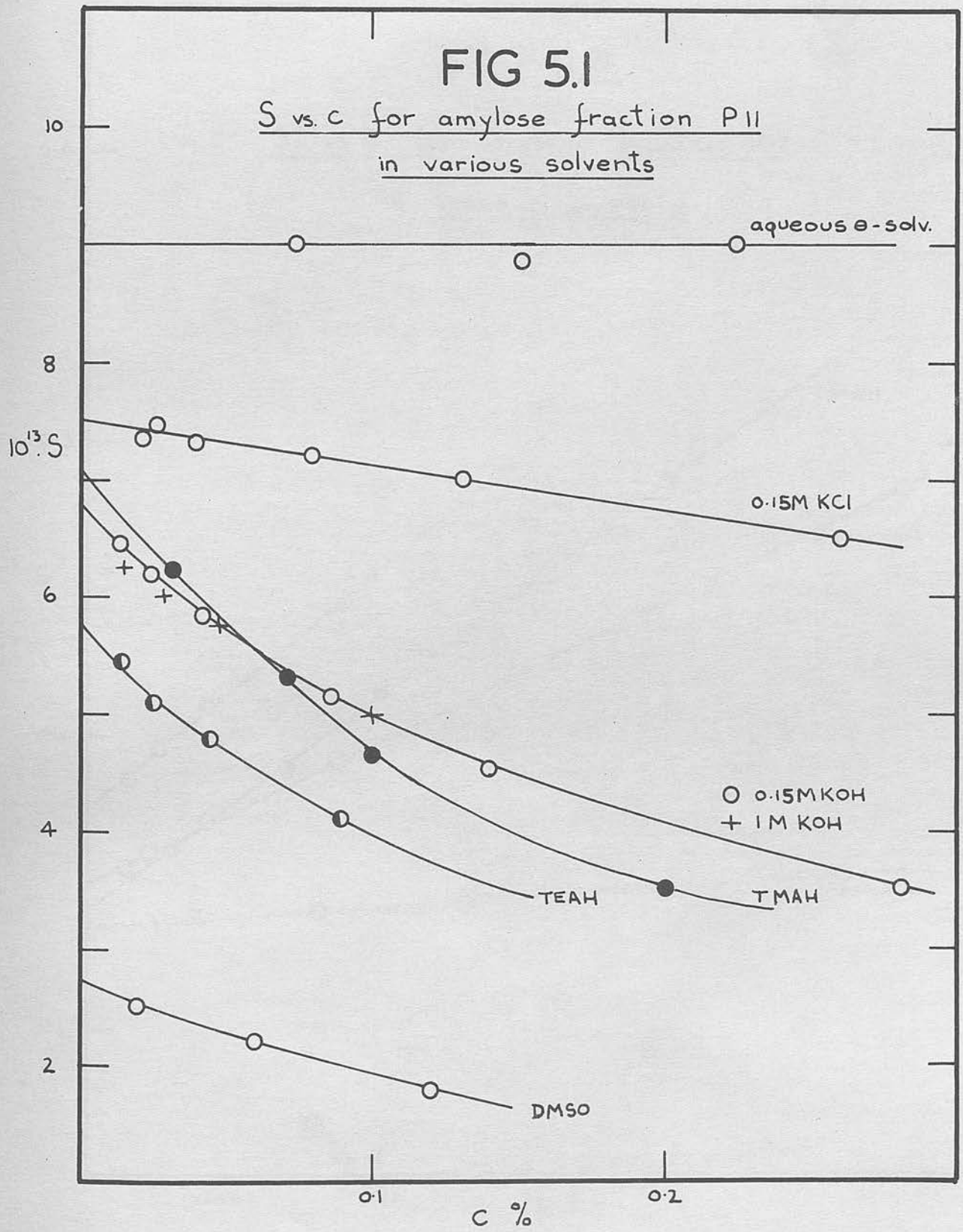
FIG 5.1
S vs. c for amylose fraction P11
in various solvents
10
8
6
4
2
10^{13}.S
aqueous θ-solv.
0·15M KCl
O 0·15M KOH
+ 1M KOH
TEAH
TMAH
DMSO
0·1
0·2
C %

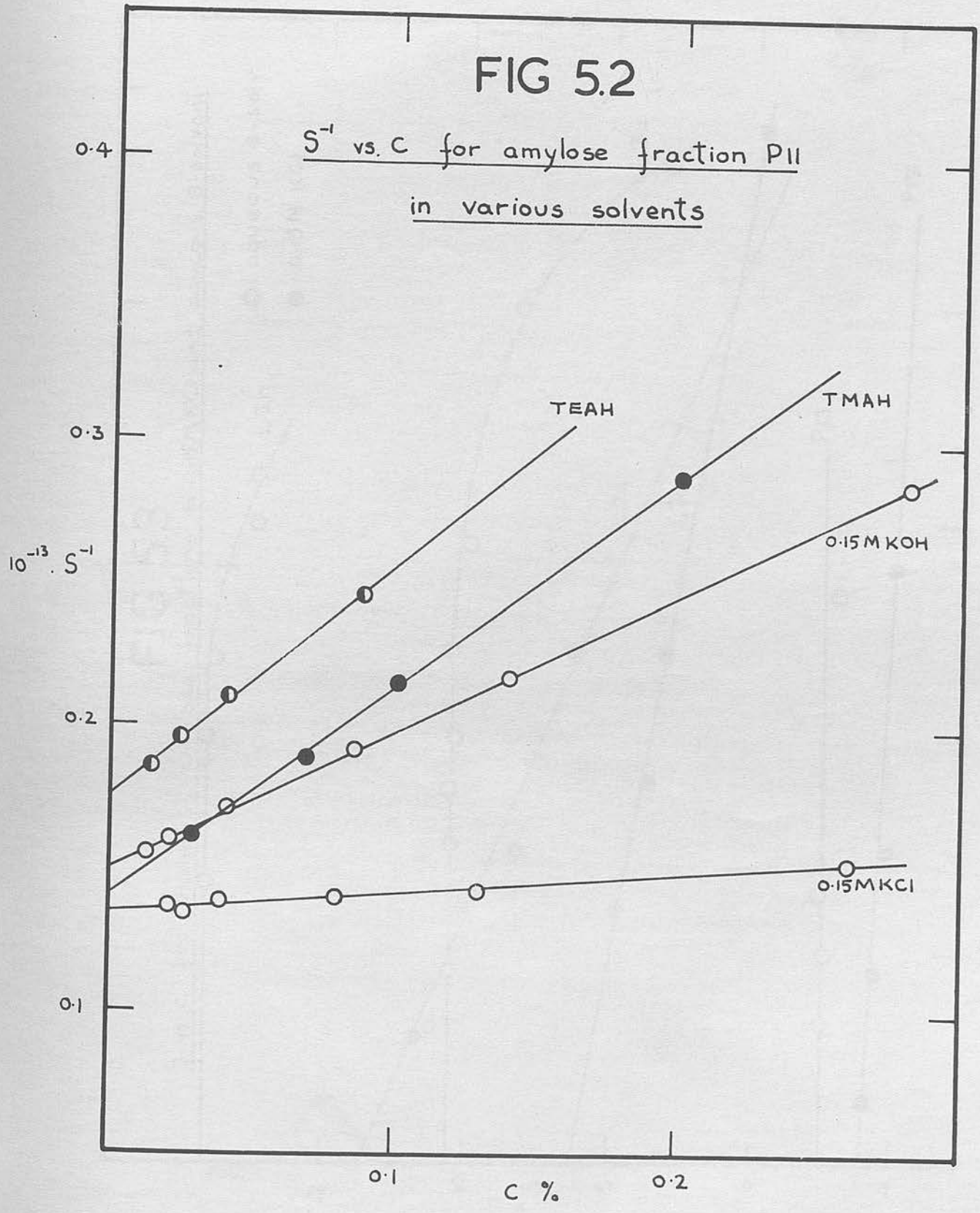
FIG 5.2
S⁻¹ vs. C for amylose fraction P11
in various solvents
0·4
0·3
0·2
0·1
10⁻¹³. S⁻¹
TEAH
TMAH
0·15 M KOH
0·15 M KCl
0·1
0·2
C %

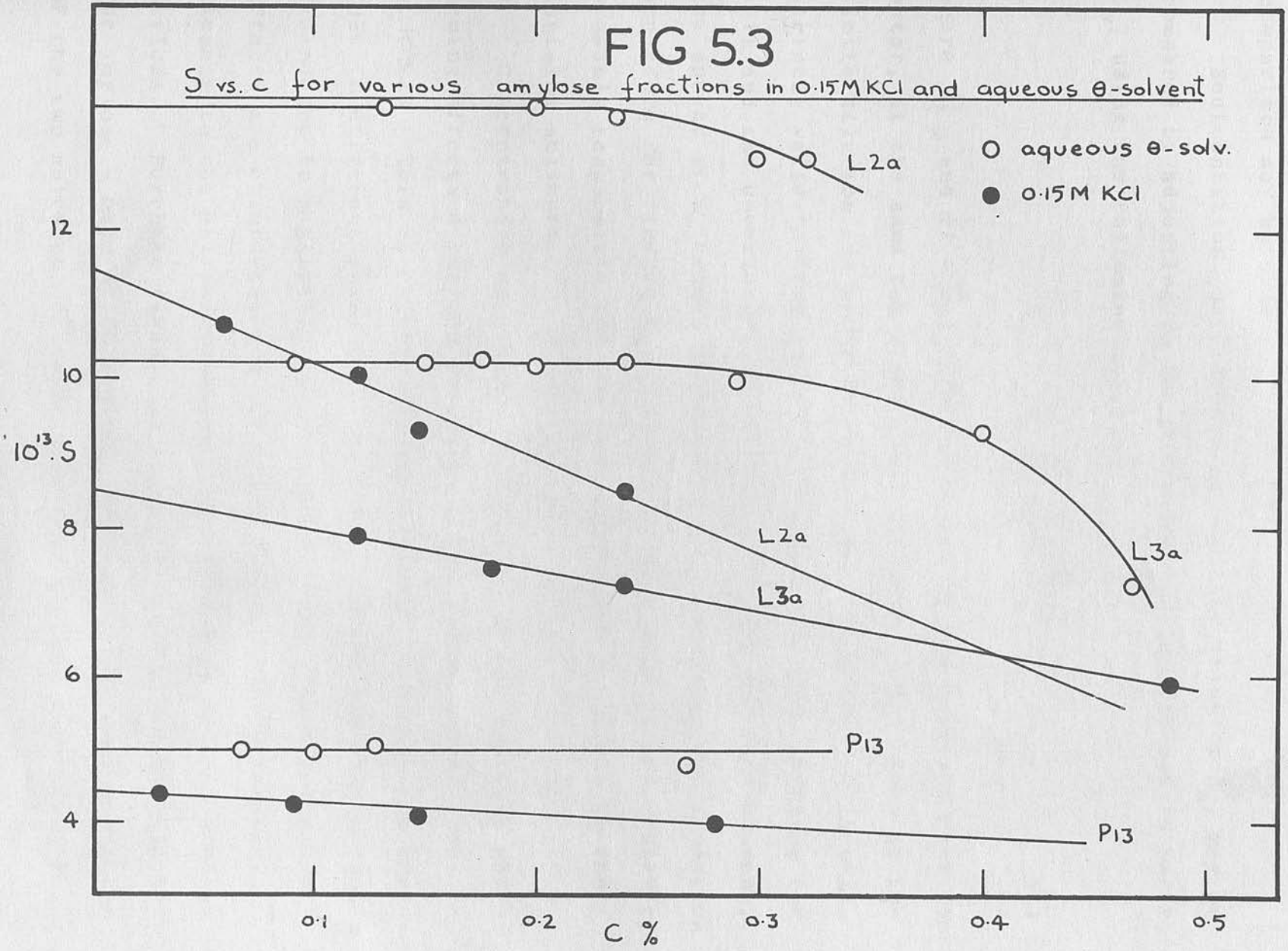
FIG 5.3
S vs. C for various amylose fractions in 0·15M KCl and aqueous θ-solvent
O aqueous θ-solv.
● 0·15M KCl
L2a
L3a
L2a
L3a
P13
P13
12
10
8
6
4
10^{13}.S
0·1
0·2
0·3
0·4
0·5
C %

ionising solvents is not strictly a poly-electrolyte, a certain comparison may be drawn.

Sedimentation coefficients at infinite dilution S_o, may be compared by adjusting to the sedimentation coefficient in water, S_w, using the following equation,

$$S_w = S_o \frac{\eta}{\eta_w} \frac{(1 - \bar{V}\rho)_w}{(1 - \bar{V}\rho)} \qquad 5.1$$

where η_w and $(1 - \bar{V}\rho)_w$ are the viscosity and buoyancy term for water, at the same temperature and pressure. S_w-values at infinite dilution are shown in Table 5.4. Equation 5.1 is only strictly valid for two component systems, but even allowing for this and the uncertainty of the buoyancy term for each solvent, the spread of S_w values illustrates the inadequate extrapolation procedure for finding S_o. Primary charge effects are, however, probably responsible for the generally lower S_o-values in the ionising solvents.

Concentration dependence of S, leads to the boundary sharpening effects described by Johnston and Ogston (1946) (see p. 103). This is apparent in the Schlieren diagrams for amylose in different solvents (Fig. 5.4). Where the concentration dependence is negligible (aqueous Θ-solvent), Johnston-Ogston effects are eliminated and the Schlieren pattern corresponds closely to the molecular-weight distribution of the sedimenting amylose. Burchard (1963) has suggested an organic Θ-solvent for amylose - DMSO/43.5% acetone, but due to the redistribution of the two solvents, sedimentation velocity was impracticable,

TABLE 5.4

The sedimentation of linear amylose fraction P11 in various solvents

Solvent	$10^{13}.S_o$	$10^{13}.S_w$
Aqueous Θ-solvent	9.0	9.0
0.15M KCl	7.5	7.5
0.15M KOH	6.7	6.7
1M KOH	6.7	7.2
0.12M TMAH	7.1	7.3
0.12M TEAH	5.7	6.2
DMSO	2.7	6.8

FIG 5.4

Schlieren diagrams for amylose in various solvents

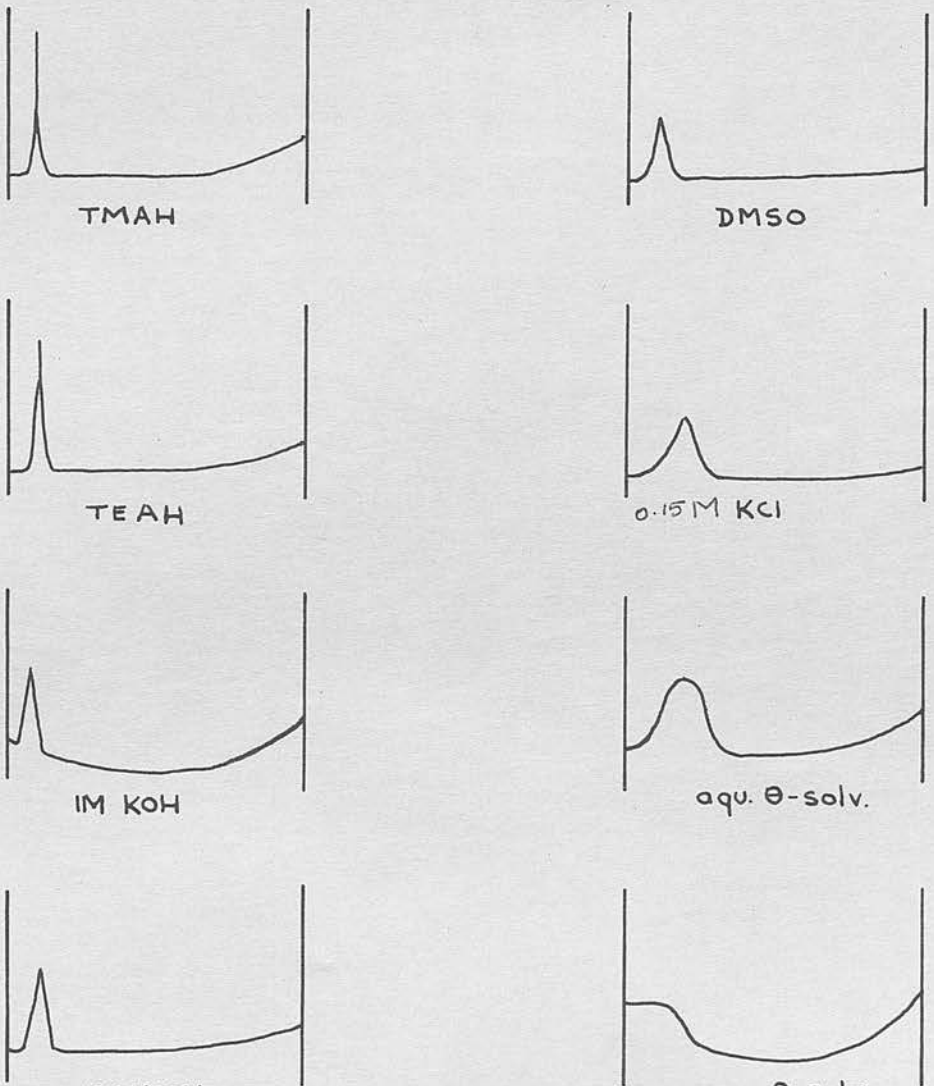

the Schlieren peak at the amylose boundary being almost obscured (Fig. 5.4).

SECTION 6

THE PRESENCE OF INTERMEDIATE POLYSACCHARIDES IN POTATO STARCH

SECTION 6 - INTRODUCTION

The existence of two components in starch is well established, but there have been reports of an intermediate material, with properties different to those of amylose and amylopectin. Lansky, Kooi and Schoch (1949) have suggested the existence of 5-7% of such material, which was precipitated by 'Pentasol' but not by butan-1-ol, in maize starches. From a study of the iodine affinities of various amylose subfractions, they suggested the structure to be intermediate between amylose and amylopectin.

Polysaccharide with a higher iodine affinity, but a lower β-amylolysis limit, than normal amylopectin, was suggested by Peat, Pirt and Whelan (1952) as the structure of a starch intermediate component. Their conclusions were based on the comparison of iodine affinity and β-amylolysis limit of potato starch with the corresponding values obtained using a synthetic mixture of amylose and amylopectin.

Although attempts to isolate this intermediate material have not met with much success, an anomalous 'thymol amylopectin' has been isolated from the supernatant liquors from the recrystallization of the initial thymol-amylose complex of a conventional potato starch dispersion, (Cowie and Greenwood, 1957a). Banks and Greenwood (1959a) studied the physical properties of this 'thymol-amylopectin' and found it to be not always homogeneous. Moreover, they suggested that this polysaccharide could be some enzymically modified amylopectin - either by premature cessation of synthesis, or by degradation. Recently, McKenzie (1964) has studied the

structure of 'thymol amylopectin' in more detail, and considered it to be merely a subfraction of the total-amylopectin, contaminated by short chain amylose.

Perlin (1958) has also reported the isolation of a similar anomalous branched fraction - 'amylopectin-C' - from wheat starch. This component represented some 5-10% of the total starch, and had a β-amylolysis limit some 7% lower than that of normal amylopectin.

Whistler and Doane (1961) separated an intermediate polysaccharide from high amylose corn starch by primary precipitation of total-amylose with butan-1-ol or 1-nitro-propane, and secondary precipitation with 2-nitro-propane from the supernatant. This polysaccharide gave a violet colour with iodine, and corresponded in properties to a long chain amylopectin (external chain length, $\overline{C.L.}$ = ca 40 anhydroglucose units).

More recently, Ulmann(1964) and Richter (1962) have shown the presence of minor components, other than amylose and amylopectin, in starch, by paper chromatography. The latter author found this material to give a blue-violet stain with iodine.

Although the existence of intermediate material seems fairly certain, the question arises as to whether it exists as a separate entity in the starch granule, or is merely a manifestation of a gradual change from linear amylose to highly ramified amylopectin.

The fractional precipitation of potato starch:- Ultracentrifugal analysis of potato starch dispersions by McGregor (1964), showed the presence of two discrete peaks - corresponding to amylose and amylopectin - but no evidence of any third component.

It was thought that any intermediate material might become more prominent if the molecular-weight distributions of the species were narrowed by fractionation.

Total-potato (var. Pentland Crown) starch was subfractionated by acetone precipitation from dimethyl sulphoxide (DMSO) solution at 20°C, in a similar manner to that for amylose (see Section 1B). Twenty subfractions were obtained from aqueous dispersions of the crude fractions by freeze-drying. All subfractions were found to be heterogeneous and were characterized by sedimentation velocity in 0.15M KCl at ca 0.2%.

The results (Table 6.1) show evidence for three components in starch. The factors governing the precipitation of such a system would be complex, however, it is clear from the S-values that the amylose is precipitated first, the amylopectin last and always with contaminating amylose. In almost all amyloses there appears a fast moving heterogeneity, which is quite separate from the amylopectin - indeed, some fractions show a total of three components. This heterogeneity, as shown in Section 4A, is associated with the larger molecular-weight amyloses, and is clearly not contaminating amylopectin. Moreover, its lower solubility than amylopectin suggests a lightly branched structure. This experiment also proves that the heterogeneity is not due to degradation or modification, as the temperature was below 25°C throughout.

Although the presence of some kind of intermediate material associated with amylose is indicated, the presence of some amylopectin-like material in the broader spectrum of structures between

TABLE 6.1

Sedimentation coefficients of DMSO/acetone fractionated potato starch in 0.15M KCl at ca 0.2%

Fraction	$10^{13}.S_s$ a)	$10^{13}.S_f$ b)	$10^{13}.S_{ap}$ c)
S 1	10	39	-
S2 + S3	9	*	-
S4 + S5	9	*	-
S6 + S7	11	*	-
S 8	11	*	-
S 9	11	24	-
S 10	9	*	-
S 11	10	22	-
S 12	11	25	-
S 13	10	*	-
S 14	10	24	-
S 15	9	23	170
S 16	8	28	130
S 17	9	-	220
S 18	7	-	270
S 19	6	-	280
S 20	5	-	110

a) Sedimentation coefficient of slowest component corresponding to amylose

b) Sedimentation coefficient of intermediate component corresponding to the amylose 'heterogeneity'.

c) Sedimentation coefficient of fastest component corresponding to amylopectin

* Not measurable - heterogeneity appeared as a shoulder on leading edge of amylose peak.

amylose and amylopectin is still a possibility.

Outline of investigation:- In attempting to isolate and elucidate the structure of any intermediate material in potato starch, the structure of all starch species from linear amylose up to the highly ramified amylopectin should be studied; intermediate material is as likely in the butan-1-ol precipitated amylose, as in amylopectin, or any intermediate fraction (e.g. 'thymol amylopectin'). For this problem, several lines of investigation were taken. Firstly, potato starch was fractionated using a new technique with nitroparaffin complexing agents (Section 6A). This procedure drew attention to the heterogeneity in amylose as the source of the intermediate polysaccharide, and the structure of amylose β-limit dextrin was therefore studied in Section 6B. Section 6C deals with the structure of the native heterogeneity as it occurs in a normal potato amylose fraction series, and in Section 6D, the technique of density gradient equilibrium ultracentrifugation was used in an attempt to elucidate structure of potato starch components.

6A. THE SUBFRACTIONATION OF AMYLOSE USING NITRO-PARAFFINS.

Whistler and Hilbert (1945) have noted that different percentages of amylose were precipitated from a starch dispersion with various nitro-paraffins. Using their results, a fractionation scheme for potato starch was evolved, which would yield fractions similar to those obtained by Whistler and Doane (1961), but which could be characterized more fully.

EXPERIMENTAL

Fractionation procedure:- 20 gm. of potato starch (var. Pentland Crown; 1963 crop) was dispersed in 3½ l. of boiling deoxygenated water. The dispersion was allowed to cool to ca 80°C under nitrogen, and 220 ml. of nitro-ethane, which had been purified of acidic contaminants by extraction with sodium bicarbonate and distilled water, was added. The nitro-ethane complex, which was formed after 72 hours (A-fraction), was removed on a Sharples super centrifuge and recrystalized twice with butan-1-ol to form a butan-1-ol complex. An aliquot of the dispersed polysaccharide was taken for a concentration estimation , in order to determine the recovery weight of the total fraction.

After removal of the nitro-ethane layer, the supernatant solution was reheated under nitrogen, boiled for 30 minutes to expel excess nitro-ethane. Excess butan-1-ol was then added, and after standing for 72 hours, the B-fraction was isolated and purified. The C-fraction was similarly isolated using 2-nitropropane,

(purified in a similar way to nitro-ethane), as a precipitant (2oo ml. per 8 l.). This fraction was isolated as a fine translucent gel, which was reprecipitated once with 2-nitro-propane, and once with ethanol. The fraction was stored as the 2-nitro-propane complex, and was obtained in a dry form by dissolving the complex in water, removing the 2-nitro-propane by ether extraction and rotary evaporation under reduced pressure, and finally freeze-drying.

The supernatant was further cleared of extraneous solvents, heated, and powdered thymol added (1 gm. l^{-1}). No thymol-complex (as D-fraction) was formed after one week, and the supernatant was therefore purified by extraction with ether, concentrated by rotary evaporation, and freeze-dried to recover the residual amylopectin (E-fraction).

Characterization of products:- Fractions were characterized with respect to,

(a) limiting viscosity number, $[\eta]$, in O.15M KOH (see Section 2A),

(b) sedimentation coefficient at infinite dilution, S_o, in O.15M KCl (see Section 2C),

(c) β-amylolysis limit and (β + Z) limit (see Section 2G),

(d) iodine stain.

An analysis for molecular weight and paucidispersity by the Archibald-Trautman method, was also made on C-fraction dissolved in aqueous Θ-solvent at 25°C (see Sections 2E and 6C).

The iodine affinities of some fractions were kindly determined by Dr. S. McKenzie and Mr. G. Adkins (see Anderson and Greenwood, 1955).

RESULTS AND DISCUSSION

General properties of fractions:- These are shown in Table 6.2. In Section 4A, the presence of a barrier to β-amylolysis was shown to be synonymous with heterogeneous material. Most of the linear material has been fractionated in A-fraction from its high β-amylolysis limit and viscosity whereas B- and C-fractions contain more heterogeneity from their lower β-limit values. The lower $[\eta]$ -value of these fractions is indicative of some branched material.

Sedimentation of A- and B-fractions showed broad Schlieren peaks which did not completely leave the meniscus. This is typical of normal total-amyloses where S_o-values are difficult to assess accurately (see Section 5B). C-fraction showed a minor fast moving component on sedimentation, the slower peak, however, has a sedimentation coefficient typical of amylose-type material. Sedimentation of E-fraction, amylopectin, showed only one broad symmetrical peak, and no trace of any slower peak indicative of amylose contamination.

Iodine stains on these fractions show E-fraction to be pure amylopectin and indicate that amylose-like material is concentrated in the A-, B- and C-fractions. Further proof of the purity of the amylopectin is deduced from its iodine affinity (Fig. 6.1) which is less than 0.1 mg/100 mg of amylopectin and is generally purer than most amylopectins obtained from conventional fractionations using a thymol precipitant. It would seem that any intermediate material present would be confined to the A-, B- and C-

TABLE 6.2

Results of a fractionation of potato starch using nitro-paraffins

Fraction	Precipitant	%	$[\beta]$	$[\beta + Z]$	$[\eta]$	$10^{13}.S_o$	I_2-stain
A	NO_2Et	17.2	81	101	470	-	blue
B	n-BuOH	7.0	67	102	320	ca 11	blue
C	2-NO_2Pr	< 1	55	83	120	8.9	blue
D	thymol	-	-	-	-	-	-
E	supernatent	75	-	-	120	63[a)]	red

a) Determined at concentration ca 0.2%.

TABLE 6.3

Results of an Archibald-Trautman analysis of C-fraction

C_1 %	C_2 %	$10^{-6}M_1$	$10^{-6}M_2$	$10^{-6}.\bar{M}_w$	$10^{-6}.\bar{M}_z$
25	75	20.6	0.07	5.3	21

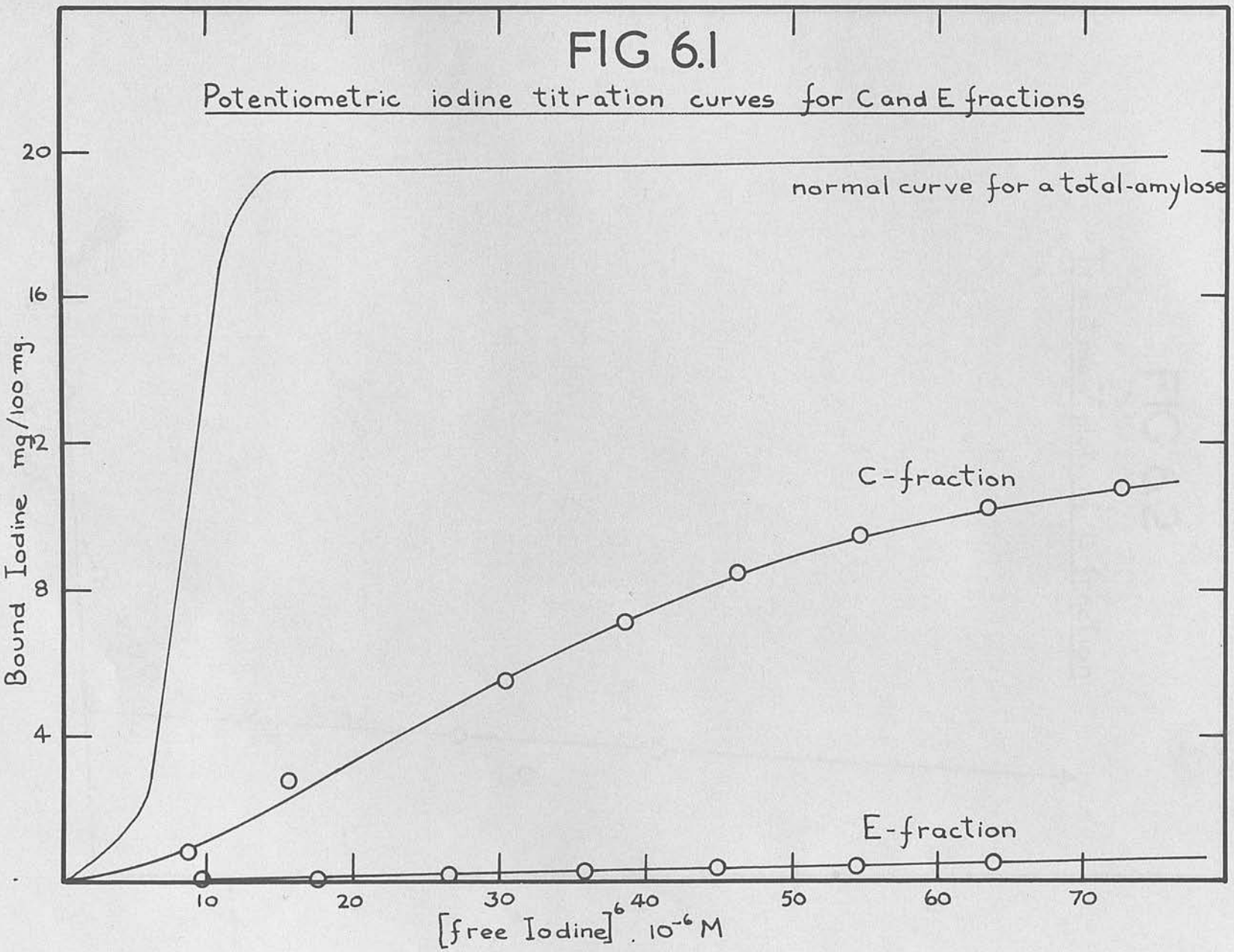
FIG 6.1
Potentiometric iodine titration curves for C and E fractions
normal curve for a total-amylose
C-fraction
E-fraction
Bound Iodine mg/100 mg.
[free Iodine]^6 . 10^{-6} M
20
16
12
8
4
10
20
30
40
50
60
70

FIG 6.2

Trautman plot of C-fraction

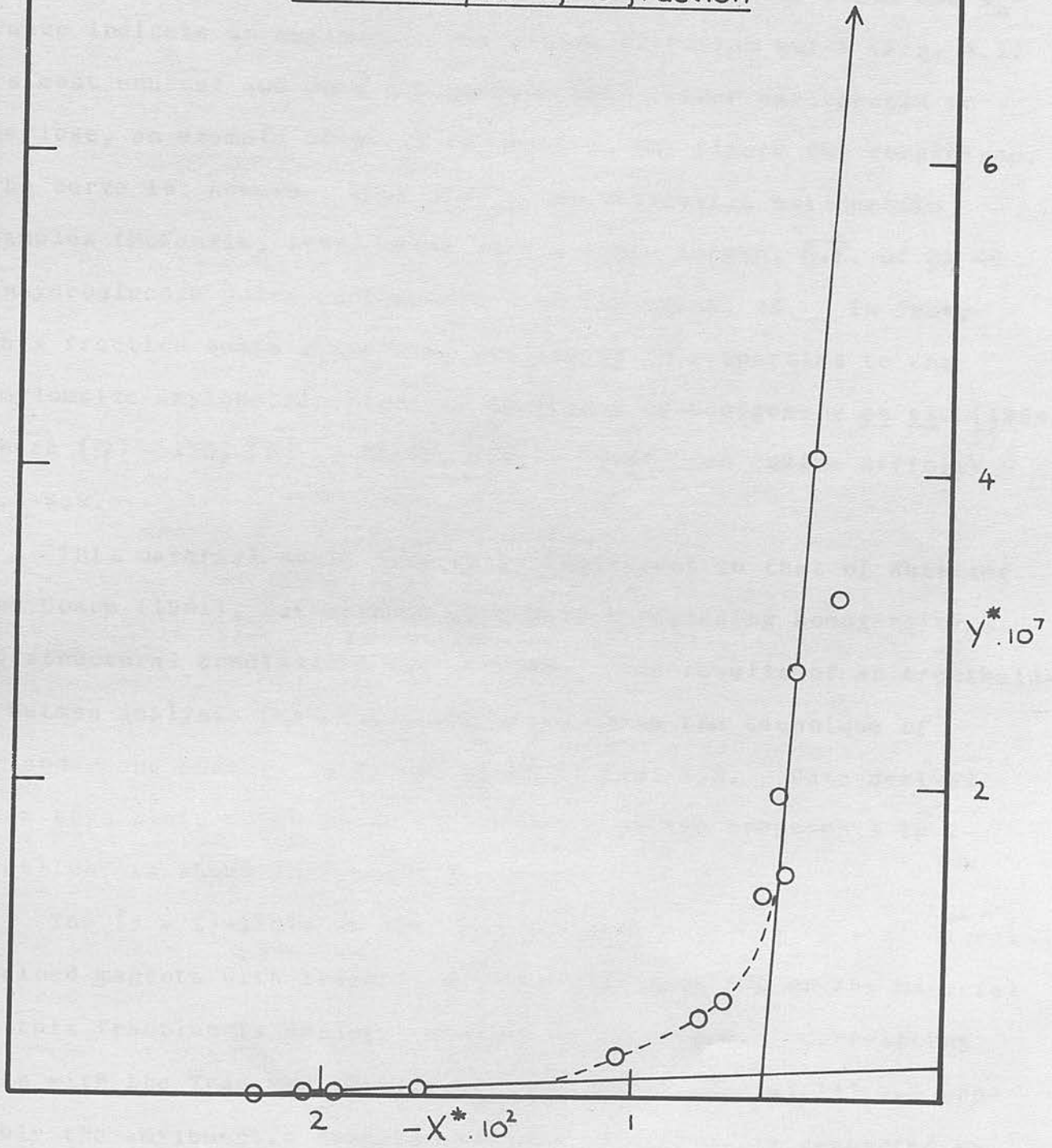

fractions, and particularly the latter which shows some unusual properties.

Properties of C-fraction:- The β-limit and viscosity suggest that this fraction is an amylopectin, yet its iodine-stain and S_o-value indicate an amylose. The iodine titration curve (Fig. 6.1) is most unusual and does not compare with either amylopectin or amylose, an example of which is shown in the figure for comparison. The curve is, however, very similar to amylomaize amylopectin samples (McKenzie, 1964) which have a chain length, $\overline{C.L.}$ of ca 40 anhydroglucose units as compared with the normal 25. In fact, this fraction bears a striking similarity in properties to the amylomaize amylopectin recently described by Montgomery et al. (1964) where $[\eta]$ = 120, $[\beta]$ = 56-77, $\overline{C.L.}$ = 27-45, and iodine affinity = 1.2-8.9.

This material would seem to be equivalent to that of Whistler and Doane (1961), but without information regarding homogeneity, no structural conclusions can be made. The results of an Archibald-Trautman analysis for paucidispersity, using the technique of Erlander and Foster (1959) are shown in Fig. 6.2. Data derived from this plot, which shows the presence of two components in C-fraction, is shown in Table 6.3.

The (β + Z)-limit of 83%, and the fact that the (β + Z) digest stained magenta with iodine indicates that some 30% of the material in this fraction is amylopectin-like in structure. Correlating this with the Trautman results, it seems that species '1' has probably the amylopectin structure; this conclusion is supported by

a molecular-weight that is far too high for any amylose. However, this molecular-weight is much lower than normal amylopectin, where $\overline{M}_w$ = ca 10^8. Since the β-amylolysis limit of the total fraction is close to 50, species '2' in the analysis must also have a barrier to β-amylolysis action. Excluding the possibility of artifacts for the moment, this would correspond to branched material. Now C-fraction complexes with 2-nitro-propane but not with butan-1-ol, which suggests the absence of any long chain amylose. Therefore, this material mustcorrespond to some kind of short chain-length, branched material of an amylose-type from a consideration of its low molecular-weight. Correlation of these conclusions with the iodine titration evidence, does suggest that the chain lengths are still sufficiently long to bind iodine, although there is no normal long chain amylose, as there is no characteristic abrupt levelling off of the curve (Fig. 6.1).

The evidence would, therefore, seem to indicate that C-fraction, which is less than 1% of the total starch, contains some 25% of small, long-chain amylopectin, and some 75% of small amylose-like material with short chain lengths. This latter material could also be identified as degraded polysaccharide, but it would be difficult to decide whether this was the case or whether the material was indeed native to the total starch. There is always the possibility that artifacts may be introduced during fractionation, (as has been discussed in Section 4A), but every precaution was taken to minimise this.

The percentage amylose in total starch:- It is noteworthy

that the percentage amylose (as precipitated by butan-1-ol) in the total starch was 25%, whereas an iodine titration of the starch indicated an amylose concentration of 20%. Schoch (1964) has pointed out the discrepancies that might be involved in assessing the percentage amylose from iodine titration curves, without knowing the status of possible intermediate fractions.

Conclusion:- The heterogeneity in amylose (as measured by the β-amylolysis limit) and an intermediate component in starch seem closely related. A closer look at the structure of the amylose heterogeneity is indicated, to find out how it is connected with that proposed for C-fraction.

6B. THE PREPARATION AND SUBFRACTIONATION OF AMYLOSE β-LIMIT-DEXTRIN

As shown in Section 4A, total-amylose is incompletely degraded by β-amylase. It was suggested that molecules with a barrier to β-amylolysis were in fact branched, and constituted a heterogeneity in natural amylose. To isolate this heterogeneity in its natural state has proved to be difficult; preparations always being contaminated with linear amylose. However, the isolation of the residual polysaccharide after β-amylolysis where all linear material is destroyed, is relatively simple, and a structural investigation of this material (the β-limit-dextrin) can lead to predictions on the structure of the amylose heterogeneity and hence the intermediate material in starch.

EXPERIMENTAL

Residue from a 60° aqueous leaching of potato starch (var. Pentland Crown) (Banks, Greenwood and Thomson, 1959) was fractionated in the usual manner (Banks and Greenwood, 1959) to obtain an amylose product rich in the heterogeneity (β-limit = ca 70). This product was then degraded by β-amylase for 24 hours at 40°C. The protein was filtered from the solution after being denatured by heating and shaking for a few minutes, and addition of butan-1-ol precipitated the dextrin as a complex after 72 hours. A small aliquot of this complex was re-incubated with fresh β-amylase, and tested for any reducing power, to ensure that β-amylolysis was complete.

The final β-limit-dextrin was then subfractionated in the usual way by acetone precipitation from a DMSO solution (cf. amylose, Section 1B), and seven subfractions isolated as butan-1-ol complexes.

Characterization of subfractions:- These were characterized with respect to $[\eta]$ -values in 0.15M KOH, and sedimentation coefficients, S, in 0.50M KCl/10^{-2}M KOH (aqueous Θ-solvent) at 20,410 r.p.m., and 25°C (see Sections 2A, 2C). Molecular-weights and an analysis for paucidispersity were also measured by the Archibald-Trautman technique on fractions dissolved in aqueous Θ-solvent at 25°C (see Sections 2E and 6C).

RESULTS AND DISCUSSION

The results are shown in Table 6.4. The fairly high $[\eta]$ - values suggest a generally open filamentous structure, as opposed to a compact branched structure. Moreover, the range in $[\eta]$ - values indicates some kind of fractionation - probably more with respect to degree of branching. All fractions were found heterogeneous from sedimentation analysis. The heavier component was generally of such a broad molecular-weight distribution, that measurements of S were impracticable. The sedimentation coefficients of the slower components, however, indicated some degree of fractionation (Table 6.4).

Although all fractions showed at least two components, only in two cases (fractions LD1 and LD 5) was the molecular-weight distribution amenable to a full Trautman analysis (Table 6.5). In other fractions, the distribution - particularly of the heavier component - made the determination of its concentration, C_1, and molecular-weight, M_1, difficult, and only approximations could be made (C_1 from the area beneath the Schlieren peak). In these fractions, and particularly in LD 3, the faster, broader component was being continually sedimented away from the meniscus, where the data for the Trautman procedure is collected. Schlieren patterns, akin to that shown in Fig. 6.3, were typical, and only an analysis of the slower component was usually possible.

Molecular-weight values calculated from $[\eta]$ using equation 4.14 (p. 123), which assumes linear-amylose, are lower than molecular-weights determined by Trautman analysis. This indicates

TABLE 6.4

Properties of subfractions of potato amylose β-limit-dextrin

% Acetone	Fraction[a)]	%[b)]	$[\eta]$	$10^{13}.s$[c)]	$10^{-6}.\bar{M}_w$	$10^{-6}.\bar{M}_z$
42.7	LD 1	22	720	23.1	7.8	13
44.9	LD 2a	17	540	19.0	*	*
	LD 2b	12	500	15.7	*	*
46.4	LD 3	5	450	15.0	*	*
47.7	LD 4	5	410	12.7	*	*
51.5	LD 5	22	380	12.2	9.5	15
excess	LD 6	17	330	10.3	*	*

a) a, b represent refractionated products

b) Calculated as percentage of recovered polysaccharide

c) Sedimentation coefficient of the major slower component

* Not accurately determinable (see text).

TABLE 6.5

Results of an Archibald-Trautman analysis of subfractions of potato amylose β-limit-dextrin

Fraction	C_1 %	C_2 %	$10^{-6}.M_1$	$10^{-6}.M_2$	Distribution[a]	$10^{-6}.M$ calc[b]
LD 1	45	55	15.7	2.4	P	2.7
LD 2a	ca40	ca60	ca 16	2.7	H - P	1.8
LD 2b	ca40	ca60	*	1.6	H - P	1.3
LD 3*	-	-	-	-	H	1.2
LD 4	ca40	ca60	*	ca 2	P	0.78
LD 5	53	47	16.6	1.7	P	0.77
LD 6	ca40	ca60	ca 5	0.52	H - P	0.50

* Heterogeneity and distribution made quantitative calculations impracticable

a) Distribution of molecular-weight, as indicated by Schlieren diagrams and Trautman plot
P = paucidisperse; H = heterogeneous

(b) Molecular-weights calculated from an approximate empirical relation* obtained from S-values (measured in aqueous Θ-solvent at 20,410 r.p.m.) of the L-fractions (see Section 4B)

$$*S = 1.45 \times 10^{-15} \bar{M}_w^{0.50}$$

that the material in these fractions is essentially branched. The faster components are broad in molecular-weight distribution, being quickly sedimented and distributed across the cell. Their molecular-weights are some 6-10 times greater than the slower components (Table 6.5). Rather surprisingly, therefore, it seems that there are two types of material making up the limit dextrin.

Molecular-weights of the slower components, calculated from their S values (using equation ~~4.17~~ 7; p. 116), were similar to those found experimentally. This calculation assumes a linear molecule, and therefore it would seem that component '2' is essentially linear in structure. The slower component is unlikely to be modified linear amylose limit dextrin, as its sedimentation coefficient and molecular-weight are too high. Such an amylose, assuming a random oxidised glucose unit, would have a limit dextrin of molecular-weight less than 10^6 (cf. Section 4B). It is further seen from Table 6.5 that species '2' is more easily fractionated with respect to molecular-weight than species '1', suggesting a filamentous structure. Thus, the evidence points to a branched structure for species '1' which could be the core of some amylopectin-like structure, whereas species '2' would seem to be smaller and essentially linear in nature, and be derived from some slightly branched amylose-like molecule. Assuming an average β-amylolysis limit of 50 for the heterogeneous material, the native polysaccharides from which these limit dextrins were derived would have molecular-weights of ca 30×10^6 and 4×10^6 for species '1' and '2' respectively. These native polysaccharides are hereafter designated intermediate-amylopectin and intermediate-amylose

TABLE 6.5

Results of an Archibald-Trautman analysis of subfractions of potato amylose β-limit-dextrin

Fraction	C_1 %	C_2 %	$10^{-6}.M_1$	$10^{-6}.M_2$	Distribution[a]	$10^{-6}.M$ calc[b]
LD 1	45	55	15.7	2.4	P	2.7
LD 2a	ca40	ca60	ca 16	2.7	H - P	1.8
LD 2b	ca40	ca60	*	1.6	H - P	1.3
LD 3*	-	-	-	-	H	1.2
LD 4	ca40	ca60	*	ca 2	P	0.78
LD 5	53	47	16.6	1.7	P	0.77
LD 6	ca40	ca60	ca 5	0.52	H - P	0.50

* Heterogeneity and distribution made quantitative calculations impracticable

a) Distribution of molecular-weight, as indicated by Schlieren diagrams and Trautman plot
P = paucidisperse; H = heterogeneous

(b) Molecular-weights calculated from an approximate empirical relation* obtained from S-values (measured in aqueous Θ-solvent at 20,410 r.p.m.) of the L-fractions (see Section 4B)

$$*S = 1.45 \times 10^{-15} \bar{M}_w^{0.50}$$

respectively.

Considerations on the mechanism of fractionation:- As the solubility of a polymer in a solvent/non-solvent mixture depends both on molecular-weight and the degree of branching, the fractional precipitation of amylose β-limit dextrin - which contains a whole spectrum of material ranging from almost linear to highly branched residues - must be complex, and any one fraction might be expected to contain two distributions of material. Therefore, although two discrete intermediate species have been indicated for the amylose heterogeneity, there could easily be a continuous distribution of branched material.

Total amylose β-limit dextrin at equilibrium in a density gradient:- To decide whether there are two discrete intermediate polysaccharides, a density gradient equilibrium experiment was made on a total β-limit dextrin butan-1-ol complex (derived from a total potato amylose) dissolved in ca 6.5M CsCl (see Section 2F). Apart from a small aggregate band (A) at a buoyant density $\rho = 1.625$ (see Section 4B), two broad, overlapping bands were observed (Fig. 6.4). Both showed density heterogeneity, and no calculation for absolute molecular-weight was therefore possible. A qualitative estimation of relative molecular-weights, to within an order of magnitude, can be made from the equilibrium time and inverse square of the band width, which is porportional to molecular-weight (Table 6.6). It is difficult to say what these two bands represent, but the major one (C) occurs at a ρ -value

TABLE 6.6

Density gradient equilibrium data for total potato amylose β-limit-dextrin

Band	ρ a) gm. ml^{-1}	Rel. conc.	T b) hours	$(b.w.)^{-2}$ c) cm^{-2}
A	1.625	1%	5	-
B	1.640	21%	26	1.0
C	1.663	79%	43	0.39

a) Buoyant density

b) Equilibrium time

c) Magnified inverse square of the band width $\propto \bar{M}_w$.

similar to that for linear amylose (see Sections4B and 6D), and therefore may be essentially linear in structure. This conclusion is substantiated by an estimation of its molecular-weight, (see Table 6.6, where a $(b.w.)^{-2}$ value of ca 0.28 corresponds to a molecular-weight of ca 10^6; Sections 4B, 6D). The minor band (B) at ρ = 1.640 may be identified as a more highly branched structure, from its higher molecular-weight. However, such a structure might be expected to have a buoyant density between that of amylose and amylopectin where ρ = ca 1.662 and ca 1.681 respectively (Section 6D).

It seems fairly certain that the amylose β-limit dextrin contains two distinct components, and it is suggested that band B represents polysaccharide derived from intermediate amylopectin, and band C from intermediate amylose.

Confirmation of the above result was obtained by the density gradient equilibrium of another total amylose β-limit-dextrin, which was independently prepared from another Pentland Crown potato starch and kindly supplied by Dr. W. Banks. In this instance, any association in aqueous systems was avoided by using a mixture of organic solvents, - N-methyl-2-pyrrolidone (NMP) and bromoform ($CHBr_3$) - to establish the density gradient (see Section 6D).

Two well defined bands were obtained (see Fig. 6.10; p.216a) at buoyant densities of ρ = 1.251 and ρ = 1.238, which contained some 30% and 70% of the total limit dextrin respectively. These are tentatively assigned to material derived from intermediate-amylopectin and intermediate-amylose respectively. From the

gradient of the $\ln c$ vs. $(r - r_o)^2$ plot, intermediate-amylose limit dextrin was found to be homogeneous with an apparent molecular weight, M_{app}, of ca 4 x 10^6, whereas the intermediate amylopectin limit dextrin was heterogeneous with respect to molecular weight. In the latter case, M_{app} varied between ca 10-3 x 10^6 over the band.

It should be noted that these polysaccharides suffer considerable preferential absorption with NMP. The extent of this for different species is unknown but ρ-values are markedly affected.

6C. THE DISTRIBUTION OF INTERMEDIATE MATERIAL IN A FRACTION SERIES

In this section, a study of the native heterogeneity or intermediate material as it occurs in a total amylose was made. The Archibald-Trautman procedure has been found satisfactory for analysing linear-amylose fractions (Section 4B), and its application in the analysis of paucidisperse systems is considered in more detail here. It is essential that the molecular-weight distribution is fairly narrow, and therefore analysis was confined to subfractions of total amylose. Moreover, it is essential that the distribution is paucidisperse rather than heterogeneous as was demonstrated in Section 6B. Non-linear amylose fractions that show two peaks on sedimentation velocity are, therefore, unsuitable for a Trautman analysis. Non-linear amylose fractions, which show one skew peak on sedimentation velocity and therefore have a paucidisperse distribution, are easily obtained (Section 4A). In addition, the subfractionation of the B-fraction total-amylose described in Section 6A, was found to yield a series of paucidisperse subfractions amenable to a Trautman analysis. This fraction series was of particular interest, as the starting material itself had a high percentage of intermediate material (β-amylolysis limit = 67).

Heterogeneous potato amylose subfractions may be analysed for the two peaks, with some knowledge of the Johnston-Ogston effects (see Section 2C). Some qualitative analysis of these systems was also made.

Finally, in an attempt to isolate the natural intermediate polysaccharides, gel filtration was tried.

EXPERIMENTAL

Preparation of subfractions:- B-fraction (Section 6A) was subfractionated by acetone precipitation from a DMSO solution to give a B-fraction series, as described in Section 1B. In order to obtain a fraction rich in intermediate material, the first fraction (B1) was refractionated to yield B1a and B1b, and fraction B1a was further subfractionated to yield B1aa and B1ab.

Subfractions obtained from total-amylose by the benzene precipitation of a DMSO solution were also used for a Trautman analysis (PB-series, see Section 4A).

A selection of heterogeneous potato amylose subfractions was taken from those described in Section 4A, and also from other sources.

Characterization of subfractions:- These were characterized with respect to $[\eta]$ -values in 0.15M KOH, and β-amylolysis limits as described in Sections 2A and 2G respectively. In addition, the iodine affinities of some fractions were kindly determined by Dr. S. McKenzie and Mr. G. Adkins.

All measurements by the Trautman procedure were on the amylose/butan-1-ol complexes dissolved in 0.50M KCl/10^{-2}M KOH (aqueous Θ-solvent) at 25°C at a concentration of ca 0.2% unless otherwise stated. The solutions were introduced into preheated cells and rotors (to 25°C), and procedure was as described in Section 2E.

In the calculation of results it was assumed that dn/dc and $\bar{V}$ were constant for all species ($\bar{V}$ = 0.65, Cowie, 1958; Everett and Foster, 1959). Since Θ-conditions were used, the second virial coefficient is zero (Sotobayashi and Ueberreiter, 1964), and no extrapolation of molecular-weight data to infinite dilution was therefore necessary.

Analysis of heterogeneous amyloses:- In view of the small amount of heterogeneous material, present as the fast moving peak (see Section 4A), the normal procedures of analysis, outlined in Section 2C, were not practical. An empirical comparison was therefore made with the sedimentation behaviour of amylose-amylopectin mixtures.

Pure samples of a fairly narrow molecular-weight distribution were required, and E-fraction (amylopectin) and amylose fraction L4 were used. Amylose and amylopectin were separately dissolved in alkali and neutralized with HCl to yield solutions in 0.16M KCl at $>$ 0.2%. The concentrations of these solutions were determined exactly by the alkali-ferricyanide method (Lampitt et al., 1955), and each adjusted to exactly 0.20% with solvent. Thus the total concentration of any mixture prepared from these solutions was always 0.20%.

Several mixtures were prepared, spun in the ultracentrifuge at 30,410 r.p.m. and 20°C. 30 mm. double-sector cells were used, with pure solvent in one sector, to facilitate area measurements by providing a base line on the Schlieren pattern. The apparent concentrations of amylose and amylopectin in any mixture were

measured from the area, corrected to a constant Schlieren bar angle of 55^{o}, beneath the corresponding Schlieren peaks. The amylose and amylopectin were also run separately in a dilution series to obtain sedimentation coefficients at infinite dilution, S_o (see Section 2C).

Gel-filtration of amylose:- Amylose fraction P-3 dissolved in O.16M KCl, was chromatographed down a G75 Sephadex column (3.5 cm. diameter x 40 cm. length) using O.15M KCl as an eluting solvent. Ca 10 ml. of amylose solution (concentration ca 0.15%) was charged to the column, allowed to soak in, washed in with 5 mls. of solvent, and the column topped up with eluting solvent. Constant volume fractions of 5 ml. were collected, and characterized with respect to (i) polysaccharide content by a phenol-sulphuric acid determination (Dubois et al., 1956) and (ii) iodine stain.

RESULTS AND DISCUSSION

Distribution of intermediate material in the B-fraction series:- The results are shown in Tables 6.7 and 6.8. All the fractions appeared paucidisperse or heterogeneous, showing at least two components. The $\bar{M}_w$-values calculated from $[\eta]$-values, assuming linear amylose (equation 4.14, p123), are all lower than the respective experimental values, indicating branched material in all fractions. This would be expected, as all fractions were incompletely degraded by β-amylase. From the shape of the Schlieren pattern in aqueous Θ-solvent, and the appearance of the Trautman plot, an estimation of molecular-weight distribution may be made. A Trautman plot with two well-defined lines indicates a paucidisperse distribution with two well-defined components (e.g. fraction B1aa, Fig. 6.5), whereas a broad distribution with a more or less continuous range in molecular-weight would give a curved Trautman plot, indicative of polydispersity (e.g. fraction B5, Fig. 6.6). In the latter case the C_1, C_2, M_1, M_2 values were not assessable with any accuracy. Fractions B1ab and B2 showed heterogeneous molecular-weight distributions, the heavier component being quickly separated from the slower, as a broad peak in the Schlieren diagram which was not included in the Trautman analysis. This behaviour was similar to that shown for some β-limit-dextrin fractions (Section 6B), and in such cases, the molecular-weight of the slower component only was determined. The remaining four fractions were amenable to a full Trautman analysis.

The concentrations, C_1 and C_2, of the different components

TABLE 6.7

Properties of subfractions from B-fraction total amylose

Fraction	$[\beta]$	$[\eta]$	$10^{-6}.\bar{M}_w$	$10^{-6}.\bar{M}_z$	$\bar{M}_z/\bar{M}_w$	$10^{-6}.M$ calc[a]
B1 aa	57	585	4.1	8.6	2.1	1.20
B1 ab	84	395	*	*	*	0.80
B1 b	76	375	1.45	3.1	2.1	0.75
B2	61	275	*	*	*	0.60
B3	77	290	0.83	1.8	2.1	0.61
B4	88	133	0.42	1.7	4.0	0.23
B5	87	140	0.29	0.67	2.3	0.23

a) Molecular-weight calculated from $[\eta]$ using equation 4.14, p.123

* Heterogeneity and distribution made calculations impracticable.

TABLE 6.8

Results of an Archibald-Trautman analysis of subfractions from B-fraction total amylose

Fraction	C_1 %	C_2 %	$10^{-6}M_1$	$10^{-6}M_2$	Distribution[a]	$10^{-6}M$ calc[b]
B1 aa	30	70	11.7	1.16	P	1.20
B1 ab	*	*	*	0.87	H	0.80
B1 b	16	84	7.5	0.74	P	0.75
B2	*	*	*	0.67	H	0.60
B3	17	83	3.9	0.40	P	0.61
B4	13	87	2.9	0.13	P	0.23
B5	*	*	*	*	BP	0.23

a) Distribution of molecular-weight, as indicated by Schlieren diagrams and Trautman plot

P = paucidisperse; H = heterogeneous; BP = broad polydisperse.

b) Molecular-weight calculated from $[\eta]$ using equation 4.14, p.123.

* Heterogeneity and distribution made calculations impractible.

FIG 6.5

Trautman plot for fraction B1aa

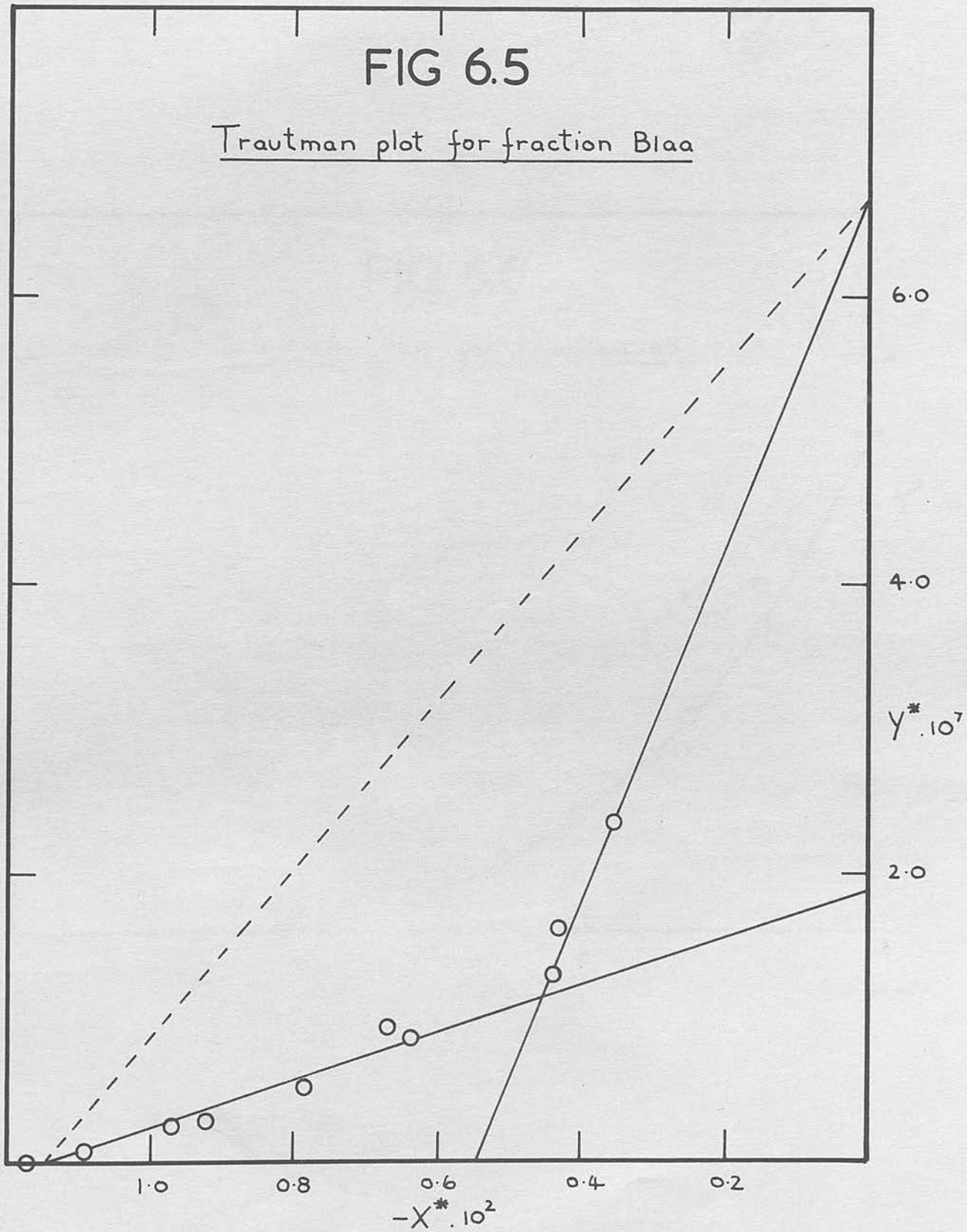

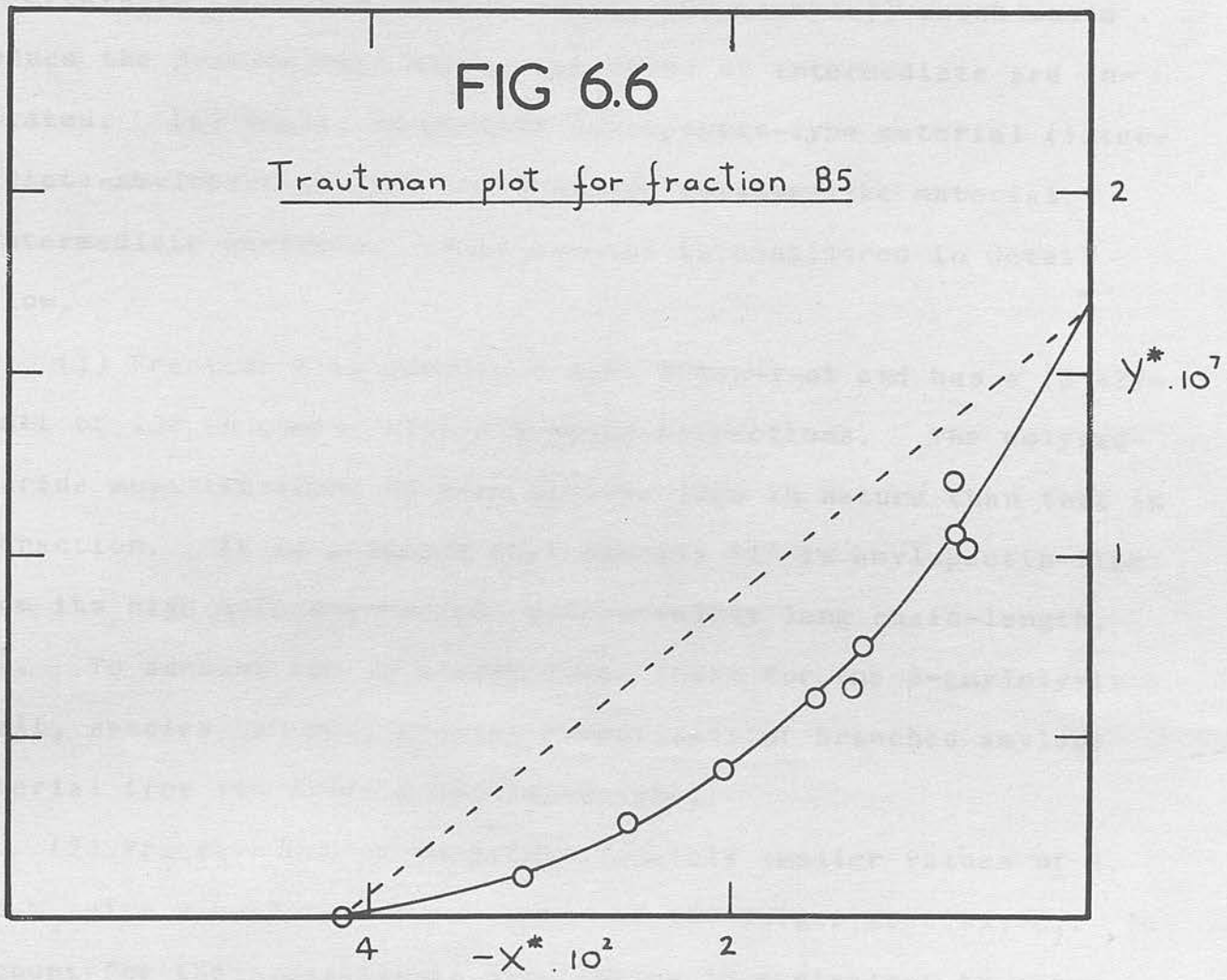
FIG 6.6
Trautman plot for fraction B5
2
y* . 10⁷
1
4
−X* . 10²
2

bear little relation to the β-amylolysis limits. If the β-amylolysis limit of non-linear amylose is assumed to be 50, then a simple mixture of linear and non-linear material for species '1' and '2' is not indicated - in each case the β-amylolysis limit is lower than would be expected. Notwithstanding the possibility of artefacts (oxidised glucose units, for example), which would reduce the β-amylolysis limit, two types of intermediate are indicated. (a) Small, long-chain amylopectin-type material (intermediate-amylopectin) and, (b) branched amylose-like material (intermediate amylose). This concept is considered in detail below.

(1) Fraction B1aa complexes with butan-1-ol and has a (β +Z)-limit of 100 in common with all other B-fractions. The polysaccharide must therefore be more amylose-like in nature than that in C-fraction. It is proposed that species '1' is amylopectin-like from its high molecular-weight with a fairly long chain-length, $\overline{C.L.}$. To account for an almost lower limit for the β-amylolysis limit, species '2' must consist essentially of branched amylose material from its lower molecular-weight.

(2) Fraction B1b shows proportionately smaller values of M_1 and M_2 with a smaller concentration of the larger species, C_1. To account for the β-amylolysis limit which is equivalent to about 50% linear material, the smaller species '2' must contain some branched amylose material as well as some linear amylose. If C_1 and C_2 were simply branched and linear material respectively, the β-amylolysis limit would be 92.

It is noteworthy that the M_2-values of B1aa and B1b are very similar to $\overline{M}_w$ values calculated from $[\eta]$ of these fractions which assumes linear-amylose. Since the heavier component is only a minor proportion of the total fraction, and being branched would have a low $[\eta]$ -value, its contribution to $[\eta]$ for the total fraction would be small. This total $[\eta]$ may therefore be regarded as essentially that of the slower component. It is therefore concluded that the intermediate amylose contained in the slower component is similar hydrodynamically to linear-amylose. This would indicate very limited branching in intermediate amylose.

(3) Fractions B3 and B4 show progressively smaller molecular weights for intermediate material and linear amylose. The lower molecular-weight species '1', is here probably more amylose-like in character and makes a significant contribution to the total $[\eta]$-value, giving calculated molecular weights intermediate between M_1 and M_2. In fraction B5 there is probably a continuous molecular distribution from linear to intermediate material which would constitute some 26% of the total fraction from its β-amylolysis limit.

The lighter component in fractions B1ab and B2 is seen to be similar to linear-amylose in hydrodynamic behaviour.

As pointed out in Section 6B, subfractionation of a mixture of linear and branched molecules would be complex. Although specific species have been assumed in this analysis, the possibility of a gradual change in molecular structure in natural total amylose should be considered.

Distribution of intermediate material in the PB-fraction

series:- The results are shown in Tables 6.9 and 6.10. This fraction series is slightly different from the B-series discussed above, in that it represents total-amylose isolated from a conventional starch fractionation. Moreover, although all subfractions had (β + Z)-limits of 100, some subfractions also had β-amylolysis limits of 100, and are therefore linear. These subfractions (PB1d and PB5) were shown to be single component on Trautman analysis with $\bar{M}_w$-values in excellent agreement with those calculated from their $[\eta]$ -values (equation 4.14, p.123). It has been shown that these PB- fractions are of broad distribution (Section 4A), and this was exemplified in gently curved Trautman plots for the two linear subfractions. All other subfractions, with β-amylolysis limits of $<$ 100 have $\bar{M}_w$-values greater than those calculated from $[\eta]$ on the basis of linear-amylose. This is indicative of branched material.

The discussion for this fraction series is similar to that for the B- fraction series above. Fraction PB1c showed a similar heterogeneous behaviour to fractions B1ab and B2 where only the slower component was analysed and found to have a similar hydrodynamic behaviour to linear-amylose. Fraction PB1a is similar to fractions B1aa and B1b, with the implication that it contains some three components - intermediate amylopectin, intermediate amylose, and linear amylose. Fractions PB2 and PB3 correspond to fractions B3 and B4, only here the concentrations of species '1'(C_1) are compatable with the β-amylolysis limits. Thus in these cases, essentially linear material must comprise

TABLE 6.9

Properties of PB- subfractions

Fraction	$[\beta]$	$[\eta]$	$10^{-6}.\bar{M}_w$	$10^{-6}.\bar{M}_z$	$\bar{M}_z/\bar{M}_w$	$10^{-6}.M$ calc[a)]
PB 1a	81	1040	8.6	24	2.8	2.4
PB 1c	81	775	*	*	*	1.7
PB 1d	98	490	1.0	1.5	1.5	1.0
PB 2	94	530	1.7	6.9	4.0	1.1
PB 3	96	340	0.93	2.4	2.6	0.67
PB 5	100	155	0.26	0.43	1.6	0.27

a) Molecular-weight calculated from $[\eta]$ using equation 4.14, p.123.

* Heterogeneity and distribution made calculations impractible.

TABLE 6.10

Results of an Archibald-Trautman analysis of PB- subfractions

Fraction	C_1 %	C_2 %	$10^{-6}.M_1$	$10^{-6}.M_2$	Distribution [a]	$10^{-6}.M$ calc [b]
PB 1a [c]	22	78	35	2.3	P	2.4
PB 1c [d]	*	*	*	1.7	H	1.7
PB 1d	-	100	-	1.0	LP	1.0
PB 2	15	85	9.2	0.81	P	1.1
PB 3	10	90	7.9	0.51	P	0.67
PB 5	-	100	-	0.26	LP	0.27

a) Distribution of molecular-weight, as indicated by Schlieren diagrams and Trautman plot

P = paucidisperse; H = heterogeneous; :P = linear-polydisperse.

b) Molecular-weight calculated from $[\eta]$ using equation 4.14, p. 123 .

c) Analysis at 30°C; d) Analysis at 26°C

* Heterogeneity and distribution made calculations impossible.

component '2', whereas component '1' would contain the intermediate material, which seems more amylopectin-like in structure, from the high molecular weights.

Potentiometric iodine titration of some potato amylose subfractions:- The iodine titration curves for some B- and PB-fractions are shown in Fig. 6.7. The variable iodine affinity can be attributed not only to the presence of intermediate material, but also to the molecular-weight (more specifically the total degree of polymerisation, $\overline{D.P.}$) of the amyloses. Although the iodine affinity of most amyloses is 19.5 (Anderson and Greenwood, 1955), samples with unusually low β-amylolysis limits or high $\overline{D.P.}$s would seem to markedly affect this value. The former effect would tend to lower the iodine affinity, whereas the latter would raise it. With two such opposing effects, quantitative conclusions are impossible, without some form of calibration for the apparatus. However, it can be seen that the titration curves for fractions B1aa and B1ab, where there is a relatively high proportion of intermediate material associated with smaller $\overline{D.P.}$s (smaller $[\eta]$ -values), are lower than for other fractions. This indicates intermediate material with fairly short chain lengths, $\overline{C.L.}$, probably approaching the long chain amylopectin structure found in C-fraction (Fig. 6.1).

The β-limit dextrins of some fractions:- The polysaccharide remaining after β-amylolysis - the β-limit dextrin - was isolated as described in Section 6B, for three amylose subfractions (viz.

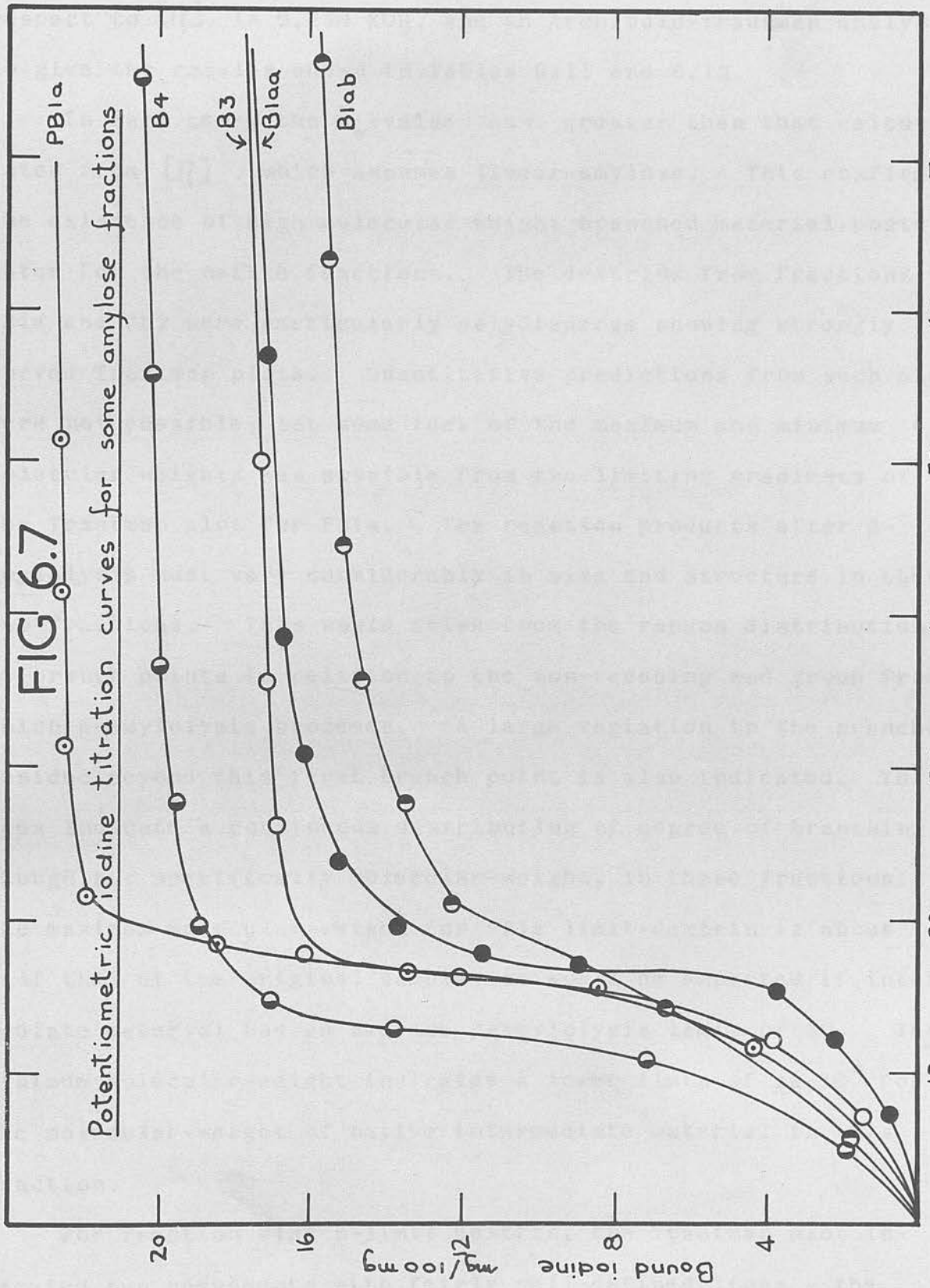
FIG 6.7
Potentiometric iodine titration curves for some amylose fractions
PB1a
B4
B3
B1aa
B1ab
Bound iodine mg/100mg
[free iodine] 10^{-6} M
4
8
12
16
20
10
20
30
40
50
60
70

B1aa, PB1a, PB2). The limit-dextrins were characterized with respect to $[\eta]$ in 0.15M KOH, and an Archibald-Trautman analysis, to give the results shown in Tables 6.11 and 6.12.

In each case, the $\bar{M}_w$-value was greater than that calculated from $[\eta]$, which assumes linear-amylose. This confirms the existence of high molecular-weight branched material, postulated for the native fractions. The dextrins from fractions PB1a and PB2 were particularly polydisperse showing strongly curved Trautman plots. Quantitative predictions from such plots were not possible, but some idea of the maximum and minimum molecular weights was possible from the limiting gradients of the Trautman plot for PB1a. The reaction products after β-amylolysis must vary considerably in size and structure in these two fractions. This would arise from the random distribution of branch points in relation to the non-reducing end group from which β-amylolysis proceeds. A large variation in the branched residue beyond this first branch point is also indicated. This does indicate a continuous distribution of degree of branching, though not specifically molecular-weight, in these fractions. The maximum molecular-weight for PB1a limit-dextrin is about half that of the original sample, as would be expected if intermediate material had an average β-amylolysis limit of 50. The minimum molecular-weight indicates a lower limit of <u>ca</u> 10^6 for the molecular-weight of native intermediate material in this fraction.

For fraction B1aa β-limit dextrin, the Trautman plot indicated two components with fairly well-defined lines - the

TABLE 6.11

Properties of β-limit dextrins from fractions B1aa, PB1a and PB2

Sample	$[\eta]$	$10^{-6}.\bar{M}_w$	$10^{-6}.\bar{M}_z$	$\bar{M}_z/\bar{M}_w$	$10^{-6}M_{calc}$ a)
β-l.d. from B1aa	215	1.7	2.2	1.3	0.40
β-l.d. from PB1a	260	ca 3.4	ca 12	ca 3.5	0.50
β-l.d. from PB2	-	1.6 - 2.6	ca 3.5	-	-

a) Molecular-weight calculated from $[\eta]$ using equation 4.14, p.123 .

TABLE 6.12

Results of an Archibald-Trautman analysis on the β-limit dextrins from fractions B1aa, PB1a and PB2

Sample	C_1 %	C_2 %	$10^{-6}.M_1$	$10^{-6}.M_2$	Distribution a)
β-l.d. from B1aa	33	67	6.0	0.9	P
β-l.d. from PB1a	*	*	max. 15	min. 0.5	BP
β-l.d. from PB2	*	*	*	*	BP

a) Distribution of molecular weight as indicated by Trautman plot

P = paucidisperse; BP = broad-polydisperse

* Distribution made calculations impracticable.

molecular-weight distribution in this sample is somewhat narrower. M_1 equals half that for the original fraction (Table 6.8), indicative of intermediate amylopectin with an average β-amylolysis limit of ca 50. The M_2-value here seems slightly higher than expected from a comparison with data of the original fraction, but this is not important, as the β-amylolysis limit of intermediate amylose may vary slightly from 50 on fractionation. However, two components of an intermediate amylopectin, and intermediate amylose-type structure are again indicated, in proportions approximately agreeing with the predicted values for the original fraction (see Table 6.8).

The limitations of the Archibald-Trautman procedure:- Many of the conclusions drawn concerning the structure of intermediate material, depend on the Archibald-Trautman analysis. Its application to the analysis of mono-molecular (linear) amyloses is fairly satisfactory (see Section 4B and Table 6.10), but its application to polymolecular (non-linear) amyloses is more uncertain (Erlander and Foster, 1959).

Because of possible heterogeneity in $^{dn}/_{dc}$ and $\bar{V}$ for different amylose species, the accuracy of the method is difficult to assess. However, semi-quantitative values for $\bar{M}_w$ and $\bar{M}_z$ are obtained, which would be inferior to values determined by sedimentation equilibrium (Section 2D).

Erlander and Foster (1959) have pointed out that natural polymers of a broad molecular-weight distribution, give a continuously curved Trautman plot. This behaviour was observed for

some amylose fractions, where the analysis for two components was very uncertain. Where full analysis was possible, M_1 and to a lesser extent, $\bar{M}_w$ and $\bar{M}_z$ are probably the least reliable values. Although the former may vary by ca 20%, the M_2 and C_1, C_2 values are fairly accurate.

There is also the question of the concentration dependence of molecular-weight at Θ-conditions. This has been shown to be zero by Kotaka and Inagaki (1964), who also point out that the Trautman plot is concave upward if the temperature is less than the Θ-temperature, and concave downward above the Θ-temperature.

The use of the Archibald-Trautman technique with non-linear amylose involves working at the limits of its applicability. Although the results of any one run would be qualitative, from the results of several runs over a fraction series, quantitative conclusions can be drawn.

Intermediate material in heterogeneous potato amylose subfractions:- Heterogeneous amylose subfractions, which show two peaks on sedimentation velocity, are not suitable to a complete Archibald-Trautman analysis. However, with an idea of the extent of the Johnston-Ogston effect in amylose-amylopectin mixtures, a qualitative analysis of these amyloses may be made.

The results for various amylopectin-amylose ratios in 0.16M KCl are shown in Table 6.13. As $S_s \ll S_f$ the procedure of Trautman et al. (1954) was not applicable, indeed with the large difference in sedimentation coefficients it was difficult to obtain measurable peaks in one photographic frame. The Johnston-Ogston

TABLE 6.13

Johnston-Ogston effect for amylopectin-amylose mixtures in 0.16M KCl[a)]

% Ap	Am [b)]	Ap [b)]	Am + Ap [b)]	$(Ap/Am)_{calc}$ [c)]	$(Ap/Am)_{obs}$ [d)]	S_{am} [e)]	S_{ap} [f)]
100	-	21.4	21.4	∞	∞	-	65
90	5.1	17.8	22.9	9.00	3.49	4.9	58
80	6.2	15.0	21.2	4.00	2.42	4.9	56
70	8.1	13.6	21.7	2.33	1.68	5.6	59
60	10.0	12.1	22.1	1.50	1.21	5.5	55
50	10.4	10.6	21.0	1.00	1.02	5.7	55
40	13.2	7.4	20.6	0.66	0.56	5.7	57
0	20.4	-	20.4	0	0	5.1	-

a) Am ≡ amylose; Ap ≡ amylopectin

b) Apparent concentration in area units, mm^2 at bar angle 55^o

c) Calculated concentration ratio

d) Observed concentration ratio

e) Sedimentation coefficient of amylose component; value at 100% amylose = S_o

f) Sedimentation coefficient of amylopectin component, value at 100% amylopectin = S_o.

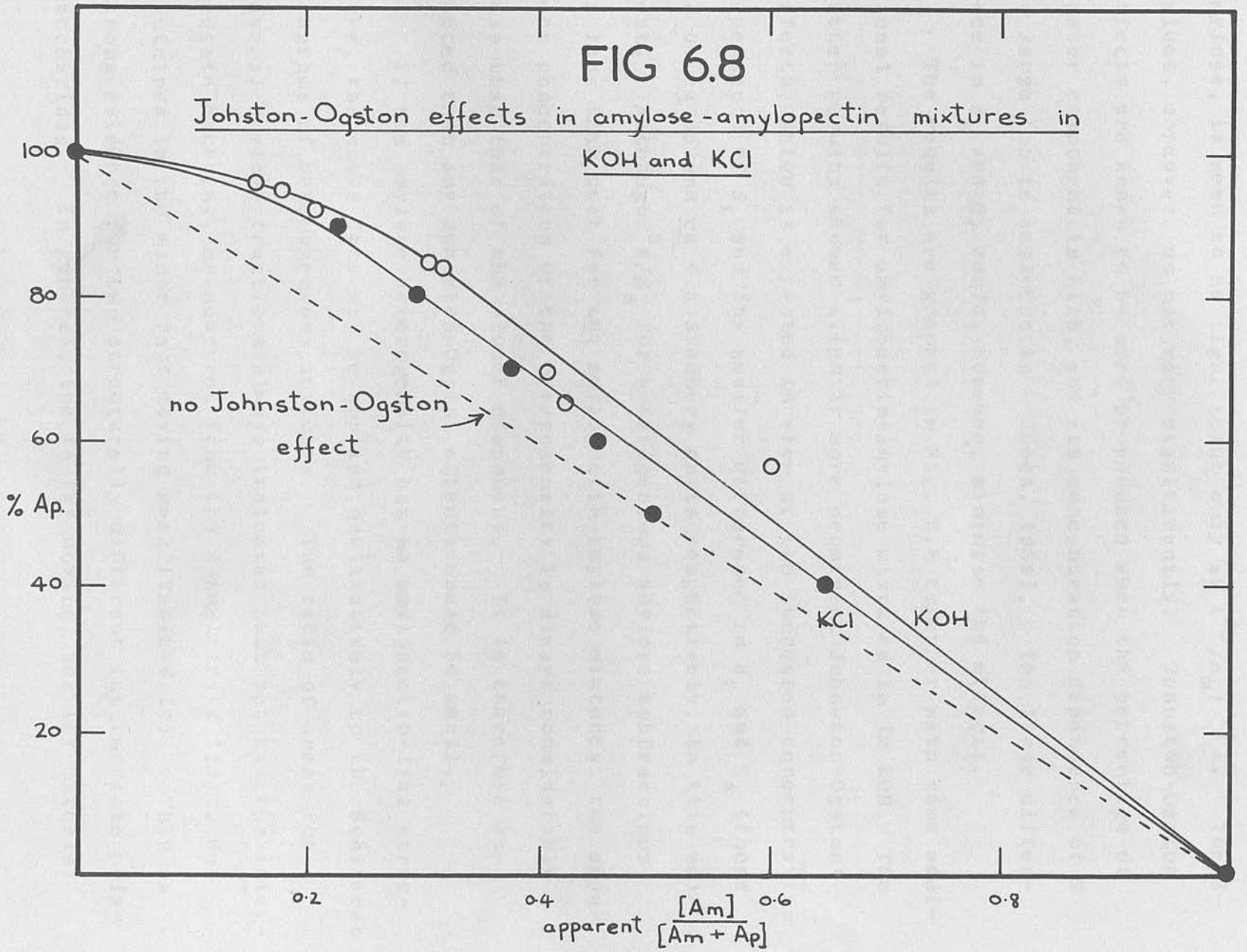
FIG 6.8
Johnston-Ogston effects in amylose-amylopectin mixtures in KOH and KCl
100
80
60
40
20
% Ap.
no Johnston-Ogston effect
KCl
KOH
0·2
0·4
0·6
0·8
apparent [Am] / [Am + Ap]

effect, demonstrated by the enhanced apparent concentration of the amylose, is seen to be significant only at $(^{Ap}/A_m) > 1$. The S-values, moreover, do not vary significantly. Johnston-Ogston effects are known to be more pronounced when the percentage of faster component is high, and its concentration dependence of S is large (as is amylopectin - Jones, 1959). The large difference in S_s and S_f would, however, minimise the effects.

The results are graphed in Fig. 6.8 together with some additional results for amylopectin-amylose mixtures in 1M KOH. The latter results showed slightly more prominent Johnston-Ogston effects, which is expected in view of the increased concentration dependence of S_f and the smaller difference in S_f and S_s (found to be ca 35 and ca 4.5 Svedberg units respectively) in this solvent. Although $^{S}f/S_s$ for heterogeneous amylose subfractions is less than that for the amylopectin-amylose mixtures, the apparent concentration of the heterogeneity is always considerably less than that of the slower component. It is therefore expected that any Johnston-Ogston effects would be small.

If the amylose heterogeneity has an amylopectin-like structure, the above data may be applied qualitatively to the Schlieren diagrams of heterogeneous amyloses. The ratio of areas for several amylose fractions always indicated that not all the intermediate material, as measured from the β-amylolysis limit, was contained in the minor fast moving peak (Table 6.14). This is strong evidence for two structurally different intermediate polysaccharides. In general, the faster moving, heavier material

TABLE 6.14

Intermediate material in some heterogeneous potato amylose subfractions

Fraction	Δ_s/Δ_f [a]	i - Ap % [b]	[β]	i - Am % [c]
1a [d]	4	23	60	57
PE1b	4	23	73	31
PE2b	5	20	80	20
P 2	6.7	15	84	17
PA1	11	9	85	21

a) Ratio of apparent concentrations of slower to faster component, as measured from Schlieren peak areas.

b) Calculated percentage of intermediate-amylopectin

c) Calculated percentage of intermediate-amylose

d) Data calculated from experiments by Banks (1960)

TABLE 6.15

Results of the gel-filtration of amylose fraction P3

Tube number	Polysaccharide concentration [a]	Iodine stain	λ_{max} [b]
8	0	nil	-
9	0.5	blue	610
10	2.9	blue	610
11	10	blue	-
12	>10	blue	-
13	>10	blue	-
14	>10	blue	-
15	>10	blue	580
16	>10	blue-magenta	570
17	10	blue-magenta	570
18	6.1	blue-magenta	570
19	6.2	blue	580
20	2.0	red	500
21	1.4	red	450
22	1.5	blue-red	-
23	0.5	nil	-
24	0.9	magenta	560
25	0.9	magenta	-
26	0.5	magenta	-
27	0	nil	-

a) In arbitrary units

b) Maximum wavelength of absorbance mμ.

always had S-values between 20 and 30 Svedberg units corresponding to molecular-weights of ca 5-12 x 10^6 (Banks, 1960), consistent with an intermediate amylopectin-like structure. It is further suggested that the slower, major component contains both linear and intermediate amylose-like material. It also appears that the percentage of intermediate amylopectin material decreases with increasing β-amylolysis limit, in qualitative agreement with the analyses of the 'single peak' fraction series by the Archibald-Trautman method.

Gel filtration of amylose:- The results for fraction P3 are shown in Table 6.15 and indicate some fractionation with respect to molecular structure. The bulk of the material was eluted in tubes 9-15 where λ_{max} has the typical value for amylose of 610 mμ. Shorter chain amylose, characterized by slightly smaller λ_{max}-values then appears to be eluted. Tubes 20-26, however, appeared to contain structurally different material - similar to amylopectin - from their iodine stains and lower λ_{max} values. Although no separation of intermediate material on a preparative scale was achieved, the existance of some amylopectin-like structure in non-linear amylose is indicated.

6A, 6B, 6C. CONCLUSIONS

The evidence from Sections 6A, 6B and 6C indicates the presence of intermediate material in potato starch, that is structurally different from normal amylopectin and linear amylose. This material seems to fall into two categories, (i) an amylopectin-like structure with long enough chain lengths to form a complex with butan-1-ol and iodine, but of a more open structure to allow for a (β + Z)-limit of 100, and a smaller molecular-weight (ca 5-30 x 10^6); (ii) a branched amylose-like structure of a similar hydrodynamic behaviour to linear amylose, which is consistent with the viscosity, sedimentation, iodine affinity and molecular weight (ca 2-6 x 10^6) evidence. These polysaccharides - intermediate-amylopectin and intermediate-amylose respectively - are confined mainly to the butan-1-ol precipitated amylose, where they comprise some 20-40% (assuming the average β-amylolysis limit of all intermediates is 50). From the density-gradient analysis of the total β-limit-dextrin, the relative proportion of intermediate amylopectin to intermediate amylose is 1:4. The existence of two discrete intermediate structures in strongly indicated by the density gradient equilibrium of total β-limit-dextrin. However, it is most likely that in the native polysaccharide, there is a continuous distribution of structures ranging from linear-amylose to highly ramified amylopectin. This is borne out by the variation in the physical properties of the natural intermediates on fractionation. This apparent contradiction may be explained in the following terms.

Intermediate material derived from linear amylose may have the 'herring bone' structure of Staudinger (1937) or, less likely, the 'laminated' structure described by Haworth (1937). On the other hand, intermediate material derived from amylopectin may have the 'tree' structure of Meyer (1940a). These structures are illustrated in Fig. 1, p. 6a. On β-amylolysis, the resultant dextrins from the three structures can be seen to be quite different. Intermediate amylose β-limit dextrin would be a linear structure, and intermediate amylopectin would be a complex branched structure. These two structures would have quite different buoyant densities, indeed, if the intermediate amylopectin had a more open structure than normal amylopectin, it is conceivable that its β-limit dextrin would have a lower buoyant density than that of a linear molecule, and conform with the experimental evidence (Section 6B). However, in the natural polysaccharides, a continuous variation in degree of branching as well as molecular-weight would be present. This would mask any transition between the Meyer and Staudinger structures, which must occur at some point in the molecular-weight distribution. This effectively continuous spectrum of structures is indicated in the continuous distribution of their physical properties; viz. $[\eta]$, $\bar{M}_w$, S, iodine affinity, $\overline{C.L.}$.

The intermediate amylopectin found in C-fraction would probably have a more branched and tighter structure than that found in B-fraction (and other butan-1-ol precipitated amyloses), as it is not completely degraded by the concurrent action of β-amylase

and Z-enzyme, nor does it form a butan-1-ol complex. However, the generally lightly branched nature of intermediate material in comparison with normal amylopectin, is implied by its lower solubility (see Table 6.1). As the branched structure becomes looser, the $\bar{M}_w$ decreases and the $[\eta]$, iodine affinity, and C.L. increase until, imperceptably, the structure becomes equivalent hydrodynamically to intermediate amylose. Intermediate amylose, on losing its fewer branch points eventually becomes linear amylose. The appearance of two discrete components in some amylose subfractions is therefore, merely an effect of fractionation with respect to molecular-weight and branching. The broad, continuous molecular-weight distribution is more truly represented by the sedimentation of total-amylose. It would seem that a refined definition for 'amylose' is required, and this could best be specified as that polysaccharide completely degraded by pure β-amylase.

The whole problem of intermediate material is complex. For a complete study of these products in different starches, a highly selective fractionation procedure would be required. Large-scale gel filtration or paper chromatography (Richter, 1962; Ulmann, 1964) offer the most promising possibilities.

6D. POTATO STARCH COMPONENTS AT EQUILIBRIUM IN A DENSITY GRADIENT

Starch intermediate material has been shown in Sections 6A, 6B and 6C to comprise of a spectrum of structures intermediate between linear amylose and highly ramified amylopectin. How these natural components behave in a density gradient is of interest and can lead to a refinement of their structure and solution behaviour.

EXPERIMENTAL

This has been described for starch components dissolved in concentrated CsCl solutions in Section 2F. Various linear and non-linear amylose subfractions were studied, as well as some total (unfractionated) amyloses, amylopectin and total starch.

RESULTS AND DISCUSSION

Molecular-weight distribution is of less importance in density gradient work than in other physiochemical techniques, as the molecules are fractionated with respect to density rather than molecular-weight.

Linear amyloses:- The results for a linear amylose fraction (L 2a) and a total-linear amylose obtained from a 60° aqueous leaching of starch granules (Banks, Greenwood, and Thomson, 1959), are shown in the first two rows of Table 6.16.

In these samples, as well as all other amyloses studied, a narrow band (A) was rapidly formed at lower buoyant densities

TABLE 6.16

Density gradient equilibrium data for potato amyloses

Fraction	Band	ρ a) gm.ml^{-1}	Rel. conc.	T b) hours	(b.w.)$^{-2}$ c) cm^{-2}
L 2a	A	1.628	6%	15	6.3
	B	1.663	94%	32	0.28
total linear amylose	A	1.628	10%	13	25
	B	1.667	90%	36	0.28
	C	1.675	< 1%	4	-
PB1a	A	1.615	-	22	100
	B	1.660	-	46	1.0
P2	A	1.615	7%	22	100
	B	1.660	93%	46	0.7
A-fraction	A	1.611	-	3	100
	B	1.663	-	24	0.8
B-fraction	A	1.612	-	3	100
	B	1.656	-	25	0.8
total amylose	A	1.611	6%	15	25
	B	1.662	94%	48	0.8
	C	1.651	< 1%	5	25

a) Buoyant density

b) Equilibrium time

c) Magnified inverse square of the band width $\propto \overline{M}_w$

FIG 6.9

Schlieren patterns for starch components at equilibrium in a density gradient

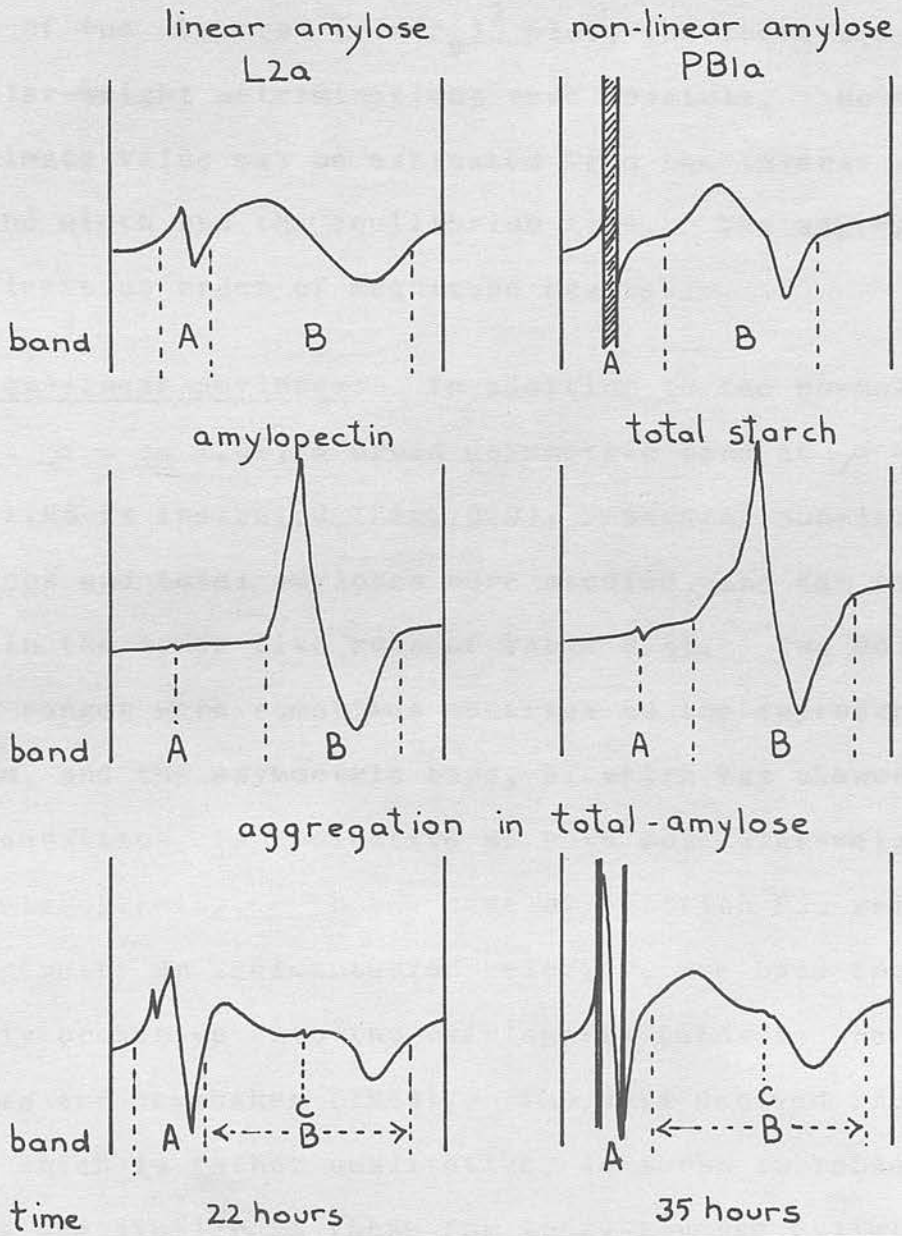

(ρ = ca 1.62; Fig. 6.9). This phenomenon has been discussed in Section 4B, and is assigned to the well-known association behaviour in aqueous natural amylose solutions.

The main proportion of the polysaccharide forms a symmetrical band (B) at ρ -values of ca 1.665. This band showed heterogeneity with respect to effective density, from the downward curvature of the ℓnc vs. $(r - r_o)^2$ plot, and therefore no accurate molecular-weight determinations were possible. However, an approximate value may be estimated from the inverse square of the band width and the equilibrium time. The aggregate band A is at least an order of magnitude heavier.

Non-linear amyloses:- In addition to the normal aggregate band at ρ = ca 1.61, a broad asymmetric band at ρ -values of about 1.66 is indicated (Fig. 6.9). Several non-linear subfractions and total amyloses were studied, and the results are shown in the lower five rows of Table 6.16. Two molecular-weight ranges were sometimes observed on the approach to equilibrium, and the asymmetric band, B, which was skewed toward lower densities, is indicative of both molecular-weight and density heterogeneity. In the case of fraction P2, which showed heterogeneity on sedimentation velocity, the band could be tentatively broken up into two overlapping bands by the procedure of Adams and Schumaker (1964). The data derived from these two bands, which is rather qualitative, is shown in Table 6.17. The results are similar to those for total-amylose β-limit-dextrin (Table 6.6, p.179), and indicate the presence of some heavier

TABLE 6.17

Density gradient data from the break-down of band B for Fraction P2

Band	ρ a) gm.ml^{-1}	Rel. conc.	(b.w.)$^{-2}$ c)
B_1	1.649	ca 25%	1.0
B_2	1.660	ca 75%	0.39

TABLE 6.18

Density gradient data for potato amylopectin and total starch

Polysaccharide	Band	ρ a) gm.ml^{-1}	Rel. conc.	T b) hours	(b.w.)$^{-2}$ c) cm^{-2}
Amylopectin	A	1.627	1%	-	-
	B	1.681	99%	10	2.1
Starch	A	1.637	1%	-	-
	B	1.681	99%	37	-

a) Buoyant density

b) Equilibrium time

c) Magnified inverse square of the band width $\propto \bar{M}_w$

branched polysaccharide of a lower density, which is identified as intermediate-amylopectin. Other asymmetric bands could not be broken up and show, therefore, a continuous distribution from linear to intermediate material (Hermans, 1963). The generally slightly lower ρ -values and higher molecular-weights support this conclusion.

In some total amyloses a small band, C, was evident (Table 6.16). This may be due to some degraded polysaccharide, or a minor amylopectin-like contaminant.

Amylopectin:- This gave a particularly polydisperse band (Fig. 6.9), with a wide range in density and molecular-weight. The buoyant density is somewhat higher than for amyloses, indicative of the more compact structure (Table 6.18). The presence of a vanishingly small band A in amylopectin as well as in a total amylose β-limit dextrin (Table 6.6, p.179), shows that aggregation is a phenomenon confined mainly to linear-amylose molecules.

Starch:- During the approach to equilibrium, several minor components banded in the region of ρ = ca 1.68 as well as at ρ = ca 1.62. However, eventually two major components were evident, amylose and amylopectin, which banded in the region ρ = 1.66-1.68 (Fig. 6.9; Table 6.18). Both bands were broad and overlapped each other, with strong density heterogeneity. The two bands were formed at different times indicating the two specific molecular-weight ranges in starch, confirming the sedimentation velocity work of McGregor (1964). A minor band (A)

identified as associated amylose is also present.

Heterogeneity with respect to effective density:- This phenomenon was common to all the polysaccharides studied, and made the calculation of any absolute molecular-weight impossible. Moreover, concentration and dispersion effects can be very important with respect to $\bar{M}_w$ determination by density gradient (Dayantis and Benoit, 1964). The inverse square of the band width and the equilibrium time, does however give some qualitative estimate of relative molecular-weights. This phenomenon may be due to intermediate degrees of association and aggregation. In such concentrated salt solutions over long time periods, amylose would be most unstable. Smaller amylose molecules are known to associate rapidly (Husemann et al., 1963) and these might form the generally observed band A. The larger molecules, with a slower association rate would comprise the main band B. Density heterogeneity in amylopectin is easily understood, in view of the probable wide range in degree of branching.

Solvation and hydration may also affect the buoyant density of the polysaccharides.

Observations on the formation of the aggregate band A:- In linear-amyloses the aggregate gave a fairly well-defined bimodal band. However, for non-linear amyloses this was complicated by the formation of a polymodal band comprised essentially of two boundaries (Fig. 6.9). This behaviour may be a consequence of the presence of intermediate material, but without further

evidence this cannot be confirmed.

The concentration of the aggregate band was found to increase with time, to form an extremely sharp Schlieren pattern in some cases. At equilibrium the percentage of aggregate was minor, but in some cases this could not be measured owing to its very large molecular weight producing excessively narrow and sharp Schlieren patterns.

Glycogen at equilibrium in a density gradient (in collaboration with Mr. R. Geddes):- Four samples of bullock liver glycogen prepared by Mr. R. Geddes using various extraction procedures all had buoyant densities of 1.662 or 1.663 in a $CsCl/H_2O$ solvent, regardless of their molecular-weight distribution. The buoyant density of glycogen is thus similar to amylose and significantly less than that of amylopectin. Glycogen is a highly branched, high molecular-weight α-1,4 glucan, but is of a more compact structure than amylopectin, and has been likened to an ellipsoid in molecular shape (Jones, 1959).

This is of interest in that the biosynthesis of starch as proposed by Erlander (1958) postulates a glycogen-type precurser, and therefore it might be expected that some starch intermediate polysaccharide may be glycogen-like. Banks (1960) could find no evidence of this from his study of 'thymol-amylopectin'. This would seem to be confirmed here, as no specific intermediate polysaccharide in potato starch banded at this buoyant density of glycogen.

The use of systems other than $CsCl/H_2O$ to establish a density

gradient:- The $CsCl/H_2O$ system is unsuitable for a complete study of natural starch polysaccharides, except perhaps for a study of aggregation (see Section 4B). An organic system, which may eliminate the aggregation difficulties was therefore sought.

Dimethylsulphoxide (DMSO), formamide (FA) and ethylene diamine (EDA) have been used as solvents for amylose (see Section 4B). N-methyl-2-pyrrolidone (NMP) and ethanol amine (EA) were also found to dissolve both dry and butan-1-ol complexed amylose, but amylose was not readily soluble in dimethyl formamide (DMF). To establish a density gradient, sufficient dense organic liquid is added to the amylose solution to make the density of the total solution nearly equal to the buoyant density of the dissolved amylose. Bromoform ($CHBr_3$) and 1,1,2,2,-tetrabromoethane (TBE) are suitable heavy additives which should, of course, be miscible with the light solvent, and not precipitate the amylose. Moreover, it is advantageous for the two organic liquids to have matched refractive indices (Wales, 1963).

The following systems were found unsuitable because of immiscibility or decomposition on mixing of the organic components:- DMSO/$CHBr_3$; DMSO/CsCl; FA/$CHBr_3$; EDA/$CHBr_3$; DMF/$CHBr_3$; FA/TBE; EDA/TBE; EA/TBE. In the DMSO/TBE system, amylose was precipitated at $>$ ca 25% TBE. The solvent systems NMP/TBE, EA/$CHBr_3$ and NMP/$CHBr_3$ were suitable for density gradient work, and as the latter solvent pair had the closest matched refractive indices, it was studied in more detail.

The bromoform concentration required to collect the polymer

in the middle of the cell was estimated from the equation

$$\rho = 1/\bar{V} = \rho_1 + (\rho_1 - \rho_1/\rho_2)\, C'_2 \qquad 6.1$$

(Buchdahl et al., 1963) where ρ is the reciprocal of the partial specific volume of the polymer, ρ_1 is the density of the pure solvent, ρ_2 the density of the additive, and C'_2 the initial concentration of the additive. A series of experiments showed that the expected $CHBr_3$ concentration of 0.757 gm ml^{-1} had to be lowered to 0.321 gm ml^{-1} to collect the dissolved amylose near the middle of the cell, because there was considerable preferential absorption of NMP on the polysaccharide.

12 mm. cells were used with plain and negative wedge windows, and equilibrium was established after ca 95 hours at 33,450 r.p.m. and ca 24 hours at 50,740 r.p.m. (The higher speed was therefore more economical with respect to wear on the ultracentrifuge drive unit).

The evaluation of data for mixtures of two organic liquids has been detailed by Hermans and Ende (1963).

The volume fraction of the additive ϕ_2, which is related to the buoyant density at the polymer band, ρ_o, through equation 6.1, was calculated from the following relations:-

$$\phi_{2/\phi_1} = \alpha.\exp\left\{\beta\, r_o^2\right\} \qquad 6.2$$

$$\beta = w^2(M_2/\rho_2)(\rho_2 - \rho_1)/2RT \qquad 6.3$$

$$U\alpha = \exp\left\{\beta(x_b^2 - x_m^2)\, \phi_2^{in}\right\} - 1 \qquad 6.4$$

$$U = \exp\left\{\beta x_b^2\right\} - \exp\left\{\beta x_b^2 \phi_2^{in} + \beta x_m^2 \phi_1^{in}\right\} \qquad 6.5$$

where ϕ^{in} is the initial volume fraction and x_m and x_b are the radial distances of the meniscus and cell bottom respectively. $(^{d}\rho/d_r)$ at any point in the liquid column was calculated from,

$$d\phi_2/dr = 2 \beta r \phi_1 \phi_2 \qquad 6.6$$

This procedure takes no account of the effect of pressure on the solvent density gradient or the polymer, and in addition non-ideality, and preferential absorption effects have been ignored. These experiments, therefore, can only be regarded qualitatively; quantitative treatments of data have been described by Dayantis and Benoit (1964) and Jacob et al. (1965).

Amylose at equilibrium in an NMP/$CHBr_3$ density gradient:- With the anhydrous conditions attained with dry amylose in an organic system, it is assumed that aggregation is absent. Indeed, the aggregate band (A) found in the $CsCl/H_2O$ system (fig. 6.9) was absent in the NMP/$CHBr_3$ system, there being only one band (see Fig. 6.10).

The data from equilibrium runs on a linear amylose (fraction L3a at 50,740 r.p.m.), a non-linear amylose (fraction P4 at 33,450 r.p.m.) and an amylose that had precipitated (as a gel) due to excess $CHBr_3$, is shown in Table 6.19.

The $\ln c$ vs $(r - r_o)^2$ plot for fraction L3a was linear, indicating homogeneity, whereas that for fraction P4 was concave

FIG 6.10

Schlieren patterns for starch components in an $NMP/CHBr_3$ density gradient

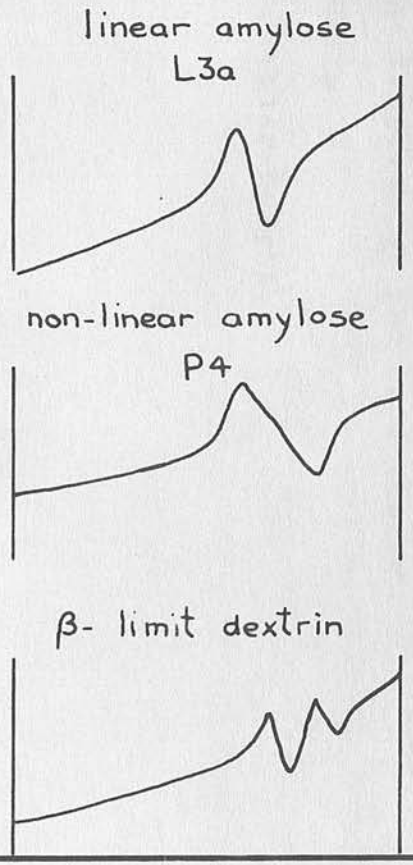

FIG 6.11

$\ln c$ vs. $(r-r_o)^2$ for two amylose fractions in an $NMP/CHBr_3$ density gradient

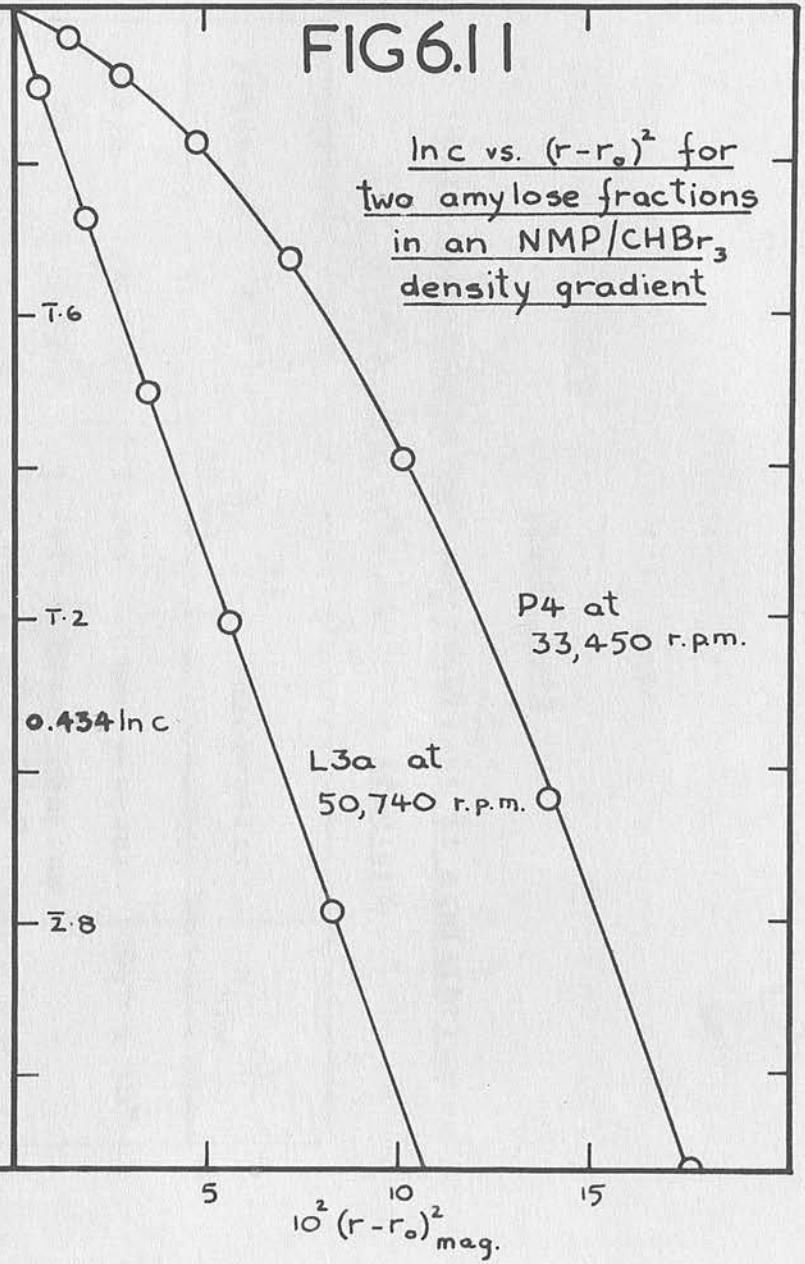

TABLE 6.19

Data from potato amylose fractions at equilibrium in an NMP/$CHBr_3$ density gradient

Fraction	ϕ_2 a)	ρ b) gm.ml^{-1}	Homogeneity	M_{app} c)
L3a	0.1110	1.246	homogeneous	0.2×10^6
P4	0.1092	1.241	heterogeneous w.r.t. ρ	-
Amylose ppt.	0.1695	1.359	-	-

a) $CHBr_3$ volume fraction at the band centre

b) Buoyant density

c) Apparent molecular-weight.

downward indicative of heterogeneity with respect to effective density (Fig 6.11). This implies the presence of a structural modification in the non-linear amylose. The nature of this material could not be deduced from this experiment, but a continuous distribution is implied by the single (polymodal) band obtained.

From the slope of the $\ell n\ c$ vs. $(r - r_o)^2$ plot for fraction L3a, the apparent molecular-weight of the solvated polysaccharide was calculated as about one-third of its expected value (see Section 4B). This would be expected as pressure and non-ideality effects had not been considered (Dayantis and Benoit, 1964).

The buoyant density of the precipitated amylose is higher than the dissolved species, but significantly different from that found in $CsCl/H_2O$. It would seem that solvent molecules are still associated with the gelled material.

Conclusion:- Density gradient experiments clearly demonstrate polydispersity or the presence of heterogeneities, but in the present instance only qualitative information is available. A detailed quantitative analysis for polydispersity is not only time consuming but probably not justified by the accuracy obtained (Jacob et al., 1965). A more precise idea about the fine structure of the various starch components, must await the preparation of structurally pure samples.

SUMMARY

Physical techniques, including rotational viscometry and several ultracentrifugal methods not previously used in these laboratories have been detailed.

The viscometric behaviour of the amylose component of potato starch dissolved in aqueous alkaline solution was found to depend on pH and counter-ion concentration. Maximum $[\eta]$-values occurred at a pH of approximately 13 and these were reduced, on the addition of salt, to values below those found in neutral solution. In these solvents, where $[\eta]$-values were minimal, the solution behaviour resembled ideal Θ-conditions. Changes in $[\eta]$ were interpreted as changes in the conformation of the amylose molecule due to the ionisation of hydroxyl groups. These effects were confirmed for amylose fractions of varying molecular-weight.

The absolute viscosity of solutions of amylose in 0.33M KCl, 0.15M KOH and 1M KOH was found to be dependent on the average shear rate $\bar{G}$, between $\bar{G}$ = 0-1200 sec^{-1}. Limiting viscosity numbers, $[\eta]$, were however, independent of shear rate even for the largest molecular weight samples of amylose.

The subfractionation of both total-amylose and linear-amylose has been studied in detail, and the fractional precipitation of amylose from a dimethyl-sulphoxide solution with acetone was found the most efficient method. In the subfractionation of total-amylose, a heterogeneity was evident in some subfractions, and its presence was related to the β-amylolysis limit. It was shown that this heterogeneity was natural to the polysaccharide, and probably

represented branched material.

From a study of the properties of subfractions of linear amylose, the polysaccharide was found to behave as a random coil in 0.50M KCl/10^{-2}M KOH (an aqueous Θ-solvent), 0.15M KCl, and 0.15M KOH. The amylose molecule was in a more expanded form in the latter two solvents. Moreover, there was some evidence for association in neutral aqueous solutions of natural amylose.

The concentration dependence of sedimentation coefficient was negligible for amylose dissolved in the above Θ-solvent, but increased with solvent power in accord with theory. In addition, the apparent sedimentation coefficient was dependent on force-field, ~~and it was concluded that this phenomenon was due to a combination of polydispersity and pressure effects.~~

By fractionating total potato starch, the presence of polysaccharide-material intermediate in structure between linear amylose and highly ramified amylopectin was confirmed. These results suggest that a continuous range in molecular structure may be present in the starch granule. Intermediate material was composed of branched polysaccharides similar to both amylose and amylopectin.

BIBLIOGRAPHY

Adams, G.H., and V.N. Schumaker (1964) Nature, 202, 490.

Alberty, R. A. (1954) J.Amer.Chem.Soc., 76, 3733.

Alfrey, T., A. Bartovics and H. Mark (1942) J.Amer.Chem.Soc., 64, 1557.

Anderson, D.M.W., and C. T. Greenwood (1955) J.Chem.Soc., 3016.

Archibald, W.J. (1947) J.Phys. and Colloid Chem., 51, 1204.

Aspinall, G.O., and C.T. Greenwood (1962) J.Inst.Brewing, 167.

Banks, W. (1960) Ph.D. Thesis, Edinburgh.

Banks, W., and C.T. Greenwood (1959) Biochem.J. (London), 73, 237.

Banks, W., and C.T. Greenwood (1959a) J.Chem.Soc., 3436.

Banks, W., and C.T. Greenwood (1961) Chem. and Ind., 928.

Banks, W., and C.T. Greenwood (1963a) Adv.Carbohydrate Chem., 18, 357.

Banks., W., and C.T. Greenwood (1963b) Makromol.Chem., 67, 49.

Banks, W., C.T. Greenwood and I.G. Jones (1960) J.Chem.Soc., 150.

Banks, W., C.T. Greenwood and J. Thomson (1959) Makromol.Chem., 31, 197.

Banks, W., C.T. Greenwood and J. Thomson (1959a) Chem. and Ind., 928.

Bates, R.G. (1954) "Electrometric pH Determinations", Chapman and Hall.

Baum, H., and G.A. Gilbert (1954) Chem. and Ind., 489.

Bear, R. (1944) J.Amer.Chem.Soc., 66, 2122.

Billick, I.H. (1962) J.Phys.Chem., 66, 1941.

Billick, I.H. (1964) A.C.S. Meeting, Chicago, 5:2, 855.

Blair, J.E., and J.W. Williams (1964) J.Phys.Chem., 68, 161.

Brown, W., D. Henley and J. Ohman (1963) Makromol.Chem., 64, 49.

Bryce, W.A.J. (1958) Ph.D. Thesis, Edinburgh.

Bottle, R.T., G. A. Gilbert, C.T. Greenwood and K.N. Saad (1953) Chem. and Ind., 541.

Burchard, W. (1963) Makromol.Chem., 64, 110.

Burchard, W. (1963a) Makromol.Chem., 59, 16.

Buchdahl, R., H.A. Ende and L.H. Peebles (1963) J.Polymer Sci., Part C, Symposia, 1, 143.

Buchdahl, R., H.A. Ende and L.H. Peebles (1963a) J.Polymer Sci., Part C, Symposia, 1, 153.

Cannon, M.R., R.E. Manning and J.D. Bell (1960) Analyt.Chem., 32, 355.

Clark, W.M. (1923) "The Determination of Hydrogen Ions", Williams and Wilkins, Baltimore.

Couette, M.M. (1890) Ann.Chim. et Phys., 21, 433.

Cowie, J.M.G. (1958) Ph.D. Thesis, Edinburgh.

Cowie, J.M.G. (1960) Makromol.Chem., 42, 230.

Cowie, J.M.G. (1961a) J.Polymer.Sci., 49, 455.

Cowie, J.M.G. (1963) Makromol.Chem., 59, 189.

Cowie, J.M.G., and C.T. Greenwood (1957) J.Chem.Soc., 2862.

Cowie, J.M.G., and C.T. Greenwood (1957a) J.Chem.Soc., 4640.

Cowie, J.M.G., and P.M. Toporowski (1964) Polymer, 5, 601.

Cragg, L.H., and H. van Oene (1962) Nature, 196, 1197.

Danielsson, C.E. (1947) Nature, 160, 899.

Dayantis, J., and H. Benoit (1964) J.Chim.phys., 61, 773, 781.

Debye, P. (1946) J.Chem.Phys., 14, 636.

Doty, P., A. Wada, J.T. Yang and E.R. Blout (1957) J.Polymer Sci., 23, 851.

Dubois, M., K.A. Gilles, J.K. Hamilton, P.A. Rebers and F. Smith (1956) Analyt.Chem., 28, 350.

Ebert, K.H., and E.Ernst (1962) Makromol.Chem., 56, 88.

Erlander, S.R. (1958) Enzymologia, 19, 273.

Erlander, S.R., and G.E. Babcock (1961) Biochim.Biophys.Acta, 205.

Erlander, S.R., and J.F. Foster (1959) J.Polymer Sci., 37, 103.

Everett, W.W., and J.F. Foster (1959) J.Amer.Chem.Soc., 81, 3459, 3464.

Flory, P.J. (1943) J.Amer.Chem.Soc., 65, 372.

Flory, P.J. (1953) "Principles of Polymer Chemistry", Cornell University Press., Ithaca, N.Y.

Flory, P.J., and T.G. Fox (1949) J.Phys.Chem., 53, 197.

Flory, P.J., and T.G. Fox (1950) J.Polymer Sci., 5, 745.

Flory, P.J., and T.G. Fox (1951) J.Amer.Chem.Soc., 73, 1904.

Foster, J.F., and R.M. Hixon (1943) J.Amer.Chem.Soc., 65, 618.

Foster, J.F., and M.D. Sterman (1956) J.Polymer Sci., 21, 91.

French, D., A.O. Pulley and W.J. Whelan (1963) Stärke, 15, 349.

Geddes, R. (1964) Measurements in these laboratories.

Germino, F.J., R.J. Moshy and R.M. Valletta (1964) J.Polymer Sci., Part A, General Papers, 2, 2705.

Gillespie, T. (1963) J.Polymer Sci., Part C, Symposia, 3, 31.

Goldberg, R.J. (1953) J.Phys.Chem., 57, 194.

Goodison, D., and R.S. Higginbotham (1950) Shirley Inst.Mem., 24, 235.

Gralén, N. (1964) Dissertation, Uppsala.

Greenwood, C.T. (1956) Adv.Carbohydrate Chem., 11, 335.

Greenwood, C.T. (1960) Stärke, 12, 169.

Greenwood, C.T. (1964) "Methods in Carbohydrate Chemistry", Vol. IV, R.L. Whistler, Acad. Press, p. 179.

Greenwood, C.T., and S. McKenzie (1963) Stärke, 7, 251.

Greenwood, C.T., and J.S.M. Robertson (1954) J.Chem.Soc., 3769.

Greenwood, C.T. and H. Rossotti (1958) J.Polymer Sci., 27, 481.

Greenwood, C.T., and J. Thomson (1962) J.Chem.Soc., 222.

Gupta, P.R., and D.A.I. Goring (1960) J.Chem.Phys., 32, 1890.

Gupta, P.R., R.F. Robertson and D.A.I. Goring (1960) Canad. J.Chem., 38, 259.

Harrington, W.F., and H.K. Schachman (1953) J.Amer.Chem.Soc., 75, 3533.

Haworth, W.N., E.L. Hirst and F.A. Isherwood (1937) J.Chem.Soc., 577.

Hearst, J.E., J.B. Ifft and J. Vinograd (1961) Proc.Nat.Acad. Sci., U.S.A., 47, 1015.

Hearst, J.E., and W.H. Stockmayer (1962) J.Chem.Phys. 37, 1425.

Hermans, J.J. (1963) J.Polymer Sci., Part C, Symposia, 1, 179,

Hermans, J.J. (1963a) J.Chem. Phys., 38, 597.

Hermans, J.J. (1964) Makromol.Chem., 74, 92.

Hermans, J.J., and H.A. Ende (1963) J.Polymer Sci., Part C, Symposia, 1, 161.

Hermans, J.J., and H.A. Ende (1964) "Newer Methods of Polymer Characterization," B.Ke, Interscience, Ch. 13.

Hess, K., and B. Krajc (1940) Ber., 73, 976.

Hess, K., and E. Steurer (1940) Ber., 73, 1076.

Hodge, J.E., E.M. Montgomery and G.E. Hilbert (1948) Cereal Chem., 25, 19.

Hollo, J., and J. Szejtle (1958) Periodica Polytech., 2, 25.

Hollo, J., J. Szejtle and J. Toth (1961) Stärke, 6, 222.

Homma, T., K. Kawahara, H. Fujita and M. Ueda (1963) Makromol. Chem., 67, 132.

Houwink, R. (1940) J.prakt.Chem., 157, 15.

Huggins, M.L. (1942) J.Amer.Chem.Soc., 64, 2716.

Hummel, B.C. W., and D.C. Smith (1962) J.Chromatog., 8, 491.

Hunt, M.L., S. Newman, H.A. Scheraga and P.J. Flory (1956) J. Phys.Chem., 60, 1278.

Husemann, E., W. Burchard, B. Pfannemüller and R. Werner (1961) Stärke, 13, 196.

Husemann, E., B. Pfannemüller and W. Burchard (1963) Makromol. Chem., 59, 1.

Husemann, E., W. Burchard and B. Pfannemüller (1964) Stärke, 16, 143.

Ifft, J.B., D.H. Voet and J. Vinograd (1961) J.Phys.Chem., 65, 1138.

Inagaki, H., and S. Kawai (1964) Makromol.Chem., 79, 42.

International Critical Tables (1929) McGraw-Hill, N.Y.)

Jacob, M., J. Dayantis and H. Benoit (1965) J.Chim.phys., 62, 73.

Johnston, J.P., and A.G. Ogston (1946) Trans.Faraday Soc., 42, 789.

Jones, I.G. (1959) Ph.D. Thesis, Edinburgh.

Kay, D.R., and J.B. Saunders (1964) J.Sci.Instr., 41, 139.

Kegeles, G., and Cho Lu Sia (1963) Biochemistry, 2, 906.

Kegeles, G., S.M. Klainer and W.J. Salem (1957) J.Phys.Chem., 61, 1286.

Kerr, R.W. (1945) J.Amer.Chem.Soc., 67, 2268.

Kerr, R.W., and H. Gehman (1951) Stärke, 3, 271.

Killion, P.J., and J.F. Foster (1960) J.Polymer Sci., 46, 65.

Kirkwood, J.G., and J. Riseman (1948) J.Chem.Phys., 16, 565.

Kjølberg, O., and D.J. Manners (1963) Biochem.J. 86, 258.

Klainer, S.M. and G. Kegeles (1955) J.Phys.Chem., 59, 952.

Koëts, P. (1936) J.Phys.Chem., 40, 1191.

Koëts, P., and H.R. Kruyt (1937) Kolloidchem.Beih., 47, 100.

Kotaka, T., and H. Inagaki (1964) Bull.Inst.Chem.Res., Kyoto Univ., 42, 176.

Kratky, O., and G. Porod (1949) Rec.Trav.chim., 68, 1106.

Kuge, T., and O. Sozaburo (1961) Bull.Chem.Soc. Japan, 34, 1264.

Kuhn, W. (1934) Kolloid-Z., 68, 2.

Kuhn, W., H. Kuhn and A. Silderberg (1953) J.Polymer Sci., 14, 193.

Kurata, M., and W.H. Stockmayer (1963) Adv.Polymer Sci., 3, 196.

Kurata, M., W.H. Stockmayer and A. Roig (1960) J.Chem.Phys., 33, 151.

Lamm, O. (1929) Z.phys.Chem. (Leipzig), A 143, 177.

Lampitt, L.H., C.H.F. Fuller and L. Coton (1955) J.Sci.Food Agric., 6, 656.

Lansky, S., M. Kooi and T.J. Schoch (1949) J.Amer.Chem.Soc., 71, 4066.

Laurent, T.C., M. Ryan and A. Pietruszkiewicz (1960) Biochim. Biophys.Acta., 42, 476.

Lohmander, U. (1964) Makromol.Chem., 72, 159.

Lohmander, U., and A. Svensson (1963) Makromol.Chem., 65, 202.

Lütje, H. (1964) Makromol. Chem., 72, 210.

McGregor, A.W. (1964) Ph.D. Thesis, Edinburgh.

McKenzie, S. (1964) Ph.D. Thesis, Edinburgh.

Mandelkern, L., and P.J. Flory (1952) J.Chem.Phys., 20, 212.

Manners, D.J., and G.A. Mercer (1963) J.Chem.Soc., 4317.

Mark, H. (1938) "Der feste Körper", Leipzig, 103.

Martin, A.F. (1942) Quoted by M.L. Huggins, J.Amer.Chem.Soc., 64, 2716.

Meselson, M., and F.W. Stahl (1958) Proc.Nat.Acad.Sci., U.S.A., 44, 671.

Meselson, M., F.W. Stahl and J. Vinograd (1957) Proc.Nat.Acad. Sci., U.S.A., 43, 581.

Meyer, K.H., and P. Bernfeld (1940a) Helv.Chim.Acta, 23, 875.

Meyer, K.H., P. Bernfeld, R.A. Boissonnas, P. Gürtler and G. Noelting (1949) J.Phys.Colloid Chem., 53, 319.

Meyer, K.H., P. Bernfeld and E. Wolff (1940) Helv.Chim.Acta, 23, 854.

Montgomery, E.M., and F.R. Senti (1958) J.Polymer Sci., 28, 1.

Montgomery, E.M., K.R. Sexson, R.J. Dimler and F.R. Senti (1964) Stärke, 11, 345.

Muetgeert, J. (1961) Adv.Carbohydrate Chem., 16, 299.

Nightingale Jr., E.R., (1962) J.Phys.Chem., 66, 894.

Ogston, A.G. (1953) Trans. Faraday Soc., 49, 1481.

Ogston, A.G., and J.E. Stanier (1953) Biochem.J., 53, 4.

Öhrn, O.E. (1958) Arkiv.Kemi, 12, 398.

Oth, J., and V. Desreux (1954) Bull.soc.chim. Belges, 63, 133.

Overbeek, J.Th.G., and H.G. Bungenberg de Jong (1949) "Colloid Science", vol. 11, H.R. Kruyt, Elsevier, p. 209.

Packter, A. (1964) J.Polymer Sci., Part A, General Papers, 2, 2771.

Paschall, E.F., and J.F. Foster (1952) J.Polymer Sci., 9, 73, 85.

Passaglia, E., J.T. Yang and N.J. Wegemer (1960) J.Polymer Sci., 47, 333.

Peat, S., S.J. Pirt and W.J. Whelan (1952) J.Chem.Soc., 705.

Peat, S., W.J. Whelan and S.J. Pirt (1949) Nature, 164, 499.

Peat, S., W.J. Whelan and G.J. Thomas (1952) J.Chem.Soc., 4546.

Pederson, K.O (1958) J.Phys.Chem., 62, 1282.

Perlin, A.S. (1958) Canad.J.Chem., 36, 801.

Peterlin, A. (1950) J.Polymer Sci., 5, 473.

Peterlin, A., and M. Copic (1956) J.Appl.Phys., 27, 434.

Peterson, J.M. (1964) J.Chem.Phys., 40, 2680.

Phyllips, I. (1961) Unpublished work.

Posternak, T. (1935) Helv.Chim.Acta., 18, 1351.

Potter, A.L., V. Silveira, R.M. McCreedy and H.S. Owens (1953) J.Amer.Chem.Soc., 75, 1335.

Rao, V.S.R., and J.F. Foster (1963) Biopolymers, 1, 527.

Reeves, R.E. (1954) J.Amer.Chem.Soc., 76, 4595.

Richter, M. (1962) Stärke, 14, 337.

Rundle, R.E., L. Daasch and D. French (1944) J.Amer.Chem.Soc., 66, 130.

Saric, S.P., and R.K. Schofield (1946) Proc.Roy.Soc. A, 185, 431.

Schachman, H.K. (1959) "Ultracentrifugation in Biochemistry", Academic Press, N.Y.

Scheraga, H.A., and L. Mandelkern (1953) J.Amer.Chem.Soc., 75, 179.

Schoch, T.J. (1942) J.Amer.Chem.Soc., 64, 2957.

Schoch, T.J. (1964) "Methods in Carbohydrate Chemistry", Vol. IV, R.L. Whistler, Acad. Press, p. 160.

Schoch, T.J., S. Lansky and M. Kooi (1949) J.Amer.Chem.Soc., 71, 4066.

Schultz, A.R., and P.J. Flory (1953) J.Amer.Chem.Soc., 75, 5681.

Schultz, R., and M-Th. Reitzer (1962) Starke, 14, 424.

Schulz, G.V., and J. Sing (1945) J.prakt.Chem., B43, 47.

Sitaramaiah, G., R.F. Robertson and D.A.I. Goring (1962) J. Phys.Chem., 66, 1364.

Smith, F., R. Montgomery (1959) "Plant Gums and Mucilages", Reinhold, N.Y., pp. 95, 59.

Sotobayashi, H., and K. Ueberreiter (1964) J.Polymer Sci., Part A, General Papers, 2, 1257.

Stacy, C.T., and J.F. Foster (1956) J.Polymer Sci., 20, 57.

Staudinger, H., and E. Husemann (1937) Ann., 527, 195.

Stockmayer, W.H., and M. Fixman (1963) J.Polymer Sci., Part C, Symposia, 1, 137.

Svedberg, T., and J.B. Nichols (1923) J.Amer.Chem.Soc., 45, 2910.

Svedberg, T., and K.O. Pederson (1940) "The Ultracentrifuge", Oxford Univ. Press, London.

Thoma, J.A., D.E. Koshland, J.J. Ruscica and R. Baldwin (1963) Biochem.Biophys.Res.Comm., 12, 184.

Thomson, J. (1961) Ph.D. Thesis, Edinburgh.

Thomson, A., and M.L. Wolfrom (1951) J.Amer.Chem.Soc., 73, 5849.

Trautman, R. (1956) J. Phys.Chem., 60, 1211.

Trautman, R. (1958) Biochim.Biophys.Acta, 28, 417.

Trautman, R., V.N. Schumaker, W.F. Harrington and H.K. Schachman (1954) J.Chem.Phys., 22, 555.

Ulmann, M. (1964) Stärke, 16, 151.

Valletta, R.M., F.J. Germino, R.E. Lang and R.J. Moshy (1964) J.Polymer Sci., Part A, General Papers, 2, 1085.

Van Holde, K.E., and R.L. Baldwin (1958) J.Phys.Chem., 62, 734.

Van Oene, H., and L.H Cragg (1962) J.Polymer Sci., 57, 175.

Van Wazer, J.R., J.W. Lyons, K.Y. Kim and R.E. Colwell (1963) "Viscosity and Flow Measurement", Interscience, ch. 3.

Vinograd, J., and J.E. Hearst (1962) Fortschr.Chem.org. Naturstoffe, 20, 373.

Wales, M. (1963) J.Appl. Polymer Sci., 7, 203.

Wales, M., and S.J. Rehfeld (1962) J.Polymer Sci., 62, 179.

Whelan, W.J. (1958) "In Encyclopedia of Plant Physiology", Springer-Verlag, Berlin, Vol. VI, p. 154.

Whistler, R.L. and W.M. Doane (1961) Cereal Chem., 38, 251.

Whistler, R.L. and G.E. Hilbert (1945) J.Amer.Chem.Soc., 67, 1161.

Williams, J.W. (1963) "Ultracentrifugal Analysis", Academic Press, N.Y.

Williams, J.W., K.E. Van Holde, R.L. Baldwin and H. Fujita (1958) Chem.Rev., 58, 715.

Wolff, I.A., L.J. Gundrum and C.E. Rist (1950) J.Amer.Chem.Soc., 72, 5188.

Yang, J.T. (1958) J.Amer.Chem.Soc., 80, 1783.

Yang, J.T. (1961) Adv.Protein Chem., 16, 323.

Young, T.F., K.A. Kraus and J.S. Johnson (1954) J.Chem.Phys., 22, 878.

Yphantis, D.A. (1960) Ann. New York Acad.Sci., 88, 586.

Yphantis, D.A. (1964) Biochemistry, 3, 297.

Zimm, B.H. (1948) J.Chem.Phys., 16, 1093.

Zimm, B.H., and D.M. Crothers (1962) Proc.Nat.Acad.Sci. U.S.A., 48, 905.

Sonderdruck aus

DIE MAKROMOLEKULARE CHEMIE

Band 79 1964 Seite 189—206

Observations on the Isolation and Subfractionation of Amylose: The Presence in Amylose of a Natural Barrier to β-Amylolysis

by

R. Geddes, C. T. Greenwood, A. W. MacGregor, A. R. Procter, and J. Thomson

HÜTHIG & WEPF VERLAG · BASEL

From the Department of Chemistry, The University, Edinburgh, 9, Scotland

Observations on the Isolation and Subfractionation of Amylose: The Presence in Amylose of a Natural Barrier to β-Amylolysis*

By R. Geddes, C. T. Greenwood, A. W. MacGregor, A. R. Procter, and J. Thomson

(Eingegangen am 29. November 1963)

SUMMARY:

Samples of amyloses isolated from potato, wheat, and iris germanica starch by conventional procedures have been subfractionated by the addition of ethanol and other precipitants to a dispersion in dimethylsulphoxide. Fractions having a very wide range in limiting viscosity number [η], were obtained, but more significantly the samples differed in their β-amylolysis limits, [β]. On ultracentrifugation all samples were apparently homogeneous in dilute alkali, but most of them with [β] < 95 were *heterogeneous* in saline, and showed a minor, faster-moving component. Evidence is presented that this component may contain the barrier to β-amylolysis. For amyloses isolated from potatoes at varying stages of maturity, an increase in [η] is associated with a decrease in [β]. The significance of this and other factors controlling the apparent molecular size and the [β]-value are discussed. Lightscattering measurements confirm the molecular weight and wide molecular weight distribution of natural amylose. Fractionation of starch pretreated with dimethylsulphoxide has been critically examined.

ZUSAMMENFASSUNG:

Amylose, die aus Kartoffel-, Weizen- und iris-germanica-Stärke nach den üblichen Methoden isoliert worden war, wurde aus einer Dispersion in Dimethylsulfoxyd durch Zugabe von Äthanol und anderen Fällungsmitteln unterfraktioniert. Es wurden Fraktionen erhalten, deren Viskositätszahl einen weiten Bereich überstreicht und die, was wichtiger ist, in dem bei dem Abbau mit β-Amylase erhaltenen Grenzwert [β] differierten. Nach Ultrazentrifugenmessungen in verdünntem Alkali schienen alle Proben homogen zu sein. Wurden die Ultrazentrifugenmessungen in Salzlösungen durchgeführt, erwiesen sich diejenigen, deren [β] < 95 war, als heterogen und zeigten eine kleine Menge einer schneller beweglichen Komponente. Die Ergebnisse scheinen darauf hinzuweisen, daß diese Komponente die Barrierenwirkung beim β-Amylaseabbau verursacht.

Bei Kartoffelamylose, die in verschiedenen Reifezuständen isoliert worden war, ist ein Anwachsen in [η] mit einer Abnahme von [β] verbunden. Die Beeinflussung der scheinbaren Molekülgröße und des [β]-Wertes durch diesen und andere Faktoren wird diskutiert. Lichtstreuungsmessungen bestätigen das Molekulargewicht und die breite Molekulargewichtsverteilung der natürlichen Amylose. Die Fraktionierung von Stärke, die mit Dimethylsulfoxyd vorbehandelt wurde, wird einer kritischen Betrachtung unterzogen.

*) This is Part XXXI in the Series "Physicochemical Studies on Starches"; Part XXX, Stärke **15** (1963) 444.

Introduction

One of the characteristic features of an amylose which has been obtained from an aqueous dispersion of starch by precipitation as a complex, is that it is incompletely degraded into maltose by the enzyme β-amylase. We have found that this phenomenon is general for the amylose from starches of many different botanical sources[1]. The incomplete conversion suggests that some type of structural modification is present in the amylose, *i.e.* the molecule is not a simple, linear chain of α-1,4-linked glucopyranose units.

β-Amylase appears to be particularly sensitive to the slightest structural anomaly in an α-1,4-glucan, and a fundamental question is whether these anomalies are *native* to the amylose, or whether they are artefacts introduced during the isolation or fractionation of the starch. This problem is complex. We have shown[2] that if amylose is dispersed in boiling water, in the presence of oxygen, the β-amylolysis limit of the sample is decreased. Oxygen is capable, therefore, of modifying – either directly, or indirectly – the α-1,4-glucan structure so that the enzyme-substrate complex cannot be formed properly, and hence the extent of degradation is reduced. (There is the possibility of oxidation at C_2, C_3 or C_6 to form carbonyl-, or carboxyl-groups[3].) It is necessary, therefore, to take great

Table 1. Properties of amylose fractions obtained on successive aqueous leaching of some starch granules[a]

Starch	Procedure	Amylose extracted[b] (%)	[β]	[η]*) (dl·g^{-1})
Iris (rhizome)	70 °C. leach	19	98	190
	80 °C. leach	25	89	230
	90 °C. leach	25	76	260
	Dispersion of residue[b]	31	72	280
Potato	58–60 °C. leach	35	99	250
(var. Redskin)	63–65 °C. leach	15	82	320
	Dispersion of residue[c]	50	75	570
Wheat	70 °C. leach	26	98	145
	98 °C. leach[d]	81	69	260

a) Results from Refs. [1] and [5].
b) From measurements of iodine affinity.
c) After addition of thymol and butanol as precipitants.
d) Direct and not successive leach.
*) Measured in 1 *M* potassium hydroxide.

care to avoid the presence of oxygen, and carry out the fractionation in an inert atmosphere[4,5]. Other experiments have shown that a "barrier" to β-amylolytic action is certainly not present in all amylose molecules. Amylose can be readily subfractionated, into samples with varying β-amylolysis limits, on successive aqueous leaching of starch granules[1–3]; with increase in temperature, amylose of *increasing* molecular size, shown by the limiting viscosity number, $[\eta]$, and *decreasing* β-amylolysis limit $[\beta]$ is obtained as shown in Table 1.

In this paper, we present more evidence for the heterogeneity of natural amylose, and for the fact that the barrier to β-amylolysis is native to the polysaccharide.

Experimental

Isolation and purification of the mature starches

Starch was isolated from potatoes (vars. Kerr's Pink, Redskin and Pentland Crown), wheat (var. Victor II), and iris rhizomes, and was purified by the general technique we have described earlier[1,5]. The potato starches were then stored in saline under toluene at 2°C., whilst the wheat and iris starches were defatted by refluxing with 80% aqueous methanol and stored under methanol.

Isolation and purification of immature potato starch

Potatoes (var. Duke of York) were grown by the Scottish Plant Breeding Station, Pentlandfield, Roslin, Midlothian. They were harvested at various intervals, and the tubers separated into sizes, which varied from smaller than 1 cm. to 8–9 cm., in their largest diameter. The starches were then isolated as above.

Characterization of starches and their components

(a) Purity

The purity of starches, amyloses, and amylopectins was determined from measurements of the iodine-binding power of the samples, using a semi-micro differential potentiometric apparatus[6]. Under the titration conditions of the experiment, the iodine affinity of potato amylose was 19.5% by weight[4]. Apparent amylose contents were calculated from:

[(Iodine affinity of sample)/19.5]·100.

(b) Enzymic characterization

The method of measuring the percentage conversion of the samples into maltose, under the action of (i) pure β-amylase, and (ii) a mixture of β-amylase and Z-enzyme*), was essentially the same as that described earlier[5,7]. The accuracy of these measurements is ± 2%.

Pretreatment of the starches

If the starch was not used directly as prepared, the granules were pretreated to disrupt their structure with either

*) See footnote on p. 197.

(i) liquid ammonia[5], or,

(ii) 1 *M* potassium hydroxide at 0 °C. with stirring for 10 mins., before careful neutralization[5], or

(iii) dimethylsulphoxide as described by KILLION and FOSTER[8]. Starch (5 g.) was added to dimethylsulphoxide (1000 ml.), and the mixture allowed to stand at room temperature to achieve dispersion (3 days). In later experiments, the starch was dispersed in dimethylsulphoxide containing 10 % of water. Dispersion was then more rapid (1 day). The starch-material was then precipitated by the addition of butanol (60 %), and the precipitate washed thoroughly with ethanol to remove the dimethylsulphoxide.

Fractionation of the starches

Dispersions of granular, or pretreated, starches in water were made under nitrogen with vigorous stirring. Various dispersion temperatures were used depending on the extent of pretreatment. The procedure for dispersion at 100 °C., and the use of thymol followed by butanol for the precipitation of the amylose, has been described elsewhere[5]. In experiments where dispersions were made at lower temperatures, butanol alone was used as the precipitant. All the amylose samples from dimethylsulphoxide-treated starches were purified by recrystallizing four times from aqueous dispersion at the appropriate temperature; the solution being filtered through a grade 3 glass sinter at each stage. Other samples were recrystallized twice.

Amyloses were stored either (i) in the form of the amylose-butanol complex, or, (ii) in the solid, after dehydration of the butanol-complex[5].

Subfractionation of the amyloses

(a) Dimethylsulphoxide/ethanol precipitation

Dried amylose was dissolved in dimethylsulphoxide to give a 0.5 % solution, to which ethanol (20 %) was added before the mixture was cooled to 4 °C., and ethanol added slowly until precipitation occurred[9]. After removal of the precipitate on the centrifuge, the stepwise addition of ethanol was continued until no more polysaccharide remained in solution (*ca.* 60 % ethanol, v/v). Precipitates were washed with ethanol and dried in vacuo at 60 °C. A typical precipitation curve for this method is shown in Fig. 1. Recovery of amylose during this procedure was *ca.* 90 %; losses being entirely mechanical.

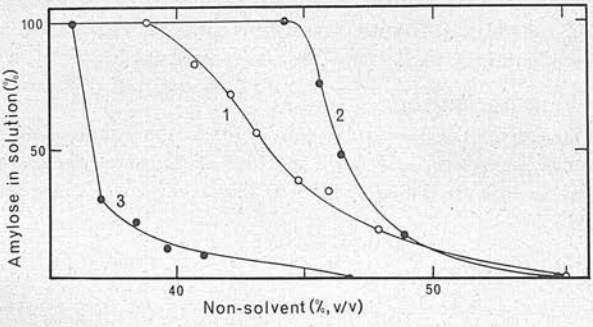

Fig. 1. Precipitation of amylose from dimethylsulphoxide solution by: 1, acetone; 2, ethanol; 3, benzene

The solid amylose fractions obtained in the above manner were sometimes difficultly soluble, and they were more easily handled if the butanol-complex was formed. This was achieved by one of two methods:

(i) By dispersing the *alcohol-washed precipitate* (without further drying) directly into boiling water (in a nitrogen atmosphere), and adding butanol to form the amylose-complex on cooling. This was then redispersed and recrystallized with butanol to ensure complete removal of dimethylsulphoxide.

(ii) The *dried solid amylose* was moistened with ethanol, and then dispersed in boiling water with vigorous stirring (under nitrogen) for 10 mins. Butanol was then added to the solution to form the complex on cooling.

(b) Dimethylsulphoxide/benzene precipitation

The procedure for this fractionation was as in (a) above, except that the experiment was carried out at 25 °C.

(c) Potassium chloride/ethanol precipitation

Amylose was dispersed in potassium chloride (0.14 *M*) as outlined below, and ethanol added in a stepwise manner to the solution at 20 °C. Precipitates were removed on the centrifuge, dispersed in boiling water, and then reprecipitated as the butanol-complex.

Physical measurements

(a) Sample dispersion

Solid amyloses were dissolved in the appropriate molarity of KOH at 0 °C. by standing overnight at this temperature. The solutions were used directly, or, if examination in aqueous KCl was required, they were carefully neutralized with HCl to p_H 7 using a p_H-meter.

Butanol-amylose complexes were dissolved directly in alkali, after centrifugation.

In all cases, concentrations were determined by hydrolysis, and estimation of the resultant glucose using the alkaline ferricyanide method[5].

(b) Viscosity

Viscosity measurements were carried out at 25 °C. using a modified UBBELOHDE viscometer. The characteristics of the instrument, and the procedure have been detailed elsewhere[7]. Measurements were made in 0.15 *M* potassium hydroxide unless otherwise stated.

(c) Sedimentation

A Spinco Model E Ultracentrifuge, incorporating a Rotor Temperature and Control-Unit, was used for the sedimentation measurements. 30 mm. path-length cells were used in conjunction with a "schlieren" optical system equipped with phase-plate optics. Sedimentation coefficients were evaluated as described earlier[7], and when dilution-series were obtained, results were expressed in the form

$$S^{-1} = S_0^{-1} + K_s C$$

where S is the sedimentation coefficient at concentration C, S_0 is the corresponding value at infinite dilution, and K_s is a constant.

(d) Lightscattering

Apparatus. The instrument used was the BRICE-HALWER-SPEISER-type[10] (supplied by the Phoenix Precision Instrument Co., Philadelphia, U.S.A.) with cylindrical cells and the narrow diaphragm-system.

Table 2. Properties of subfractions obtained from various amyloses by dimethylsulphoxide/ethanol precipitation

Iris germanica amylose					Wheat amylose					Potato (var. Redskin) amylose			
Fraction[a]	%[b]	$[\eta]$*)	$[\beta]$	$[\beta + Z]$	Fraction[a]	%[b]	$[\eta]$*)	$[\beta]$	$[\beta + Z]$	Fraction[a, c]	$[\eta]$	$[\beta]$	$[\beta + Z]$
I 1	1.9	540	62	101	W 1 a[d]	0.9	—	—	—	P 1 a	1200	58	101
I 2 a	3.5	410	65	100	W 1 b	3.7	560	66	100	P 1 b	700	66	101
I 2 b	2.6	360	100	101	W 2 a	11.6	535	71	101	P 2	800	65	100
I 3 a	2.1	380	70	101	W 2 b	10.9	310	94	101	P 3	525	72	99
I 3 b	31.5	320	88	101	W 3 a	12.1	410	80	101	P 4	480	76	99
I 3 c	9.4	260	100	100	W 3 b	8.0	330	85	101	P 5	410	82	101
I 4 a	11.4	280	86	100	W 3 c	5.6	265	99	100	P 6	300	95	99
I 4 b	10.4	150	92	100	W 4	13.4	210	94	100	P 7	160	100	100
I 5	10.4	130	95	101	W 5	9.7	175	96	101	P 8	90	100	100
I 6	11.4	110	95	101	W 6	10.9	130	99	100				
I 7	3.5	85	100	100	W 7	6.2	90	99	100				
I 8	1.9	80	100	100	W 8	7.0	60	100	101				
Σ-values[e]	100	240	86	—	Σ-values[e]	100	270	88	101	Σ-values[e]	—	—	—
Orig. amylose	100	240	85	100	Orig. amylose	100	270	86	100	Orig. amylose	550	80	100

[a] a, b, c, represent refractionation products.

[b] Expressed as percentage of total polysaccharide recovered.

[c] Fraction weights were not determined as samples were obtained directly as butanol-complexes.

[d] Insoluble fraction.

[e] Calculated assuming percentage loss of each sample is identical.

*) Measured in 1 *M* potassium hydroxide.

Clarification of solvent and solutions

Measurements were made on amyloses dispersed in 0.33 *M* KCl as above and dimethylsulphoxide, and on amylose acetates dissolved in nitroethane. 0.33 *M* KCl was clarified by filtration through a Millipore filter, type VC, whilst the nitroethane and dimethylsulphoxide were fractionally distilled. Solutions were clarified by ultracentrifugation at 20,000 r.p.m. for 1 hr., removed from the rotor using the technique of SCHNEIDER[11], and filtered through a grade 4 glass sinter directly into the lightscattering cell.

Procedure. The experimental procedure for dilution and evaluation of results by the method of ZIMM[12] has been detailed earlier in this series[7].

Preparation of acetyl-derivatives of amylose

Some potato amylose sub-fractions were acetylated, from the butanol-complex, with pyridine and acetic anhydride under conditions of minimum degradation to form the triacetate[13].

Results and Discussion

In the past, the successful subfractionation of native amylose into species of differing molecular weight has not proved to be easy[14–16]. However, we have found that the method of EVERETT and FOSTER[9], is remarkably successful. In this technique, amylose is dissolved in dimethylsulphoxide and subfractionated by the stepwise addition of ethanol

Table 3. Properties of subfractions of potato (var. Pentland Crown) amylose obtained by precipitation from dimethylsulphoxide solution

Acetone[a]				Ethanol[a]				Benzene[a]			
Fraction[b]	%[c]	[η]	[β]	Fraction[b]	%[c]	[η]	[β]	Fraction[b]	%[c]	[η]	[β]
PA 1	17.1	1040	85	PE 1a	10.8	1205	70	PB 1a	23.9	1040	81
PA 2	13.2	905	92	PE 1b	9.7	1135	73	PB 1b	2.8	—	84
PA 3	16.1	555	99	PE 1c	6.4	615	98	PB 1c	25.0	775	91
PA 4	20.2	460	100	PE 2a	15.5	690	82	PB 1d	14.2	490	98
PA 5	4.1	—	99	PE 2b	3.6	555	80	PB 2	8.5	530	94
PA 6	16.1	280	99	PE 2c	5.9	410	85	PB 3	11.9	340	96
PA 7	13.1	135	99	PE 3	32.0	340	97	PB 4	2.3	—	98
				PE 4	16.1	120	99	PB 5	11.4	155	101
Σ-values[d]	100	570	95	Σ-values[d]	100	560	89.	Σ-values[d]	100	650	92
Original sample	100	575	92	Original sample	100	575	92	Original sample	100	575	92

[a] Precipitant.

[b] a, b, c represent refractionation products.

[c] Expressed as the percentage of total amylose recovered.

[d] Calculated assuming percentage loss of each sample is identical.

at 4 °C. Typical results for the amyloses from the starch of iris rhizomes, wheat, and potatoes are shown in Table 2. The efficiency of molecular weight fractionation is shown by the wide range in values of the limiting viscosity number, $[\eta]$, and by the agreement between the summative value and the observed value of $[\eta]$ for the original amyloses. The method appears to be successful without extreme precautions being necessary in the fractionation procedure. Fractionation at 25 °C. is as successful as that at 4 °C., and the removal of subfractions can be completed in 2–3 hours.

We have extended this technique by using acetone, ethanol and benzene as precipitants. The precipitation curves shown in Fig. 1 and the results in Table 3 indicate that the efficiency of fractionation would be in the order acetone > ethanol > benzene.

The actual success of these fractionations in terms of the narrowness of the molecular weight distribution of the fractions will be discussed later.

Subfractionation by the addition of ethanol to potato amylose (var. Pentland Crown) dissolved in 0.14 *M* potassium chloride was not as satisfactory as that involving the use of a dimethylsulphoxide solution:

Fraction	0	1	2	3	4
% of ethanol	0	20.6	20.7	24.6	29.8
% of total amylose recovered	100	83.5	5.5	7.0	4.0
$[\eta]$	575	560	345	230	125

Subfractionation and its relation to structural anomalies

It is very significant that the subfractions from the dimethylsulphoxide/ethanol precipitations varied not only in their $[\eta]$-values, but also in the extent to which they were degraded by β-amylase (see Table 2).

This result is comparable to that found on aqueous leaching of starch granules (Table 1). It would substantiate our claim that native amylose is heterogeneous, some molecules consisting of a linear chain of unmodified glucose-units, whilst others must contain some type of structural anomaly. In addition, the values of $[\eta]$ indicate that this anomaly is associated primarily with the high molecular-weight fractions, and the low molecular-weight samples are essentially all linear.

Further investigation showed that the distribution of material containing a barrier to β-amylolysis was dependent on the non-solvent used to precipitate the amylose from the dimethylsulphoxide solution as shown in Table 3.

It is to be noted that the incomplete enzymic degradation is not due to contaminating branched-material, as conversion into maltose under the concurrent action of β-amylase and Z-enzyme*), [β + Z], was complete for all samples. Further, it seems unlikely that an *artificial* barrier should be associated only with the high molecular-weight fractions of amylose.

The ultracentrifugation of amylose and its subfractions

We have studied the behaviour of amylose and its subfractions on ultracentrifugation in 0.16 *M* potassium chloride and 0.16 *M* potassium hydroxide. The sedimentation coefficients, *S*, of polysaccharides in both of these solvents were dependent on the concentration, *C*, as shown in Fig. 2, but the concentration dependence was reduced in the salt solution. This is in agreement with our earlier investigations[7], in which we found 0.33 *M* potassium chloride to behave as a theta-solvent at 20 °C. (It is of interest to note that the sedimentation results presented in this work substantiate the claim of FUJITA and his workers[17] that when the molecular weight of the polymer is above about 10^5, the sedimentation coefficient in a theta-solvent is dependent on the concentration to an appreciable extent.)

However, the more important facet of these investigations was the finding that, although all the subfractions in alkaline solution behaved

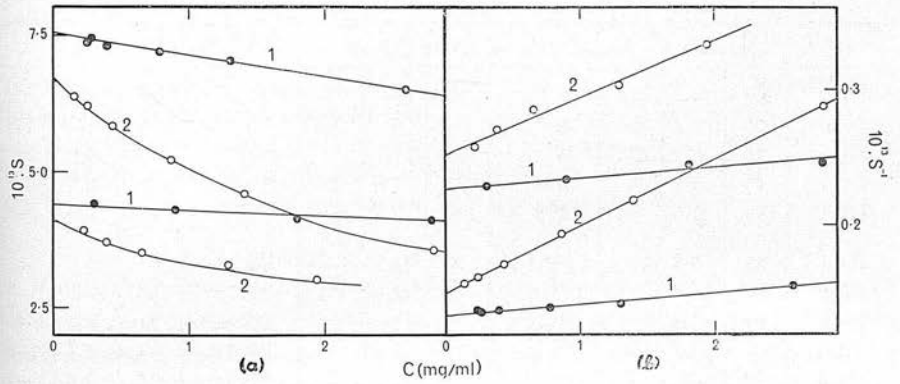

Fig. 2. Graph of (a) *S versus C*, and (b) S^{-1} *versus C* for fractions P 7 and P 8 (Table 2) in: 1, 0.16 *M* potassium chloride; 2, 0.16 *M* potassium hydroxide

*) We have shown that Z-enzyme has some of the properties of an α-amylase, but we are here retaining the conventional nomenclature (see W. BANKS, C. T. GREENWOOD, and I. G. JONES, J. chem. Soc. [London] **1960**, 150).

as homogeneous polymers, most samples with a β-amylolysis limit appreciably less than 100 *showed evidence of heterogeneity (i.e. contained a minor fast-moving component) when examined in 0.16 M potassium chloride solution.* This effect is shown in Fig. 3. The apparent homogeneity in the alkali is presumed to be due to the fact that the increased dependence of S on C in this solvent causes pronounced boundary sharpening

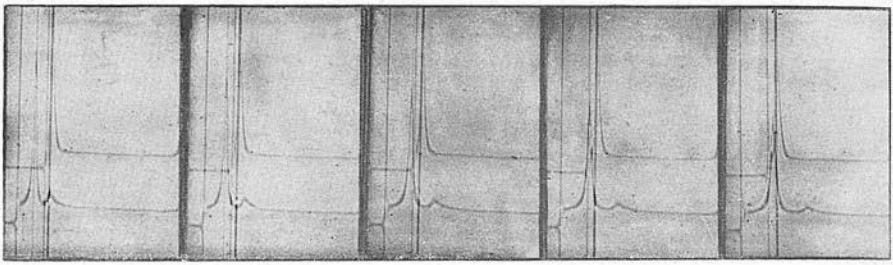

Fig. 3. Typical schlieren patterns for amylose subfraction PA 1 (Table 2); [β] = 85; 2-cell operation, with 1° wedge window; upper pattern, sample in 0.16 *M* potassium hydroxide; lower pattern, sample in 0.16 *M* potassium chloride; concentration, 0.3 g./100 ml. for both solutions; speed, 39,460 r.p.m.; angle of phase-plate, 60°; times of photographs, (from left to right), 1, 16, 32, 48, 64 mins. after reaching fullspeed

Table 4. Apparent sedimentation coefficients for amylose subfractions dissolved in 0.16 *M* potassium chloride at a concentration of *ca.* 0.2 g./100 ml.

Fract.[a]	[β]	S_s	S_f	Fract.[a]	[β]	S_s	S_f	Fract.[a]	[β]	S_s	S_f
I 1[b]	62	14 ⟶		W 1*b*	66	13	32	P 1a	58	12.9	27
I 3*a*	70	7.2	35	W 2*b*	94	6.7	16	P 2	65	11.0	24
I 4*a*	86	8.3	22	W 3*a*	80	11	24	P 6	95	8.6	21
I 5	95	5.0	–	W 4	94	7.6	23	P 7	100	6.7	–
I 7	100	3.6	–	W 8	100	4.5	–	P 8	100	4.0	–
PA 1	85	9.5	17.4	PE 1*a*[b]	70	11.2 ⟶		PB 1*a*	81	12.8	–
PA 2	92	11.0	*	PE 1*b*	73	12.9	23	PB 1*b*	84	–	–
PA 3	99	12.4	–	PE 1*c*	98	14	–	PB 1*c*	91	9.3	–
PA 4	100	8.2	–	PE 2*a*	82	15	*)	PB 1*d*	98	6.9	–
PA 5	99	–	–	PE 2*b*	80	11	26	PB 2	94	8.0	–
PA 6	99	7.9	–	PE 2*c*	85	7.2	29	PB 3	96	6.2	–
PA 7	99	6.0	–	PE 3	97	6.5	–	PB 4	98	–	–
				PE 4	99	4.6	–	PB 5	101	4.9	–

a) Fractions labelled as in Table 2 and 3.

b) Pronounced asymmetrical peak.

*) Not measurable, minor peak present as a shoulder.

effects, which mask the presence of the minor component. It has to be emphasised that this heterogeneity is not apparent when a *total* amylose is ultracentrifuged in saline solution. For such an amylose sample, the distribution of molecular weights – as is shown by the fractionation results above – is so broad that again boundary sharpening must overwhelm any possible heterogeneity effects.

Table 4 shows the apparent sedimentation coefficients for the amylose subfractions dissolved in 0.16 *M* potassium chloride at a concentration of *ca.* 0.2 g./100 ml. It can be seen that, in general, whenever the value of [β] for a fraction is less than 95, the sample shows the presence of a minor fast-moving component with a sedimentation coefficient, S_f, some 2–4 times greater than that for the main slower-moving component, S_s. Some typical schlieren patterns are shown in Fig. 4.

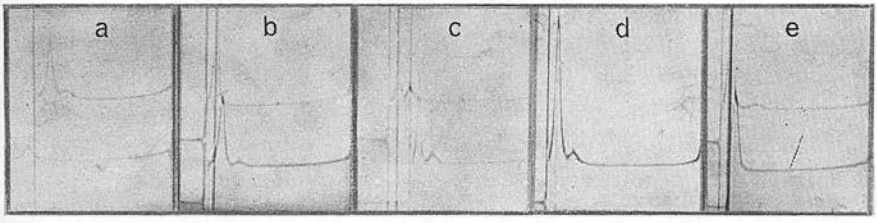

Fig. 4. Typical schlieren patterns for the ultracentrifugation of amylose subfractions in 0.16 *M* potassium chloride

Fraction numbers as in Tables 2 and 3; 2-cell operation (except (d)) with 1° wedge window; speed, 39,460 r.p.m.; concentration, 0.2 g./100 ml. except where otherwise stated; angle of phase-plate, 60°; times are those after reaching full-speed

(a) Time, 17 mins.; fraction PE 1b at two concentrations; lower pattern, c = 0.1 g./100 ml
(b) Time, 12 mins.; upper pattern, fraction PA 6; lower pattern, fraction, PA 1.
(c) Time, 7 mins.; upper pattern, fraction PE 2b; lower pattern, PE 2c.
(d) Time, 8 mins.; sample 1 from KCl/EtOH fractionation.
(e) Time, 14 mins.; upper pattern, fraction W 4; lower pattern, fraction W 9.

When the value of [β] is less than 95 %, it would appear that a fraction of relatively narrow molecular weight distribution is necessary before heterogeneity appears on ultracentrifugation. For example, none of the fractions of potato amylose obtained by precipitation with benzene from dimethylsulphoxide (PB in Table 4) were heterogeneous. This we would attribute to the fact that benzene is a "poor" precipitant (see earlier) which yields fractions with a relatively wide range of molecular weights. Indirect evidence for this is shown by comparing the properties of the fractions PB with those of the linear PA-fractions. For fractions with

comparable values of S_s, the PB-fractions have much greater values of $[\eta]$, and it would appear that the minor-component is retarding the movement of the major one although the heterogeneity is not apparent in the schlieren pattern. Further, some fractions (*e.g.* I1 and PE1*a*) gave an extremely broad and asymmetrical peak, which indicated incipient heterogeneity.

Some of the fractions obtained by ethanol/potassium chloride fractionation (see p. 196) also showed heterogeneity on ultracentrifugation in aqueous salt solution.

Estimation of the concentration of a fast-moving component in the presence of a slow-moving one has been discussed by JOHNSTON and OGSTON[18] and SCHACHMAN[19]. In our investigation, no quantitative measurements were attempted, but the Schlieren patterns showed that the peak area for the fast-moving component was related to the β-amylolysis limit of the sample. For example the ratio of slower- to faster-moving component for fraction PA1, where $[\beta] = 85$, was 11, whilst the corresponding ratio for fraction PE1b, where $[\beta] = 73$, was 4 (see Fig. 4). It should be noted that the JOHNSTON-OGSTON effect will reduce the apparent amount of faster-moving component. We intend to investigate the quantitative aspects of this behaviour later.

Ultracentrifugal examination of a heterogeneous subfraction after β-amylolysis showed the absence of the major slow-moving component, but the appearance of a peak with a sedimentation coefficient intermediate between S_f and S_s. We would suggest, therefore, that the structural anomaly responsible for incomplete β-amylolysis of amylose is present in the minor fast-moving component, which must correspond to the high molecular-weight material.

Studies on amyloses isolated from plants of varying maturity

There is now substantial evidence that, during growth of a plant, there are changes in the amount of starch and its characteristics, but the properties of the components isolated from such starches have not been so extensively investigated[20–24].

In this work, we have carried out experiments on potatoes, as shown in Table 5. During growth of the potato, there is an increase in the average size of the starch granules, and in their gelatinization temperature and the amount of amylose that they contain. The amylose components showed (i) a decrease in β-amylolysis limit from 92 to 72 %, indicating the introduction of some structural modification with growth, (ii) complete conversion into maltose under the concurrent action of β-amylase

and Z-enzyme, indicating the absence of contaminating amylopectin, and (iii) a viscosity increase from 100 to 450, indicating an increase in molecular size.

Table 5. Properties of starches and amylose components[a] isolated from potatoes (var. Duke of York) at varying stages of maturity

Size of tuber (cm.)	< 1	1–2	2–3	3–4	4–5	6–7	7–8	8–9
Starches								
Size of granules (μ)[b]	18	22	29	34	38	46	50	54
Gelatinization temp. (°C.)[b]	56.0	56.5	58.0	58.5	59.0	59.5	59.5	60.0
Iodine affinity	2.3	3.4	3.6	3.8	4.3	4.4	4.4	4.4
% of amylose	12	17	18	19	22	22	22	22
Amyloses								
Iodine affinity	19.0	19.0	19.1	19.1	19.2	19.0	19.0	19.1
[β]	92	86	84	84	83	79	75	72
[β + Z]	100	101	100	100	100	100	101	100
[η]*)	100	130	160	240	290	360	430	450

[a] Fractionation by conventional dispersion after liquid ammonia pretreatment of starches Precipitants: thymol followed by butanol.

[b] Methods as in Ref. 1; gelatinization temperature is the temperature at which 50% of the granules have lost their birefringent properties.

*) Measured in 1 *M* potassium hydroxide.

As all starch samples had received identical treatment during isolation and fractionation, it seems unlikely that the anomaly is an artefact, which is just introduced more readily into the starches from the more mature plants. In our view, this evidence indicates extremely strongly that the barrier to β-amylolysis in amylose is a natural one.

Factors controlling the apparent molecular size of amylose and its β-amylolysis

It is obvious from the above results that generalizations regarding the molecular weight of natural amylose are not possible. For a given fractionation procedure, the apparent molecular weight – as shown by viscosity measurements – and also the β-amylolysis limit – depend on the state of maturity of the plant material. On this basis, comparisons of different fractionation procedures can only be made on *the same sample of starch*: this essential prerequisite is often not observed.

Fractionation must be carried out in the absence of oxygen to avoid degradation, but pretreatment of the granule is also often essential for effective dispersion. Because potato starch can be directly dispersed into

water, it provides a useful standard by which the effect of various pretreatments can be examined. Table 6 shows experiments of this type; although [β] is independent of the pretreatment, the [η] for the amylose from a liquid-ammonia pretreated starch tends to be slightly higher.

Table 6. Properties of amyloses obtained by precipitation from aqueous dispersions of potato starch, var. Pentland Crown (at 100 °C.) after various pretreatments of the granules

Sample	Methods of pretreatment of granule	[β]	[β + Z]	[η]	% of amylose in corresponding amylopectin
1	None	88	100	630	0.4
2	NH_3 (l)	86	100	730	0.4
3	KOH/HCl at 0 °C.	86	101	625	0.5
4	NH_3 (l)*)	87	100	720	0.4
5	None*)	88	100	610	0.4

*) Re-examination of samples after storage of the butanol-complex at room temperature for six months.

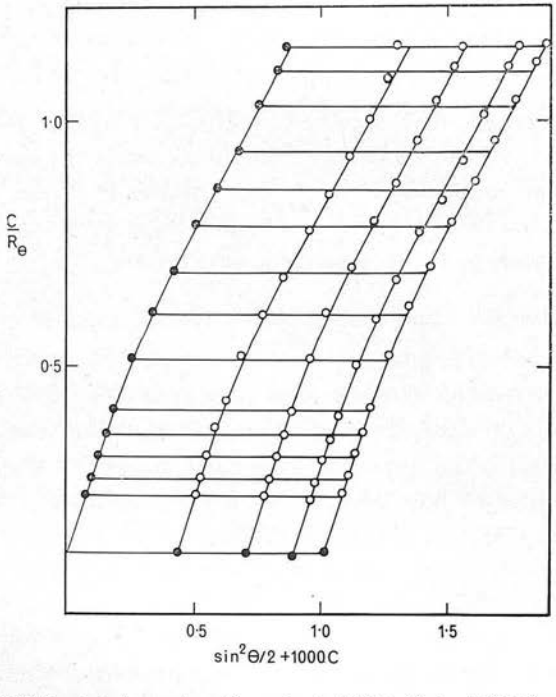

Fig. 5. Zimm-plot[12] for total amylose (sample 5, Table 6) in 0.33 *M* potassium chloride

Although values of $[\eta]$ vary with plant maturity, the total amyloses isolated in these laboratories, from random selections of potato tubers, have consistently been found to have values of $[\eta]$ of 400–500 when measured in 1.0 *M* alkali. We have also considered that these values give an estimate of the molecular size of the amylose. However, MUETGEERT[25] has suggested that the maximum value of $[\eta]$ for potato amylose is 280. We cannot regard this idea as being correct.

To confirm that the $[\eta]$-values correspond to high molecular weights, lightscattering measurements were carried out on some of the total potato amylose samples. A typical ZIMM-plot[12] for such a sample in 0.33 *M* potassium chloride is shown in Fig. 5. As found earlier[7], the second virial coefficient is essentially zero for this solvent in the concentration range investigated (compare Refs. 26 and 27). The pronounced curvature of the ZIMM-plot is due to the extremely wide molecular weight distribution; this curvature disappeared when sub-fractions were examined, in agreement with our earlier results[7]. Values of the weight-average molecular weight, $\overline{M}_w$, and the approximate number-average molecular weight, $\overline{M}_n$, are shown in Table 7. (The theory underlying this evaluation has been discussed by BENOIT, HOLTZER and DOTY[28].) Potato amylose from the sample of starch studied has a $\overline{M}_w$-value of about $5 \cdot 10^6$, thus confirming the high molecular weight indicated by the $[\eta]$-value. The ratio of $\overline{M}_w/\overline{M}_n$ shows the large width of the molecular weight distribution. Values of the root-mean-square radius of gyration $(\bar{\rho}_z^2)^{1/2}$ are also shown in Table 7.

Table 7. Results of lightscattering measurements on total amylose samples

Sample[a]	$[\eta]$	$10^{-6}\overline{M}_w$	$10^{-6}\overline{M}_n$	$\overline{M}_w/\overline{M}_n$	$(\bar{\rho}_z^2)$ (Å)[b]
NH_3 (1)*)	720	5.8	1.4	4.2	1990
None*)	610	4.2	0.8	5.2	1430

[a] As in Table 6.

[b] Calculated as in Ref. 28.

Preliminary experiments were carried out to show that these high values for $\overline{M}_w$ were not due to associative effects. Two fractions of potato amylose (var. Redskin; prepared by the late Mr. I. PHILLIPS) were acetylated, and the molecular weight of the esters in nitroethane found to be $5.2 \cdot 10^6$ and $6.9 \cdot 10^6$ by lightscattering. When the corresponding free amyloses in dimethylsulphoxide solution were studied, $\overline{M}_w$ was found to be $3.1 \cdot 10^6$ and $4.0 \cdot 10^6$, respectively, which compared well with values of $2.9 \cdot 10^6$ and $3.8 \cdot 10^6$ calculated from the molecular weights of the esters.

Dispersion of starch in dimethylsulphoxide followed by fractionation

At some stage in all the fractionation procedures described above, the starch granules have been heated at temperatures greater than 60 °C., and thus the possibility has to be considered that this treatment modifies the amylose-structure. The experiment outlined by KILLION and FOSTER[8] was therefore repeated on potato starch, and the properties of the resultant amylose were then compared to those for a sample obtained from a conventional dispersion without pre-treatment. Results were as follows:

Treatment	Dispersion Temp. (°C.)	$[\eta]$	$[\beta]$	$[\beta + Z]$
None	100	525	84	100
Dimethylsulphoxide ...	70	500	84	101

We obtained amylose with a large value of $[\eta]$, but the β-amylolysis limit was the same as that from a conventional dispersion and *not* higher.

The method was examined, therefore, in more detail for two potato starches which yielded amyloses with different values of $[\beta]$, *i.e.* 80 and 85, respectively. Amyloses were isolated at various dispersion temperatures as shown in Table 8. It is to be noted that although KILLION and

Table 8. Fractionation scheme for dimethylsulphoxide-pretreated potato starches

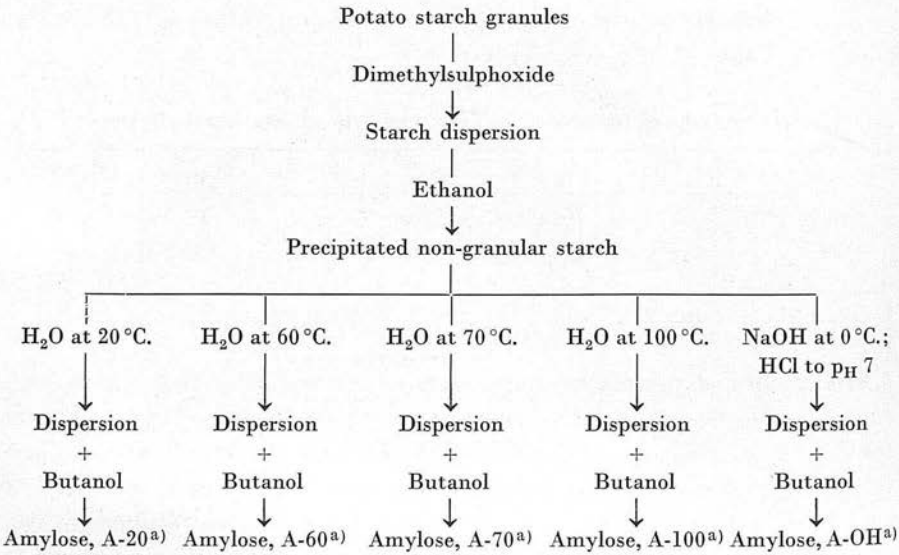

a) The corresponding amylopectin was obtained from the supernatant liquors after removal of the amylose-complex.

FOSTER[8] reported that precipitation of a butanol-complex was not possible unless the dispersion was heated (in their experiments to 70 °C.), the use of the "critical concentration of precipitant", introduced by MUETGEERT[25], enabled a complex to be formed at any temperature (see below). The properties of the various amyloses are shown in Table 9 for the two different samples of potato starch. It can be seen that all the amyloses have essentially the same β-amylolysis limits and limiting viscosity numbers; there is no evidence that the samples from the pretreated starches were of larger molecular size, or contained a smaller number of structural anomalies. (We think, in fact, that it is very likely that the sample of starch used by KILLION and FOSTER[8] was that from immature potato tubers, and so would naturally have had a high β-amylolysis limit.) Further, in view of the increased experimentation required for the dimethylsulphoxide pretreatment, it offers no advantages over the conventional fractionation method.

Table 9. Properties of amyloses obtained from potato starch granules treated with dimethylsulphoxide

Fraction[a]	[β]	[β + Z]	[η]	% of amylose in amylopectin[b]
var. Redskin				
A-20	79	99	540	0.8
A-60	82	101	560	1.0
A-70	84	100	550	1.0
A-OH	82	99	540	0.8
A[c]	80	100	550	0.8
var. Pentland Crown				
A-20	85	99	620	0.8
A-60	85	99	690	1.0
A-70	85	102	640	0.3
A-100	86	101	630	0.5
A[c], ...	88	100	630	0.8

[a] Amylose obtained as in Table 8.
[b] From measurements of iodine affinity.
[c] Amylose from conventional dispersion at 100 °C. in water; no pretreatment.

Conclusions

All the evidence presented above indicates that the incomplete β-amylolysis of amyloses, obtained by precipitation from aqueous dispersion of

the granules, is due in the main to the presence of a natural structural anomaly. However, it is realized that a few barriers may be inadvertently introduced during fractionation, but it will be difficult to establish this point. Further experiments will be necessary to establish unambiguously the nature of this anomaly.

The authors thank the Department of Scientific and Industrial Research for maintenance grants (to R.G., A.W.M., A.R.P., and J.T.).

[1] C. T. Greenwood and J. Thomson, J. chem. Soc. [London] **1962**, 222.
[2] W. Banks, C. T. Greenwood, and J. Thomson, Chem. and Ind. **1959**, 928.
[3] G. O. Aspinall and C. T. Greenwood, J. Inst. Brewing **1962**, 167.
[4] J. M. G. Cowie and C. T. Greenwood, J. chem. Soc. [London] **1957**, 4640.
[5] W. Banks, C. T. Greenwood, and J. Thomson, Makromolekulare Chem. **31** (1959) 197.
[6] D. M. W. Anderson and C. T. Greenwood, J. chem. Soc. [London] **1955**, 3016.
[7] W. Banks and C. T. Greenwood, Makromolekulare Chem. **67** (1963) 49.
[8] P. J. Killion and J. F. Foster, J. Polymer Sci. **46** (1960) 65.
[9] W. W. Everett and J. F. Foster, J. Amer. chem. Soc. **81** (1959) 3459.
[10] B. A. Brice, M. Halwer, and R. Speiser, J. opt. Soc. America **40** (1950) 768.
[11] N. Schneider, J. Polymer Sci. **32** (1958) 255.
[12] B. H. Zimm, J. chem. Physics **16** (1948) 1093.
[13] C. T. Greenwood and J. S. M. Robertson, J. chem. Soc. [London] **1954**, 3769.
[14] S. Lansky, M. Kooi, and T. J. Schoch, J. Amer. chem. Soc. **71** (1949) 4066.
[15] J. Holló and J. Szejtli, Stärke **14** (1962) 75.
[16] D. Goodison and R. S. Higginbotham, Shirley Inst. Mem. **24** (1950) 235.
[17] T. Homma, K. Kawahara, H. Fujita, and M. Ueda, Makromolekulare Chem. **67** (1963) 132.
[18] J. P. Johnston and A. G. Ogston, Trans. Faraday Soc. **42** (1946) 789.
[19] H. K. Schachman, Ultracentrifugation in Biochemistry, Academic Press, New York and London 1959, pp. 108–128.
[20] M. J. Wolf, M. M. MacMasters, J. E. Hubbard, and C. E. Rist, Cereal Chem. **25** (1948) 321.
[21] E. Maywald, R. Christensen, and T. J. Schoch, J. agric. Food Chem. **3** (1955) 521.
[22] S. Harris and I. C. MacWilliam, Cereal Chem. **35** (1958) 82.
[23] S. R. Erlander, Cereal Chem. **37** (1960) 81.
[24] C. T. Greenwood and J. Thomson, Biochem. J. **82** (1962) 156.
[25] J. Muetgeert, Advances in Carbohydrate Chem. **16** (1961) 299.
[26] E. Husemann, B. Pfannemüller, and W. Burchard, Makromolekulare Chem. **59** (1963) 1.
[27] W. Burchard, Makromolekulare Chem. **59** (1963) 16.
[28] H. Benoit, A. M. Holtzer, and P. Doty, J. physic. Chem. **58** (1954) 639.